

**Alfred-Wegener-Institut für Polar- und Meeresforschung,
Forschungsstelle Potsdam und
Humboldt-Universität zu Berlin, Geographisches Institut**

**Glacier and ground ice as archives of Late Holocene climate and
environmental change in the Russian Arctic**

Dissertation

**zur Erlangung des akademischen Grades
doctor rerum naturalium
(Dr. rer. nat.)**

im Fach Geographie

eingereicht an der
Mathematisch-Naturwissenschaftlichen Fakultät II
der Humboldt-Universität zu Berlin

von
Diplom-Geograph Thomas Opel
(16.09.1977, Berlin)

Präsident der Humboldt-Universität zu Berlin
Prof. Dr. Dr. h.c. Christoph Marksches

Dekan der Mathematisch-Naturwissenschaftlichen Fakultät II
Prof. Dr. Peter Frensch

Gutachter

1. Prof. Dr. Wilfried Endlicher
2. Prof. Dr. Hans-Wolfgang Hubberten
3. Prof. Dr. Heinrich Miller

Tag der Verteidigung: 13.11.2009

Table of contents

Zusammenfassung	v
Abstract	vi
Chapter 1: Introduction	1
1.1 Scientific background	1
1.1.1 Arctic climate change	1
1.1.2 Eurasian Arctic paleoclimate records	3
1.1.3 Glacier and ground ice as paleoclimate archives	5
1.2 Aims and approaches	6
1.3 Study region	8
1.3.1 Geological and geographical characteristics	9
1.3.2 Climate characteristics	9
1.4 Thesis outline	11
1.5 The author's contribution to the individual parts	12
Chapter 2: 115 year ice-core data from Akademii Nauk ice cap, Severnaya Zemlya: high-resolution record of Eurasian Arctic climate change	14
Abstract	14
2.1 Introduction	15
2.2 Previous Severnaya Zemlya ice cores	16
2.3 Study Area	17
2.3.1 Climate conditions on Severnaya Zemlya	17
2.3.2 Drilling-site characterization and melting processes	18
2.4 Methods	19
2.5 Dating approach and age model	20
2.6 Results, climatic implications and discussion	23
2.6.1 Stable water-isotope ratios $\delta^{18}\text{O}$ and δD	23
2.6.2 Deuterium excess	29
2.6.3 Melt-layer content	32
2.6.4 Major ions	33
2.7 Conclusions	37

Chapter 3: Late Holocene climate change in the Central Russian Arctic – evidence from Akademii Nauk ice core (Severnaya Zemlya)	39
Abstract	39
3.1 Introduction	40
3.2 Regional Setting	43
3.2.1 Severnaya Zemlya (SZ)	43
3.2.2 Akademii Nauk (AN) ice cap	43
3.3 Materials and Methods	44
3.3.1 Ice core drilling	44
3.3.2 Ice core processing and sampling	45
3.3.3 Laboratory analytics	47
3.4 Results	47
3.4.1 Ice core chronology	47
3.4.2 High resolution record of the last three centuries	51
3.4.2.1 Stable water-isotopes ratios $\delta^{18}\text{O}$ and δD	52
3.4.2.2 Deuterium excess d	54
3.4.2.3 Melt-layer content	55
3.4.3 The Late Holocene record	55
3.4.3.1 Stable oxygen-isotope ratio $\delta^{18}\text{O}$	56
3.4.3.2 Deuterium excess d	56
3.4.3.3 Major ions	58
3.5 Discussion	60
3.5.1 Holocene AN ice cap history	60
3.5.2 Paleoclimatic implications of AN ice core records	61
3.6 Conclusions	67
Chapter 4: Paleoclimatic information from stable water isotopes of Holocene ice wedges at the Dmitrii Laptev Strait (Northeast Siberia)	69
Abstract	69
4.1 Introduction	70
4.2 Ice wedges and stable isotopes	71
4.3 Study region	72
4.4 Materials and Methods	74

4.4.1 Sampling and field measurements	74
4.4.2 Laboratory methods	75
4.5 Isotopic composition of recent precipitation	76
4.6 Isotopic composition of recent ice wedges	78
4.7 Holocene ice wedges	80
4.7.1 Description	80
4.7.2 Chronology	84
4.7.3 Isotopic composition and paleoclimatic implications	87
4.8 Conclusions	94
Chapter 5: Synthesis	96
5.1 Main paleoclimatic results and implications for the Late Holocene climate history of the Eurasian Arctic	96
5.2 Potentials and limitations of the studied paleoclimate archives	101
5.2.1 Akademii Nauk ice core	101
5.2.2 Syngenetic ice wedges (Oyogos Yar)	103
5.3 Outlook and ideas for future research	104
5.3.1 Akademii Nauk ice core	104
5.3.2 Syngenetic ice wedges	105
Appendix I: A 275 year ice-core record from Akademii Nauk ice cap, Severnaya Zemlya, Russian Arctic	107
Abstract	107
I.1 Introduction	108
I.2 Analytical methods	109
I.3 Results and discussion	110
I.4 Conclusions	117
Appendix II: Permafrost evidence for a Younger Dryas cold event in northern Alaska	118
Abstract	118
Methods	125

Appendix III: $^{36}\text{Cl}/\text{Cl}$ ratio in ground ice of East Siberia and its application for chronometry	128
Abstract	128
III.1 Introduction	129
III.2 Sampling of ground ice	133
III.3 Methods	138
III.4 Results	139
III.4.1 Concentration and Ratio	139
III.4.2 Age determination	141
III.4.3 Discussion	141
III.5 Summary and Conclusions	144
References	146
Acknowledgments	163

Zusammenfassung

Die Arktis ist stärker von den aktuellen Klima- und Umweltveränderungen betroffen als andere Regionen der Erde. Für das nächste Jahrhundert wird eine Verstärkung dieser Änderungen erwartet. Nur wenige arktische meteorologische Zeitreihen reichen bis ins 19. Jahrhundert zurück. Deshalb sind Klimaarchive von besonderer Bedeutung, um vergangene Klimaänderungen und deren Ursachen zu rekonstruieren und zu bewerten. In dieser Arbeit wurde Gletscher- und Grundeis aus der Russischen Arktis untersucht, genauer ein Eiskern von der Eiskappe Akademii Nauk (Severnaya Zemlya) und syngenetische Eiskeile der Oyogos Yar Region (Dmitrii-Laptev-Straße). Beide Archive umfassen das Spätholozän und wurden hauptsächlich mittels stabiler Isotope des Wassers untersucht.

Diese Arbeit zeigt das große Potential des Akademii Nauk Eiskerns für eine hoch aufgelöste Rekonstruktion der regionalen Klima- und Umweltgeschichte. Insbesondere seine $\delta^{18}\text{O}$ Daten können als Proxy für Temperaturen in der westlichen Eurasischen Arktis genutzt werden. Sie belegen deutliche Veränderungen auf verschiedenen Zeitskalen. Das 20. Jahrhundert mit einem zweigipfeligen Maximum zwischen 1920 und 1940 war demnach die wärmste Zeit der letzten 2000 Jahre. Von besonderem Interesse sind schnelle dekadische Klimaänderungen sowohl im 15./16. Jahrhundert als auch um 1900, vermutlich verursacht durch die interne Dynamik des Arktischen Klimasystems. Der Deuterium excess d bietet Informationen zur Beteiligung von regionalen Feuchtequellen am Niederschlag, der die Eiskappe speist, in Abhängigkeit von der Meereisaustrückung. Das spätholozäne Wachstum der Eiskappe wird durch abnehmende Trends von $\delta^{18}\text{O}$ - und Meersalz-Ionen-Daten belegt.

Ein neuer Ansatz zur Gewinnung von Paläo-Umwelt-Informationen aus syngenetischen Eiskeilen der Oyogos Yar Region basiert auf hoch aufgelöster Analyse und Radiokarbondatierungen. Auch wenn noch keine kontinuierlichen Zeitreihen gewonnen werden konnten, wurden paläoklimatische Informationen abgeleitet. $\delta^{18}\text{O}$ Daten der Eiskeile zeigen, dass die Winter der letzten Jahrzehnte die wärmsten im Spätholozän waren. Diese Tatsache wurde begleitet von Änderungen der Feuchtequellen, verbunden mit Änderungen in der Atmosphärischen Zirkulation und/oder der Meereisdynamik.

Die geplante weitere Forschung wird die Arbeit an beiden Archiven fortsetzen und neue Einblicke in die Paläoumweltgeschichte der Eurasischen Arktis ermöglichen.

Abstract

The Arctic has been affected by the ongoing climate and environmental change more than other regions of the Earth. For the next century, increasing rates of change have been predicted. Only a few Arctic meteorological records date back to the 19th century. Hence paleoclimate archives are of particular importance for the reconstruction and assessment of past climate variability and its causes. In this thesis, glacier and ground ice from the Russian Arctic, more precisely an ice core from Akademii Nauk ice cap (Severnaya Zemlya) and syngenetic ice wedges from Oyogos Yar (Dmitrii Laptev Strait), both covering the Late Holocene, were studied to contribute new paleoenvironmental information. Both archives were mainly analyzed by using stable water isotopes.

This thesis demonstrates the great potential of Akademii Nauk ice core for the high resolution reconstruction of regional climate and environmental variability. In particular, its $\delta^{18}\text{O}$ data can be used as proxy for temperature in the Western Eurasian Arctic revealing significant changes on different timescales. The 20th century was the warmest period of the last two millennia, with an absolute double-peaked maximum around AD 1920-1940. Of particular interest are rapid decadal-scale climate changes, which occurred in the 15th and 16th century as well as at about AD 1900, most probably caused by internal dynamics of the Arctic climate system. Deuterium excess d provides valuable information on the participation of regional moisture in the precipitation feeding Akademii Nauk ice cap, which is linked to the regional sea ice extent. Decreasing $\delta^{18}\text{O}$ and sea salt ion values due to the increasing ice cap altitude prove the growth of Akademii Nauk ice cap in the Late Holocene.

A new approach, comprising high resolution sampling and radiocarbon dating, was used to gain paleoenvironmental information from the syngenetic Oyogos Yar ice wedges. Even though no continuous records could be obtained due to still inconsistent dating results, paleoclimatic information could be extracted. Ice wedge $\delta^{18}\text{O}$ data show evidence that winters in the last decades were the warmest in the Late Holocene. These were accompanied by changes in the moisture sources, related to changes in the atmospheric circulation patterns and/or sea ice dynamics.

Envisaged follow-up research will continue the work on the studied objects and will facilitate new insights into the paleoenvironmental history of the Eurasian Arctic.

1 Introduction

1.1 Scientific background

1.1.1 Arctic climate change

The last two centuries have been characterized by a significant worldwide climate warming. On the global scale, the mean surface temperature increased by 0.76°C from 1850-1899 to 2001-2005 (Trenberth et al., 2007). In the Arctic, this general warming has been amplified (e.g. Overpeck et al., 1997; Serreze et al., 2000; Moritz et al., 2002). In particular, warming in the Arctic is more than double the warming in the global mean from the 19th century to the 21st century (Figure 1.1; ACIA, 2005; Trenberth et al., 2007).

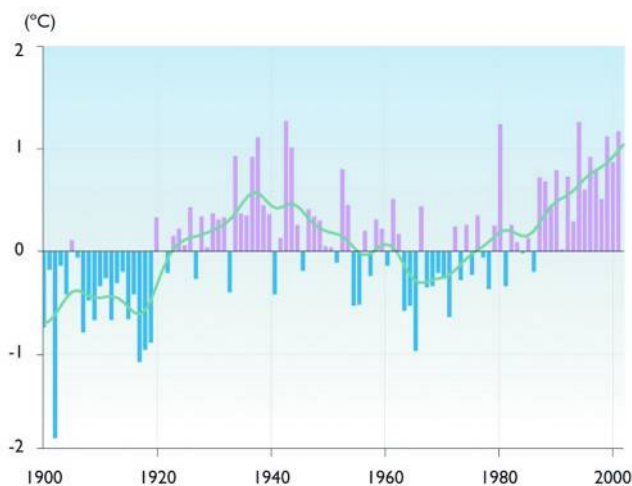


Figure 1.1: Observed Arctic (here: 60-90°N) near surface air temperature changes from land stations relative to the average of 1961-1990 (Source: ACIA 2005).

This Arctic warming has been accompanied by a significant decrease in sea ice extent and thickness, a decrease of the snow-covered area as well as by a warming of the terrestrial permafrost (e.g. Serreze et al., 2000; ACIA, 2005; Osterkamp, 2005; Lemke et al., 2007; Romanovsky et al., 2007), revealing the high sensitivity of Arctic regions to climate changes.

In turn, the Arctic environmental dynamics influence the global climate system by changing river runoff as well as snow and ice cover, affecting the thermohaline circulation and the surface albedo. They furthermore impact atmospheric circulation patterns and the concentrations of the greenhouse gases carbon dioxide and methane (e.g. Overpeck et al., 1997; ACIA, 2005). Consequently, the

Arctic, in this thesis defined as the area northwards of the timberline (corresponding roughly to the 10°C isotherm of the warmest month), is a key region for global climate change and, thus, climate change research.

Projections of future climate changes indicate a stronger ongoing warming of the Arctic relative to other regions (Figure 1.2). This warming will be accompanied by positive feedback mechanisms such as an intense sea ice retreat, a further decrease of the snow-covered areas, shrinking glaciers and an increased thawing of permafrost (thermokarst), including increased release of greenhouse gases (e.g. ACIA, 2005; Walter et al., 2006; Zimov et al., 2006; Christensen et al., 2007). The Arctic climate change, however, will not only influence the global climate system, but will also have substantial ecological, social and economic impacts.

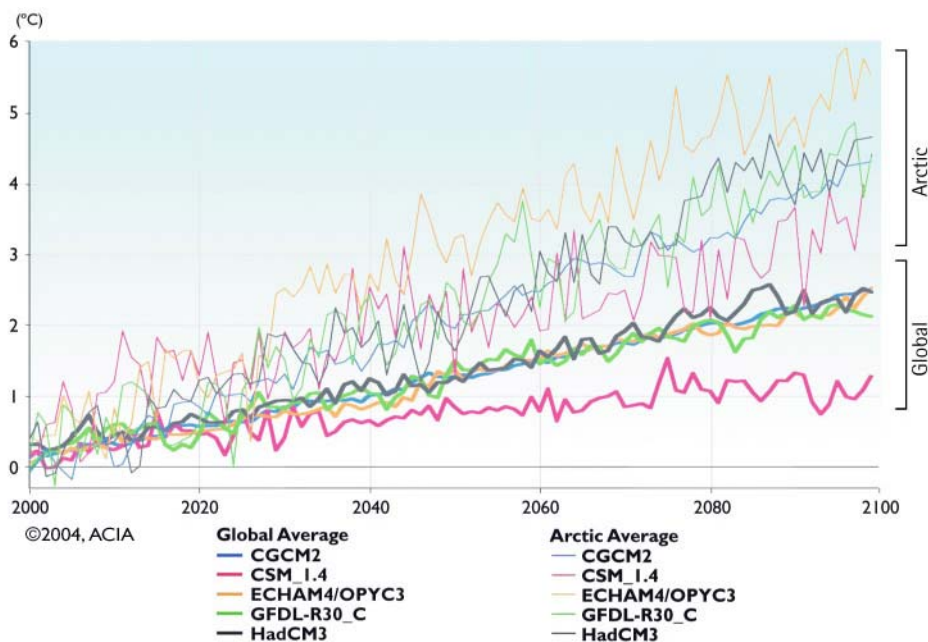


Figure 1.2: Projected surface air temperature change (change from the 1981-2000 average), projected by the five ACIA climate models for the B2 emission scenario. The thick lines (bottom) represent the projected global temperatures, the thin lines (top) the projected Arctic temperatures (Source: ACIA, 2005).

A better understanding and assessment of the recent climate and environmental changes in the Arctic require detailed information on past changes, their interactions and their controlling factors. This information is also needed to improve climate projections. The Arctic meteorological records are, however, both temporally and spatially limited. In the Eurasian Arctic only a few meteorological time series reach back to the 19th century, while instrumental observations at

several stations started only in the course of the 2nd International Polar Year in 1932/33. The longest Eurasian Arctic time series of surface air temperature (SAT) from Vardø (Northern Norway) dates back to the first half of the 19th century; whereas the longest continuous SAT record in the Russian Arctic did not start before 1917 at Dikson. This lack of long meteorological time series emphasizes the relevance of sub-recent high-resolution climate archives for the study of regional Arctic climate and environmental changes (e.g. Overpeck et al., 1997) and the assessment of the recent Arctic warming from a centennial to millennial scale perspective. Of particular interest are climate changes in the Middle to Late Holocene, which is characterized by relative stable boundary conditions of the climate system as compared to Glacial-Interglacial cycles and by a negligible anthropogenic influence in the preindustrial period before about AD 1750 (Wanner et al., 2008). Studying these changes provides insight into the natural climate variability. However, past climate variations and their causes are still contested, such as in the case of the hockey-stick shaped Northern Hemisphere temperature reconstruction for the last millennium by Mann et al. (1999) (for a short overview of the debate see Jansen et al., 2007). For a better assessment it is therefore important to gain new regional high-resolution paleoclimatic information.

1.1.2 Eurasian Arctic paleoclimate records

The most prominent Arctic climate archives are the Central Greenland ice cores (e.g. GRIP, GISP2, NorthGRIP). They provide comprehensive information of climate and environmental changes over more than 100 thousand years on Arctic to global scales (e.g. Dansgaard et al., 1993; Grootes et al., 1993; NorthGRIP members, 2004).

In the Eurasian Arctic, a lot of paleoclimatic studies have been conducted within the scope of the QUEEN (Quaternary Environment of the Eurasian North) program. Substantial results comprise the reconstruction of the Late Quaternary ice-sheet extents (Svendsen et al., 2004) as well as the reconstruction of the Late Pleistocene periglacial climate and environment (Hubberten et al., 2004), particularly in the Russian Arctic.

Several joint German-Russian projects dealt with the Late Quaternary climate and environmental history of the East and Central Siberian Arctic, applying multi-disciplinary approaches to analyze ice-rich permafrost sequences and lake

sediments predominantly along the coastal lowlands of the Laptev Sea and East Siberian Seas (e.g. Meyer et al., 2002a, 2002b; Schirrmeister et al., 2002a; Kienast et al., 2005; Andreev et al. 2009; Wetterich et al., 2009), but also on Taimyr Peninsula (e.g. Siegert et al., 1999; Kienast et al., 2001; Andreev et al., 2003) and on Severnaya Zemlya (e.g. Raab et al., 2003). Due to the specific characteristics of the studied paleoclimate archives (including unconformities and low sedimentation rates) as well as dating issues, the resulting records provide valuable paleoclimatic information on long timescales (covering the Holocene and parts of the Late Pleistocene), at a low resolution (maximum centennial to millennial) but not at high resolution (annual to decadal scale).

Additional relatively low-resolution Holocene paleoenvironmental information comes from dated glacier advances on Franz Josef Land (e.g. Lubinski et al., 1999) and Novaya Zemlya (e.g. Murdmaa et al., 2004; Polyak et al., 2004) as well as from marine sediment cores drilled in the Kara Sea (e.g. Stein et al., 2004) and Laptev Sea (Bauch et al., 2001).

A comprehensive assessment of Arctic climate changes, their causes and feedbacks requires temporally higher resolved data. This is particularly obvious in the Eurasian Arctic, which has only a few of such Middle to Late Holocene records as revealed e.g. by the overview study of Solomina et al. (2004). Compared to the American Arctic (e.g. Overpeck et al., 1997; Kaufmann et al., 2004) the lack of comparable records is evident.

High-resolution records in the Eurasian Arctic are sparse and restricted to tree-ring chronologies as well as ice-core records. Tree-ring time series exist for single suited study sites at the timberline, e.g. on Taimyr Peninsula (Naurzbaev et al., 2002). They primarily reflect summer temperatures.

Ice-core records in the Eurasian Arctic are bound to the occurrence of glaciers or ice caps and therefore limited to High Arctic archipelagos such as Svalbard, Franz Josef Land and Severnaya Zemlya. These ice caps are characterized by summertime melting. Ice core analysis and interpretation therefore require special consideration of melt water infiltration processes (Koerner, 1997). Kotlyakov et al. (2004) reviewed the records of Eurasian Arctic ice cores, mainly drilled by Soviet/Russian teams, revealing that their age models are often significantly overestimated and, thus, require re-evaluation. Recently drilled ice cores from Svalbard (e.g. Isaksson et al., 2005a), Franz Josef Land (Henderson, 2002) and

Severnaya Zemlya (Fritzsche et al., 2002) have revealed a high potential for gaining regional high resolution climate records of at least the last centuries.

In the wide tundra areas of the Siberian Arctic, where tree ring and ice core archives are not available, ground ice contained in the permafrost sequences serves as additional climate archive. However, up to now, only low-resolution information on Late Quaternary paleoclimate has been obtained from ice wedges (e.g. Vaikmäe, 1989; Vasil'chuk, 1991, 1992; Meyer et al., 2002a, 2002b).

1.1.3 Glacier and ground ice as paleoclimate archives

Ice is a natural paleoclimate archive as it preserves atmospheric precipitation and air, which contain numerous physical and chemical parameters. These parameters (proxies) are related to climate and environmental conditions on different scales and allow the reconstruction of valuable information on past climate and environmental changes.

Glaciers and ice caps are large ice bodies arising from the continuous accumulation of snow and its transformation via firn to ice over long periods of up to several hundred thousands of years. Consequently, ice cores have been drilled since about 1950 predominantly in the polar regions and are recognized as one of the best paleoclimate archives.

Generally, paleoclimatic information from ice cores can be obtained by four approaches (Bradley, 1999): the analysis (1) of stable water isotopes, (2) of air bubbles trapped in the ice, (3) of dissolved and particulate matter and (4) of the physical characteristics of the ice core.

(1) The stable water isotope composition of precipitation depends mainly on the condensation temperature (e.g. Dansgaard, 1964; Rozanski et al., 1993) and can therefore be used as proxy for local to regional temperature conditions. Furthermore, information on the primary evaporation conditions can be obtained that way. (2) The air bubbles contained in ice represent samples of a former atmospheric composition and allow direct analyses of the paleo-atmosphere. (3) Dissolved ions and particulate matter, such as dust can be used for the reconstruction of atmospheric aerosol content, of atmospheric circulation patterns as well as of wind speed. (4) Physical characteristics of the ice core (e.g. density and stratigraphic features) allow, for instance, the identification of melt layers, which are a proxy for summer warmth on the glacier surface (Koerner, 1977).

Ground ice, comprising all types of ice in freezing or frozen ground (van Everdingen, 1998), is a major component of permafrost, which is defined by ground temperatures below or at 0°C for two or more consecutive years. Most ground ice types, ice wedges in particular, are fed by precipitation and can therefore be used as climate archives (e.g. Vaikmäe, 1989; Vasil'chuk, 1991, 1992; Meyer et al., 2002a, 2002b). Ice wedges arise from the periodically repeated filling of frost cracks by snow melt water, which trickles down and refreezes quickly (Lachenbruch, 1962; MacKay, 1974). Ice wedge growth can occur during the freezing of previously deposited sediments (epigenetic ice wedges) or approximately simultaneously to the accumulation and freezing of the enclosing sediments (syngenetic ice wedges). Up to now, the paleoclimatic study of ice wedges has primarily focused on the stable water isotope composition, which is related to winter climate conditions.

1.2 Aims and approaches

Up to now, glacier and particularly ground ice in the vast areas of the Siberian Arctic have not been used sufficiently for the reconstruction of Holocene paleoenvironmental changes. The overarching aim of this thesis, therefore, is to use these archives to gain new insights into the Late Holocene climate and environmental history of the Eurasian Arctic. For this purpose, new paleoclimatic data have been derived from both glacier and ground ice in the Russian Arctic (Table 1.1). On the one hand, the recently drilled ice core from Akademii Nauk (AN) ice cap (Severnaya Zemlya; Fritzsche et al., 2002) provides stable isotope and major ion records for a regional reconstruction of paleoclimatic changes. On the other hand, an innovative approach has been used to extract winter temperature records from Holocene ice wedges at Oyogos Yar (Dmitrii Laptev Strait, Northeast Siberia; Dereviagin and Opel, 2009) using stable water isotope data.

More specifically, this thesis pursues the following objectives:

- The assessment of the proxy data contained in Akademii Nauk ice core concerning their paleoclimatic significance under consideration of melt water infiltration and with a strong focus on ice core stable water isotope data.

- The establishment of a chronology for Akademii Nauk ice core and the creation of proxy time series.
- The reconstruction of the Late Holocene climate and environmental conditions from Akademii Nauk ice cap with respect to climate forcing and feedbacks as well as rapid climate changes.
- The use of syngenetic ice wedges as climate archives and the reconstruction of Holocene relative winter temperature changes based on the analysis of the stable water isotope composition and AMS ^{14}C dating.
- The combination of the new information and integration into the regional paleoenvironmental context.

Table 1.1: Comparison of the study objects and methods used in this thesis.

	Akademii Nauk ice cap Severnaya Zemlya Central Siberian Arctic	Syngenetic ice wedges Oyogos Yar East Siberian Arctic
Time range	Late Holocene to present	
Chronology	Annual layer counting using stable water isotopes and volcanic reference horizons	Radiocarbon dating by Accelerator Mass Spectrometry (AMS)
Temporal resolution	Annual to decadal	Centennial to millennial
Spatial resolution	Local to supra-regional	Local to regional
Sampling	Vertical	Horizontal
Information source	Annual precipitation	Winter precipitation
Stable water isotopes $\delta^{18}\text{O}$, δD , d excess	Mass spectrometry	
Major ions	Ion chromatography Continuous flow analysis (CFA)	Ion chromatography Inductively Coupled Plasma Optical Emission Spectrometry (ICP OES)
Electrical conductivity	Dielectrical profiling	Conductivity meter
pH	–	pH meter
Density	γ -absorption	–
Melt-layer content	Line-scan camera	–
Reconstruction potential of the derived proxies	Annual temperatures Summer temperatures Moisture source Sea ice extent Atmospheric aerosol content Atmospheric circulation patterns	Winter temperatures Moisture source Sea ice extent Atmospheric circulation patterns

In order to extract the new paleoclimatic information, the relevant proxy data have been derived mostly by standard laboratory methods (Table 1.1), such as mass spectrometry (stable isotope composition of glacier and ground ice) and ion chromatography (major ion concentration in glacier ice). Details are given in the respective chapters.

1.3 Study Region

The paleoclimatic data presented here originate from two study sites in the Central Russian and East Siberian Arctic (Figure 1.3). The Akademii Nauk ice core was drilled on Severnaya Zemlya archipelago at 80.5°N, 94.8°E, while the Holocene ice wedges were studied at Oyogos Yar (72.7°N, 143.5°E; Dmitrii Laptev Strait).

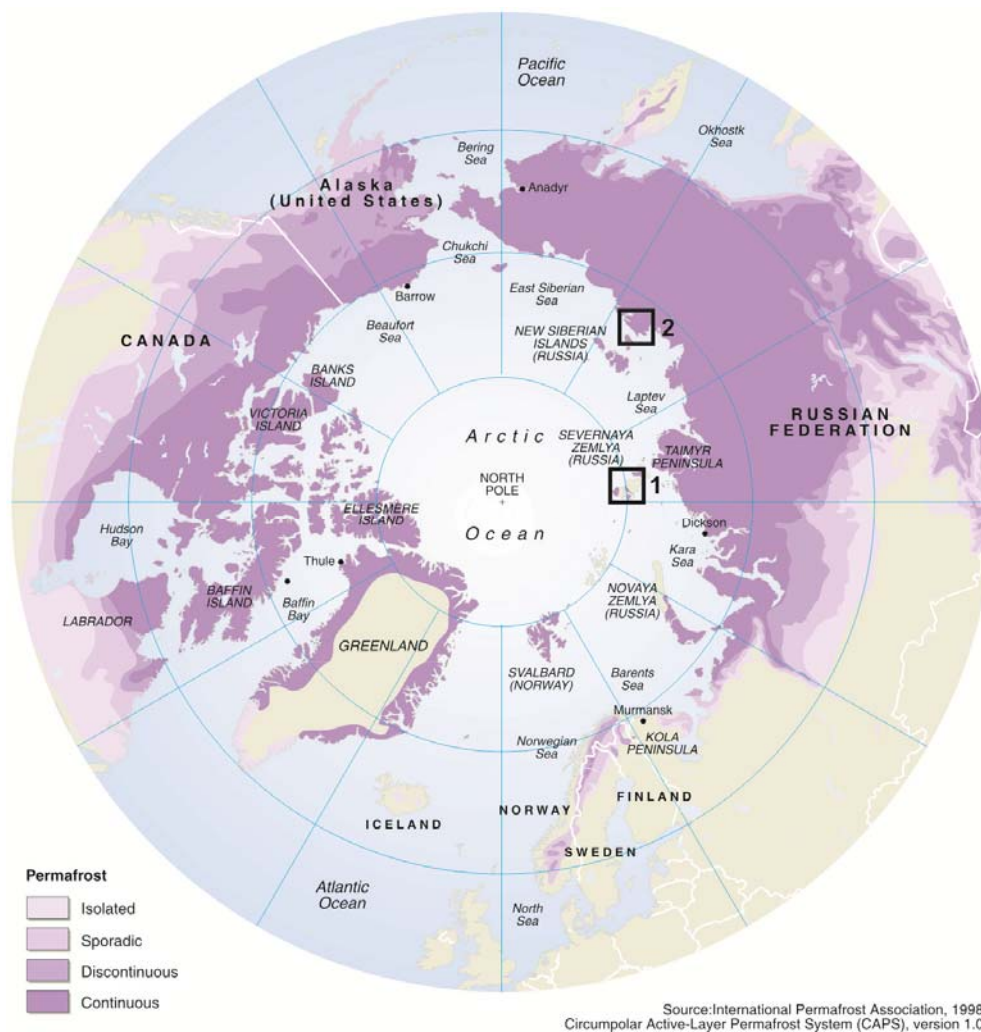


Figure 1.3: Overview map of the Arctic, showing the permafrost distribution and the position of the study areas in the Central and East Siberian Arctic: 1 – Severnaya Zemlya archipelago, 2 – Dmitrii Laptev Strait with Oyogos Yar as its southern coast (source: IPA 1998, modified).

1.3.1 Geological and geographical characteristics

Severnaya Zemlya is located on the northern shelf of the Eurasian continent between the Kara and Laptev Seas. It belongs to the Taymyr-Severnaya-Zemlya folded area (Koronovsky, 2002). The bedrock geology is dominated by Neoproterozoic to Palaeozoic sedimentary successions (Lorenz et al., 2008). The low-lying parts of Severnaya Zemlya are covered by Quaternary marine sediments (Bolshiyakov and Makeyev, 1995).

The Dmitrii Laptev Strait divides the Bol'shoy Lyakhovsky Island from the Eurasian mainland and connects the Laptev and East Siberian Seas. The bedrock of this area belongs to the Verkhoyansk-Kolyma orogen and is dominated by Palaeozoic and mainly Mesozoic folded shallow marine sediments (Koronovsky, 2002). It is overlain by Cenozoic sediments.

Both study areas belong to the area of continuous permafrost (Figure 1.3), which is characterized by deeply frozen ground. Only the upper part, comprising several centimeters to decimeters thaws during the summer (active layer). Several permafrost-related processes, such as frost cracking and subsequent ice wedge growth, thermokarst, thermoerosion and geli-solifluction, form typical periglacial land surfaces like patterned ground and polygonal ice wedge relief (French, 2007). In contrast to the non-glaciated East Siberian coastal lowlands such as Oyogos Yar, about 50 percent of Severnaya Zemlya is glaciated. Due to its location in the High Arctic, Severnaya Zemlya exhibits typical polar desert vegetation, whereas Oyogos Yar is characterized by tundra vegetation.

1.3.2 Climate characteristics

The climate of both study areas is mainly characterized by their position in the high northern latitudes and by their continentality. The latter is caused by the huge Eurasian landmass, but reduced by the adjacent Arctic Ocean (Endlicher, 2000; Shahgedanova, 2002). This leads to high seasonal contrasts with large seasonal temperature amplitudes as well as generally low precipitation amounts (Figure 1.4). Long, cold winters with monthly mean temperatures of about -30°C are followed by short, cool summers. Monthly mean temperatures above 0°C appear only in two to three months. Severnaya Zemlya is positioned in the transition zone from the rather maritime West Siberian to the continental East Siberian Arctic climate, which is characteristic for Oyogos Yar.

The general atmospheric circulation patterns are dominated by temperature induced pressure areas (Endlicher, 2000; Shahgedanova, 2002). In response to the strong radiative cooling of the earth surface, a stable high pressure area (Siberian High) develops in winter over Central Siberia, extended to the Northeast Siberian lowlands, and accompanied by a lower pressure over the Arctic Ocean. In summer, conversely, high temperatures and insulation result in low pressure areas over Eastern Siberia, whereas a high pressure area develops over the cold Arctic Ocean. Spring and autumn are characterized by transition states between winter and summer circulation.

The mean annual precipitation is relatively low, reaching close to sea level about 250 mm at Oyogos Yar and 300 mm at Severnaya Zemlya (Figure 1.4). The annual precipitation pattern in the study areas is related to the seasonal pattern of cyclones and anticyclones. Therefore, the precipitation is particularly low in winter. Precipitation maxima occur in summer and autumn. They are connected to the higher moisture content of the air due to the higher temperatures, and to increased cyclonic activity.

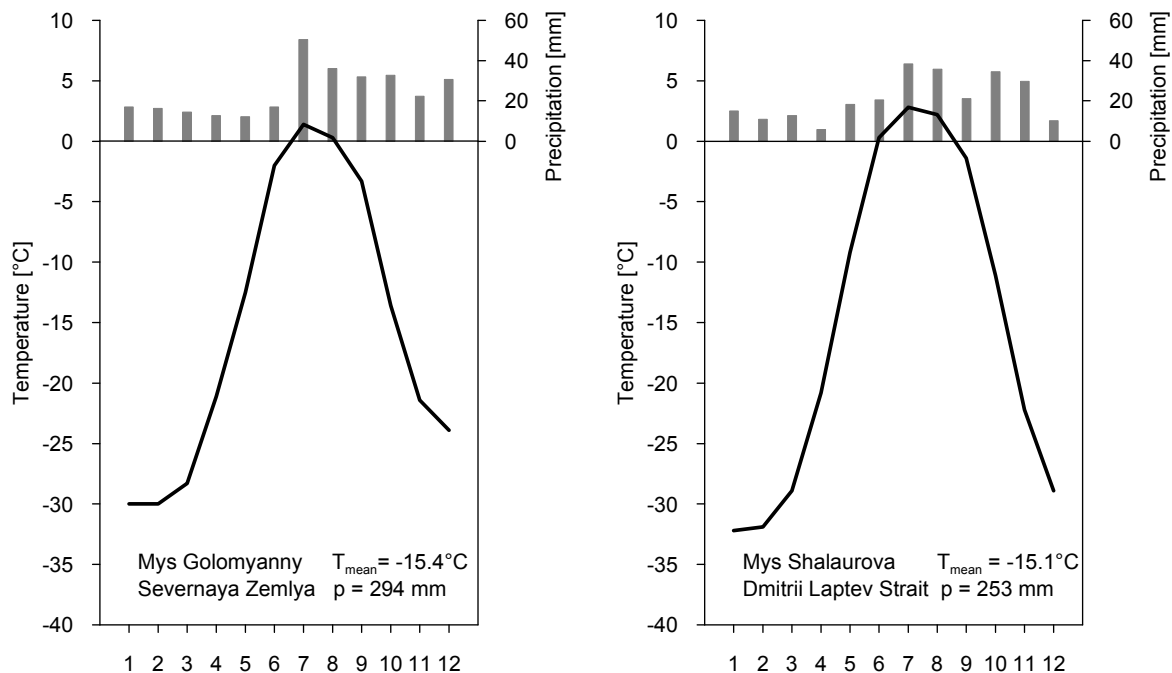


Figure 1.4: Climate diagrams for the meteorological stations Mys Golomyanny (Severnaya Zemlya) and Mys Shalaurova at Bol'shoy Lyakhovskiy Island, the closest meteorological station to Oyogos Yar (Dmitrii Laptev Strait). The data cover the period 1984-1994 and are from Rivas-Martínez and Rivas-Saenz (1996-2009).

1.4 Thesis outline

This thesis is divided into an introduction providing background information, three main chapters, a synthesis and an appendix. The three main chapters and the appendix, subdivided in three parts, consist of original research papers, which have been designed for publication in international peer-reviewed journals. While two papers have already been published, another two publications are currently resubmitted and two manuscripts are presented here as final drafts for submission (Table 1.2).

Table 1.2: Overview of publications presented within this thesis.

Chapters	Publication
Chapter 2	<u>Opel T</u> , Fritzsche D, Meyer H, Schütt R, Weiler K, Ruth U, Wilhelms F, Fischer H. 2009b. 115 year ice-core data from Akademii Nauk ice cap, Severnaya Zemlya: high-resolution record of Eurasian Arctic climate change. <i>Journal of Glaciology</i> 55(189), 21-31.
Chapter 3	<u>Opel T</u> , Fritzsche D, Meyer H, Schütt R, Ruth U, Wilhelms F, Fischer H. 2009. Late Holocene climate change in the Central Russian Arctic – evidence from Akademii Nauk ice core (Severnaya Zemlya). In preparation for submission to <i>Quaternary Science Reviews</i> .
Chapter 4	<u>Opel T</u> , Dereviagin AYu, Meyer H, Schirrmeister L, Wetterich S. 2009a. Paleoclimatic information from stable water isotopes of Holocene ice wedges at the Dmitrii Laptev Strait (Northeast Siberia). <i>Permafrost and Periglacial Processes</i> . Resubmitted after minor revisions.
Appendix I	Fritzsche D, Schütt R, Meyer H, Miller H, Wilhelms F, <u>Opel T</u> , Savatyugin LM. 2005. A 275 year ice core record from Akademii Nauk ice cap, Severnaya Zemlya, Russian Arctic. <i>Annals of Glaciology</i> 42, 361-366.
Appendix II	Meyer H, Schirrmeister L, Yoshikawa K, <u>Opel T</u> , Hubberten H-W, Brown J. 2009. Permafrost evidence for a Younger Dryas cold event in northern Alaska. In preparation for submission to <i>Nature</i> .
Appendix III	Blinov A, Alfirmov V, Beer J, Gilichinsky D, Schirrmeister L, Kholodov A, Nikolskiy P, <u>Opel T</u> , Tihomirov D, Wetterich S. 2009. $^{36}\text{Cl}/\text{Cl}$ ratio in ground ice of East Siberia and its application for chronometry. <i>Geochemistry, Geophysics, Geosystems (G³)</i> . Resubmitted after revisions.

Chapter 2 examines the paleoclimatic significance of proxy data (covering 115 years) of the Akademii Nauk ice core based on comparisons with meteorological and other paleoclimatic data from the Eurasian sub-Arctic and Arctic (Opel et al., 2009b). The long-term paleoclimatic records of Akademii Nauk ice core in relation

to other Arctic climate records are discussed in terms of Late Holocene climate and environmental change in Chapter 3 (Opel et al., in preparation). Chapter 4 deals with high-resolution stable-isotope profiles from Late Holocene ice wedges in Northeast Siberia and their use as paleoclimate archives (Opel et al. 2009a, resubmitted after minor revisions). Appendix I introduces the methods applied to the analysis of the Akademii Nauk ice core and presents a first overview of paleoclimatic results (Fritzsche et al., 2005). Appendix II deals with the first ice-wedge evidence of the Younger Dryas cold event, highlighting the potential of ice wedges as paleoclimate archive (Meyer et al., in preparation c). First results of a recently developed geochronological method for the age determination of ground ice are discussed in Appendix III (Blinov et al., resubmitted after revisions). The synthesis (Chapter 5) summarizes and discusses the main results and the implications of the individual publications as well as provides an outlook on further paleoclimatic research based on glacier and ground ice in the Russian Arctic. Owing to the structure of the individual stand-alone articles, overlapping sections and repetitive statements may occur within the three main chapters and the appendix.

1.5 The author's contribution to the individual papers

Paper 1 (Chapter 2)

I designed the study, reviewed the relevant literature, analyzed and interpreted the data, and wrote the entire manuscript. The co-authors participated in the laboratory work, contributed data and/or critically reviewed and discussed earlier drafts of the manuscript. Diedrich Fritzsche advised me in the whole process.

Paper 2 (Chapter 3)

I reviewed the relevant literature, analyzed and interpreted the data, and wrote the entire manuscript. Diedrich Fritzsche and I jointly developed the core chronology. All co-authors were involved in the laboratory work and/or contributed data. All co-authors critically reviewed and discussed interpretation and earlier versions of the manuscript, and Diedrich Fritzsche supervised the whole process.

Paper 3 (Chapter 4)

I did the entire fieldwork together with Alexander Dereviagin within the scope of the joint Russian-German expedition “Lena – New Siberian Islands” 2007 (Dereviagin and Opel, 2009). I designed the study, prepared the relevant literature review, analyzed and interpreted the data and drafted the manuscript. All authors were involved in the field and/or laboratory work and critically reviewed and discussed earlier versions of the manuscript. Hanno Meyer advised me in the whole process.

Paper 4 (Appendix I)

This paper was coordinated and drafted by Diedrich Fritzsche. I contributed to laboratory work, data interpretation, internal review and writing of the final manuscript.

Paper 5 (Appendix II)

This study was designed and coordinated by Hanno Meyer, who conducted the laboratory work and drafted the manuscript. I was involved in data interpretation, internal reviews and writing of the final manuscript.

Paper 6 (Appendix III)

Alexander Blinov led the overall effort and drafted the manuscript. As a member of the German INTAS project team, I was involved in the fieldwork, the data interpretation and in writing the manuscript.

2 115 year ice-core data from Akademii Nauk ice cap, Severnaya Zemlya: high-resolution record of Eurasian Arctic climate change

Thomas Opel^{1,2}, Diedrich Fritzsche¹, Hanno Meyer¹, Rainer Schütt¹, Karin Weiler^{3,4}, Urs Ruth³, Frank Wilhelms³, Hubertus Fischer^{3,4}

¹Alfred Wegener Institute for Polar and Marine Research, PO Box 600149, D-14401 Potsdam, Germany

²Department of Geography, Humboldt-Universität zu Berlin, Unter den Linden 6, D-10099 Berlin, Germany

³Alfred Wegener Institute for Polar and Marine Research, PO Box 120161, D-27515 Bremerhaven, Germany

⁴Climate and Environmental Physics, Physics Institute, University of Bern, Sidlerstrasse 5, CH-3012 Bern, Switzerland

Journal of Glaciology 55(189), 21-31.

Abstract

From 1999 to 2001 a 724m deep ice core was drilled on Akademii Nauk ice cap, Severnaya Zemlya, to gain high-resolution proxy data from the central Russian Arctic. Despite strong summertime meltwater percolation, this ice core provides valuable information on the regional climate and environmental history. We present data of stable water isotopes, melt-layer content and major ions from the uppermost 57m of this core, covering the period 1883-1998. Dating was achieved by counting seasonal isotopic cycles and using reference horizons. Multi-annual $\delta^{18}\text{O}$ values reflect Eurasian sub-Arctic and Arctic surface air-temperature variations. We found strong correlations to instrumental temperature data from some stations (e.g. $r = 0.62$ for Vardø, northern Norway). The $\delta^{18}\text{O}$ values show pronounced 20th-century temperature changes, with a strong rise about 1920 and the absolute temperature maximum in the 1930s. A recent decrease in the deuterium-excess time series indicates an increasing role of the Kara Sea as a regional moisture source. From the multi-annual ion variations we deduced decreasing sea-salt aerosol trends in the 20th century, as reflected by sodium and

chloride, whereas sulphate and nitrate are strongly affected by anthropogenic pollution.

2.1 Introduction

Ice cores are well known as one of the best archives for providing information on palaeoclimatic and palaeoenvironmental changes. These data are very valuable for climate research, especially for regions or time periods with only few meteorological observations. For the Arctic, ice cores from the dry snow zone of the Greenland ice sheet contribute data of more than 100 000 years (e.g. North Greenland Ice Core Project (NorthGRIP) members, 2004). However, for a more comprehensive view on the climate changes on a more regional scale and over shorter timescales, more data from Arctic regions outside Greenland are needed. Therefore, in the Eurasian Arctic several ice cores from ice caps on Svalbard (Isaksson et al., 2001; Watanabe et al., 2001) and on Franz Josef Land (FJL) (Henderson, 2002) have been drilled and analysed recently. Ice caps in the Eurasian Arctic are relatively small and have a relatively low altitude compared with the Greenland ice sheet as well as with Canadian Arctic ice caps. Moreover, they have higher accumulation rates. Thus, they mostly contain records of only several hundred years. Additionally, they are characterized by summer surface melting and infiltration processes, which alter these ice-core records further (e.g. Koerner, 1997). Nevertheless, the small Arctic ice caps contain valuable palaeoclimatic and palaeoenvironmental records (e.g. Henderson, 2002; Isaksson et al., 2005b).

The easternmost considerable ice caps of the Arctic exist on the Severnaya Zemlya (SZ) archipelago, located in the central Russian Arctic between the Kara Sea in the west and the Laptev Sea in the east (Figure 2.1). SZ is vulnerable to climatic and environmental changes due to its position in the high latitudes and in the transition zone from the Atlantic-influenced western Siberian to continental eastern Siberian Arctic climate. In the last few decades, several ice cores have been drilled on SZ ice caps (see section 2.2). They were analysed only at a relatively low resolution, resulting in an uncertain maximum time resolution and questionable timescales. To improve the resolution of palaeoclimatic data, to check the previous timescales and to evaluate the alteration of the original atmospheric deposition by melting and infiltration, a new 724 m long surface-to-

bedrock core was drilled on Akademii Nauk (AN) ice cap from 1999 to 2001 at 80831' N, 94849' E (Fritzsche et al., 2002).

In this paper, we present high-resolution data of stable water isotopes, melt-layer content as well as major ions from the uppermost 57 m of this core, covering the time period 1883-1998. The uppermost 57 m section was chosen because this is the only section with high-resolution ion data. We discuss the palaeoclimatic significance of the ice-core proxies by comparing them with meteorological and palaeoclimatic data from the Eurasian sub-Arctic and Arctic and the deduced climatic features.

2.2 Previous Severnaya Zemlya ice cores

Between 1978 and 1988, scientists from the former Soviet Union drilled eight ice cores on SZ (seven on Vavilov ice cap and one on AN ice cap) (Kotlyakov et al., 2004). Six of these cores were sampled and analysed, but only at low resolution (about 2 m and less). Some of these data are available, provided by the database 'Deep Drilling of Glaciers in Eurasian Arctic' (DDGA) at <http://www.pangaea.de/search?q=ddga>.

Dating of these cores was achieved by a combination of annual-layer counting (based on variations of optical density, electrical conductivity and non-specified stratigraphic features), ice-flow modelling and wiggle matching with icecore records from Greenland and Antarctica. These methods led to different age models for the SZ ice cores. For the near-bottom ice layers of AN ice cap as well as of Vavilov ice cap, ages between 10 and 40 kyr were published, but due to uncertainties in the applied dating methods, these ages seem to be distinctly overestimated (Kotlyakov et al., 2004, and references therein). However, according to Koerner and Fisher (2002), AN ice cap, as the thickest and coldest ice cap on SZ, is the only one in the Eurasian Arctic with the potential for a Late Pleistocene age.

Stable-isotope data ($\delta^{18}\text{O}$, δD) from the previous ice cores revealed a marked warming trend for the last 150 years (Tarussov, 1992; Kotlyakov et al., 2004). The older climatic implications, though, are questionable due to the aforementioned inadequate dating methods.

2.3 Study Area

2.3.1 Climate conditions on Severnaya Zemlya

In general, the climate of SZ is typical for the High Arctic. The large-scale atmospheric circulation is dominated by the low-pressure area over the Barents Sea and Kara Sea and by the high-pressure areas over Siberia and the Arctic Ocean (Bolshiyarov and Makeev, 1995; Alexandrov et al., 2000). During wintertime, anticyclone circulation connected with the Siberian and Arctic highs dominates, but cyclones coming from the Kara Sea reach the archipelago. In spring, the circulation shows winter characteristics, but with lower pressure gradients and cyclone activity. The summer is characterized by continually decreasing cyclone activity and the formation of a high-pressure area. In autumn, wintertime pressure fields start to develop and the cyclone activity increases to its annual maximum.

Meteorological measurements on SZ started only in 1930. Unfortunately, there are some data gaps in the 1930s and 1940s. Golomyanny station (Figure 2.1; World Meteorological Organization (WMO) number 20087), located on a small island at the western tip of SZ (7 m a.s.l.), has an annual mean surface air temperature (SAT) of -14.7°C for the period 1951-80 (Alexandrov et al., 2000). After a SAT maximum in the 1950s, Golomyanny data show a cooler period until 1980 and a warming trend since 1990, though without reaching the values of the 1950s (data from Polyakov et al., 2003b, <http://www.frontier.iarc.uaf.edu/~igor/research/data/airtempres.php>).

Annual mean precipitation is 186 mm at Golomyanny station (Alexandrov et al., 2000), whereas the ice caps receive about 400 mm distributed throughout the year, with maxima in summer and autumn (Bolshiyarov and Makeev, 1995). According to the general circulation pattern, Bolshiyarov and Makeev (1995) demonstrated that the main part of precipitation on Vavilov ice cap occurs in connection with southerly and southwesterly winds, caused by northeastward movement of moisture-bearing cyclones over the Kara Sea. The autumn precipitation maximum is connected to the increase in cyclonic activity: depressions causing much precipitation move from the North Atlantic. Cyclones, formed over northern Europe and western Siberia, are responsible for the summer precipitation maximum. An air-mass transport mainly from Asia, northern Eurasia,

Europe and the Atlantic Ocean, as identified by trajectory analysis for spring (Vinogradova and Egorov, 1996) and summer (Vinogradova and Ponomareva, 1999), confirms these findings. We assume a similar pattern and origin of precipitation for the nearby AN ice cap, situated about 150 km north of Vavilov ice cap.

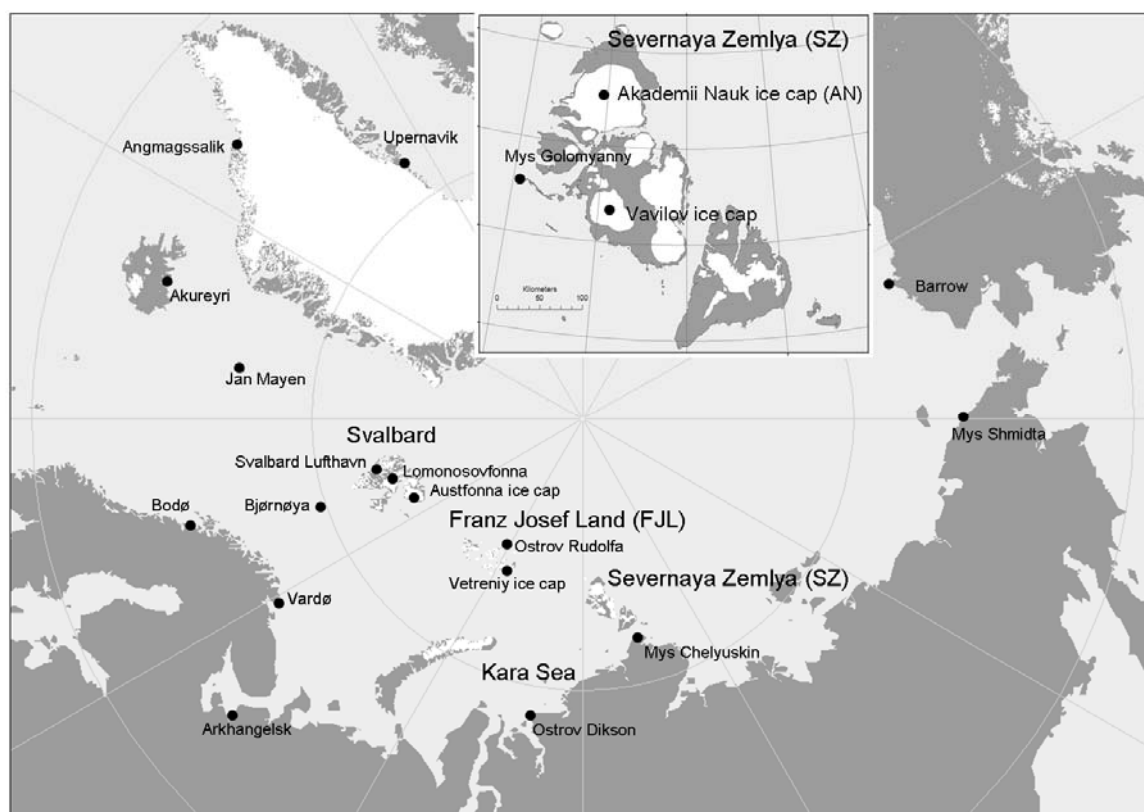


Figure 2.1: Map of the Arctic. Inset shows a detailed map of Severnaya Zemlya (SZ) archipelago. All locations referred to in the text are labelled.

2.3.2 Drilling-site characterization and melting processes

Covering an area of 5575 km², the dome-shaped AN ice cap is the largest in the whole Russian Arctic, reaching a maximum elevation of about 750 m a.s.l. (Dowdeswell et al., 2002). To avoid a disturbed core stratigraphy, the drilling site was chosen in an area with flat subglacial topography and low horizontal ice-flow velocity (Fritzsche et al., 2002). Although situated near the summit, the drilling site is located in the percolation zone and therefore, like almost all Arctic ice caps outside interior Greenland, is affected by infiltration of meltwater during summer. We assume that melting and infiltration processes occur in almost every summer due to temperatures above 0°C and/or high insolation.

An automatic weather station (AWS) was run at the drilling site between May 1999 and May 2000, with a data gap of 2 months (during February and April 2000) due to a breakdown in power supply (Kuhn, 2000). The AWS data give the opportunity to characterize the temperature conditions near the drilling point for the 1999 summer season. Figure 2.2 illustrates daily mean values of air temperature (2.5 m above snow cover at the start in May 1999), snow height (calculated from the distance between sensor and snow cover, relative to the start) and snow temperature (0.5 m below snow cover at the start). Clearly visible are temperatures above 0°C in July and August, causing snowmelt and decrease of snow height. Strong increases in snow temperature within a few days, corresponding with decreasing snow height, indicate infiltration events. The meltwater pulses connected with latent-heat flow reach depths of 1 m (height difference between snow height and snow temperature logger) as a minimum, at least in fresh snow. At the end of August, almost all the snow that had fallen since May had sintered and melted, before new snow accumulation began. The maximum percolation depth on AN ice cap is uncertain. However, percolation deeper than two to three annual layers seems unlikely, since the ice layers, formed by refrozen meltwater, should be barriers to further infiltration. For the Lomonosovfonna ice core, extensive study by Pohjola et al. (2002b) showed that the infiltrated meltwater typically refreezes within the recent annual layer.

The annual mean air temperature for May 1999 - April 2000 was calculated as -15.7°C (Kuhn, 2000). Compared with the measured 10m depth temperature of -10.2°C in April 2000, this indicates latent-heat flow of infiltrating meltwater, as mentioned above. From a comparison of AWS and Golomyanny SAT data, we calculated a mean temperature gradient of -0.5°C per 100 m altitude, with lowest values in summer and highest values in autumn as a result of sea-level freezing processes with release of latent heat.

2.4 Methods

The AN ice core was processed and sampled in the cold laboratory of the Alfred Wegener Institute for Polar and Marine Research in Bremerhaven. At first, electrical conductivity and density were determined in 5 mm resolution by using dielectrical profiling and γ -absorption techniques (Wilhelms, 2000). Thereafter, two core-axis-parallel slices were cut. Samples for stable water-isotope measurements

were taken from the first 11 mm thick slice at a very high resolution of 25 mm. To determine $\delta^{18}\text{O}$ and δD we used a Finnigan-MAT Delta S mass spectrometer with an analytical precision of better than $\pm 0.1\text{‰}$ for $\delta^{18}\text{O}$ and $\pm 0.8\text{‰}$ for δD (Meyer et al., 2000). In total, we analysed 2248 samples for the 57 m considered here.

The second 30 mm thick slice was polished and scanned with a line-scan camera (Svensson et al., 2005) for stratigraphical analysis and identification of melt layers. Subsequently, these slices were used for glaciochemical studies. For the uppermost 53 m, discrete samples were taken continuously under clean conditions at a resolution of 60 mm (for details of sampling see Weiler et al., 2005). For the remaining 4 m of the considered core section, we took discrete samples at a resolution of about 30 mm by using a melting device for continuous flow analysis (CFA) coupled with an autosampler system, which was also used for the analysis of the ice cores from Greenland (NorthGRIP) and Antarctica (European Project for Ice Coring in Antarctica (EPICA)) (for details see Ruth et al., 2004). A Dionex IC20 ion chromatograph was used to analyse the melted samples for anions (methanesulphonate (MSA^-), Cl^- , NO_3^- , SO_4^{2-}) and cations (Na^+ , NH_4^+ , Mg^{2+} , Ca^{2+}) (for details see Weiler et al., 2005).

2.5 Dating approach and age model

We dated the presented ice-core section and determined the annual layer thickness by identifying different reference horizons as well as by counting seasonal isotopic cycles. As reference horizon, we used the 1963 radioactivity peak caused by the fallout from nuclear bomb tests, as determined by ^{137}Cs measurements (Fritzsche et al., 2002; Pinglot et al., 2003). Additionally, we interpreted two peaks in electrical conductivity as well as sulphate as deposits of the volcanic eruptions of Bezymianny, Kamchatka, in 1956 (Weiler et al., 2005) and of Katmai, Alaska, in 1912 (section 2.6.3). Seasonal signals of $\delta^{18}\text{O}$, δD and deuterium excess d ($d = \delta\text{D} - 8 \delta^{18}\text{O}$) are detectable in AN ice-core isotopic data, even though altered from the originally deposited signal in the snowpack and smoothed due to melting and infiltration processes. The counted annual marks ($\delta^{18}\text{O}$ winter minima and corresponding d maxima) confirm the reference horizons and yield an age of 116 years at annual resolution for the 57 m core section studied. As a result of the high-resolution sampling, each year is represented by a mean of 20 samples (min. 9, max. 44). However, the possibility of substantial

runoff or strong modification of the original isotopic signature has to be taken into account. This could lead to complete smoothing of annual cycles or creation of additional peaks, which could possibly be counted as additional years.

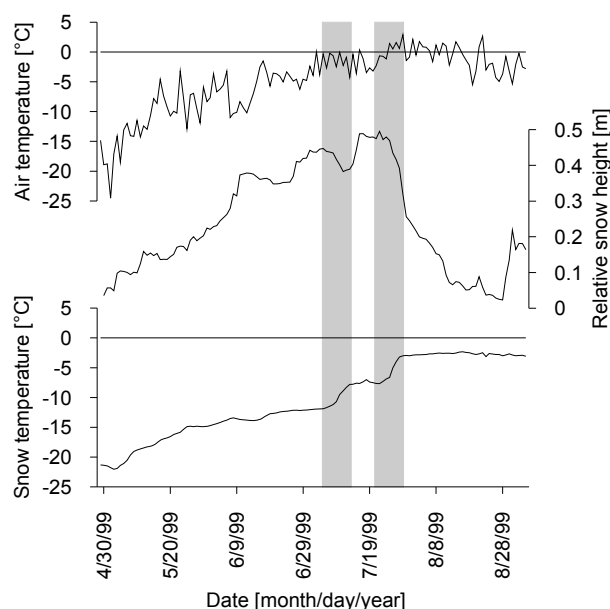


Figure 2.2: Data from an AWS near the drilling site for time period May-August 1999: air temperature (2.5 m above snow cover at the start in May 1999), relative snow height (relative to start in May 1999) and snow temperature (0.5 m below snow cover at start in May 1999). The horizontal black lines indicate 0°C. Grey shaded areas indicate infiltration events with decreasing snow height and increasing snow temperature.

The resulting depth-age relationship and annual layer thickness are displayed in Figure 2.3. The annual layer thickness shows distinct variations on different scales. The mean value for the period 1883-1998 is 0.41 m w.e. In general, the mean annual layer thickness shows lower values (0.36 m w.e.) before and higher values (0.44 m w.e.) after 1935. A similar increase of annual layer thickness in the second half of the 20th century also occurred on Lomonossovfonna, Svalbard (Pohjola et al., 2002a).

As another approach for dating the upper AN ice-core section, Weiler et al. (2005) counted Na⁺ peaks as assumed annual markers. They determined 94 years in the 0-53 m core section, 15 years less than by the abovementioned dating method for the same depth interval. Deviations between the two dating approaches occur over the whole core section, but mainly in the 1950s and 1920s, probably caused by strong melting.

Evidence for the reliability of our age model is given by the coincidence of a strong rise at about 1920 in both the $\delta^{18}\text{O}$ and SAT data (as shown in Figure 2.5 below), which could be used as additional reference horizon (Watanabe et al., 2001). This leads to the conclusion that the chemical profile of the AN ice core is modified more by infiltration processes than the isotopic record, as reported also for a Svalbard ice core from Lomonosovfonna (Pohjola et al., 2002b). Therefore, counting seasonal isotopic cycles and cross-checking with reference layers seem to be more promising for dating the AN ice core than counting chemical signals. In the following discussion, we use the dating shown in Figure 2.3 and estimate the dating accuracy to be better than ± 3 years after 1920 and up to ± 5 years at the end of the 19th century.

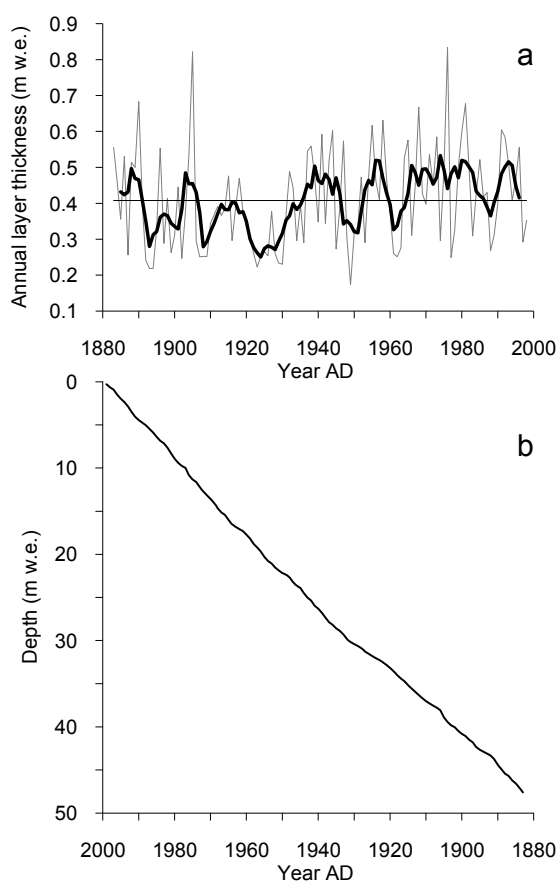


Figure 2.3: (a) Thickness of the thinned (not decompressed) annual layers (grey line: annual values; thick black line: 5 year running mean (5yrm) values; horizontal line: long-term mean) and (b) depth-age relationship as result of the age model.

Fritzsche et al. (2005) found that AN ice cap was not in dynamic steady state, but had been growing until recent times. They calculated the age of the near-bottom ice of the AN ice core at approximately 2500 years. Therefore, it is distinctly

younger than assumed before drilling this ice core. Most likely, the AN ice cap had disappeared almost completely during the Holocene thermal maximum and started growing again to the present state thereafter.

2.6 Results, climatic implications and discussion

2.6.1 Stable water-isotope ratios $\delta^{18}\text{O}$ and δD

Due to their dependence on condensation temperatures, stable water-isotope ratios $\delta^{18}\text{O}$ and δD in precipitation are commonly accepted as valuable proxy for local- to regional-scale temperatures in high polar latitudes. For the AN ice core, the relationship between all $\delta^{18}\text{O}$ and δD values in the presented core section is $\delta\text{D} = 7.46 \delta^{18}\text{O} - 0.11$ ($R^2 = 0.98$, $n = 2248$; Figure 2.4). Considering only the annual mean values, derived by averaging all isotope values between the defined annual marks, the isotopic relationship is calculated as $\delta\text{D} = 7.55 \delta^{18}\text{O} + 1.84$ ($R^2 = 0.99$, $n = 116$; Figure 2.4). Both relationships are close together and can be interpreted as a local meteoric waterline (LMWL). Additionally, they differ only slightly from the global meteoric waterline (GMWL), which is defined theoretically as $\delta\text{D} = 8 \delta^{18}\text{O} + 10$ (Craig, 1961) and calculated on a global scale as $\delta\text{D} = 8.17 \delta^{18}\text{O} + 10.35$ (Rozanski et al., 1993). From this, it follows that the mean isotopic composition of the AN ice core is not affected by considerable changes owing to evaporation. Therefore, the AN ice-core stable-isotope data seem to be suitable for palaeoclimate studies. Statistical descriptions of the stable water-isotope data (single values and annual mean values) are given in Table 2.1.

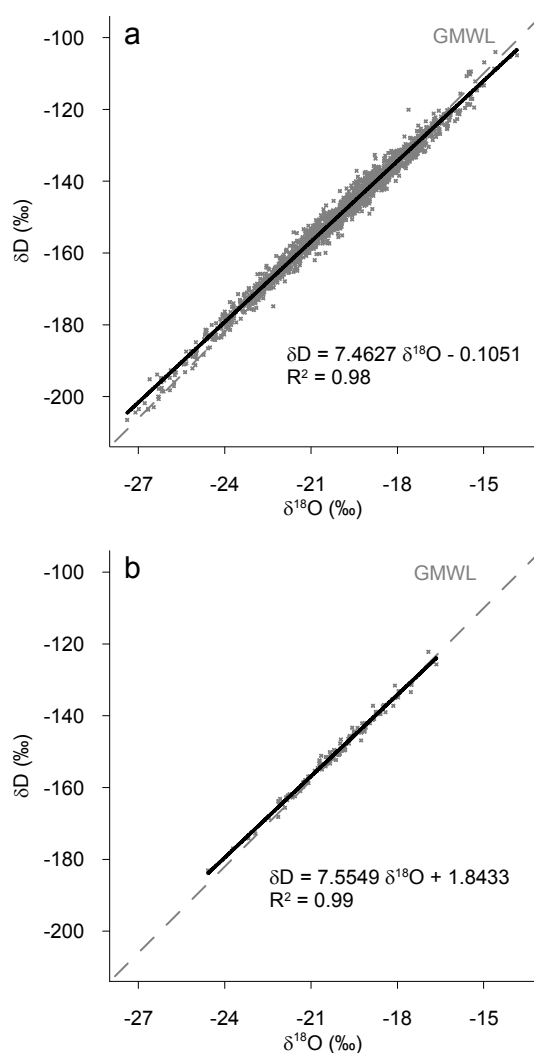


Figure 2.4: $\delta^{18}\text{O}$ - δD diagram for single values (a) and annual values (b) of the AN ice core. Grey dots represent single values, the thick black lines represent the regression fit and the dashed grey line represents the GMWL.

Table 2.1: Statistical descriptions of AN ice-core stable water-isotope data

	$\delta^{18}\text{O}$ [‰]		δD [‰]		d [‰]	
	Single values	Annual mean values	Single values	Annual mean values	Single values	Annual mean values
n	2248	116	2248	116	2248	116
Max	-13.8	-16.6	-104.0	-122.2	20.8	14.0
Min	-27.4	-24.6	-206.5	-183.1	2.7	6.8
Range	13.6	7.9	102.5	60.9	18.1	7.2
Mean	-20.1	-20.2	-150.0	-150.7	10.7	10.8
Median	-20.0	-20.2	-149.1	-150.8	10.7	10.9
Variance	4.0	2.0	225.8	114.6	4.9	2.1
Standard deviation	2.0	1.4	15.0	10.7	2.2	1.4

For palaeoclimatic consideration of stable-isotope data, we focused on $\delta^{18}\text{O}$, which is more common in Arctic ice-core studies and therefore suitable for comparisons. To evaluate the palaeoclimatic significance of AN $\delta^{18}\text{O}$ data, we compared them with instrumental as well as composited SAT time series and other ice-core data. For the calculation of correlation coefficients the time series were detrended by removing the linear trends. We used annual mean values and 5 year running mean (5yrm) values of AN $\delta^{18}\text{O}$ and SAT data, since the effects of melting, infiltration and refreezing processes on the stable-isotope data should be reduced or even negligible when smoothing the dataset over 5 years.

We did not find any good agreement between AN $\delta^{18}\text{O}$ data and SAT time series from the nearest meteorological station, Golomyanny ($r_{5\text{yrm}} = 0.27$; data from Polyakov et al., 2003b). Since Golomyanny is situated on a small island only 7 m a.s.l., we assume that its SAT is controlled mainly by the local occurrence of sea ice, especially in the summer and autumn seasons. It therefore represents a very local climate. In contrast, temperature conditions at the AN ice-cap summit, as well as at the precipitation condensation level, are relatively independent of the local sea-ice occurrence at Golomyanny.

Since there are no Central Russian Arctic SAT time series reaching back to the 19th century, we chose additional stations, mainly from the Atlantic and Eurasian sub-Arctic, with respect to their spatial vicinity on the one hand and temporal extension of the time series on the other. We present the correlations for some of these SAT time series in Table 2.2. The best accordance between AN $\delta^{18}\text{O}$ and instrumental SAT time series (1883-1998) was found for Vardø ($r_{5\text{yrm}} = 0.62$) and Arkhangelsk ($r_{5\text{yrm}} = 0.61$) stations, located at the Barents Sea and White Sea coasts, respectively (Figure 2.5; data from Climatic Research Unit (CRU), Norwich, UK; Brohan et al., 2006). Compared with Golomyanny, their SATs are not (or in the case of Arkhangelsk to a much lesser extent) influenced by the occurrence of sea ice. The good correlations and similarities of the time series reveal again the influence of the Atlantic Ocean via the Barents Sea and Kara Sea on SZ region SAT conditions. Additionally, we found a strong correlation ($r_{5\text{yrm}} = 0.72$; Figure 2.5) with the composite Arctic (north of 62° N) SAT anomalies time series of Polyakov et al. (2003b). However, one should note that these strong correlations are mainly due to common multi-annual variability (Table 2.2).

The strong correlations to instrumental and composite SAT data show that AN $\delta^{18}\text{O}$ data are representative for SAT changes, not only for the central Russian Arctic, but also for the western and possibly whole Eurasian Arctic and sub-Arctic. Since there are no meteorological data from the central Russian Arctic and only a few time series in the Eurasian Arctic spanning more than 100 years, our high-resolution AN $\delta^{18}\text{O}$ data are very valuable for further palaeoclimatic studies in the Eurasian Arctic.

Table 2.2: Correlation coefficients between the detrended time series of AN $\delta^{18}\text{O}$ and of selected sub-Arctic and Arctic SAT (r_y for annual mean values, $r_{5\text{yrm}}$ for 5 year running mean values) in the given time periods. The reduced degrees of freedom due to autocorrelation were taken into account for the calculation of the levels of significance. The WMO stations are sorted from east to west (see Figure 2.1).

WMO station	WMO number	time period	r_y	$r_{5\text{yrm}}$
Mys Shmidta ¹	25173	1933-1998	0.20 ⁺	0.66 ⁺⁺⁺
Mys Chelyuskin ¹	20292	1933-1998	0.21 ⁺	0.40
Mys Golomyanny ¹	20087	1946-1998 [*]	0.02	0.27
Ostrov Dikson ¹	20674	1917-1998	0.16 ⁺	0.32
Ostrov Rudolfa ¹	20049	1948-1995 [*]	0.10	0.42
Arkhangelsk ²	22550	1883-1998	0.34 ⁺⁺⁺	0.61 ⁺⁺
Vardø ²	01098	1883-1998	0.35 ⁺⁺⁺	0.62 ⁺⁺⁺
Svalbard Lufthavn ²	01008	1912-1998	0.33 ⁺⁺⁺	0.56 ⁺
Bjørnøya ²	01028	1946-1998 [*]	0.12	0.43
Bodø ²	01152	1883-1998	0.21 ⁺⁺	0.53 ⁺⁺
Jan Mayen ²	01001	1921-1998	-0.04	0.27
Akureyri ¹	04063	1883-1998	0.27 ⁺⁺	0.54 ⁺
Angmagssalik ¹	04360	1895-1998	0.14	0.43
Upernavik ¹	04210	1883-1998	0.13	0.36
Barrow ¹	70026	1893-1998	0.14	0.41 ⁺
Arctic ¹	-	1883-1998	0.44 ⁺⁺⁺	0.72 ⁺⁺

¹ Data source: Polyakov et al., 2003b.

² Data source: CRU Norwich.

^{*} Time series were shortened due to data gaps.

⁺ Correlation coefficient statistically significant at the level of $p=0.1$

⁺⁺ Correlation coefficient statistically significant at the level of $p=0.05$.

⁺⁺⁺ Correlation coefficient statistically significant at the level of $p=0.01$.

The AN $\delta^{18}\text{O}$ time series shows a distinct increasing trend with pronounced changes since 1883. Starting from a low level of about -22‰, $\delta^{18}\text{O}$ values

increased to values of -18‰ at about 1920 and 1940. From 1950 to the 1980s they oscillated about -20‰ and rose again afterwards. Besides the strong warming in the first two decades of the 20th century the most prominent feature of the AN $\delta^{18}\text{O}$ time series is the double-peaked SAT maximum between 1920 and 1940. These values were not reached again until the end of our record in the 1990s. This agrees with the instrumental sub-Arctic and Arctic SAT data (Figure 2.5). The double-peak structure of this SAT maximum seems to be a specific feature of the Eurasian Arctic, since the 1920 peak is not visible in other SAT time series (e.g. Bodø or Akureyri). Based on instrumental data, Przybylak (2007) stated that for the whole Arctic the decade 1936-45 and the year 1938 were the warmest in the 20th century. Only the period 1995-2005 and the year 2005, respectively, reached and exceeded these values. This SAT pattern shows the Arctic peculiarity compared with the whole Northern Hemisphere (NH), where the SAT maximum values at about 1940 have been exceeded since the end of the 1980s (Figure 2.5; data: <http://data.giss.nasa.gov/gistemp/taledata/NH.Ts.txt>).

AN $\delta^{18}\text{O}$ data show distinct similarities to the ice-core $\delta^{18}\text{O}$ time series from Austfonna ice cap, Svalbard, (Isaksson et al., 2005b) and Vetreniy ice cap, FJL, (Henderson, 2002) whereas the accordance to Lomonosovfonna (Isaksson et al., 2005b) is not as good. AN, Austfonna (750 m a.s.l.) and Vetreniy (500 m a.s.l.) ice caps are located at relatively low altitudes and are therefore more sensitive to SAT changes. In contrast, glaciers of higher elevation like Lomonosovfonna (1250 m a.s.l.) seem to reflect primarily free atmospheric climate signals (Isaksson et al., 2005b). The higher sensitivity of the lower-altitude ice caps is also visible in the broader range of $\delta^{18}\text{O}$ values (about 4‰ for AN and Austfonna for 5yr in the 20th century) compared with Lomonosovfonna (about 2‰). The range differences may also be influenced by different impacts of sea ice and of the dampening North Atlantic, as well as by the more frequent temperature inversions at the lower altitudes as reported for Austfonna compared with Lomonosovfonna (Isaksson et al., 2005b).

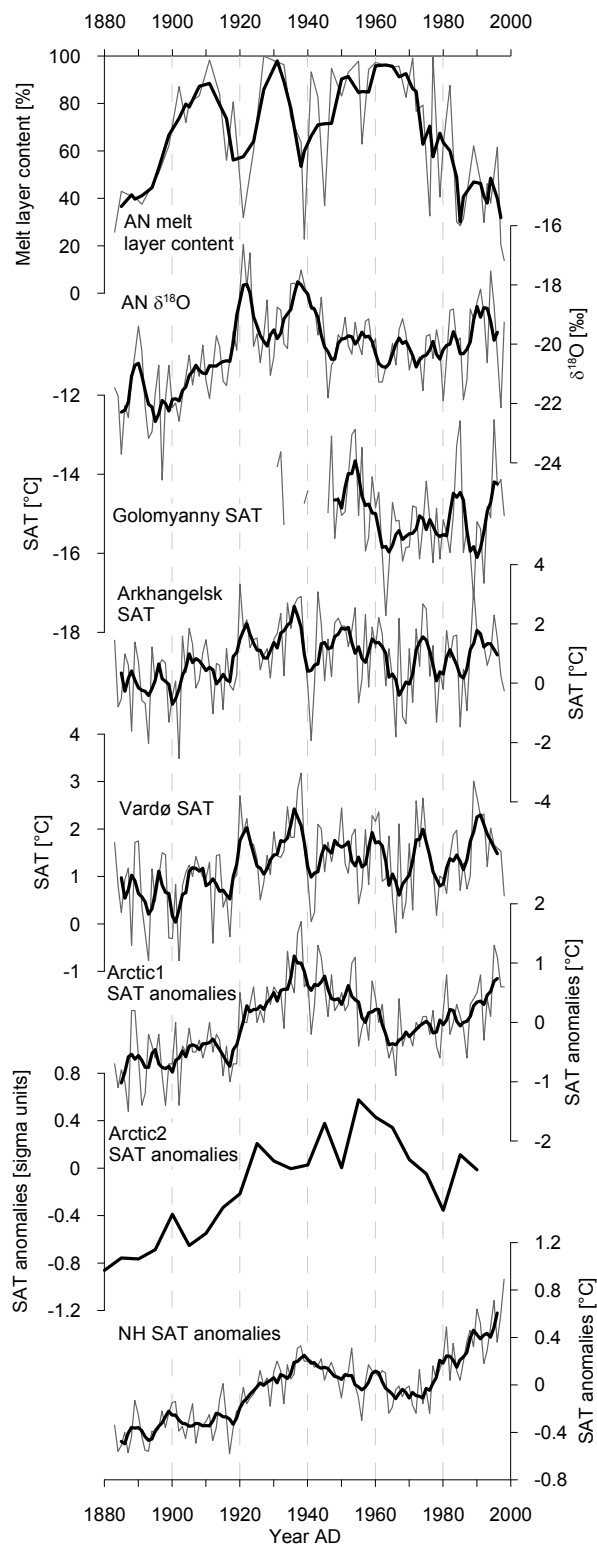


Figure 2.5: Time series of the AN melt-layer content, AN $\delta^{18}\text{O}$, sub-Arctic and Arctic SAT and NH SAT. The thin grey lines indicate annual mean values. The thick black lines represent 5yr values (for AN melt-layer content 1 and 3 m running mean values, respectively) except for Arctic2, where it represents 5 year mean values. Arctic1 displays the Arctic SAT anomalies (relative to 1961-90) dataset of Polyakov et al. (2003b), Arctic2 the reconstructed Arctic SAT anomalies (relative to 1901-60) of Overpeck et al. (1997).

In contrast to these Eurasian Arctic ice-core data, the accordance between AN $\delta^{18}\text{O}$ data and the often used proxy-deduced SAT time series of Overpeck et al. (1997) is less pronounced (Figure 2.5). This is probably caused by the predominance of Canadian and Alaskan Arctic proxy sites in this composite record, whereas just a few proxy records of the Eurasian Arctic are considered.

2.6.2 Deuterium excess

The second-order parameter deuterium excess d (Dansgaard, 1964) in precipitation depends largely on the evaporation conditions in the moisture source region, to a lesser degree on condensation temperatures but also on secondary kinetic fractionation processes. The main controlling factors are the relative air humidity and the sea-surface temperature (SST) and, to a lesser extent, wind speed during evaporation (Rozanski et al., 1993). Assuming no significant changes in the spatial distribution of the moisture source regions, variations of d can be interpreted in terms of changing SST and relative humidity conditions (e.g. Hoffmann et al., 2001).

The mean d values of the considered core section account for 10.7‰ for all single samples and 10.8‰ for the annual mean values, respectively (Table 1). These values are typical for precipitation in high-latitude coastal areas (Johnsen et al., 1989). Therefore, we assume an oceanic main moisture source, whereas substantial water recycling from the continents seems unlikely. However, the AN mean d value is slightly higher than the 9.5‰ for the period 1883-1990 in the Lomonosovfonna ice core (Divine et al., 2008), the only Arctic ice core outside of Greenland for which a study of d was performed so far. This points to different moisture generation and transport regimes, probably due to the more remote location of SZ compared with the much more Atlantic-influenced western Svalbard. In general, high (low) d values are caused by high (low) SST as well as by low (high) relative humidity during evaporation (Johnsen et al., 1989). However, on seasonal timescales d seems to be controlled mainly by the relative humidity. In the AN d record, high (low) d values in winter (summer) are connected with lower (higher) relative humidity in the moisture source region, outbalancing lower (higher) SSTs during that time. This pattern of opposite behaviour of $\delta^{18}\text{O}$ and d corresponds with the isotopic data of the Global Network of Isotopes in

Precipitation (e.g. Rozanski et al., 1993) and model calculations (Fröhlich et al., 2002).

Based on the assumption of nearly constant annual mean values of relative humidity in the moisture source region, multi-annual variations of d should be related mainly to SST changes (Hoffmann et al., 2001). The AN d time series shows a distinct decreasing trend over the 115 years considered. This is a reverse picture compared with $\delta^{18}\text{O}$ (Figure 2.6), corresponding with the findings in the seasonal cycles of d and $\delta^{18}\text{O}$. Only the strong $\delta^{18}\text{O}$ peak about 1920 shows no counterpart in d (see below). The highest d values (about 12‰) occurred about 1900 and the lowest (about 9‰) in the 1990s. A similar decreasing trend is visible in the ice cores from central Greenland (Hoffmann et al., 2001), but not in the Lomonosovfonna ice core (Divine et al., 2008), where an increasing d trend is visible for the period considered here.

The main feature of the AN d time series is the strong decrease since 1970, also detectable in the ice-core records from central Greenland (Hoffmann et al., 2001), but not in the Lomonosovfonna ice core, which shows an increase (Divine et al., 2008). Assuming the positive d -SST relationship both the general decreasing trend and the strong d decrease after 1970 in the AN d record would indicate corresponding SST decreases in the main moisture source region. However, no comparable cooling trends are visible in the SST time series of the North Atlantic (0-70° N) (Gray et al., 2004; data: <ftp://ftp.ncdc.noaa.gov/pub/data/paleo/treering/reconstructions/amo-gray2004.txt>), which is the supposed main moisture source for precipitation reaching AN ice cap (Figure 2.6), as well as in the NH SAT record (Figure 2.5). Opposed to the AN d record, the North Atlantic SST has increased strongly since 1970. Such an opposite behaviour is also detectable about 1940, where a distinct d minimum was accompanied by high SST values. This pattern indicates that in hemispherical warmer periods (e.g. about 1940 and since 1970; Figure 2.5) AN ice cap receives more precipitation from moisture evaporated at lower SSTs, for example due to a northward shift of the moisture source or a significant moisture contribution of a secondary regional source (Johnsen et al., 1989). Since most precipitation on SZ is caused by air masses moving from the south and southwest, the Kara Sea could be a regional moisture source (Figure 2.1) with its sea-ice cover as the main controlling factor for summer and autumn evaporation. The time series of Kara Sea August sea-ice extent

anomalies (Polyakov et al., 2003a; data: <http://www.frontier.iarc.uaf.edu/~igor/research/ice/icedata.php>) shows a pattern similar to AN d data ($r_{5\text{yrm}} = 0.51$ for detrended data, $p = 0.05$; Figure 2.6). A low sea-ice extent in the Kara Sea allows higher evaporation rates and leads to higher contribution of regional moisture to AN ice-cap precipitation. This results in lower d values due to the lower SST of the Kara Sea compared with the North Atlantic. In contrast, high sea-ice extent prevents a considerable regional moisture contribution, preserving the initially higher d values. The missing d counterpart of the 1920 $\delta^{18}\text{O}$ peak can also be explained with this approach. The first part of the strong early 20th century warming about 1920 occurred primarily in the winter season (Polyakov et al., 2003b). This did not lead to a substantial decrease in sea-ice extent in the Kara Sea and therefore not to a considerable regional moisture contribution and a decrease of d values. Since 1930 a warming of the non-winter season is perceptible, causing the absolute SAT maximum about 1938 (Polyakov et al., 2003b). This resulted in a corresponding decrease of sea-ice extent, leading to an amplified regional evaporation and, thus, a minimum in d .

Therefore, we assume the Kara Sea to be an important secondary moisture source region for the air masses reaching SZ, as well as the AN deuterium excess to be an indicator of temperature changes in the surrounding seas and the connected sea-ice extent changes. However, this is not the case for the d record of the Lomonosovfonna ice core, which can be interpreted as a proxy for the SST variability of the mid-latitude western North Atlantic (Divine et al., 2008).

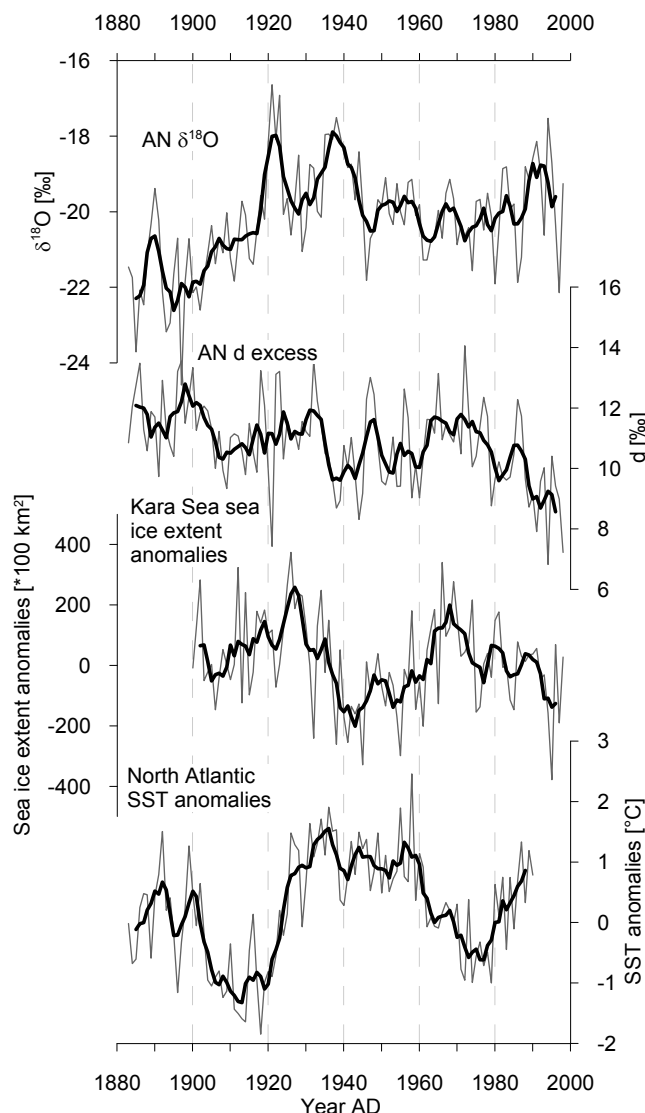


Figure 2.6: Time series of AN $\delta^{18}\text{O}$, AN d , Kara Sea August sea-ice anomalies (Polyakov et al., 2003a, computed against mean of the entire period) and North Atlantic SST anomalies (Gray et al., 2004). The thin grey lines indicate annual mean values; the thick black lines show 5yr.

2.6.3 Melt-layer content

The amount of melt layers in ice cores is a proxy for the summer warmth at the ice-cap surface (Koerner, 1977). We calculated the melt-layer content by the proportion of meltlayer ice per metre by weight. As melt layer we considered ice, which consists of firn, infiltrated by a visible content of meltwater, independent of the amount of meltwater. Summertime meltwater infiltration on AN ice cap is irregular, as shown by Fritzsche et al. (2005). Percolation deeper than the corresponding annual layer leading to the formation of superimposed melt features may occur, at least in the warmest summers (section 2.3.2). Consequently, as a

nearly annual resolution is not possible, we identified the melt-layer content per metre.

The melt-layer content in the AN ice core shows a strong increase at about the beginning of the 20th century, remains on a high level until about 1970, despite distinct variations, and exhibits a strong decrease in the most recent decades (Figure 2.5). The ice cores from Vetreniy ice cap (Henderson, 2002) and Austfonna ice cap (Watanabe and other, 2001) show similar melt-layer records, in contrast to the Lomonosovfonna melt-layer time series (Kekonen et al., 2005).

Whereas the first increase in the AN melt-layer record is also perceptible in a rise in the $\delta^{18}\text{O}$ time series, there are distinct differences between both proxies later on. Around the $\delta^{18}\text{O}$ -derived SAT maxima at about 1920 and 1940, as well as in the last decades, the melt-layer content shows sharp declines, whereas it exhibits higher values in the cooler 1950s and 1960s, indicating different seasonal temperature trends. For example, the strong warmings at about 1920 and 1940 occurred primarily in winter and autumn, which is supported by the studies of Polyakov et al. (2003b; see above) and of Henderson (2002) for the Vetreniy ice core. We did not find any correspondence between the melt-layer content and the Golomyanny summer SAT record (not shown here), which is influenced mainly by the cold Kara Sea due to melting sea ice. However, we assume that the melt-layer content in the AN ice core reflects predominantly the local summer conditions at the ice-cap surface, determined not only by the temperature, but also by the energy balance. Hence the significance of the melt-layer content in terms of regional SAT conditions is limited, at least on such short timescales as considered here.

2.6.4 Major ions

The ion record of ice cores reflects the atmospheric aerosol concentrations (e.g. Legrand and Mayewski, 1997). However, ions deposited in glaciers with percolation are subject to post-depositional changes (Koerner, 1997). The initially deposited AN chemical profile is superimposed by melting, infiltration and refreezing processes. Weiler et al. (2005) found that the AN ion record does not reflect seasonal atmospheric changes, but can be considered as an annually varying melting/refreezing signal. Most years seem to be represented by a peak of the more conservative ions such as sodium, which was used to achieve a depth-

age scale (Weiler et al., 2005; see also section 2.5). However, using mean values (here: 5yr values) seems to be promising to detect lower-resolution changes in ice-core chemistry. In this subsection, we focus on 20th-century trends in AN ion data and two singular events, which are assumed to be of volcanic origin (see below).

The sea-salt ions sodium and chloride increased from a relatively low level at about 1900 to maximum values between 1910 and 1925 (Figure 2.7). From this time the sea-salt ions show a decreasing trend. In the most recent years, values comparable to those at about 1900 were reached. Nevertheless, until about 1970 they remained on a high level characterized by a high-frequency variability. The period 1900-70 is characterized by the highest melt-layer content in the core section shown here. Therefore, the high variability could be caused or strengthened by meltwater percolation due to accumulation of leached ions in or above a melt layer. This assumption is supported by similar variations of the other ions of sea-salt origin: magnesium, calcium and (not shown here) potassium.

Similar records of sea-salt ions with a mid-20th-century maximum and a distinct decrease thereafter are also found in the Vetreniy ice core (Henderson, 2002), in the Austfonna ice core (Watanabe et al., 2001) with maximum values for 1920-63 and, less pronounced, in the Lomonosovfonna ice core (Isaksson et al., 2001; Kekonen et al., 2005). Kekonen et al. (2005) attributed this decrease to a substantial loss of ions due to increased melting and runoff, whereas Isaksson et al. (2001) stated a decreasing deposition.

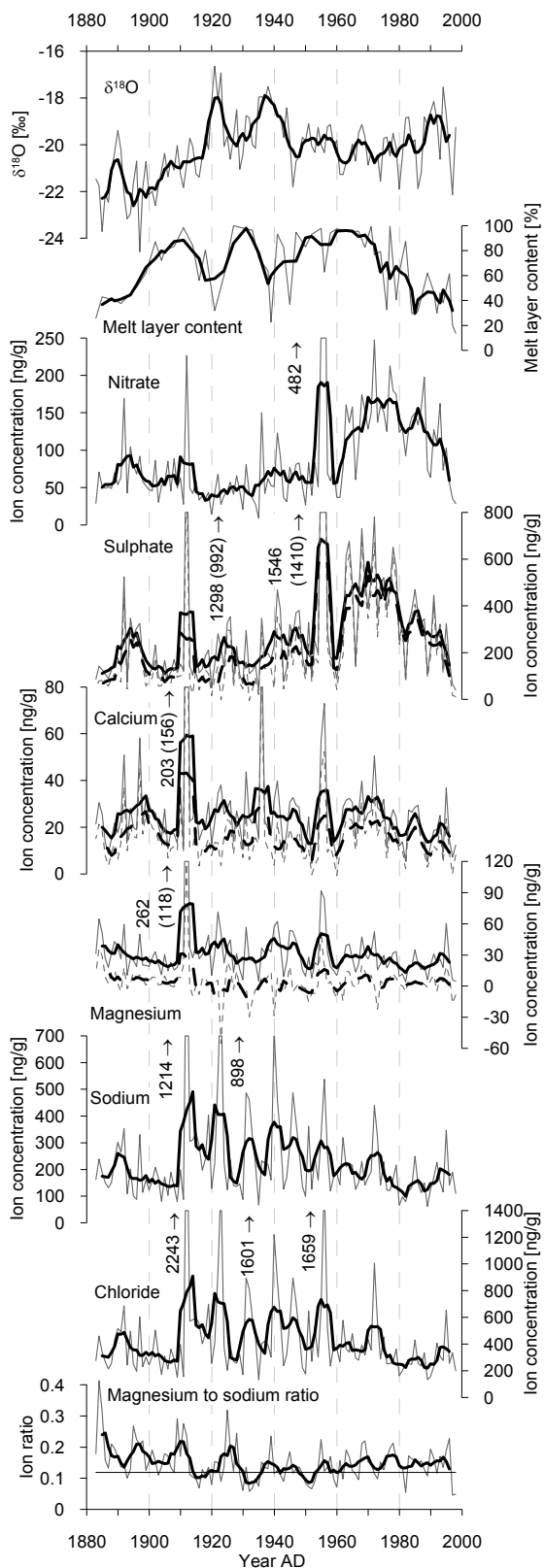


Figure 2.7: Time series of AN $\delta^{18}\text{O}$, AN melt-layer content, AN major ions and magnesium to sodium ratio by weight. The thin grey lines indicate annual mean values; the thick black lines indicate 5yr (for AN melt-layer content 1 and 3 m running mean values, respectively). The dashed lines as well as numbers in parentheses represent non-sea-salt values. The horizontal black line indicates the magnesium to sodium ratio of sea water.

The magnesium to sodium ratio, introduced as a sensitive indicator for meltwater percolation in the Austfonna ice core by Lizuka et al. (2002), shows no long-lasting decrease (Figure 2.7). Only three short-term drops about 1920, 1930 and 1950 are detectable, accompanied by increased values in the years before. This indicates short phases of preferential elution of magnesium with respect to sodium and accumulation in deeper layers. However, no decline of this ratio in the last few decades is perceptible, corresponding to the decrease in sea-salt ion concentration. Additionally, the melt-layer content shows the lowest values of the 20th century for this period, indicating that an increased loss of ions owing to increased melting and runoff seems unlikely. Hence the decreasing sea-salt ion trend favours a decreasing deposition due to lower wind speed, a change of dominating air masses or storm tracks. Since the Svalbard and FJL ice cores show similar patterns, the reasons for this decrease seem not to be only regional, but on a larger scale, covering at least parts of the Eurasian Arctic. However, a possible further growth of AN ice cap with a subsequent rise in altitude due to higher values of mean annual layer thickness since 1935 (see section 2.5) could also have contributed.

Short-term peaks in ice-core ion time series are often caused by major volcanic eruptions. During these eruptions large amounts of aerosols are injected into the atmosphere, leading to increased ion concentrations, particularly of sulphate (e.g. Legrand and Mayewski, 1997). In the AN sulphate record, two outstanding sharp peaks are visible, ascribed to the years 1956 and 1912 by $\delta^{18}\text{O}$ cycle counting (Figure 2.7). These values represent the highest values of sulphate concentrations for at least the last 1500 years, and of electrical conductivity in the whole AN ice core. The peaks were interpreted as imprints of the large volcanic eruptions of Bezymianny in 1956 and Katmai in 1912 and were therefore used as reference horizons for our age model. It is notable that for both events not only sulphate increased significantly, but all ions show enlarged values (Figure 2.7). In both cases the magnesium to sodium ratio shows smaller declines in the layers directly above the peaks (Figure 2.7), indicating leaching of ions. Therefore, it is likely that these peaks were amplified by infiltration processes and accumulation of ions. However, the peak linked to the Bezymianny eruption was identified clearly as of volcanic origin by Weiler et al. (2005), whereas this was not necessarily the case for the 1912 peak. The Bezymianny eruption was also detected in the

Lomonosovfonna ice-core sulphate record, whereas there was no hint for the Katmai-related peak (Isaksson et al., 2001; Kekonen et al., 2005). However, there are spikes in the Austfonna sulphate profile (Figure 6 in Iizuka et al., 2002) which could be related to the two peaks in the AN ice core. Also, in the ice core from Vetreniy ice cap, a strong peak in sulphate is perceptible about 1956 (Henderson 2002), even though not attributed to the Bezymianny eruption.

The concentrations of nitrate and sulphate in the AN ice core show a distinct anthropogenic imprint with a strong increase in the 1960s, maximum values about 1970 and decreasing values thereafter. This pattern corresponds to the records of the Svalbard and FJL ice cores (Isaksson et al., 2001; Watanabe et al., 2001; Henderson, 2002; Kekonen et al., 2005) and was attributed to regional industrial sources by Weiler et al. (2005), who discussed these records in detail, even though with the slightly different age model mentioned above.

2.7 Conclusions

This study deals with the uppermost 57 m of the recently drilled ice core of AN ice cap, covering the time period 1883-1998. To evaluate the palaeoclimatic significance of the ice-core data, we compared them to meteorological and other proxy data. We show that the AN ice core reflects Eurasian Arctic climate and environmental changes, although the ice cap is affected by summertime melting and infiltration processes. The main conclusions are:

1. Despite overprinting by summertime melting and infiltration processes, seasonal stable water-isotope cycles can be recognized over most of the section of the AN ice core considered here. In combination with the use of reference horizons, they enable a high-resolution dating of the AN ice core.
2. The multi-annual AN $\delta^{18}\text{O}$ time series shows strong similarities and correlations to instrumental SAT data from a couple of meteorological stations from the sub-Arctic and Arctic. Hence AN $\delta^{18}\text{O}$ data are a valuable proxy for mean Eurasian Arctic SAT, providing unique information for this poorly investigated region, particularly beyond the instrumental records.

3. In the warmest periods of this record, low d values connected with minima in the Kara Sea sea-ice extent indicate an increasing role of the Kara Sea as an important regional moisture source for the precipitation feeding AN ice cap.

4. The melt-layer content has no large-scale significance as proxy for SAT, since it reflects predominantly summer conditions at the ice-cap surface.

5. The AN ion record is more affected by meltwater percolation than the stable-isotope record. Nevertheless, long-term trends in atmospheric aerosol content as well as short-term events like the volcanic eruptions of Bezymianny in 1956 and Katmai in 1912 can be deduced.

Acknowledgements

We thank all the people who, in various ways, have contributed to the Severnaya Zemlya ice-core project. This study was funded by the state of Berlin (NaFöG PhD scholarship). The drilling project was funded by the German Ministry of Education and Research (03PL027A). We thank E. Isaksson and an anonymous reviewer for helpful comments which improved the quality of the manuscript.

3 Late Holocene climate change in the Central Russian Arctic – evidence from Akademii Nauk ice core (Severnaya Zemlya)

Thomas Opel^{1,2}, Diedrich Fritzsche¹, Hanno Meyer¹, Rainer Schütt^{1,3}, Urs Ruth⁴, Frank Wilhelms⁴, Hubertus Fischer^{4,5}

¹Alfred Wegener Institute for Polar and Marine Research, Telegrafenberg A43, 14473 Potsdam, Germany

²Department of Geography, Humboldt-Universität zu Berlin, Unter den Linden 6, D-10099 Berlin, Germany

³Now at Applied Geophysics and Geothermal Energy, RWTH Aachen University, Lochnerstraße 4 - 20, D-52056 Aachen

⁴Alfred Wegener Institute for Polar and Marine Research, PO Box 120161, D-27515 Bremerhaven, Germany

⁵Now at Climate and Environmental Physics, Physics Institute, University of Bern, Sidlerstrasse 5, CH-3012 Bern, Switzerland

In preparation for submission to Quaternary Science Reviews

Abstract

A 724 m deep ice core was drilled recently on the relatively low-altitude Akademii Nauk (AN) ice cap (Severnaya Zemlya) to gain high resolution proxy data from the Central Russian Arctic. The AN ice core provides significant climate and environmental proxy data; although the ice cap is affected by strong summertime melt water infiltration. We present data of stable water isotopes ($\delta^{18}\text{O}$, deuterium excess) and major ions of the upper 535 m, covering about 1700 years. The core chronology is based on volcanic reference layers and stable-isotope annual layer counting. The AN $\delta^{18}\text{O}$ data are highly correlated with instrumental temperature data from the Western Eurasian Arctic and can therefore be used as valuable near-surface temperature proxy for this region. AN $\delta^{18}\text{O}$ data reveal major changes in the last centuries, e.g. the absolute minimum around AD 1800 and the exceptional double-peaked early 20th century maximum. No pronounced Medieval Warm Period or Little Ice Age occurred, but several rapid warming and cooling events are detected, indicating considerable shifts in atmospheric circulation,

accompanied by sea ice extent changes. The long-term decrease of AN $\delta^{18}\text{O}$ and sea salt ions reflects the growth of AN ice cap over large parts of the Late Holocene. Warmer periods show evidence of higher sea-salt ion concentrations due to smaller sea-ice extent. The 20th century ion records indicate major shifts in atmospheric circulation and significant anthropogenic pollution.

3.1 Introduction

The Arctic has been influenced more than other regions by the ongoing climate change (e.g. ACIA, 2005; Trenberth et al., 2007). Temperature increase has been amplified compared to the global or Northern Hemispheric (NH) scale (Trenberth et al., 2007) during the rapid Arctic warming events 1920-1940 (Bengtsson et al., 2004) and in the last two decades (Przybylak, 2007). Accompanying processes like the decrease of sea ice extent and thickness (Lemke et al., 2007), as well as the warming of permafrost (Osterkamp, 2005; Romanovsky et al., 2007) clearly demonstrate the high climate-sensitivity of the Arctic ecosystems. Moreover, due to its impact on the global surface albedo and ocean currents as well as due to the large amounts of carbon stored in permafrost, the Arctic is a key region to study climate changes, particularly as for the future a strong temperature increase, a strong retreat of sea ice and increased thawing of permafrost are predicted (e.g. ACIA, 2005; Christensen et al., 2007). This raises the question, whether the Arctic warming since the 19th century and the amplification of global temperature variations are exceptional with regard to their magnitude and rate in the last millennia.

In the European Arctic, meteorological records are relatively short (Polyakov et al., 2003b). The longest surface air temperature (SAT) time series dates back to the first half of the 19th century only (Vardø; Figure 3.1), whereas in the Central Russian Arctic the longest SAT time series started in 1917 only (Dikson, Figure 3.1). Even greater is the relevance of high-resolution climate archives for reconstructing and understanding temporal and spatial patterns of climate variability and its causes (e.g. Overpeck et al., 1997).

Among climate archives available for the Arctic, glaciers and ice caps are most prominent. They provide unique records of physical and chemical properties of the atmosphere in past times. Greenland ice core records date back to the last Interglacial and play a major role in understanding NH climate history (e.g. NorthGRIP members, 2004). In the Eurasian Arctic, glaciers and ice caps are

limited to archipelagos and islands (Figure 3.1) such as Svalbard, Franz Josef Land (FJL) and Severnaya Zemlya (SZ). Koerner and Fisher (2002) assumed a Late Holocene origin for most of them. Even though these glaciers and ice caps are characterized by summertime surface melting and hence require special consideration of percolation processes (Koerner, 1997), due to their position at relatively low altitude and their high accumulation rates they provide high-resolution records of climate and environmental changes on a regional scale. Consequently, ice cores from such glaciers and ice caps at Svalbard (Isaksson et al., 2001; Watanabe et al., 2001) and FJL (Henderson, 2002) were drilled in the last decades. The ice core records of Svalbard and FJL span only several hundred years (Isaksson et al., 2005a, 2005b; Henderson, 2002), whereas the ice caps of SZ are considered to be older. For the near-bottom layers of Akademii Nauk (AN) ice cap as well as of Vavilov ice cap (Figure 3.1), maximum ages between 10 000 and 40 000 years were suggested (Klementyev et al., 1988, 1991; Kotlyakov et al., 1990), but due to low data resolution and uncertainties in the applied dating methods, these ages seem to be distinctly overestimated (Kotlyakov et al., 2004). However, Koerner and Fisher (2002) stated that AN ice cap, as the thickest and coldest ice cap on SZ, is the only one in the Eurasian Arctic with the potential of a Late Pleistocene age.

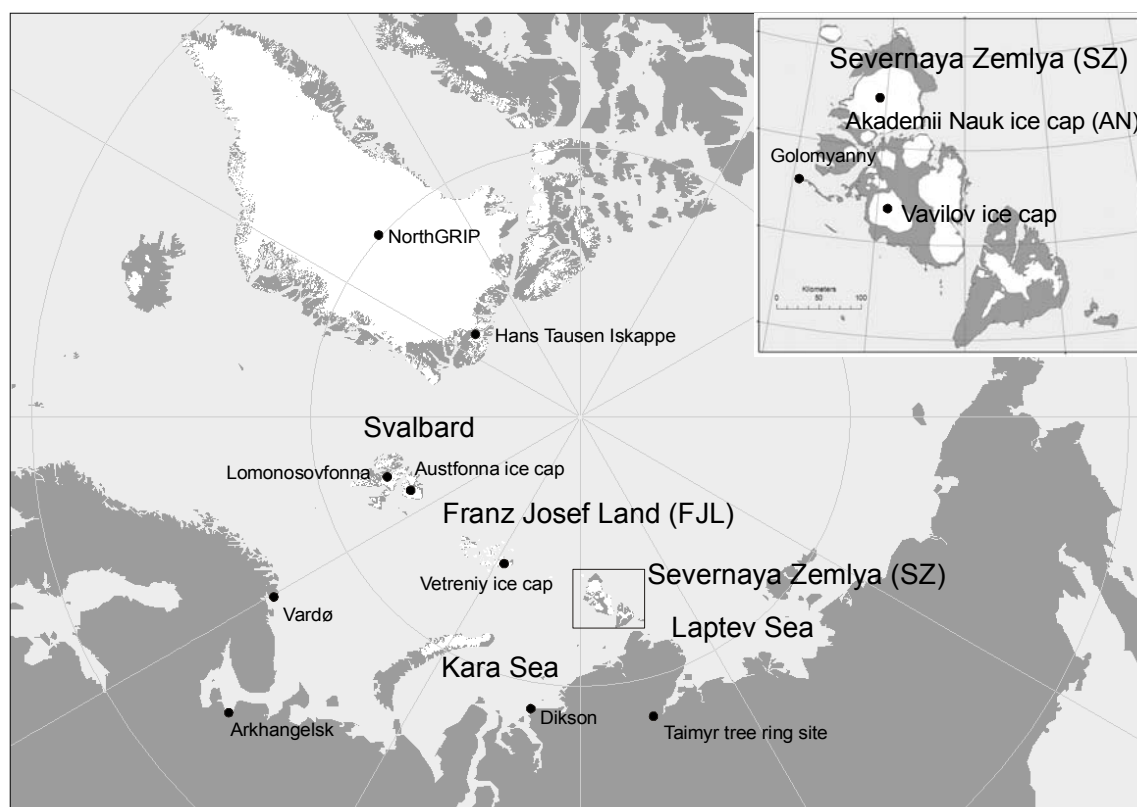


Figure 3.1: Map of the Eurasian Arctic. Inset: detailed map of Severnaya Zemlya (SZ) archipelago. All locations referred to in the text are labelled.

To verify the suggested timescales and extend high-resolution paleoclimate information from Eurasian Arctic ice cores eastwards, a joint German-Russian team drilled a new 724 m long surface-to-bedrock ice core on AN ice cap from 1999 to 2001 (Fritzsche et al., 2002). Hitherto existing results indicate that the AN ice core is a key archive for the reconstruction of the Late Holocene climate and environmental history of the Central Russian Arctic (Fritzsche et al., 2005; Weiler et al., 2005; Opel et al., 2009b). Despite melt water infiltration, AN $\delta^{18}\text{O}$ data of the last 115 years are highly correlated with SAT data of several meteorological stations from the Eurasian Arctic and Subarctic and can therefore be used as proxy for regional SAT (Opel et al., 2009b).

In this paper, we present a continuous record of stable water isotopes and major ions from the upper 535 m (487 m water equivalent (w.e.)) of the AN ice core based on overview datasets as well as high resolution data for selected core sections. We focus on the establishment of a core chronology and the detection of climate and environmental variations on different timescales.

3.2 Regional Setting

3.2.1 Severnaya Zemlya (SZ)

SZ is located north of the Taimyr Peninsula on the continental shelf in the Central Russian High Arctic, between the Kara Sea in the West and the Laptev Sea in the East. It represents the easternmost archipelago with considerable ice caps in the Eurasian Arctic (Figure 3.1). Due to its geographical position in the transition zone from the Atlantic-influenced western Siberian Arctic to the continental dominated eastern Siberian Arctic SZ is a key area for paleoclimate research. Consequently, several studies focused on SZ, mainly on the extent of Middle to Late Quaternary ice sheets and the corresponding paleoenvironments (e.g. Raab et al., 2003; Möller et al., 2007), Holocene pollen records (Andreev et al., 2008), but also on ice cores from AN and Vavilov ice caps (for a review of Soviet/Russian ice core activities see Kotlyakov et al., 2004).

The present-day climate conditions on SZ are harsh, according to its position in the High Arctic. The low-pressure area over the Barents Sea and Kara Sea and high-pressure areas over Siberia and the Arctic Ocean dominate the general atmospheric circulation. Meteorological observations on SZ started in AD 1930. The mean annual air temperature at Golomyanny station (Figure 3.1, WMO number 20087, 7 m a.s.l.) on a small island at the western tip of SZ was -14.7°C in the period AD 1951-1980 (Alexandrov et al., 2000). Mean monthly temperatures reach their maximum values around 0°C from June to August and their minimum values about -28°C from January to March. Annual precipitation increases from 186 mm at Golomyanny station (Alexandrov et al., 2000) to about 400 mm on the ice caps, with most of precipitation falling as snow. Even though precipitation takes place throughout the year, maxima in summer and autumn, connected with cyclonic activity are evident (Bolshiyarov and Makeev, 1995). This pattern is primarily caused by moisture-bearing cyclones from the North Atlantic as well as from Northern Europe and Western Siberia, which move in north-easterly direction over the Kara Sea towards SZ.

3.2.2 Akademii Nauk (AN) ice cap

Among the ice caps of SZ, AN is the largest one covering $5\,575\text{ km}^2$ with a volume of $2\,184\text{ km}^3$ (Dowdeswell et al., 2002). The dome-shaped ice cap reaches a

maximum elevation of about 750 m a.s.l. With a bottom temperature of -7.5°C (Kotlyakov et al., 2004) AN ice cap is a cold glacier without basal melting. A mean air temperature of -15.7°C for May 1999 to April 2000 was calculated from data of an automatic weather station near the 1999-2001 drilling site. However, air temperatures near ice cap summit reached values above 0°C in July and August, leading to snowmelt (Opel et al., 2009b). The melt water irregularly infiltrates into deeper snow and firn layers, where it refreezes and forms ice layers by filling the pore volume of the firn. Consequently, the ice cap stratigraphy is characterised by an alternation of layers of bubble-rich firn, partly saturated firn and clear bubble-free ice. The infiltration of “warm” melt water and its subsequent refreezing leads to an input of latent heat into the ice cap. This is visible in the measured 10 m depth temperature of -10.2°C in April 2000, which is significantly higher than the annual mean air temperature of -15.7°C . The maximum percolation depth on AN ice cap remains unclear, but an infiltration of more than two to three annual layers seems unlikely, as ice layers, formed by the refrozen melt water, should act as barriers and prevent a deeper percolation. Even though the percolation of melt water and occasionally rain modified the originally deposited isotopic and chemical records, significant high-resolution data can be obtained from AN ice core (Opel et al., 2009b).

3.3 Materials and Methods

3.3.1 Ice core drilling

The AN ice core was drilled at 80.52°N , 94.82°E in German-Russian cooperation of Alfred Wegener Institute for Polar and Marine Research (AWI) Bremerhaven/Potsdam, and the Arctic and Antarctic Research Institute (AARI) and the Mining Institute, both St. Petersburg. Due to logistical issues, the drilling took place during three field campaigns from 1999 to 2001. The bedrock was reached in a depth of 724 m. For drilling, a KEMS electromechanical ice-core drill was used, the same type as at Vostok, Antarctica (Fritzsche et al., 2002). For technical details of the drilling see Savatyugin et al. (2001). The drilling site was selected close to the ice cap summit, considering geophysical studies of ice cap form and flow (Dowdeswell et al., 2002). Although situated near the summit, the drilling site

is located in the percolation zone and therefore, affected by infiltration of melt water during summer (see section 3.2.2).

3.3.2 Ice core processing and sampling

The processing of the AN ice core took place in the cold laboratory of the AWI in Bremerhaven and comprised the following steps (see Table 3.1 for an overview; see also Fritzsche et al., 2005):

1. The electrical conductivity and density of the ice core were non-destructively measured in a resolution of 5 mm using dielectrical profiling and γ -absorption techniques (Wilhelms, 2000).
2. A two-step-strategy was applied for the sampling for measurements of the stable water isotope composition ($\delta^{18}\text{O}$ and δD) of the ice core: First, we carried out a screening by taking a mean sample from each core segment (bag, about 0.3 to 1.0 m). Second, we took samples in a very high (sub-annual) depth resolution of 2.5 cm. These data are available for the core parts 0-163 m, 204-251 m and some shorter sections (about 5 m each) distributed every about 25 to 40 m down to 535 m depth.
3. For analysing the ice core stratigraphy and the identification of melt layers, we scanned ice-core slices with a line-scan camera (Svensson et al., 2005). We calculated the melt-layer content for the upper 244 m using the proportion of melt-layers per meter ice core. As melt layer we considered ice, consisting of firn, infiltrated by a visible content of melt water, independent of the amount of melt water.
4. For glacio-chemical studies, the uppermost 53 m were sampled continuously with a subannual resolution of about 6 cm (for details, see Weiler et al., 2005). For the core section 53-535 m, we used a melting device for a continuous flow analysis (CFA), coupled with an auto-sampler-system (for details, see Ruth et al., 2004) to take screening samples (bag means) for the whole core section and high resolution (about 5 cm) samples for selected core sections.

Table 3.1: Overview of methods applied to AN ice core and data used for this study.

Processing Step	Ice core parameter	Method	Reference	Resolution	Proxy for	Core section
1a)	Electrical Conductivity	Dielectrical profiling	Wilhelms (2000)	5 mm	Total ion concentration	0-535 m
1b)	Density	γ -absorption	Wilhelms (2000)	5 mm	Stratigraphy	0-535 m
2	Stable water isotopes	Mass spectrometry	Meyer et al. (2000)	a) 2.5 cm (high resolution)	Temperature, moisture source region conditions	a) 0-163 m, 204-251 m, 280-285 m, 301-306 m, 372-377 m, 445-453 m, 483-488 m, 518-523 m, 530-535 m, some shorter sections
3	Melt layer content	Line-scan camera	Svensson et al. (2005)	1 m	Summer warmth, Stratigraphy	0-244 m
4	Ion concentration	Ion chromatography, Continuous flow analysis (CFA)	Weiler et al. (2005), Ruth et al. (2004)	a) 5 cm b) 0.3-1.0 m (screening)	Atmospheric aerosol content	a) 0-56 m, 102-108 m b) 55-535 m

3.3.3 Laboratory analytics

The oxygen ($\delta^{18}\text{O}$) and hydrogen (δD) stable isotope ratios of the melted ice core samples were analysed at the stable isotope laboratory of AWI Potsdam, using a Finnigan MAT Delta-S mass spectrometer. Both isotope ratios were determined for the same water aliquot, using equilibration techniques. The values are expressed in delta per mil notation (δ , ‰) relative to the Vienna Standard Mean Ocean Water (V-SMOW). The analytical precision is better than $\pm 0.1\text{‰}$ for $\delta^{18}\text{O}$ and $\pm 0.8\text{‰}$ for δD (Meyer et al., 2000).

The major ion concentrations were analysed at the glaciochemistry laboratory of AWI Bremerhaven. To analyse the melted ice core samples for anions (methanesulphonate (MSA^-), Cl^- , NO_3^- , SO_4^{2-}) and cations (Na^+ , NH_4^+ , Mg^{2+} , Ca^{2+}), a Dionex IC20 ion chromatograph was used (for details see Weiler et al., 2005).

3.4 Results

3.4.1 Ice core chronology

We dated the core section 0-535 m presented in this paper by using reference horizons and annual-layer counting. Besides the AD 1963 radioactivity peak caused by the fallout of nuclear bomb tests (Fritzsche et al., 2002; Pinglot et al., 2003), we used some extraordinary peaks in non-sea-salt (nss) sulphate as reference horizons, which we interpreted as deposited ions following major volcanic eruptions. Due to the high amount of sea-salt ions (see section 3.4.3) as well as the altering effects of infiltration and refreezing, peaks in electrical conductivity are not necessarily connected with volcanic events (Weiler et al., 2005). They are therefore less relevant for the detection of volcanic signals. The volcanic reference horizons used for the chronology of the AN ice core and the derived mean annual layer thicknesses are displayed in Table 3.2. For the volcanic horizons of Bezymianny (Kamchatka) in AD 1956, Katmai (Alaska) in AD 1912 and Laki (Iceland) in AD 1783 (Fritzsche et al., 2005; Weiler et al., 2005; Opel et al., 2009b) high resolution stable isotope and major ion data are shown in Figure 3.2. Extraordinarily elevated signals in all major ion concentrations and consequently in electrical conductivity for both the Bezymianny AD 1956 and Katmai AD 1912 horizons indicate an amplification of the originally deposited

signal due to infiltration processes and additional accumulation of ions as discussed by Weiler et al. (2005) and Opel et al. (2009b). In contrast, the AD 1783 horizon exhibits elevated values only for nss-sulphate and is clearly caused by the Laki eruption. Additionally, from screening data we newly interpreted an outstanding nss-sulphate peak in a depth of 303.75 m (274.35 m water equivalent (w.e.)) as the deposited volcanic aerosols of the 1259 eruption. This eruption of an up to now unknown volcano is, however, one of the largest Holocene volcanic signals evident in the Greenland (e.g. Zielinski et al., 1994) as well as Antarctic ice cores, too (e.g. Traufetter et al., 2004; Castellano et al., 2005). It was also detected and similarly interpreted in the Vetreniy (FJL; Henderson, 2002) and Lomonosovfonna (Svalbard; Moore et al., 2006) ice cores.

Table 3.2: Volcanic reference horizons used for ice core chronology and derived mean annual layer thickness.

Reference horizon	Year	Depth		Mean annual layer thickness between	
	AD	(m)	(m w.e.)	reference horizons (m w.e.)	reference horizon and 1999 (m w.e.)
Bezymianny eruption	1956	25.85	19.65	0.457 (1956-1999)	0.457
Katmai eruption	1912	44.30	36.20	0.376 (1912-1956)	0.416
Laki eruption	1783	104.93	91.32	0.427 (1783-1912)	0.423
Unknown eruption	1259	303.75	274.36	0.349 (1259-1783)	0.371

Seasonal signals of $\delta^{18}\text{O}$, δD , and deuterium excess d ($d = \delta\text{D} - 8 \cdot \delta^{18}\text{O}$) are detectable in the high-resolution sampled sections of the entire ice core part presented here. An alteration of the isotope signal originally deposited in the snowpack due to melting and infiltration of melt water is obvious in several sections, resulting in a smoothing of the isotope records or a shifting of signals. However, also in core sections which suffered intense melting and infiltration, the combination of $\delta^{18}\text{O}$ and δD minima and d excess maxima as winter signals enables us to count annual layers continuously in the long highly resolved core sections (0-163 m and 204-251 m). In the ice core parts with high resolution stable isotope data available only in several shorter sections, we determined the mean annual layer thickness for these sections by counting seasonal isotope cycles. To fill the gaps between the high-resolution sections, we calculated the missing years based on the mean annual layer thickness of these sections. Using this approach,

the mentioned volcanic reference horizons were cross-checked and their age estimate could be confirmed.

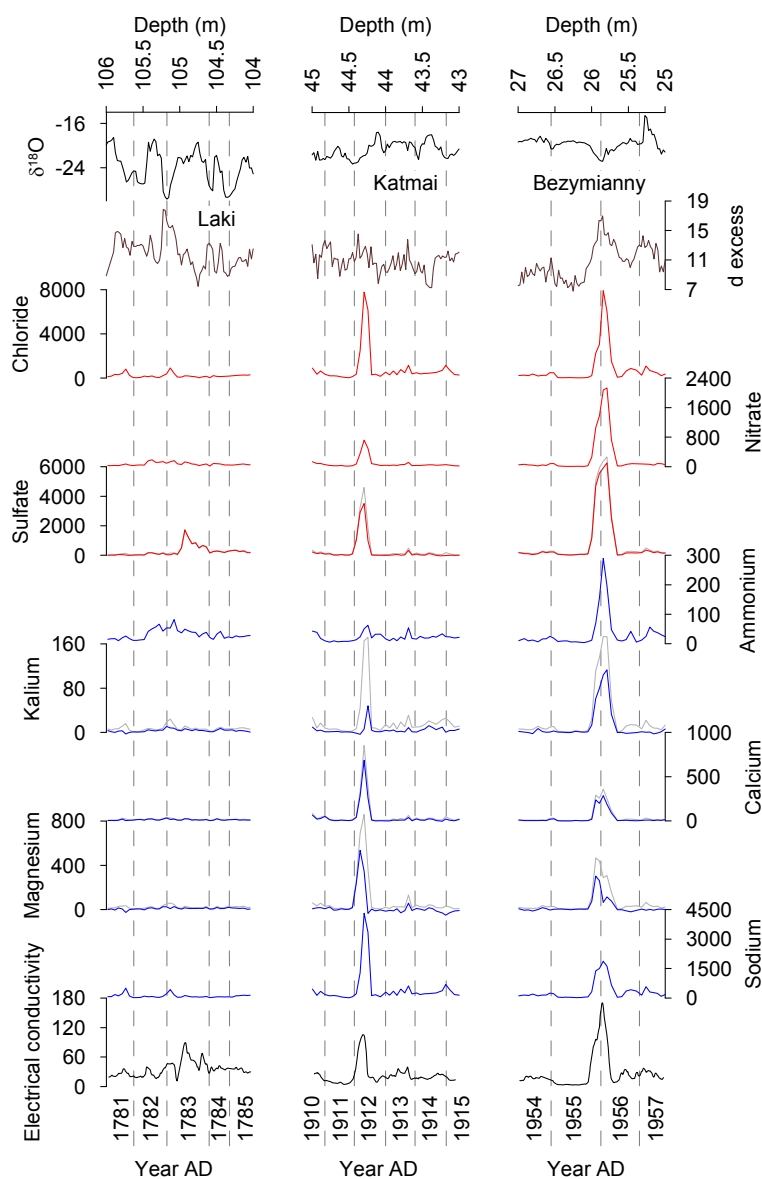


Figure 3.2: High resolution (0.5 to 5 cm) records of stable isotope (black, top), anions (red), cations (blue) and electrical conductivity (black, bottom) data for the core sections 104-106 m (left), 43-45 m (middle), 25-27 m (right), containing the volcanic horizons of Laki AD 1783, Katmai AD 1912 and Bezymianny AD 1956. The units are (‰) for stable isotopes, (ng g^{-1}) for major ions and ($\mu\text{S m}^{-1}$) for electrical conductivity. Coloured lines for ions indicate the nss-fraction, grey lines the total ion concentration.

The applied dating approach resulted in an ice core chronology (AN 2009/04) spanning about 1 700 years for the core section 0-535 m presented here (Figure 3.3). We estimated the dating accuracy as better than ± 3 years after AD 1783, ± 5 years between AD 1650 and 1783, ± 20 years between AD 1259 and 1650, and \pm

50 years before AD 1259. This chronology is distinctly younger as compared to the published age models of the first AN ice core drilled in 1986/87 (Kotlyakov et al., 1990), which propose ages of about 4 200 years for the corresponding depth. These overestimated ages seem to be caused by a considerable underestimation of annual layer thickness over the entire core length. However, comparing the 1986/87 and 1999-2001 AN $\delta^{18}\text{O}$ records on a depth scale reveal a striking similarity (Figure 3.4), if different core lengths (1986/87: 761 m, 1999-2001: 724 m) due to slightly different coring locations are taken into account. This similarity demonstrates that both ice cores contain the same climate record and are directly comparable.

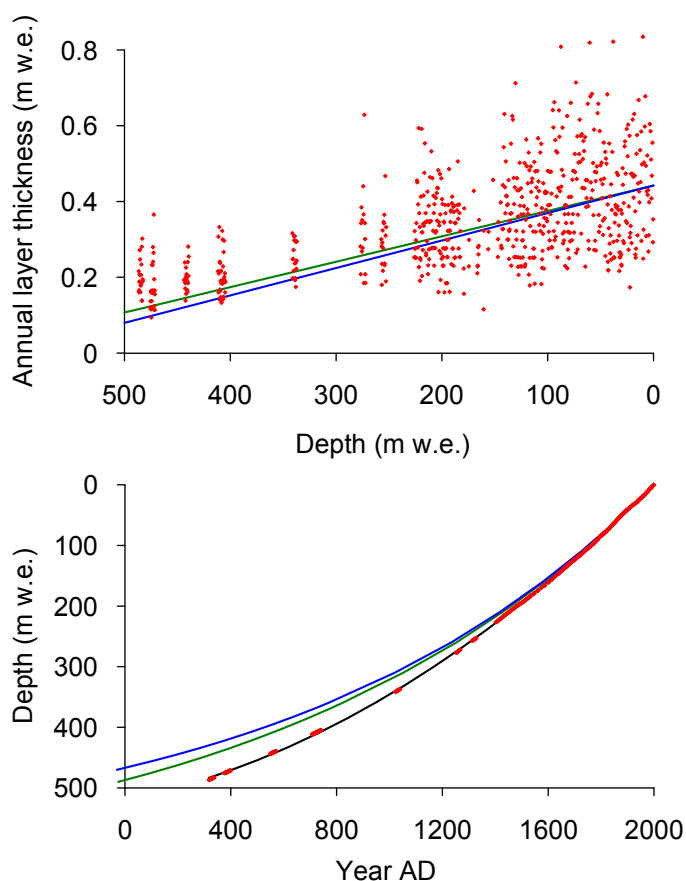


Figure 3.3: Annual layer thickness (top) and depth-age-relationship (bottom) for core chronology AN 2009/04. Red dots represent the stable isotope based annual layer thickness (top) and the corresponding ages considering the volcanic reference horizons (bottom). The green and blue lines show Nye and Dansgaard-Johnsen models (Paterson, 1994), respectively, applied to AN ice core. The black line displays a polynomial fit for the core chronology.

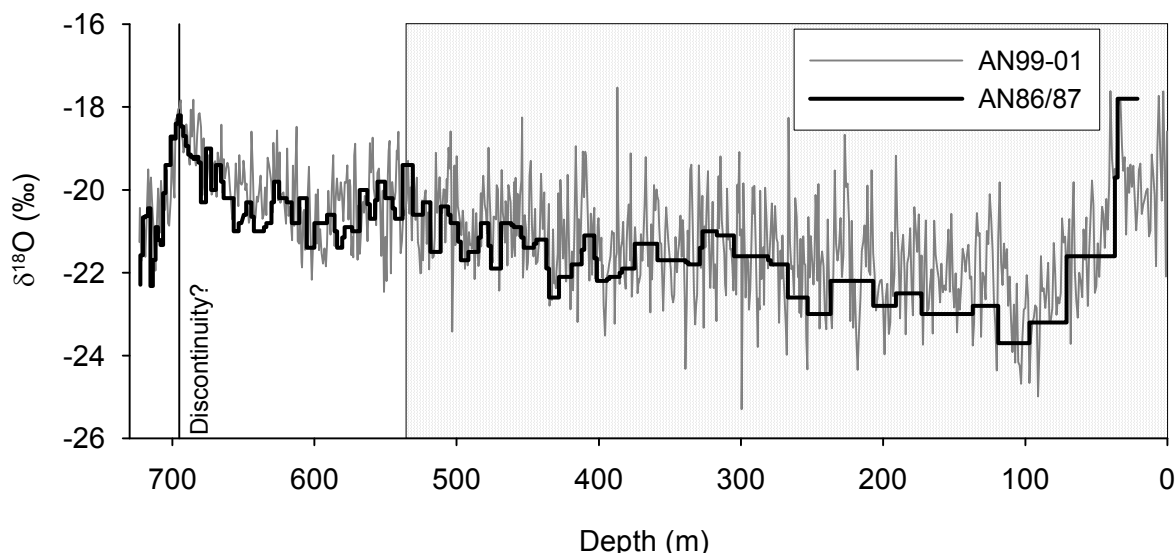


Figure 3.4: Comparison of 1986/87 (sparse data available only) and 1999-2001 (bag mean values) AN ice core $\delta^{18}\text{O}$ records. The 1986/87 record is adjusted to the depth scale of the 1999-2001 core by a) adding 11 m (representing the accumulation between 1986 and 1999) and b) fitting of two reference points and interpolating in between. The grey shaded area marks the ice core section presented in this paper. The vertical line at a depth of 695 m indicates the potential discontinuity (see section 3.5.1).

The stable isotope based annual layer thickness does not decrease significantly to a depth of about 140 m (about 0.40 m w.e.; Figure 3.3). From that depth it decreases nearly linearly to a mean value of 0.17 m w.e. at a depth of 518-523 m. The core section 530-535 m exhibits a slightly increased mean annual layer thickness of 0.20 m w.e. Simple ice-flow models (i.e. the Nye and Dansgaard-Johnson models; Paterson, 1994) underestimate the real annual layer thickness and therefore tend to overestimate the corresponding ages (Figure 3.3). This is supported by an annual layer thickness of 8-10 cm w.e. in the lowest core section (below 700 m), where these ice flow models predict annual layer thickness converging to zero caused by layer thinning due to increasing load and horizontal ice flow. Consequently, AN ice cap was not in dynamic steady state in the time span discussed here and therefore did not fulfil the assumption for the application of the mentioned ice flow models. We assume that AN ice cap has been growing until recent times.

3.4.2 High resolution record of the last three centuries

This section focuses on high resolution (2.5 cm) stable water isotope data ($\delta^{18}\text{O}$ and d excess) and melt-layer content of the last three centuries (AD 1700-1998;

represented by the uppermost 140 m ice core) while high resolution ion concentrations (continuously available only for the last 115 years) were already presented and discussed by Weiler et al. (2005) and Opel et al. (2009b).

3.4.2.1 Stable water-isotopes ratios $\delta^{18}\text{O}$ and δD

Stable water isotope ratios ($\delta^{18}\text{O}$ and δD) in precipitation mainly depend on condensation temperatures. Therefore, they are generally accepted as proxies for temperature conditions in high polar latitudes on a local to regional scale. We calculated annual mean values of AN stable water isotope data by averaging all isotope values between the defined annual marks. The co-isotopic relationships for AN ice core are

$$(1) \delta\text{D} = 7.6261 \delta^{18}\text{O} + 3.0513 \quad (R^2 = 0.99, n = 5549, \text{ single values})$$

and

$$(2) \delta\text{D} = 7.6957 \delta^{18}\text{O} + 4.5729 \quad (R^2 = 0.9933, n = 298, \text{ annual mean values}).$$

This slope is typical for the Siberian Arctic and is close to the Global Meteoric Water Line (GMWL) which has been defined theoretically as $\delta\text{D} = 8 \delta^{18}\text{O} + 10$ (Craig, 1961) and calculated for precipitation on a global scale as $\delta\text{D} = 8.17 \delta^{18}\text{O} + 10.35$ (Rozanski et al., 1993). Therefore, we assume only minor influence of kinetic fractionation effects. Consequently, AN ice core stable isotope relationships can be considered as a Local Meteoric Water Line (LMWL) for SZ and reliable information from a paleoclimatic point of view can be obtained. In the following, we focus on $\delta^{18}\text{O}$ as this isotopic ratio is commonly used in Arctic paleoclimate studies. Smoothing the dataset over 5 years results in strongly reduced or even negligible effects of melting, infiltration and refreezing on the stable-isotope data as well dating uncertainties.

Annual mean AN $\delta^{18}\text{O}$ and corresponding 5 year running means (5yrm) are displayed in Figure 3.5 together with other SAT time series for the last three centuries. Generally, the AN $\delta^{18}\text{O}$ curve clearly exhibits an increasing trend between AD 1700 and 1998, superimposed by a marked variability. Highly variable $\delta^{18}\text{O}$ values from AD 1700 to 1750 are followed by a strong decrease to the

absolute minimum (around -24‰) between AD 1780 and 1820. Thereafter, the $\delta^{18}\text{O}$ values increased gradually until the beginning of the 20th century, and strongly until the double-peaked absolute maximum (-18‰) between AD 1920 and 1940. After a decrease to about -20‰ in the mid-20th century, $\delta^{18}\text{O}$ values again started to increase from the AD 1980s. However, the maximum values between AD 1920 and 1940 were not yet reached until AD 1998.

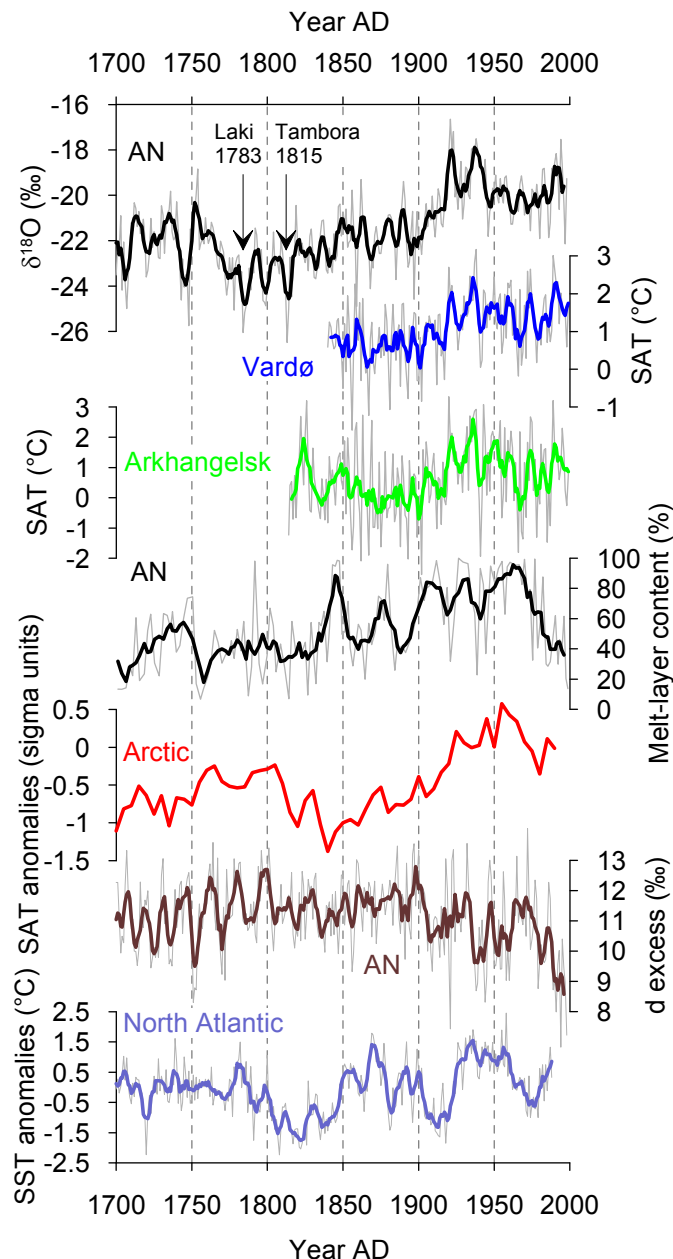


Figure 3.5: AN stable isotope and melt-layer content records together with the SAT records of Vardø and Arkhangelsk, the reconstructed Arctic SAT anomalies and the reconstructed North Atlantic (0-70°N) SST for AD 1700 to 2000. The thin grey lines indicate annual and the thick lines 5yr running mean values (for AN melt-layer content 1 m and 5 m running mean values, respectively).

The similarity between the AN $\delta^{18}\text{O}$ data and the instrumental SAT time series of Vardø (WMO station 01098, AD 1840-1999) is striking (Figure 3.5). Vardø, about 2000 km west of AN ice cap, is situated at the year-round ice-free Northern Norway Barents Sea coast (Figure 3.1). The linear correlation coefficient is $r_{5\text{yrm}} = 0.76$ (data from CRU Norwich; Brohan et al., 2006). Even though the correlation between Vardø SAT and AN $\delta^{18}\text{O}$ is lower for annual values ($r = 0.37$), many maxima and minima in annual mean SAT correspond to those of the AN $\delta^{18}\text{O}$ curve, also underlining the validity of our core chronology. The lower correlation was expected considering infiltration of summer melt into the layers of previous years, and dating uncertainties. Additionally, the instrumental SAT time series of Arkhangelsk (White Sea Coast, WMO station 22550, Figure 3.1; AD 1814-1998 with small gaps), the longest of the Russian Subarctic, exhibits distinct similarities to the AN $\delta^{18}\text{O}$ time series, even though somewhat less than that of Vardø, particularly before 1850 (Figure 3.5). Consequently, the correlation coefficients are slightly lower compared to those of Vardø, but still strong (AD 1814-1998: $r_{5\text{yrm}} = 0.57$, AD 1840-1998: $r_{5\text{yrm}} = 0.68$).

In contrast, the SAT time series from the nearest meteorological station Golomyanny (WMO station 20087, AD 1931-1998 with gaps) on a small island at the western tip of SZ about 150 km southwest of AN ice cap (Figure 3.1) exhibit only minor similarities with the AN $\delta^{18}\text{O}$ curve (AD 1946-1998, $r_{5\text{yrm}} = 0.14$; Opel et al., 2009b). Due to its location on a small island only 7 m a.s.l., SAT at Golomyanny is mainly controlled by the local occurrence of sea ice, predominantly in the summer and autumn seasons. It therefore is valid only on a local scale, in contrast to the regional climate signals recorded in AN ice cap.

Other SAT time series of the Eurasian Arctic and Subarctic, which do not date back to the 19th century, were compared to AN $\delta^{18}\text{O}$ for shorter time periods in a former study (Opel et al., 2009b). They reveal some good accordance as well. Consequently, we regard AN $\delta^{18}\text{O}$ as a suitable proxy for SAT on a regional to (at least) Western Eurasian Arctic scale.

3.4.2.2 Deuterium excess d

Deuterium excess d (Dansgaard, 1964), a second-order parameter calculated from $\delta^{18}\text{O}$ and δD (see section 3.4.1), is largely influenced by the evaporation conditions in the moisture source region. It is mainly determined by relative air

humidity and the surface temperature (SST) and, to a lesser extent, by wind speed (Rozanski et al., 1993). The mean annual AN d excess of 11.1‰ is a typical value for precipitation in high-latitude coastal areas and indicates an oceanic main moisture source. Therefore, substantial continental water recycling contributing to precipitation at AN ice cap is unlikely. Considering the general atmospheric circulation patterns, we assume the Northern Atlantic to be the main moisture source for precipitation feeding the AN ice cap.

The last three centuries of the AN ice core d excess record are characterised by a marked variability (Figure 3.5). A slightly increasing trend from AD 1700 to 1900 is superimposed by short-term oscillations between 9.5‰ and 12.5‰ until AD 1800 and more stable values (about 11.5‰) until AD 1900. The 20th century shows a strongly decreasing trend, also with high fluctuations. It is remarkable that the opposite behaviour of d excess and $\delta^{18}\text{O}$ on a seasonal scale (Opel et al., 2009b) is also evident on a longer time scale. Maxima (minima) in d excess are often connected to minima (maxima) in $\delta^{18}\text{O}$.

3.4.2.3 Melt-layer content

The amount of melt layers in ice cores is generally accepted as a proxy for the summer warmth at the ice cap surface (Koerner, 1977). As summertime melt water infiltration at AN ice cap is irregular and percolation may exceed the corresponding annual layer (Opel et al., 2009b), the temporal resolution of that proxy is lower as compared to $\delta^{18}\text{O}$. The AN melt-layer content varies between less than 10% and 100% per core meter (Figure 3.5). Slight maxima are detected around AD 1740 and AD 1875 whereas a strong maximum occurred around AD 1850. From AD 1900 to 1970, the melt-layer content is generally high representing the warmest summers of the last 300 years, interrupted only by two slight minima at about AD 1920 and AD 1940. From AD 1970, the melt-layer content decreased strongly. AN melt-layer content differs considerably from AN $\delta^{18}\text{O}$ record (Figure 3.5). Moreover, it seems that $\delta^{18}\text{O}$ maxima coincide with minima in melt-layer content, whereas melt-layer peaks are located immediately before that of $\delta^{18}\text{O}$.

3.4.3 The Late Holocene record

The screening data (bag mean values) of stable isotopes and major ions were resampled to annual values using a polynomial fit function based on the ice core

chronology AN 2009/04. For the period AD 1650-1998, continuous high-resolution stable isotope data are available and replace therefore the resampled data. The AN stable isotope ($\delta^{18}\text{O}$, d excess) and major ion records are displayed in Figure 3.6 and are discussed in the following chapters as running means over 15 years, which is appropriate for long-term climate information.

3.4.3.1 Stable oxygen-isotope ratio $\delta^{18}\text{O}$

The $\delta^{18}\text{O}$ record shows a continuous decreasing trend from -20‰ in the 4th and 5th century to around -21.5‰ at about AD 1750, characterised by a considerable variability. Around AD 1750, a strong drop to the absolute minimum around AD 1800 ($\delta^{18}\text{O} = -23\text{‰}$) occurred, followed by the increase to the absolute maximum (19‰) in the early 20th century. This $\delta^{18}\text{O}$ rise reflects a strong warming, which is unprecedented in this record. The corresponding $\delta^{18}\text{O}$ maximum represents the warmest time period of the whole AN record (see also Figure 3.4). In the centuries before, no pronounced century-lasting warmer or cooler periods such as the Medieval Warm Period (MWP) or the Little Ice Age (LIA) are recorded at AN ice cap. Long periods of the AN $\delta^{18}\text{O}$ record exhibit a persistent but relatively low variability of 1 to 1.5‰ for 15yr values. However, there are some periods, e.g. around AD 900 and particularly in the 15th and 16th century, which are characterised by rapid warming and cooling events up to 3‰ for 15yr values. These events culminate in sharp short-term $\delta^{18}\text{O}$ maxima and minima, indicating drastic SAT changes within a few decades in the Western Eurasian Arctic.

3.4.3.2 Deuterium excess d

The AN d excess curve does not show a general trend, but displays a marked irregular variability with d excess values mainly fluctuating between 10.5‰ and 12‰ . Several but not all short-term maxima (minima) in d excess are accompanied by $\delta^{18}\text{O}$ minima (maxima) as counterparts, underlining the connection between both proxies. The AN record reveals some longer periods with generally slightly higher d excess values (e.g. AD 470-660, AD 720-870, AD 940-1070 and AD 1480-1650) as well as slightly lower (AD 1220-1480) d excess values (Figure 3.6), possibly indicating shifts of the moisture source region. A similar pattern is not detectable in the $\delta^{18}\text{O}$ record. Several rapid changes in d excess by up to 2‰ for 15yr values within one to two decades are visible in the

AN record. Distinct short-term minima around AD 450, AD 600 and AD 700, as results of rapid changes reach, the minimum d excess values of the late 20th century.

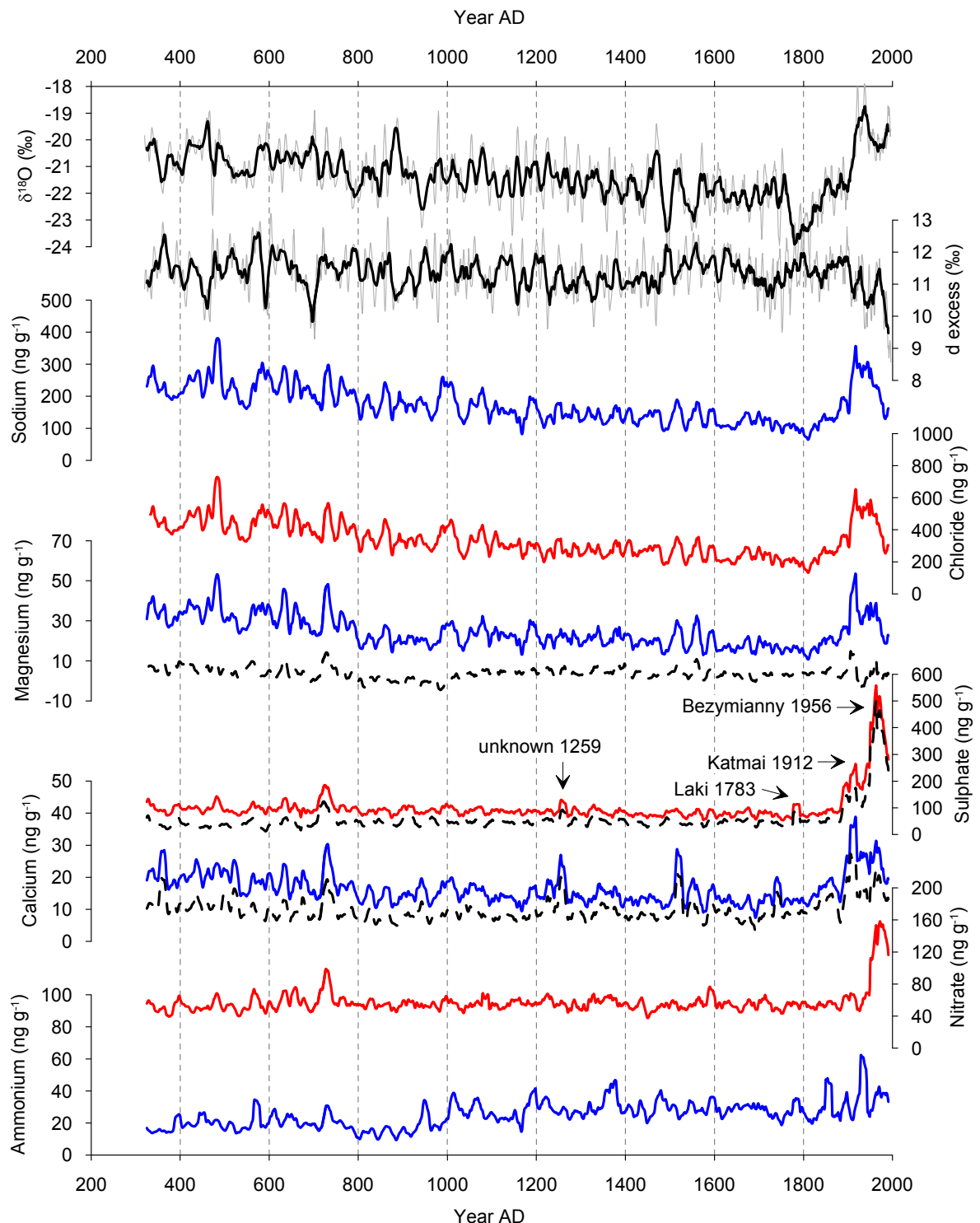


Figure 3.6: Long-term records of AN stable isotope (black), anion (red) and cation (blue) data. The thin grey lines indicate 5yr and the thick lines 15yr values. The dashed lines represent nss-values. Volcanic eruptions used for the core chronology are marked in the sulphate record.

3.4.3.3 Major ions

The ion concentration in ice cores reflects the atmospheric aerosol content (e.g. Legrand and Mayewski, 1997). In ice cores from the percolation zones of glaciers, the ion record is altered by post-depositional processes (Koerner, 1997), i.e. melting, infiltration and refreezing. Even though seasonal atmospheric effects are often blurred, conclusions on multi-annual and long-term changes can be drawn from the AN ice core (Opel et al., 2009b; Weiler et al., 2005). The AN major ion concentrations are displayed in Figure 3.6. Assuming that all sodium comes from sea water, sea-salt (ss) and non sea-salt (nss) fraction of other ion species with a sea-salt proportion are calculated based on the corresponding ion ratios to sodium.

The sea-salt ions chloride and sodium are the dominating ions in the AN ice core. The mean chloride to sodium ratio of 1.98 in AN ice core is close to that of sea water (1.8), indicating that essentially all of the sodium originates from marine sea-salt sources, whereas chloride seems to have additional sources. The concentrations of chloride and sodium exhibit a similar pattern along the whole record presented here (Figure 3.6). Both show a marked decline from the beginning of the record until a common minimum around AD 1820, only a few years after the absolute SAT minimum. Whereas the decrease is rather strong until about AD 1200, characterised by a considerable variability and some rapid changes (i.e. about AD 500 and about AD 1000), the ion concentration remained on a relatively constant level until about AD 1450, when the variability increased strongly similar to the $\delta^{18}\text{O}$ record. From about AD 1650 to about AD 1820, the sea salt ion concentrations again decreased to the absolute minimum. Subsequently, they started to increase gradually until about AD 1900, when they rose sharply to a maximum from AD 1910 to 1940 and declined strongly thereafter to values comparable to the long-term mean from about AD 1200 to 1600. The early 20th century increase in sea-salt ion concentrations is exceptional regarding magnitude and rate. However, it started and reached its maximum some 10 to 20 years before the corresponding $\delta^{18}\text{O}$ maximum around AD 1930, which was, in turn, of shorter duration. The subsequent sea-salt ion decrease was longer-lasting and more pronounced as compared with $\delta^{18}\text{O}$.

About 75% of the magnesium in AN ice core is of sea-salt origin. Consequently, the AN magnesium record reveals a general similarity to that of chloride and

sodium (Figure 3.6). However, the decrease is interrupted by an about 200 years lasting period of comparatively low magnesium values from about AD 800 to 1000. Thereafter, magnesium concentrations decreased further to the absolute minimum at about AD 1820, interrupted by a period of a high variability in the 16th century. The nss-magnesium level remains on a relatively constant level throughout the record. However, the period AD 800 to 1000 is characterised by slightly negative nss-magnesium values. Consequently, the magnesium to sodium ratio (not shown), as sensitive indicator for melt-water percolation introduced in the Austfonna ice core on Svalbard (Iizuka et al., 2002), exhibits a distinct minimum and dropped partly below that of sea water (0.12), pointing to a preferential elution of magnesium with respect to sodium in this period, probably due to enhanced melting.

The most prominent feature of the AN sulphate record is the marked rise in the 20th century followed by a strong decrease (Figure 3.6). The long-term sulphate record reveals a pattern similar as compared to chloride and sodium, due to a substantial proportion of sea-salt sulphate. Due to the relatively low altitude, about 50% of the sulphate comes from sea salt, viewing only the time period before the anthropogenic influenced 20th century. Consequently, only about 50% of the sulphate originates from marine biogenic, terrestrial or volcanic sources. Therefore, volcanic sulphate peaks are masked. So far, only four remarkable peaks in nss-sulphate could be certainly attributed to distinct volcanic eruptions (unknown eruption in AD 1259, Laki in AD 1783, Katmai in AD 1912 and Bezymianny in AD 1956) and thus used as reference horizons for ice core dating (see also section 3.4.1). The large peak around AD 720 in total sulphate as well as nss-sulphate could not be attributed to a volcanic eruption. This peak is detectable in all ion concentrations, pointing to another than volcanic origin.

About 60% of the calcium ions in AN ice core are of non sea-salt origin. The nss-calcium fraction remains relatively constant, whereas the sea-salt fraction and therefore also the total calcium concentration exhibit distinctly higher values before about AD 800 than thereafter (Figure 3.6). From about AD 800 the total calcium concentrations decrease slightly until the 18th century. After AD 1800 the calcium values increase to distinctly higher values in the 20th century with a higher proportion of the sea-salt fraction. Generally, the AN calcium record exhibits several striking peaks in nss- and total calcium, indicative of short-term inputs, e.g.

dust storms or rapid shifts in wind regimes. Two of the peaks are accompanied by peaks in nss-sulphate and are therefore interpreted as being related to the explosive volcanic eruptions of AD 1259 (unknown volcano) and AD 1912 (Katmai), possibly associated with volcanic ash or continental crust particles. Two considerable nss-calcium peaks occurred in the 16th century, corresponding with the highly variable records of $\delta^{18}\text{O}$ and sea salt ions in this period.

The nitrate concentration in AN ice core reveals a relatively constant level with minor fluctuations throughout the record until about AD 1900 (Figure 3.6). In the 20th century, the nitrate values first increased dramatically and then declined steeply in the last two to three decades. We assume that the nitrate variations in the centuries before represent the natural variability (soil exhalation) of preindustrial times with some short-term peaks, possibly due to singular events such as biomass burning.

Generally, the ammonium concentrations in AN ice core show a slightly increasing trend, overprinted by several short term spikes (Figure 3.6). These may be caused by large forest fires in the Siberian Taiga, whereas the long-term record might reflect a slight increase in microbial soil activity.

3.5 Discussion

3.5.1 Holocene AN ice cap history

Even though SZ was not covered by the Kara Sea ice sheet during the Last Glacial Maximum (LGM; Möller et al., 2007) the occurrence of local glaciers on SZ is likely, probably comparable to the present situation. These glaciers had only a relatively small extent and/or were relatively thin due to drier climate conditions during the LGM (Raab et al., 2003; Stiévenard et al., 1996). Recent pollen studies of Andreev et al. (2008) revealed optimum conditions for local biota warmer than today and peat accumulation in the transition from Late Glacial to Holocene at 11 500 to 9 500 cal. years BP. At 9 400 cal. years BP the environmental conditions changed significantly and the vegetation became similar to today due to colder and dryer climate conditions. Most likely, AN ice cap disappeared or at least extremely shrunk during that thermal maximum covering the Late Glacial and Early Holocene, as supposed for all other Eurasian Arctic ice caps as well (Koerner and Fisher, 2002). Accordingly, induced by the following cooling trend

and/or change in moisture supply due to changed atmospheric and oceanic circulation, AN ice cap started growing again in Middle to Late Holocene times (at least 2 000 to 2 500 years ago) and probably did not reach steady state conditions until recent times. As similarly suggested also for Hans Tausen Iskappe, North Greenland (Hammer et al., 2001), the possibility of Late Holocene growth has to be taken into account when interpreting ice core records from smaller Arctic ice caps.

However, a discontinuity in the AN ice core record, possibly separating an older part from the more recent one, cannot be excluded so far. A change in ice core consistency in the range of the first $\delta^{18}\text{O}$ maximum at a depth of about 695 m (marked in Figure 3.4) is evident and gives hints to changing physical conditions, even though no peculiar changes in the stable isotope composition or electrical conductivity are detectable. Moreover, the lowermost core section (below 696 m) is characterised by CO_2 and CH_4 concentrations of one to two orders of magnitude higher than the atmospheric values for Interglacials (Samyn et al., 2008). This indicates biogenic activity during the formation of these ice layers and/or melting-refreezing processes. The latter did, however, not change the stable water isotope composition, which forms a slope close to the GMWL.

3.5.2 Paleoclimatic implications of AN ice core records

The long-term decrease of AN $\delta^{18}\text{O}$ until about AD 1750 does not solely reflect a climate cooling, as also the growth of AN ice cap influences the $\delta^{18}\text{O}$ record (see sections 3.4.1 and 3.5.1). An increasing ice-cap altitude and therefore a higher condensation level, with lower temperatures leading to more depleted $\delta^{18}\text{O}$ values is likely responsible for at least parts of this decline. This interpretation is supported by similar decreasing trends of the sea salt ions (Figure 3.6). We conclude that sea salt aerosol concentration decreases due to a less efficient sea-salt aerosol deposition with increasing ice cap altitude. However, the long-term records of nitrate and ammonium seem to be not affected by the growing ice caps altitude. Furthermore, maxima (minima) of $\delta^{18}\text{O}$ are often, but not always accompanied by maxima (minima) of sea-salt ion concentrations (Figure 3.6). That points to higher sea-salt ion deposition in warmer periods, possibly because of a smaller sea ice extent in periods of higher temperatures. Vice versa, lower

temperatures, combined with an assumed larger sea ice cover, could have caused lower sea salt ion deposition.

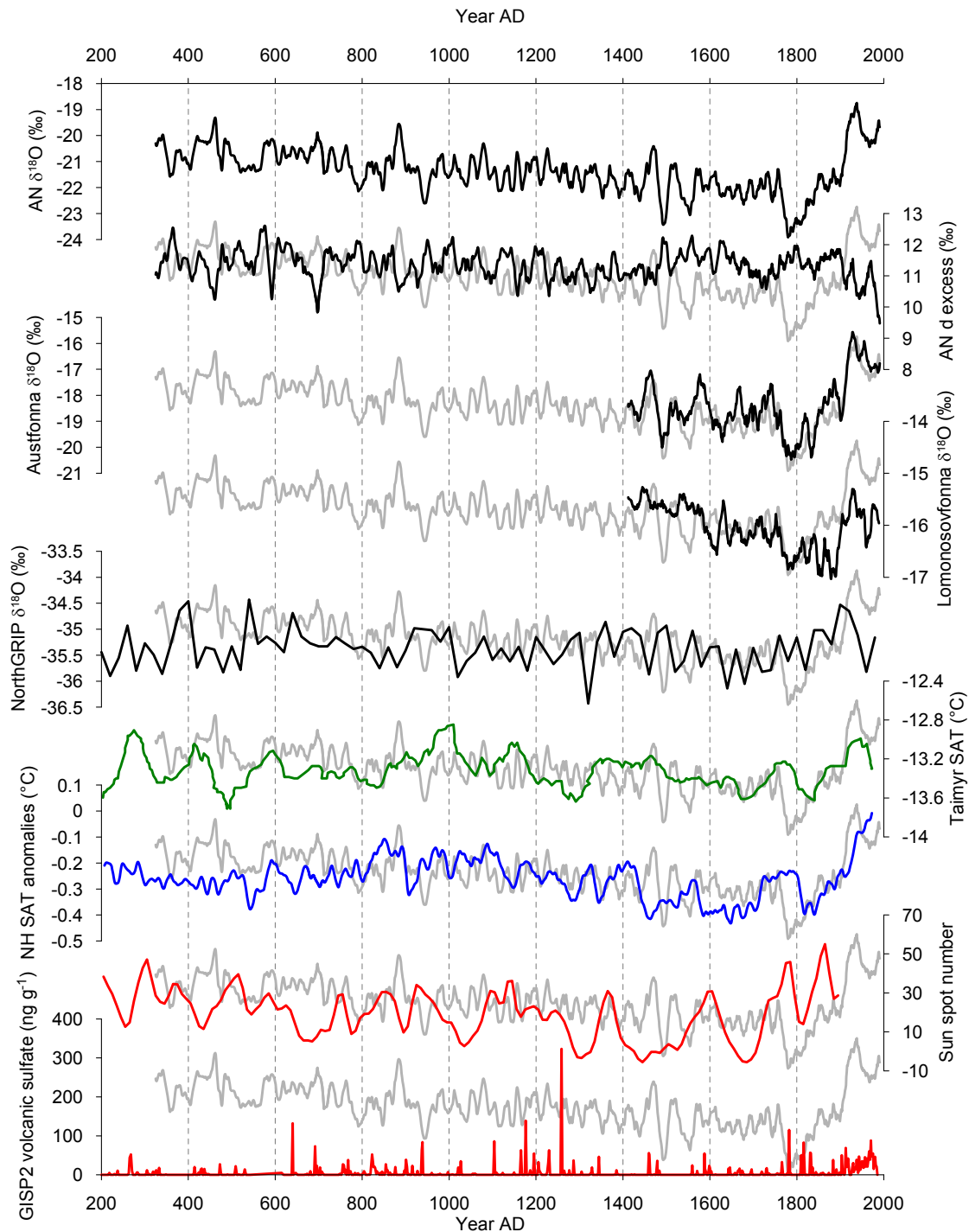


Figure 3.7: AN $\delta^{18}\text{O}$ and d records together with the Austfonna, Lomonosovfonna (Isaksson et al., 2005a) and NorthGrip (NorthGRIP members, 2004) $\delta^{18}\text{O}$ records, the annual Taimyr SAT (reconstructed from tree rings; Naurzbaev et al., 2002), the NH SAT reconstruction of Mann & Jones (2003), the reconstructed sun spot number record (Solanki et al., 2004) and the GISP2 volcanic SO_4 record (Zielinski et al., 1994). All records are displayed as 15yr values, except NorthGrip (20 year mean values), Taimyr (50 year smoothes), reconstructed sun spot numbers (10 year mean values) and GISP2 volcanic SO_4 (about bi-annual values). For a better comparison, AN $\delta^{18}\text{O}$ curve is added to each of the other curves on the same vertical scale as above.

The AN $\delta^{18}\text{O}$ record reveals striking similarities to that of Austfonna ice cap (Svalbard; Isaksson et al., 2005a) for the last 600 years including the rapid shifts in the 15th and 16th century (Figure 3.7) and to that of Vetreniy ice cap (FJL; Henderson, 2002; not shown) for the last 300 years. This includes decreasing temperatures from about AD 1750 to the common minimum at about AD 1800 followed by strongly increasing temperatures until the AD 1930s and lower temperatures thereafter. It is noteworthy that all three ice core locations are of a relatively low altitude (AN 750 m a.s.l., Austfonna 750 m a.s.l., Vetreniy 500 m a.s.l.). Therefore, we conclude that they record climate signals which are more representative for SAT changes on sea level in contrast to higher elevated ice-core sites. Although some general features are similar to the AN $\delta^{18}\text{O}$ curve, the $\delta^{18}\text{O}$ record from Lomonosovfonna (Svalbard, 1250 m a.s.l.; Figure 3.7) accordingly displays a distinctly different picture and appears to reflect free atmospheric climate signals (Isaksson et al., 2005b). Moreover, the range of $\delta^{18}\text{O}$ values is particularly broader for AN and Austfonna ice caps than for Lomonosovfonna (Figure 3.7), even though the Austfonna $\delta^{18}\text{O}$ record shows generally shifted values (about 3‰) compared to AN data, indicating the more maritime and warmer climate of Svalbard. The similarities of AN $\delta^{18}\text{O}$ values to the Austfonna and Vetreniy data and the good accordance with the Vardø and Arkhangelsk SAT time series indicate the common distinct climatic influence of the North Atlantic on this Eurasian Arctic region. Furthermore, it can be concluded that AN $\delta^{18}\text{O}$ data are a significant proxy for SAT changes in this region.

Due to the high altitude of the relatively isolated Central Greenland ice core sites, their $\delta^{18}\text{O}$ records, e.g. from NorthGRIP (NorthGRIP members, 2004), reflect atmospheric signals from higher atmospheric layers compared to AN ice cap. Consequently, the recorded temperature signals differ between both ice cores, i.e. the AD 1800 minimum and the AD 1930s maximum are not visible in the NorthGRIP record (Figure 3.7).

The AN $\delta^{18}\text{O}$ curve differs considerably from the multi-proxy derived SAT reconstruction for the Arctic (Overpeck et al., 1997; Figure 3.5). Even though both time series show similar general trends, distinct differences are detectable regarding the timing of major SAT minima and maxima. The Arctic time series exhibits a pronounced minimum at about AD 1840, some 40 years later than in AN data. Additionally, the double-peaked early 20th century maximum in AN $\delta^{18}\text{O}$ is

exceptional, whereas the Arctic reconstruction exhibits its maximum only in the AD 1950s. This indicates different climatic trends in the Central Russian and Western Eurasian Arctic as compared to the American Arctic, from which much more proxy records are available and included in the Overpeck time series. That lack of Eurasian Arctic proxy data in this Arctic SAT reconstruction as well as the pronounced differences compared to the Central Greenland ice cores emphasize the relevance of our AN $\delta^{18}\text{O}$ record for a regionalisation of paleoclimate information in the Arctic as well as in the whole Northern Hemisphere. This is underlined by the considerable discrepancies between the High Arctic AN $\delta^{18}\text{O}$ record and SAT reconstruction from nearby Taimyr Peninsula (Naurzbaev et al., 2002; Figure 3.7). Their tree-ring based time series represents a more continental climate owing to its more southern location and is dominated by summer temperatures which determine the vegetation period. Despite some minor similarities, the AN $\delta^{18}\text{O}$ time series furthermore differs significantly from the often used NH SAT reconstruction of Mann and Jones (2003; Figure 3.7), which is based only on a few proxy records that cover more than some centuries.

In contrast to several NH climate records (compiled e.g. in Jones and Mann, 2004; Wanner et al., 2008), the Russian Arctic SAT as deduced from AN $\delta^{18}\text{O}$ data, does not show evidence of pronounced long-lasting warmer (MWP) or colder (LIA) periods. In the AN $\delta^{18}\text{O}$ record, only the AD 1800 minimum and the subsequent warming could be interpreted as the termination of the LIA, whereas Northern Greenland ice core data indicate distinct climate cooling in the 17th and the first half of the 19th century (Fischer et al., 1998). The period AD 1700 to 1900 was the coldest of the last two millennia at the Hans Tausen Iskappe in Northern Greenland (Hammer et al., 2001). However, the period AD 1600 to 1750 in the AN $\delta^{18}\text{O}$ is characterised by a marked low variability, while the preceding 15th and 16th centuries show evidence of strong SAT changes (up to 3‰ within two to three decades for 15yr values), visible also in the AN d excess and sea salt ion data (Figure 3.6) and the Austfonna $\delta^{18}\text{O}$ record (Figure 3.7). The rapid warming (cooling) events are accompanied by increasing (decreasing) sea salt aerosol deposition (see above), indicating a sea-ice response on the SAT changes or vice versa. These rapid SAT changes affected at least the Western Eurasian Arctic from Svalbard to SZ.

Similar rapid changes occurred e.g. around AD 1750 and AD 1920 (up to 4‰ within a few years for 5yr values; Figure 3.5). This indicates drastic changes in Eurasian Arctic SAT, which could have been caused by short-term variations of the forcing factors or by internal climate variability. A few AN $\delta^{18}\text{O}$ minima coincide with major volcanic eruptions, e.g. the absolute minimum $\delta^{18}\text{O}$ AD 1784/85 with the Laki eruption AD 1783 and a minimum at about AD 1815 with the Tambora eruption AD 1815 (Figures 3.5 and 3.7), possibly indicating the importance of volcanic forcing for Eurasian Arctic SAT, at least in terms of short-term variability. However, other major volcanic eruptions, e.g. AD 1259, are not accompanied by rapid cooling events in AN $\delta^{18}\text{O}$ (Figure 3.7). Since prominent maxima and minima in the solar forcing (expressed as sun spot number) also does not coincide with major SAT changes (Figure 3.7), internal climate variability seems to be responsible for the rapid changes in the AN $\delta^{18}\text{O}$ record. This assumption is supported by climate modelling results for the late 15th century (Crespin et al., 2009) and early 20th century warming events (Bengtsson et al., 2004). These studies indicate that changes in the atmospheric circulation may have led to these warming events, probably caused by stronger Icelandic Low and Siberian High as proposed e.g. for the 15th and 16th century (Mayewski et al., 2004; Maasch et al., 2005).

The melt-layer content in the AN ice core is not useable as regional SAT proxy as it predominantly reflects the local snowmelt and infiltration conditions at the ice caps surface, which are determined not only by the temperature but by the energy balance in general. Most likely, the discrepancies between melt-layer content and $\delta^{18}\text{O}$ (Figure 3.5) are caused by different seasonal temperature trends, as evident for the early 20th century warming events (Opel et al., 2009b). However, the AN ice core exhibits a distinctly higher melt-layer content in the 20th century compared to the preceding centuries (Figure 3.5). This is similarly evident in the melt-layer records of Austfonna ice cap (Watanabe et al., 2001) and Vetreniy ice cap (Henderson, 2002). Considerable differences between these records in contrast to similar $\delta^{18}\text{O}$ records underline the limited spatial significance of the melt-layer contents.

Generally, high (low) d excess values are caused by high (low) SST and/or by low (high) relative humidity during evaporation (Johnsen et al., 1989). Provided that the moisture source region does not undergo substantial spatial changes in the

considered time period, variations of d excess can be interpreted in terms of changing SST and relative humidity conditions (Hoffmann et al., 2001). If we assume additionally nearly constant annual mean values of relative humidity in the moisture source region, variations of d excess may be mainly related to SST variations (Hoffmann et al., 2001). We consider the North Atlantic to be the main moisture source for AN ice cap. However, the North Atlantic (0-70°N) SST time series (Gray et al., 2004) shows only minor similarities with the AN d excess record, e.g. between AD 1780 and 1850 (Figure 3.5). This indicates that changes in the AN d excess record cannot primarily be related to the mean North Atlantic SST. Consequently, other factors such as changes of the main moisture source region, of moisture transport pathways, of relative humidity conditions during primary evaporation or of changing contributions of different moisture sources (e.g. regional moisture) have to be taken into account.

The evident opposite characteristics of $\delta^{18}\text{O}$ as regional SAT proxy and d excess for large sections of the record (Figures 3.5 and 3.7) indicate that in warmer periods the precipitation-forming moisture was generated at lower SST than in colder periods. This indicates that the mean AN d excess values are significantly influenced by the contribution of regional moisture, evaporated at distinctly lower SSTs compared to the North Atlantic, on. For the 20th century such a relation between a decline in the sea ice extent of the Kara Sea and an increasing contribution of regional moisture to the precipitation at AN leading to lower d excess values has already been proposed (Opel et al., 2009b). However, it must be stated that the most prominent minima in AN d record, which would indicate the highest proportion of regional moisture, did not occur in the warmest periods (Figures 3.6 and 3.7).

A comparison of AN d excess data with that of Central Greenland (Hoffmann et al., 2001) and of Lomonosovfonna (the only Arctic d excess record outside of Greenland; Divine et al., 2008) reveals significant differences. Only the 20th century decrease is also detectable in the Central Greenland record. This indicates considerable differences in moisture generation and transport patterns, probably also influenced by the different ice caps altitude and therefore different dominating atmospheric layers. Divine et al. (2008) relates the d excess variation in the Lomonosovfonna ice core to SST variability of a distinct North Atlantic region, whereas the contribution of regional moisture is of minor significance.

All studied major ions show evidence for distinctly elevated values in the 20th century. Sulphate and nitrate reflect primarily the anthropogenic pollution of the Eurasian Arctic with rising values after about AD 1950 and a strong decline after AD 1980 (Weiler et al., 2005, Opel et al., 2009b), also prominent in the Svalbard (e.g. Kekonen et al., 2005) and FJL (Henderson, 2002) ice cores. However, the sea-salt ions had started to increase already at about AD 1910, some years before the strong warming recorded in AN $\delta^{18}\text{O}$ record, and decreased again since about AD 1950. This pattern of sea-salt ions does not fit to the record of sea-ice extent anomalies in the Kara and Laptev Seas (Polyakov et al., 2003a, see also Opel et al., 2009b), indicating that the regional sea-ice extent changes do not play a major role concerning these sea-salt ion changes, even though the sea-ice record may be biased due to a lower data density in the early 20th century. A loss of ions by melting and runoff as cause for the 20th century decrease is unlikely, as this decrease is accompanied by a strong decrease in melt-layer content (see Figure 3.5). As similar sea-salt ion patterns have also been detected in the Austfonna (Watanabe et al., 2001) as well as Vetreniy ice cores (Henderson, 2002), considerable large-scale changes of dominating air masses or storm tracks may have caused this sea-salt ion pattern. These atmospheric circulation changes, in turn, may have been caused by internal climate variability, i.e. a changing Icelandic Low (Kekonen et al., 2005) and a stronger Siberian High (Maasch et al., 2005) and related to the early 20th century warming event (Bengtsson et al., 2004), which has started some years after the strong rise in sea-salt ion concentrations.

3.6 Conclusions

This study has presented new paleoclimatic records from the upper 535 m of a recently drilled ice core from AN ice cap on SZ, covering about 1 700 years. It has been shown that even though AN ice cap is characterised by melt water infiltration, high resolution records can be obtained.

AN ice cap is much younger than assumed before the start of the Severnaya Zemlya ice-core project and it has been growing at least over large parts of the Late Holocene as reflected by long-term decreasing $\delta^{18}\text{O}$ and sea-salt ion data. Consequently, the combination of volcanic reference horizons and stable-isotope annual layer counting is more suitable for dating than simple ice-flow models.

The AN $\delta^{18}\text{O}$ curve reveals striking similarities with instrumental SAT (Vardø) and $\delta^{18}\text{O}$ ice core (Austfonna, Svalbard) records. These similarities underline the significance of $\delta^{18}\text{O}$ data from the relatively-low altitude AN ice cap as a sensitive regional SAT proxy for the Western Eurasian Arctic. This is particularly important as the climate history of this region differs considerably from that of other Arctic and NH records. AN $\delta^{18}\text{O}$ data show no evidence for pronounced warmer (MWP) or colder (LIA) time periods. The absolute SAT minimum around AD 1800 is followed by an unprecedented increase to the double-peaked early 20th century maximum, which represents the warmest period in the entire ice core record.

The ion contents are dominated by ions of sea-salt origin. Generally, warmer periods are characterised by higher sea-salt ion concentrations, indicating a more efficient deposition, possibly due to less sea-ice extent.

The variations in d excess can not primarily be related to SST variations of the North Atlantic, but seem to reflect the varying moisture contribution of the surrounding seas as regional sources.

Rapid changes, e.g. in the 15th/16th and early 20th centuries, detected in stable isotope and sea-salt ion data, indicate major shifts in atmospheric circulation as well as sea ice patterns, possibly caused by internal climate variability.

Acknowledgements

The drilling project was funded by the German Ministry of Education and Research (03PL027A/3). This study was partly funded by a NaFöG PhD scholarship from the state of Berlin. We thank all the people who have contributed to the Severnaya Zemlya ice-core project, particularly the joint Russian-German drilling team for drilling the ice core. Anika Schmidt, Birthe Twarloh and Lutz Schönicke greatly supported the sampling and analytical work.

4 Paleoclimatic information from stable water isotopes of Holocene ice wedges at the Dmitrii Laptev Strait (Northeast Siberia)

Thomas Opel^{1,2}, Alexander Yu. Dereviagin³, Hanno Meyer¹, Lutz Schirrmeister¹, Sebastian Wetterich¹

¹Alfred Wegener Institute for Polar and Marine Research, Telegrafenberg A43, 14473 Potsdam, Germany

²Department of Geography, Humboldt-Universität zu Berlin, Unter den Linden 6, 10099 Berlin, Germany

³Faculty of Geology, Moscow State University, 119899 Moscow, Russia

Permafrost and Periglacial Processes. Resubmitted after minor revisions

Abstract

To gain paleoclimatic signals, we studied ice wedges at the Dmitrii Laptev Strait (Oyogos Yar Coast, 72.7°N, 143.5°E). In this paper, we present data on the stable isotope composition ($\delta^{18}\text{O}$, δD , d) of actively growing Holocene ice wedges in a vast thermokarst depression. Three 2.5 to 3.5 m wide ice wedges were sampled in high resolution (100 to 200 samples each). AMS ^{14}C ages prove the Late Holocene age of the studied horizontal ice wedge profiles, indicating a growth syngenetically to sediment accumulation. We assume that the initial ice wedge growth started in the Early Holocene (ca. 8-9 ka BP) after drainage of a thermokarst lake. The ice wedges' co-isotopic relationships close to the GMWL point to a good suitability for paleoclimate studies. All three profiles show similar isotopic features. $\delta^{18}\text{O}$ data reflect a Late Holocene winter warming trend from about -26‰ to values of -23‰ to -21‰, superimposed by a marked variability. This trend is accompanied by a shift in the d excess from 8‰-11‰ to 5‰-8‰, probably caused by varying proportions of different moisture sources to the precipitation. The highest winter temperatures and an increased influence of regional moisture in the last decades may reflect ongoing Arctic climate change.

4.1 Introduction

The Arctic is a key region of climate change as it has experienced one of the greatest temperature rises in the 20th and 21st centuries (ACIA, 2005, Trenberth et al., 2007). For the future, a strong temperature increase and a strong retreat of sea ice as well as permafrost warming are predicted (e.g. ACIA, 2005, Christensen et al., 2007, Lemke et al., 2007). The Arctic itself influences the global climate system by changes in surface albedo and ocean currents as well as carbon release from thawing permafrost. Understanding the ongoing climate change and improving climate predictions requires detailed information about past changes. But direct meteorological observations started mostly in the 20th century, only a few records reach back into the 19th century (e.g. Polyakov et al., 2003b). Therefore, the use of paleoclimatic archives is valuable for the reconstruction of past climate variations.

As compared to the better studied Central Russian Arctic, where several records from ice cores (Severnaya Zemlya, e.g. Opel et al., 2009b; Franz Josef Land, Henderson, 2002), lake sediments (Severnaya Zemlya, Raab et al., 2003; Taimyr peninsula, e.g. Andreev et al., 2003) as well as tree rings (Taimyr peninsula, e.g. Naurzbaev et al., 2002) provide paleoclimatic information for the last centuries to millennia, such archives are not present (ice cores, tree rings) or less available (lake sediments) in the vicinity of Dmitrii Laptev Strait (Northeast Siberia). Thus, we use ice wedges in order to obtain paleoclimatic information.

Northeast Siberia is characterised by ice-rich permafrost deposits that provide a paleoclimate archive, including paleoecological proxies such as pollen (e.g. Andreev et al., 2009), ostracods (e.g. Wetterich et al., 2009), chironomids (e.g. Ilyashuk et al., 2006) and plant macro fossils (e.g. Kienast et al., 2008). The frozen ground contains different types of ice that are summarised as ground ice (van Everdingen 1998, revised 2005). Since ground ice is mostly fed by precipitation, the stable water isotope composition can be used for paleoclimatic reconstructions (Vaikmäe, 1989). Ice wedges are the most abundant type of ground ice in the ice-rich permafrost deposits of Northeast Siberia and the most suitable ground ice type for such stable-isotope based paleoclimatic studies (e.g. Vaikmäe, 1989; Vasil'chuk, 1991, 1992).

In the last decade, ice wedges in the Laptev Sea region in Northeast Siberia have been used in a variety of Russian-German cooperative paleoclimate studies.

These stable-isotope based studies focused on modern ice wedge growth (Dereviagin et al., 2002) as well as on the classification and interpretation of different ice wedge generations, resulting in overview winter temperature trends for the last 60 ka (Meyer et al., 2002a; 2002b; in preparation a).

Following a pilot study in 2002 (Schirrneister et al., 2003a), a variety of paleoclimatological, paleoecological and sedimentological investigations was carried out at the Oyogos Yar Coast of the Dmitrii Laptev Strait within the scope of the joint Russian-German expedition “Lena – New Siberian Islands” in August 2007 (Schirrneister et al., 2008a). As one approach to gain paleoclimatic information, we studied ice wedges of different sedimentological and geochronological units. In this paper, we present stable isotope data of Holocene and recent ice wedges, whereas the Pleistocene ice wedges of different stratigraphical units will be subject of an upcoming study. Here, we focus on the detection and interpretation of isotopic variability, the comparison with other regional ice wedge data and the paleoclimatic implications.

4.2 Ice wedges and stable isotopes

Polygonal ice wedge formation is based on a combination of frost cracking and freezing processes. In winter time, frost cracking occurs in the upper permafrost layers due to thermal contraction caused by rapid cooling at very low temperatures (Lachenbruch, 1962), mostly between mid-January and mid-March (Mackay, 1974). In spring, elementary ice veinlets form, when snow-melt water trickles down into the frost cracks and refreezes there. Periodic repetitions of these cracking-freezing-cycles lead to a gradual horizontal ice wedge growth, even though the crack frequency may vary considerably (Mackay, 1974; 1992). Thereby, ice wedges crack preferentially near the centre and often year by year at the same location (Mackay, 1974).

The stable water isotope composition of precipitation is determined by several fractionation processes. However, due to their dependence on condensation temperatures, the stable isotope ratios $\delta^{18}\text{O}$ and δD are commonly accepted as suitable proxies for local to regional scale temperatures in polar latitudes (e.g. Rozanski et al., 1993). The deuterium excess d ($d = \delta\text{D} - 8 * \delta^{18}\text{O}$), introduced by Dansgaard (1964), reflects the evaporation conditions in the moisture source region. Stable water isotope ratios, such as that from ice cores (e.g. North

Greenland Ice Core Project (NorthGRIP) Members, 2004), are widely used for paleoclimate reconstructions. It is generally accepted that melting of snow is the main source for ice wedge ice (Mackay, 1983; Vaikmäe, 1989; Vasil'chuk, 1991, 1992). Consequently, the stable water isotope composition of ice wedges can be interpreted as proxy for past winter temperatures and can be used for the reconstruction of paleotemperature trends as well as of moisture generation and transport patterns (Meyer et al., 2002a, 2002b). According to Michel (1992), melt water in a frost crack refreezes rapidly enough to prevent fractionation. An elementary ice vein represents the refrozen precipitation of a discrete winter and preserves therefore its specific isotope signal. Assuming regular frost cracking and subsequent formation of an elementary ice vein, ice wedges should contain a continuous stable isotope time series. Studies of Vasil'chuk (1992) and Nikolayev and Mikhalev (1995) reveal that stable isotope ratios of ice wedges can be correlated with mean annual winter and January temperatures.

4.3 Study region

Oyogos Yar is the southern coast of the Dmitrii Laptev Strait, which connects the Laptev and the East Siberian Seas, and divides the Bol'shoy Lyakhovsky Island from the Eurasian mainland (Figure 4.1). Since the 19th century, the coasts of the Dmitrii Laptev Strait have been of geographical and geological interest (e.g. Bunge, 1887; von Toll, 1895). However, detailed geocryological and paleoenvironmental studies at the Oyogos Yar Coast started much later, not before the second half of the 20th century (e.g. Gravis, 1978; Konishchev and Kolesnikov, 1981).

This region builds the northern part of the Yana-Indigirka lowland and belongs to the zone of continuous permafrost with a thickness of 400 to 600 m. The mean annual ground temperature is about -12 to -14°C (Yershov, 1989), the mean thickness of the active layer accounts for about 40 cm. Along the coasts of the Dmitrii Laptev Strait, frozen sediments of different ages and accumulation types are exposed in steep bluffs, which have been subject of paleoclimatological and paleoecological investigations (e.g. Andreev et al., 2009; Wetterich et al., 2009).

Long severe winters and short cold and rainy summers characterise the climate of the Oyogos Yar Coast. From data of the nearest meteorological stations Cape Shalaurova, Cape Kigilyakh (both at Bol'shoy Lyakhovsky Island) and Cape

Svyatoy Nos (west of Oyogos Yar) we conclude for Oyogos Yar a mean annual air temperature of about -15°C , with mean winter and summer temperatures of about -21.5°C and 1.5°C . The mean annual precipitation is about 150-200 mm with more than 60% in the summer season. Snow accumulation starts in September-October and reaches its mean maximum of about 20-25 cm in spring.

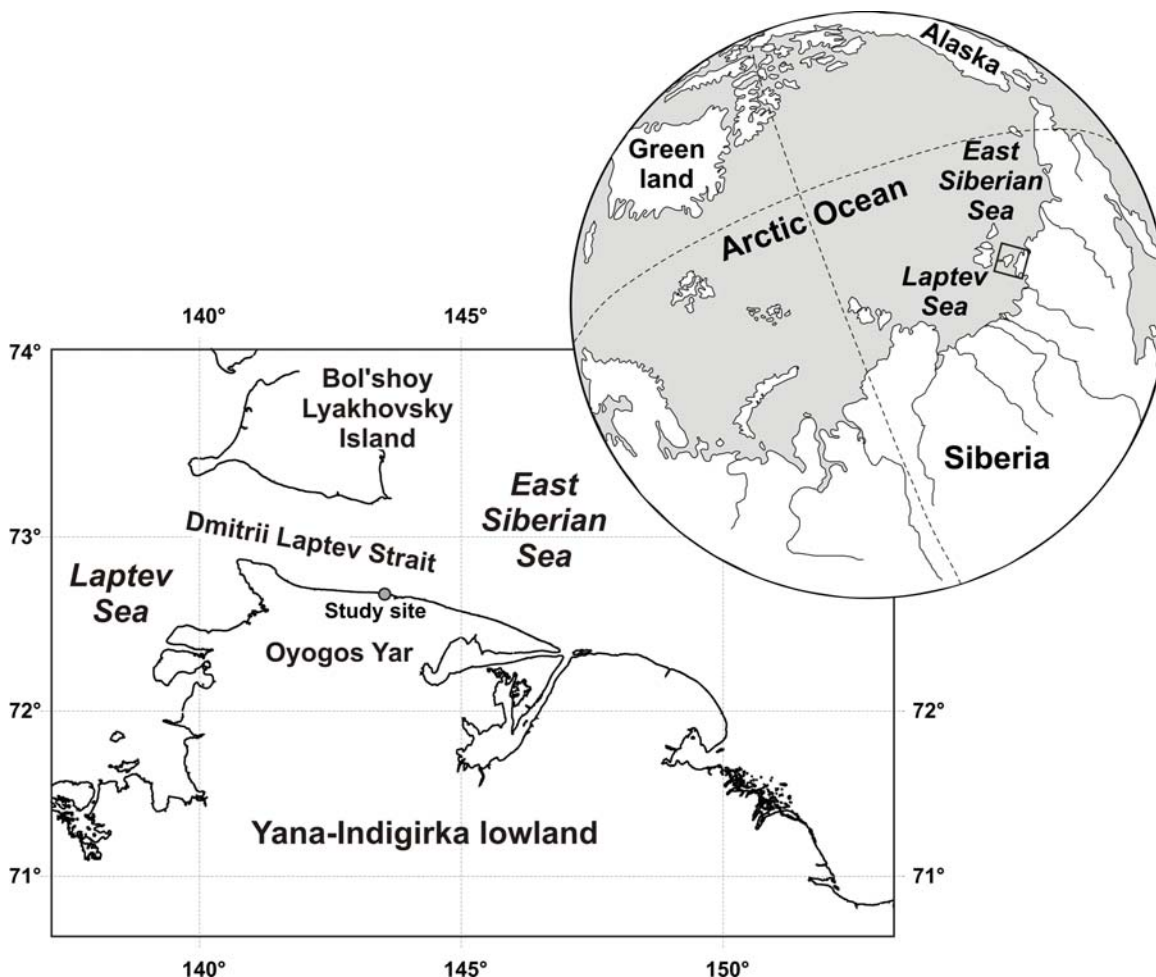


Figure 4.1: Overview map of the study site at the Oyogos Yar coast of the Dmitrii Laptev Strait.

The modern relief of the Oyogos Yar Coast region is characterised by an alternation of wide thermokarst depressions (Alases) and hills of Ice Complex remains (Yedoma). Thermokarst depressions reach about 5-10 km in diameter and have a flat bottom surface with numerous ponds and small thermo-erosional valleys with creeks and brooks. The Alas surface is characterised by nets of ice wedge polygon systems with a size of 10 to 20 m. Whereas the Alas bottoms reach altitudes of about 8-12 m a.s.l., the maximum elevation of the adjacent Ice Complex hills is about 40 m a.s.l. A typical sediment sequence of the studied Alas exposures at the Oyogos Yar Coast (72.7°N , 143.5°E ; Figure 4.1) shows a

subdivision in three parts (Wetterich et al., 2009). Taberal (thawed and refrozen) Weichselian Ice Complex deposits are overlain by sediments of the Late Glacial and Holocene Alas stage: Lacustrine sediments with ice wedge casts are covered by a characteristic peat horizon and further upward boggy deposits, all consisting dominantly of poorly-sorted silt with peat inclusions and plant detritus (Figure 4.2).

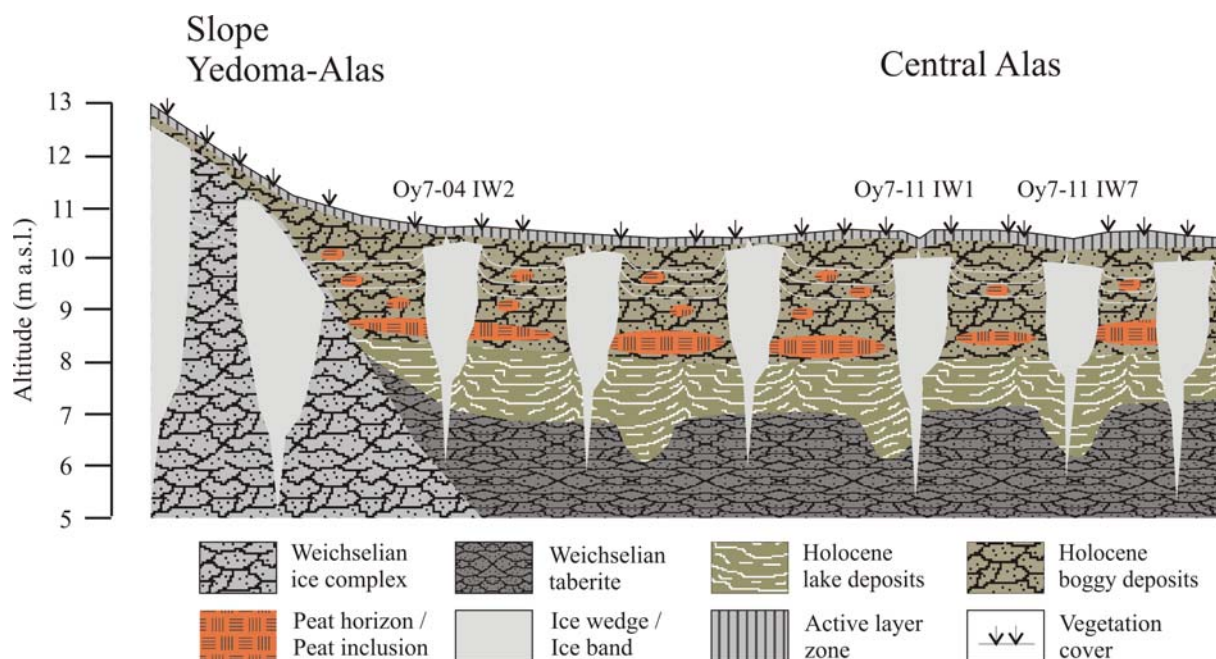


Figure 4.2: General stratigraphic situation of the Oyogos Yar study site with the Alas depression and the slope to the Yedoma hill. Included are the approximate locations of the studied ice wedges.

4.4 Material and Methods

4.4.1 Sampling and field measurements

After an overview survey along the coastal bluff which cuts the thermokarst depression, we selected the studied ice wedges according to the best perpendicular cut. Steep walls of permafrost outcrops and extensive mudflows limited the accessibility of the ice wedges and complicated the fieldwork. Before sampling, we described, photographed and sketched the selected ice wedges. In total, we studied eight Holocene ice wedges, from three of them also the most recent part separately, and from six additional ice wedges only the recent parts (recent ice veins, indicating modern growth).

The ice wedges were sampled using a chain saw, a special ice screw (diameter 15 mm, length 150 mm) or an axe, depending on the ice wedge size and the sampling strategy. We sampled two horizontal high-resolution profiles by chain

saw, cutting thin ice slices (about 2-3 cm). After cutting, the samples were cleaned to prevent contamination. The ice wedge samples (N=292) were melted on site. For stable water isotope analyses melt water was stored in 30 ml PE bottles, which were completely filled and tightly closed to avoid evaporation. We collected organic material contained in the melted samples (plant remains, lemming coprolites) for age determination (^{14}C AMS). From selected samples melt water was taken for hydrochemical characterisation of the ice wedges. A part was filtered and collected in 8 ml and 15 ml HDPE flasks for measurements of anion and cation concentrations, respectively. We determined pH and electrical conductivity (EC) with a handheld multi-parameter instrument (WTW 340i) equipped with appropriate sensors (pH: SenTix 41; EC: Tetracon 325) in the field camp.

For a third high resolution profile, we cut blocks (length ca. 20-25 cm) from the ice wedge, which were transported in frozen state to the Alfred Wegener Institute (AWI) Potsdam and sampled there in the cold lab.

Additionally, fresh precipitation samples (N=33) as well as samples of snow patches from the last winter (N=2) were collected for measurements of stable water isotopes and stored in the same way as ice wedge samples.

4.4.2 Laboratory methods

For all samples, the oxygen ($\delta^{18}\text{O}$) and hydrogen (δD) stable isotope ratios were analysed at the stable isotope lab of AWI Potsdam, using a Finnigan MAT Delta-S mass spectrometer. Both isotope ratios were determined for the same water sample, using equilibration techniques. The values are expressed in delta per mil notation (δ , ‰) relative to the Vienna Standard Mean Ocean Water (V-SMOW). The analytical precision is better than $\pm 0.1\text{‰}$ for $\delta^{18}\text{O}$ and $\pm 0.8\text{‰}$ for δD (Meyer et al., 2000).

Plant remains of selected ice wedge samples were radiocarbon-dated using the Accelerator Mass Spectrometry (AMS) facilities at the Leibniz Laboratory for Radiometric Dating and Stable Isotope Research (Kiel University, Germany). Details on the AMS facility in Kiel were published by Nadeau et al. (1997, 1998). Conventional ^{14}C ages were calculated according to Stuiver and Polach (1977). For the determination of calibrated ages, the IntCal04 data set (Reimer et al., 2004) was used.

For a hydrochemical characterisation, we analysed selected ice wedge samples for ion concentrations in the hydrochemistry lab of AWI Potsdam. The anion concentrations were determined by means of an Ion Chromatography (IC, Dionex-320), whereas cation concentrations were analysed using Inductively Coupled Plasma Optical Emission Spectrometry (ICP-OES, Perkin-Elmer Optima 3000 XL).

4.5 Isotopic composition of recent precipitation

To characterize the modern stable water isotope environment of the study region, we used samples from all precipitation events as well as from snow patches. Due to the late summer field season, only two snow patch samples could be taken in deep cracks along the coastal cliff, whereas a lot of rain samples were collected in the four weeks of field work. Statistical features on the stable isotope composition of these samples can be drawn from Table 4.1. The scatter of these data is displayed in a $\delta^{18}\text{O}$ - δD diagram (Figure 4.3). It exhibits a wide range, representing extreme values of the seasonal isotope and temperature variation.

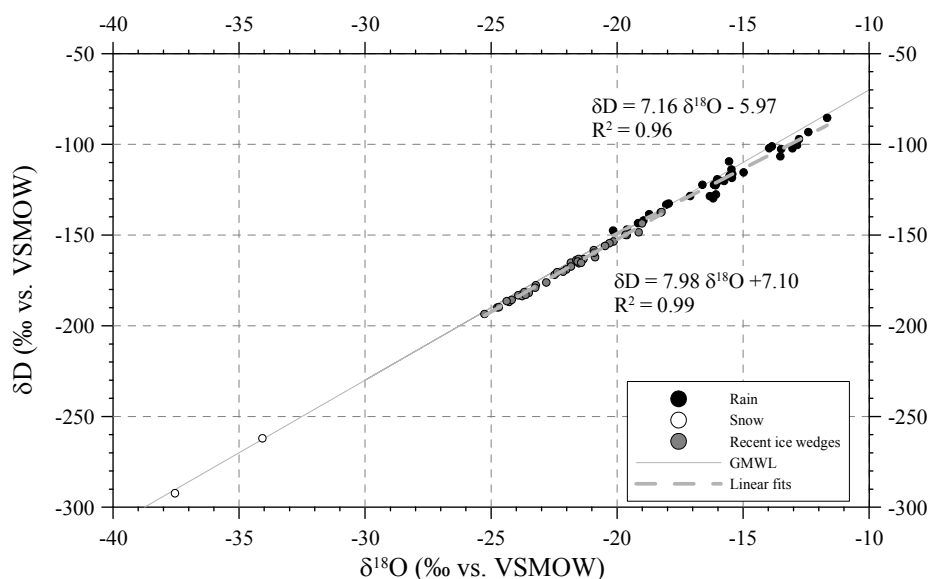


Figure 4.3: $\delta^{18}\text{O}$ - δD diagram for samples of snow patches, recent ice wedges and rain water. GMWL is the Global Meteoric Water Line.

The isotope data of the rain samples (N=33) vary between -20.2‰ and -11.7‰ for $\delta^{18}\text{O}$ and -147.5‰ and -85.4‰ for δD , with mean values of -15.8‰ and -119.0‰ , respectively. The d excess varies between -0.2‰ and 15.1‰ with a mean of 7.3‰ . The co-isotopic relationship as displayed in the $\delta^{18}\text{O}$ - δD -diagram (Figure 4.3) accounts for $\delta\text{D} = 7.16 \delta^{18}\text{O} - 6.0$ ($R^2=0.96$), which is deviated from the Global

Meteoric Water Line (GMWL), theoretically defined as $\delta D = 8 \delta^{18}O + 10$ (Craig, 1961) and calculated on a global scale as $\delta D = 8.17 \delta^{18}O + 10.35$ (Rozanski et al., 1993). However, Meyer et al. (2002b) found a similar slope of 6.8 for Bol'shoy Lyakhovsky Island summer precipitation. The deviation from the GMWL as well as the highly variable d excess point to the occurrence of kinetic fractionation processes for summer precipitation. These processes may be connected with a mixing of air masses bearing moisture from sources that differ isotopically from the North Atlantic Ocean, the assumed main moisture source (Kuznetsova, 1998). Presumably, such moisture originates from recycled water, i.e. from the continental tundra ponds and lakes as well as from the active layer. As shown by Kurita et al. (2004), the isotopic composition of precipitation in Siberia is largely influenced by such recycling of continental water. Evaporation from the ice free Laptev and East Siberian Seas could increase the proportion of regional moisture. Generated at relatively cold temperature conditions, this moisture proportion might lead to lower d excess values as similarly deduced for the Akademii Nauk ice core (Severnaya Zemlya; Opel et al., 2009b). Due to its position relatively close to the Pacific Ocean, Pacific moisture might contribute to the precipitation reaching the study region as well.

The snow-patch samples as reference of the winter precipitation show very low isotope values of -37.6‰ and -34.1‰ for $\delta^{18}O$ (-292.3‰ and -262.0‰ for δD), with d excess values of 8.1‰ and 10.6‰ (Table 1). The co-isotopic relationship of $\delta D = 8.72 \delta^{18}O + 35.26$ ($R^2=1$) is not significant due to the limited sample number ($N=2$). However, the d excess values plot close to the GMWL, thus indicate no considerable participation of kinetic fractionation. This is most probably caused by the isolated location of these snow patches, preventing substantial sublimation. The very light isotope values point to extreme precipitation events, since they exceed the lower end of the range of snow patch samples known from Bol'shoy Lyakhovsky Island ($\delta^{18}O$: -31.4‰ to -16.1‰, mean: -26.3‰; δD : -239.0‰ to -125.6‰, mean: -198.7‰) on the northern shore of the Dmitrii Laptev Strait about 100 km NW of our study site (Meyer et al., 2002b). However, East Siberian Arctic winter precipitation exhibits a wide scatter of stable isotope composition as shown by Kurita et al. (2005) and Kloss (2008). For the site Tiksi southeast of the Lena Delta at the central Laptev Sea coast (about 500 km west of Oyogos Yar), isotope data of snow samples on a daily basis range from -46.1‰ to -9.7‰ (mean: -

28.7‰) for $\delta^{18}\text{O}$ and -359.4‰ to -94.3‰ (mean: -225.6‰) for δD (Kloss, 2008). Therefore, the presented snow patch stable isotope data fit well into the regional winter isotopic pattern, even though they seem to represent single precipitation events at very low temperatures.

4.6 Isotopic composition of recent ice wedges

For an isotopic characterisation of the modern ice wedge growth, we sampled the most recent parts from nine ice wedges, i.e. a collection of elementary ice veins penetrating from the permafrost table into the ice wedge due to modern frost cracking. We took samples from the parts overtopping the ice wedge as well as from corresponding parts located in the actual ice wedge body (Figure 4.4). The occurrence of such recent ice-vein assemblages points to extensive thawing in recent times (the last decades). This thawing led to a considerably increased thickness of the active layer whose lower part refroze afterwards. Due to the field work period in late summer we were not able to sample the elementary ice vein of the last winter/spring, but the mentioned collection of ice veins, formed after the last extensive thawing event. These recent ice veins may also be interpreted as a new ice wedge generation. The assemblages of recent ice veins were between 2 and 8 cm wide (Figure 4.4), overtopping the ice wedge by about 10 to 15 cm and containing 6 to 30 elementary ice veins; in so far as single veins were distinguishable. Elementary ice veins reached a thickness of up to 3 mm, mostly varying between 0.5 and 2 mm. These recent veins consisted mostly of white, milky ice, characterised by a lot of small air bubbles and some mineral inclusions, but also clear ice veins were visible. In total, we took 38 samples of such recent ice wedges.

The isotopic composition of the recent ice wedges ranges from -25.3‰ to -18.2‰ (mean: -22.0‰) for $\delta^{18}\text{O}$ and from -193.5‰ to -137.3‰ (mean: 168.1‰) for δD (Table 1). As expected, the δ values are located between the extreme winter and summer precipitation data (Figure 4.3), but relatively near to the summer samples. Probably, recent frost cracks were fed by melt water from later stages of snow melt, characterised by a heavier isotopic composition compared to the initial snow (Lauriol et al., 1995; Meyer et al., 2002b). Due to the sparse and extreme light winter samples it is not possible to connect their stable isotope composition directly to that of recent ice wedges. However, the isotope values of recent ice

wedges coincide well with isotope data of recent ice veins at Bol'shoy Lyakhovsky Island ($\delta^{18}\text{O}$: -22.5‰ to -19.2‰, mean: -20.4‰; δD : -175.5‰ to -149.2‰, mean: -158.9‰), which exhibit a connection to winter precipitation (Meyer et al., 2002b, Dereviagin et al., 2002).

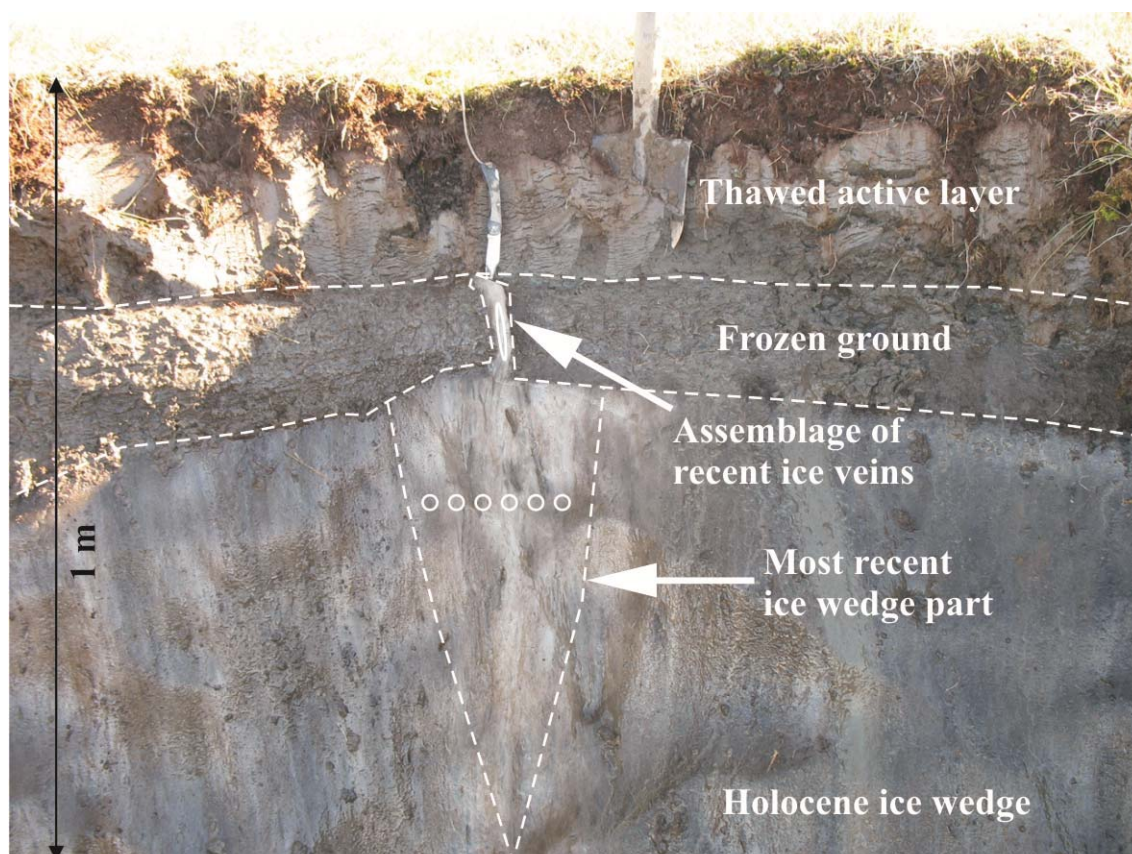


Figure 4.4: Example of recent ice wedge growth in ice wedge Oy7-11 IW7 as considered in this study: assemblage of recent ice veins overtopping the ice wedge and corresponding parts located in the actual ice wedge body. Circles and ellipse mark sample points.

In the $\delta^{18}\text{O}$ - δD diagram (Figure 4.3), recent ice wedge data of Oyogos Yar display a slope of 7.98 and an intercept of 7.1, parallel to the GMWL. This indicates that the mean isotopic composition of recent ice wedges was not considerably affected by kinetic fractionation during sublimation of snow, melt water percolation through the snowpack, or refreezing of melt water in the frost crack. From that and the similarity of our data to the nearby study site at Bol'shoy Lyakhovsky Island, we conclude that the stable isotope composition of Oyogos Yar recent ice wedges is mainly determined by the mean isotopic composition of the winter precipitation. However, d excess values, varying between 4.7‰ and 9.5‰ (mean: 7.6‰), are slightly shifted below the GMWL. This shift points to the possibility that additional

moisture sources besides the North Atlantic Ocean, presumably the main moisture source, have contributed to the precipitation at Oyogos Yar. Following Kuznetsova (1998), the boundary between prevailing western and eastern flows in Northern Eurasia, transporting Atlantic and Pacific moisture respectively, is located between 130° and 150°E in winter. Therefore also Pacific moisture could have contributed to the ice wedge feeding winter precipitation at Oyogos Yar Coast (Kurita et al., 2005) as could have polynyas (areas of open water) in the generally ice covered Laptev or East Siberian Seas.

4.7 Holocene ice wedges

4.7.1 Description

The following results are mainly based on high resolution profiles of three ice wedges but consider also samples taken from other Holocene ice wedges. The ice wedge Oy7-04 IW2 was located in the transition zone from the Yedoma-Alas-slope to the Alas bottom, whereas the ice wedges OY7-11 IW1 and Oy7-11 IW7 were located in the central Alas depression (Figure 4.2). All ice wedges were sampled at the coastal bluff at an altitude of about 10 m a.s.l. At the altitude level of the sampling profile the studied ice wedges were enclosed by the typical boggy Alas deposits: dominating grey silts with varying amounts of clay and sand with some peat inclusions. At the contact zone with the ice wedges, brownish layers were observed. These sediments were characterised by a banded as well as a regular to non-regular reticulate cryostructure. The vertical distances between single horizontal ice belts (2-5 cm thick) were about 10-20 cm. Close to the ice wedges the ice belts were bent upwards indicating an ice wedge formation syngenetic to the accumulation of the surrounding sediment layers. In general, the ice wedges were overlain by 35-70 cm of sediment, mainly grey-brownish silty loams, covered by a layer of peaty soil. Whereas the uppermost 20-40 cm of sediments were attributed to the active layer, the frozen transition zone between ice wedge and active layer accounted for 10-30 cm.

Table 4.1: Stable isotope ($\delta^{18}\text{O}$, δD and d) minimum, mean and maximum values, standard deviations as well as slopes and intercepts for all sampled ice wedges and for recent precipitation samples at the Oyogos Yar Coast.

Ice wedge	Remarks	N	$\delta^{18}\text{O}$ (‰)		$\delta^{18}\text{O}$ (‰)	δD (‰)	δD (‰)		d (‰)	d (‰)	slope	intercept	R^2				
			min	mean			max	sd						min	mean	max	sd
Oy7-04 IW2	horizontal profile	104	-27.09	-25.10	-21.59	1.26	-207.8	-192.0	-164.2	9.6	6.2	8.8	11.3	1.1	7.58	-1.83	0.99
Oy7-11 IW1	horizontal profile	119	-26.64	-25.01	-21.62	1.03	-203.9	-192.1	-167.2	7.8	5.1	8.0	9.8	0.9	7.59	-2.19	0.99
Oy7-11 IW7	horizontal profile	193	-26.53	-24.99	-20.73	0.91	-203.2	-192.3	-159.9	7.1	4.8	7.7	9.3	0.8	7.72	0.76	0.99
Other Holocene ice wedge samples		20	-26.28	-25.25	-23.15	0.89	-201.3	-193.9	-178.0	6.5	5.9	8.1	10.6	1.2	7.26	-10.59	0.97
Recent ice wedge samples		38	-25.27	-21.96	-18.24	1.87	-193.5	-168.1	-137.3	15	4.7	7.6	9.5	1.1	7.98	7.10	0.99
Rain water		33	-20.16	-15.79	-11.67	2.16	-147.5	-119.0	-85.4	15.8	-0.2	7.3	15.1	3.7	7.16	-5.97	0.96
Snow patches		2	-37.55	-35.81	-34.08	2.45	-292.3	-277.2	-262.0	21.4	8.1	9.3	10.6	1.8	8.72	35.26	1

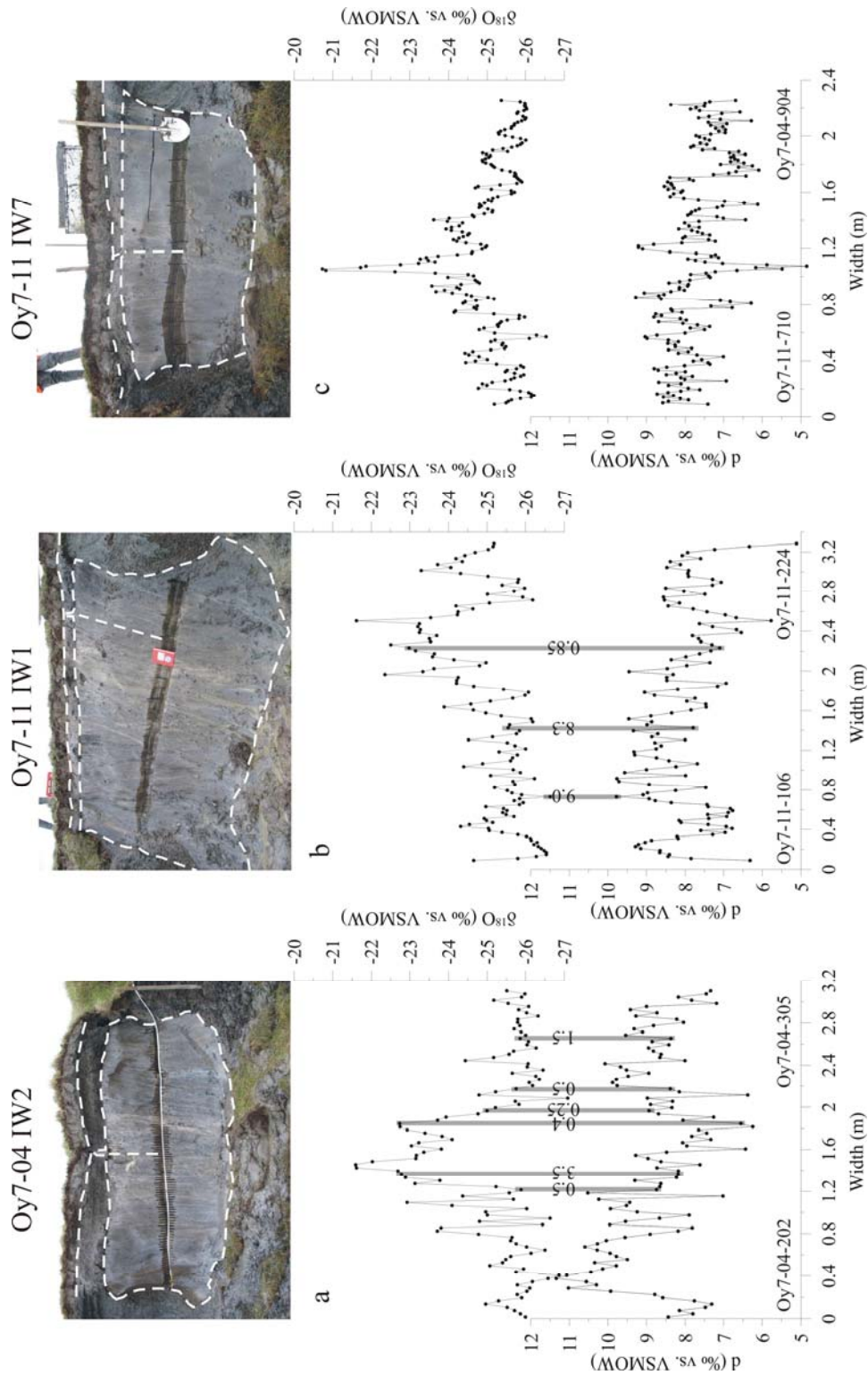


Figure 4.5: Photographs and high resolution $\delta^{18}\text{O}$ as well as d excess profiles of Holocene ice wedges Oy7-04 IW2 (a), Oy7-11 IW1 (b), Oy7-11 IW7 (c). The ice wedges and boundary layers between frozen ground and thawed active layer are marked by white dashed lines. Sub-vertical white dashed lines indicate the most recent ice wedge part as deduced from field observation. Black dots show single values, connected by thin lines to better illustrate the variations. Grey bars indicate dated samples with corresponding AMS ages in ka BP. The first and last samples of each profile are indicated in the diagram.

Ice wedge Oy7-04 IW2

The ice wedge Oy7-04 IW2 was about 3.2 m wide and the visible height was about 1.5 m (Figure 4.5a). The lower ice wedge part was buried under muddy debris. However, from similar well exposed ice wedges nearby we concluded a mean vertical extension of about 5-6 m. A well pronounced collection of recent ice veins overtopped the ice wedge in its central part. The ice wedge consisted of white to transparent ice with a lot of vertically-oriented air bubbles up to a length of 1 cm, especially in the central part. Mineral inclusions and organic matter were found in the generally clean ice as well. Vertically to subvertically oriented ice veins were evident for the ice wedge. Elementary ice veins had a thickness of 1 to 3 mm. In total, we took 107 samples in a resolution of about 2.5 cm by chainsaw in a horizontal profile at about 1.60 m below the surface. This profile represents a cut perpendicular to the frost cracking of this ice wedge. The mean values of electrical conductivity and pH are 44 μ S/cm and 6.5, respectively.

Ice wedge Oy7-11 IW1

The ice wedge Oy7-11 IW1 was about 3.5 m wide. Its bottom part was buried under debris, so the visible height was about 2 m (Figure 4.5b). The ice wedge was obviously not symmetrically structured, because the most recent ice veins were not located in the central part of the ice wedge but 70 to 80 cm away from the western edge. This might point to an imbalanced growth with different ice wedge generations, interrupted by inactive phases, and/or to a change in the orientation of the polygonal system. The ice wedge consisted mostly of greyish dirty ice and was rich in organic and mineral inclusions as well as small vertically-oriented gas bubbles. The high resolution sampling transect was located about 1.5 m below the surface, omitting the ice-sediment interface. In total, we took 123 samples in a resolution of about 2.5 cm. Electrical conductivity and pH exhibit mean values of 58 μ S/cm and 6.2, respectively.

Ice wedge Oy7-11 IW7

The perpendicularly cut ice wedge Oy7-11 IW7 had a width of about 2.5 m and a visible height of 1.2 m with a buried bottom part (Figure 4.5c). This ice wedge exhibited a central, very well pronounced recent ice veins assemblage of about 3 cm width (Figure 4.4). These recent ice veins and the central part of the ice wedge

were more milky-white due to more air bubbles than the other parts. Subvertically oriented ice veins were common in the whole ice wedge, single ice veins showed a width of up to 1 cm. We sampled a horizontal profile 1 m below the surface and took 12 blocks (20-25 cm, including the ice-sediment interface at both rims), which were sampled later under cold laboratory conditions in Potsdam in a resolution of 1 cm (210 stable isotope samples) and 4-5 cm (45 hydrochemistry samples). The mean values of electrical conductivity and pH are 40 μ S/cm and 6.0, respectively. No significant differences regarding the major ion content exist between the three high-resolution profiles.

Other ice wedges

We also took samples from five other Holocene ice wedges which were similar to the ones mentioned above. These samples were taken by ice screw. Except for one, all samples were taken from the middle to lower parts of the ice wedges in altitudes of 5 to 7 m a.s.l.

4.7.2 Chronology

The dating of ice wedges is crucial for a paleoclimatic interpretation of the derived proxy records. Even though a direct dating method for ground ice was recently developed (Gilichinsky et al. 2007) and successfully applied to different Pleistocene ice wedge generations (Blinov et al. in preparation), ice wedges have commonly been dated indirectly by age determination of enclosing sediments (Meyer et al., 2002a, 2002b) or by direct ^{14}C dating of organic remains within ice wedges (e.g. Vasilchuk et al., 2000). The latter method is based on the incorporation of organic material of herbal (blades of grass, leaves, roots) or animal origin (e.g. lemming coprolithes) fallen or moved by melt water into the open frost crack. This material marks the age of one discrete frost crack filling event, if contamination or reworking of the organic material can be excluded. As recently shown by Meyer et al. (in preparation b, c), ^{14}C dating of organic remains in ice wedges entails the possibility to generate even high resolution stable isotope time series from ice wedges.

In this study, plant remains of nine samples of ice wedges Oy7-04 IW2 and Oy7-11 IW1 were AMS ^{14}C dated (samples are marked in Figure 4.5a and 4.5b). We present the corresponding ages in Table 4.2. The ^{14}C ages reveal the Holocene

age of the studied ice wedges. These results are in accordance with Wetterich et al. (2009) who found Late Glacial ages of 14.8 to 10.7 ka BP for lacustrine Alas deposits with age reversals, most probably due to cryoturbation (Table 2). After the thermokarst lake fell dry, first ice wedges might have formed epigenetically. Wetterich et al. (2009) dated the overlying boggy sediments, which contain the studied syngenetically formed parts of the ice wedges, to 10.0 to 3.3 ka BP with an unconformity between the Early (10 to 8.3 ka BP) and Late Holocene (3.3 ka BP), possibly caused by a phase of erosion or without sedimentation.

In general, the ^{14}C ages of Holocene ice wedges from Oyogos Yar can be classified into two groups: Early Holocene (8 to 9 ka BP) and Late Holocene (0.25 to 1.5 ka BP). We did not get any Middle Holocene ages (about 5 to 6 ka BP) for our ice wedge samples. This is in line with the fact that mid-Holocene Alas deposits could not be verified in recent investigations at Oyogos Yar Coast (Wetterich et al., 2009) as well as on Bol'shoy Lyakhovsky Island (Andreev et al., 2009; Wetterich et al., 2009), whereas a previous study of Gravis (1978) reported such deposits at Oyogos Yar Coast.

Only organic material from one sample (Oy7-04-247, dated to 3.5 ka BP, Table 4.2) was characterised by a low carbon content and derived most probably from reworked plant detritus (Grootes, pers. comm.). Therefore, it was excluded from further interpretation.

Ice wedge Oy7-04 IW2

All significant dated samples of ice wedge Oy7-04 IW2 were of Late Holocene age (Table 4.2, Figure 4.5a). The youngest samples (0.25 to 0.5 ka BP) were from the central part of the ice wedge, whereas the sample dated to 1.5 ka BP was located more to the ice wedge rim. This corresponds to the general ice wedge scheme with higher ages at the rim and the youngest ice in the central part. However, a continuous relation between age and distance from the central ice wedge part towards the rim was not detectable, most probably due to irregular frost cracking, resulting in different frost-crack positions (see below). Additionally, the plant material used for dating could have been relocated at the earth surface or within the active layer before filled in the frost cracks.

Table 4.2: Radiocarbon AMS ages of plant remains in ice wedge samples as well as in sediment samples of the studied Oyogos Yar Alas. The ice wedge samples are numbered as follows: Oy7 represents Oyogos Yar 2007, the numbers 04 and 11 mark different outcrops. The three-digit numbers are labelled continuously from left to right (see Figures 4.5a-c). The sediment samples were taken from bottom to top (for details see Wetterich et al., 2009).

Sample	Lab no	uncal. AMS age [a BP]	cal. age (2 σ) [a]	
Ice wedge samples (this study)				
Oy7-04-242	KIA 35630	525	± 45	AD 1385-1449
Oy7-04-247	KIA 35631	3520	± 30	BC 1925-1750
Oy7-04-263	KIA 35632	410	± 30	AD 1430-1520
Oy7-04-267	KIA 35633	260	± 50	AD 1481-1684
Oy7-04-274	KIA 35634	490	+ 60 / - 55	AD 1384-1516
Oy7-04-290	KIA 35635	1480	+ 110 / - 100	AD 340-729
Oy7-11-138	KIA 35636	8960	± 45	BC 8278-8166
Oy7-11-162	KIA 35637	8300	± 43	BC 7486-7246
Oy7-11-189	KIA 35638	855	± 45	AD 1118-1264
Sediment samples (Wetterich et al., 2009)				
Oy7-11-14	KIA 35234	3325	± 35	BC 1685-1527
Oy7-11-12	KIA 35233	8335	± 45	BC 7522-7297
Oy7-11-10	KIA 35232	8260	± 40	BC 7458-7142
Oy7-11-09	KIA 36687	9985	± 35	BC 9666-9321
Oy7-11-08	KIA 36686	11145	± 40	BC 11191-10993
Oy7-11-07	KIA 35231	14830	+ 70 / - 60	BC 16550-15781
Oy7-11-06	KIA 36688	10720	+ 40 / - 35	BC 10889-10750
Oy7-11-04	KIA 35230	11995	± 50	BC 12034-11798

Ice wedge Oy7-11 IW1

In contrast, ice wedge Oy7-11 IW1 contains organic matter of Late Holocene as well as of Early Holocene age (Table 4.2, Figure 4.5b). A Late Holocene growth corresponding to ice wedge Oy7-04 IW2 is proved by the 0.85 ka BP age of the sample Oy7-11-189. The organic material (peat) of the ice wedge samples Oy7-11-138 and Oy7-11-162 (dated to 9 and 8.3 ka BP, respectively) corresponds well to the characteristic Early Holocene peat horizon dated to 8.3 ka BP (sample Oy7-11-10, Table 4.2) in the transition zone from lacustrine to boggy deposits (Wetterich et al., 2009). However, this peat horizon was located much below the ice wedge top and also about 1-1.5 m below the position of the dated organic material in the ice wedge. The samples Oy7-11-138 and Oy7-11-162 were taken from the upper ice wedge part (about 1.5 m below surface, Figure 4.5b), which

was growing syngenetically to the enclosing sediments as revealed by the upward bent ice belts. These were clearly of Late Holocene origin as proved by a 3.3 ka BP age (sample Oy7-11-14, Table 4.2) and typical Pollen spectra (Wetterich et al. 2009). As the peat in the samples Oy7-11-138 and Oy7-11-162 was incorporated into the ice wedge by frost crack filling events, it must be relocated material of the Early Holocene peat layer. A redistribution of parts of this horizon, e.g. due to cryoturbatic processes, is revealed by sample Oy7-11-12 (Table 2) located about 1 m above the peat layer and dated to 8.3 ka BP (Wetterich et al., 2009). Consequently, we consider these Early Holocene ages as relocated and exclude them from paleoclimatic interpretation.

Ice wedge Oy7-11 IW7

No AMS ^{14}C ages for organic remains of this ice wedge have been available so far. However, since this ice wedge is in a similar stratigraphical situation but less wide than the ice wedges Oy7-04 IW2 and Oy7-11 IW1, we assume a Late Holocene age for the sampled profile of this ice wedge, too. But it may be even younger.

Assuming a temporal mean frost cracking frequency of 50% (Mackay 1992) and a mean elementary ice vein thickness of 2 mm, 2.5 to 3.5 m wide ice wedges may grow in about 2,500 to 3,500 years. Consequently, we assume only Late Holocene ice wedge growth at the altitude level of the studied ice wedge profiles at the Oyogos Yar Alas. However, an initial stage of epigenetic ice wedge growth in deeper layers even in the Early Holocene directly after the drainage of the thermokarst lake seems possible.

Late Holocene ice wedge growth in thermokarst depressions, thermo-erosional valleys and fluvial terraces, though, is evident from the study sites of Bol'shoy Lyakhovsky Island (Meyer et al., 2002b), Bykovsky Peninsula (Meyer et al., 2002a), Cape Mamontov Klyk (Meyer et al., in preparation a) and different sites in the Lena Delta (Meyer, unpublished data), mainly for the last millennium.

4.7.3 Isotopic composition and paleoclimatic implications

To gain a pure ice wedge signal, we excluded some of the outermost samples that reach out beyond the ice-sediment interface (containing sediment and texture ice)

as well as samples exhibiting a clearly modified isotopic composition due to water migration between ice wedge and enclosing sediments (Meyer et al. 2002a). Such samples were observed only in the outermost 2 to 3 cm of the ice wedge. They have distinctly increased $\delta^{18}\text{O}$ values (about 2‰ to 7‰ higher) and extremely low d excess values (-7‰ to 5‰) compared to the adjacent, presumably unaffected ice wedge samples. Assuming an exchange rate between ice wedge and surrounding sediments of about 10-15 cm per 10,000 years (Meyer et al., in preparation b), the small number of affected samples indicates a relatively young age of the studied ice wedges, confirming the expected Late Holocene age. Accordingly, we used 104 out of 107 samples from ice wedge profile Oy7-04 IW2, 119 out of 123 from Oy7-11 IW1, 193 out of 210 from Oy7-11 IW7 and 20 out of 24 from other Holocene ice wedge samples.

We present statistical features of the stable isotope composition of the three high-resolution ice wedge profiles in Table 4.1. The scatter of these data is displayed in $\delta^{18}\text{O}$ - δD diagrams (Figure 4.6a-c). Obviously, the minimum, maximum and mean values for $\delta^{18}\text{O}$, δD and d excess as well as slopes (7.58 to 7.72) and intercepts (-2.19 to 0.76) in the $\delta^{18}\text{O}$ - δD diagrams are very similar to each other, and relatively close to the GMWL as well as to recent ice wedge data, pointing to only low influence of kinetic fractionation processes. The d excess values (about 8‰) are close to the GMWL, too. The co-isotopic relationships of the high-resolution profiles can therefore be regarded as reliable Late Holocene LMWL (Local Meteoric Water Line) for winter precipitation at Oyogos Yar Coast. Thus, climate-relevant data are obtained from these ice wedges.

Other Holocene ice wedge samples, not taken from profiles in the upper parts but predominantly from lower ice wedge parts around the characteristic peat layer (3 to 5 m below the surface), differ slightly. Whereas the mean values of $\delta^{18}\text{O}$, δD and d excess are close to that of the high resolution profiles, the slope (7.26) as well as the intercept (-10.59) are somewhat lower (Figure 4.6d, Table 4.1). Most probably, these samples represent an earlier stage of ice wedge formation. Climate conditions were slightly different, but kinetic fractionation processes were involved (such as mixing of air masses and moisture from different sources or evaporation/sublimation of snow). However, their isotopic composition corresponds well with data from generally comparable Alas ice wedges from nearby Bol'shoy Lyakhovsky Island (Meyer et al., 2002b), which also include

samples from lower and therefore older ice wedge parts. In the following, we focus on $\delta^{18}\text{O}$, since this isotopic ratio is common in Arctic and Siberian paleoclimate studies.

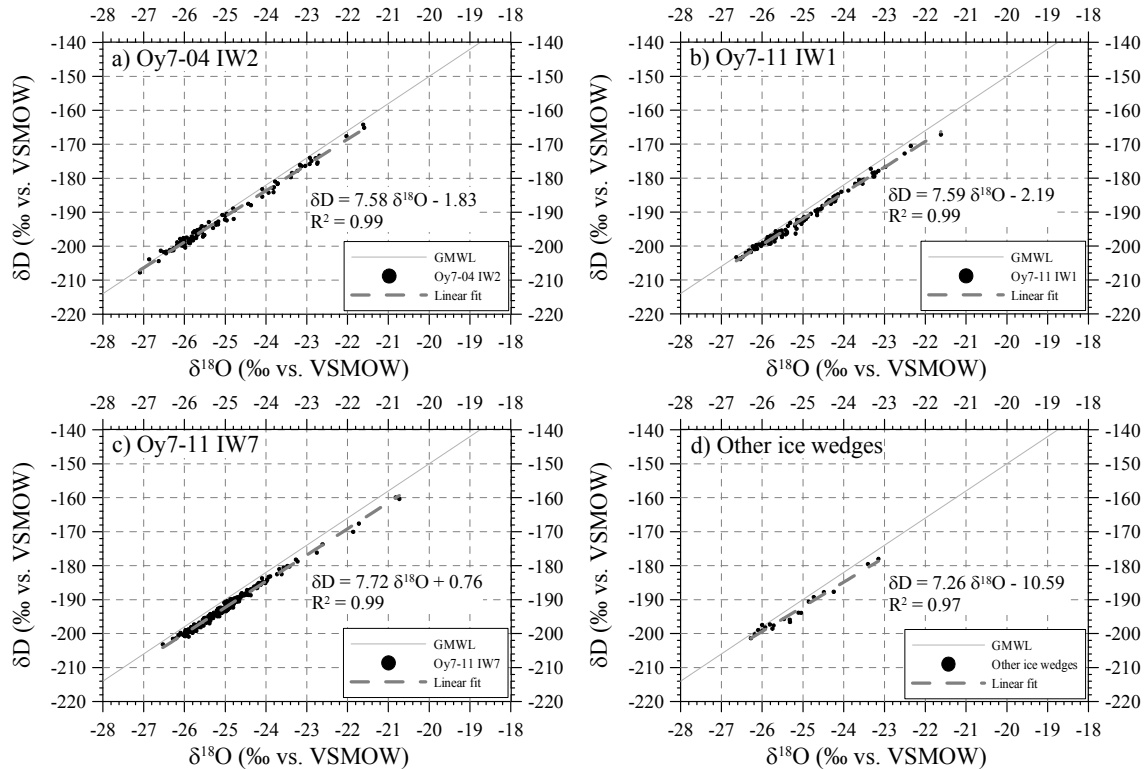


Figure 4.6: $\delta^{18}\text{O}$ - δD diagrams for the ice wedges Oy7-04 IW2 (a), Oy7-11 IW1 (b), Oy7-11 IW7 (c) and other Holocene ice wedges (d).

The three sampled profiles have a similar size and the same composition regarding maximum, mean and minimum stable isotope data. However, a classification of stable isotope data by means of $\delta^{18}\text{O}$ classes reveals different distributions of $\delta^{18}\text{O}$ values, especially pronounced in the medial classes (Figure 4.7). For all isotope profiles the $\delta^{18}\text{O}$ class -25‰ to -25.99‰ contains the highest proportion (41-50%) of $\delta^{18}\text{O}$ values. The $\delta^{18}\text{O}$ class -26‰ to -26.99‰ represents 24% of Oy7-04 IW2 data, but only 14% and 6% of Oy7-11 IW1 and Oy7-11 IW7, respectively. In turn, the $\delta^{18}\text{O}$ class -24.00‰ to -24.99‰ contains only 11% of Oy7-04 IW2 data, but 24% and 34% of Oy7-11 IW1 and Oy7-11 IW7, respectively. This pattern may be caused by the timing of frost cracking and ice wedge growth as well as by the location of the studied ice wedges in the thermokarst depression (Figure 4.2): Oy7-04 IW2 was located close to the slope to the Yedoma hill, whereas Oy7-11 IW1 and Oy7-11 IW7 were situated in the central part. However,

viewing the $\delta^{18}\text{O}$ class -23‰ to -23.99‰ , the ice wedges Oy7-04 IW2 and Oy7-11 IW1 exhibit a double proportion of corresponding data (about 13.5%) compared to the ice wedge Oy7-11 IW7 (7%). This suggests the width as one determining factor, as the ice wedges Oy7-04 IW2 and Oy7-11 IW1 were about 3.5 m wide whereas the ice wedge Oy7-11 IW7 was only 2.5 m wide and, therefore, probably younger. In the $\delta^{18}\text{O}$ class -22‰ to -22.99‰ , Oy7-04 IW2 shows an elevated amount (8%) compared to Oy7-11 IW1 and Oy7-11 IW7 with 2.5% and 1%, respectively. The remaining classes can be neglected since they contain too little data.

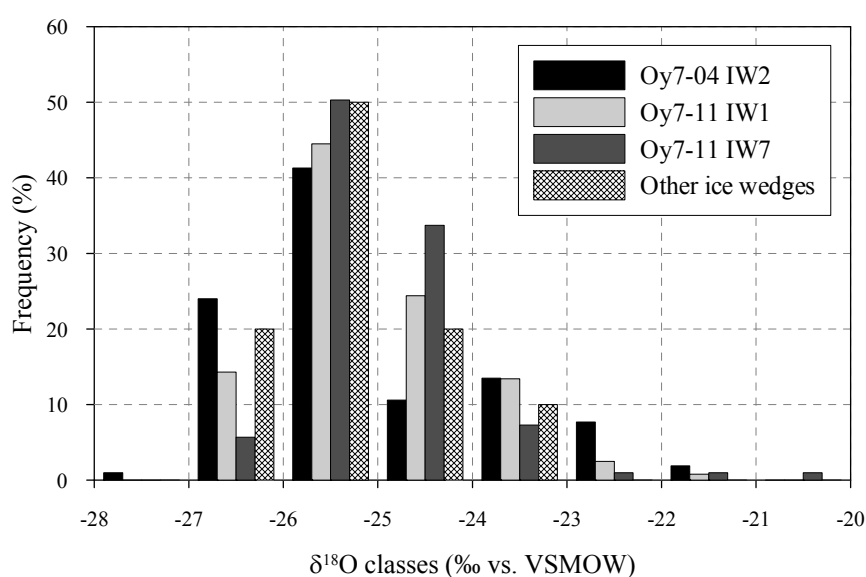


Figure 4.7: Frequency of $\delta^{18}\text{O}$ values in classes for the ice wedges Oy7-04 IW2, Oy7-11 IW1, Oy7-11 IW7 and the other studied Holocene ice wedges.

These variations clearly demonstrate that ice wedges are not uniform bodies but differ regarding frost cracking and ice wedge growth. The incorporation of the precipitation isotope signal into an ice wedge has to be taken into account as well. From monitoring, Mackay (1992) revealed that ice wedge cracking is a temporally random process, depending on different factors of which the snow cover thickness plays an important role. Beside the climate-derived year-to-year differences in winter precipitation amount, seasonality, isotopic composition and frost intensity, local effects like non-uniform snow accumulation due to surface irregularities within the ice wedge polygon or wind drift could have resulted in different frost cracking frequencies for the studied ice wedges at different time slices. Another possible cause for the different isotopic distributions leads to the question, which

part of winter precipitation the ice veins contain. Melt water from different stages of snow melt exhibits different isotope signatures due to isotopic fractionation during snow melt; first melt water will show more negative $\delta^{18}\text{O}$ and higher d excess values than the last (Lauriol et al., 1995). Beside that, snow directly fallen into the frost crack or hoar frost may contribute to ice vein formation. Additionally, one has to keep in mind the issue of sampling resolution. One elementary ice vein integrates different precipitation events of one winter. In turn, one ice wedge sample comprises some 5 to 20 ice veins and represents therefore again a mixed signal of different cracking events in an about decadal resolution.

Even though such local factors may have an influence, similar general isotope characteristics (minima, mean, maxima, slope; Table 4.1) and similar features in the ice wedge isotope profiles (maxima, minima) lead to the conclusion that climate signals are visible in the variations of $\delta^{18}\text{O}$ and d excess data. We present the high-resolution stable isotope profiles ($\delta^{18}\text{O}$ and d excess) from ice wedges Oy7-04 IW2, Oy7-11 IW1, and Oy7-11 IW7 in Figures 4.5a-c. The profiles are characterised by a high variability, indicating that isotopic diffusion, which would smooth the record, probably did not take place in the studied ice wedges.

The $\delta^{18}\text{O}$ profiles generally reflect the ice wedge structure: The highest values (about -23‰ to -21‰) are found in the youngest ice wedge parts below the assemblages of recent ice veins with similar $\delta^{18}\text{O}$ values, confirming recent growth of ice wedges at the altitude level of the studied profiles. The lowest values (about -27‰ to -25 ‰) are evident in the outer ice wedge parts. In contrast to Oy7-11 IW1, ice wedges Oy7-04 IW2 and Oy7-11 IW7 generally exhibit symmetric $\delta^{18}\text{O}$ profiles (Figure 4.5a-c). In these profiles, especially in the case of Oy7-11 IW7, probably corresponding $\delta^{18}\text{O}$ maxima are detectable at both sides of the central part, indicating a more or less continuous and symmetric growth with regular frost cracking at nearly the same position (Figures 4.5a and c).

The range of $\delta^{18}\text{O}$ variation in the profiles is about 4 to 6‰. This corresponds to similar values observed in Holocene Alas ice wedges on Bol'shoy Lyakhovsky Island (Meyer et al., 2002b) and Bykovsky Peninsula, the latter with overall more negative values (Meyer et al., 2002a); whereas at Cape Mamontov Klyk a variation of only about 3‰ was observed (Meyer et al., in preparation a). Drawing on the attempts of Vasil'chuk (1992) and Nikolayev and Mikhalev (1995) to relate the $\delta^{18}\text{O}$ range to absolute temperatures, which, however, were based only on sparse

data, our data would result in Late Holocene temperature ranges of 9°C to 12°C and 6°C to 7°C for mean January and mean winter temperatures, respectively. The most negative $\delta^{18}\text{O}$ values (-27‰ to -25‰) in the outer part of the profiles correspond well to the samples from lower and therefore older ice wedge parts (other Holocene samples, Table 4.1). This indicates similar winter temperature conditions in the Late Holocene around 3,500 a BP to 2,500 a BP and in the initial phase of ice wedge growth, probably in the Early Holocene after the drainage of the thermokarst lake. The heaviest $\delta^{18}\text{O}$ values (-23‰ to -21‰) of the profiles correspond well to that of recent ice wedges (mean: -22‰). Therefore, we consider these highest values as recent end point of the examined time period. Consequently, the $\delta^{18}\text{O}$ data reflect a marked Late Holocene winter warming trend with several shorter temperature maxima and minima towards a generally warmer last millennium. This is in contradiction to other Northern Hemisphere high-latitude paleo-records, which show decreasing temperature trends during the last 6,000 years (e.g. Wanner et al., 2008). However, Andreev et al. (2001) reconstructed a general warming trend since 1.5 to 1.7 ka BP from pollen data in the nearby Yana lowland, interrupted by a temperature maximum about 1 ka BP and a subsequent minimum about 500 a BP. These temperature patterns might correspond to the Medieval Warm Period (MWP; about AD 900-1200) and the Little Ice Age (LIA; about AD 1300-1850), in the Northern Hemisphere commonly attributed to warmer and colder temperatures, respectively (e.g. Wanner et al., 2008). Similar features are also detectable in the ice wedge profile $\delta^{18}\text{O}$ data: The warm isotope signal of sample Oy7-11-189 (-23‰) dated to 855 a BP (cal. AD 1118-1264) may be related to MWP. Three samples with low $\delta^{18}\text{O}$ values (-26‰ to -25‰), dated to 525 a BP (cal. AD 1385-1449 AD; Oy7-04-242), 490 a BP (cal. AD 1384-1516; Oy7-04-267) and 260 a BP (cal. AD 1481-1684; Oy7-04-274), may be related to LIA. However, the warm signal of sample Oy7-04-263 ($\delta^{18}\text{O}$ -22.7‰) dated to 410 a BP (cal. AD 1430-1520) would also fit into the time period of LIA. Up to now, only little is known about the climate characteristics of these time periods in Northeast Siberia. Therefore, the ice wedge data from Oyogos Yar provide valuable information on climate variability, i.e. winter temperatures, during the last millennia. However, to verify these preliminary interpretations and to develop a continuous time series of Late Holocene winter temperatures, more absolute dating of ice wedge samples would be needed.

The most recent parts of the high resolution $\delta^{18}\text{O}$ profiles, particularly that of ice wedge Oy7-11 IW7, reveal a pronounced maximum of -22‰ to -20.5‰ for the last decades (approximately the last 30 to 50 years). The related rapid warming (increase of 4‰ to 5‰) might have taken place during the last 100 to 200 years, as it comprises only a few samples (Figures 4.5a-c). A similar strong warming in the Russian Arctic was recorded in the Akademii Nauk ice core (Severnaya Zemlya) from about AD 1800 to the AD 1930s (Fritzsche et al., 2005). Using the attempts of Vasil'chuk (1992) and Nikolayev and Mikhalev (1995), this $\delta^{18}\text{O}$ increase of about 4‰ to 5‰ would be equivalent to a warming of 4°C to 6°C (winter temperature) and 6°C to 10°C (January temperature). However, modern winter temperatures at the Oyogos Yar coast have clearly been the warmest of the Late Holocene and most probably also the warmest since Early Holocene optimum.

The d excess values of the ice wedge profiles vary considerably and range between 5‰ and 11‰ . They resemble the range observed in Holocene Alas ice wedges on Bol'shoy Lyakhovsky Island (Meyer et al., 2002b), whereas Holocene Alas ice wedges on Bykovsky Peninsula (Meyer et al., 2002a) and at Cape Mamontov Klyk (Meyer et al., in preparation a) show distinctly higher values (about 8‰ to 18‰).

Low (high) d excess values are generally linked to high (low) $\delta^{18}\text{O}$ values. Accordingly, d excess and $\delta^{18}\text{O}$ are anticorrelated (Oy7-04 IW2: $r = -0.49$, Oy7-11 IW1: $r = -0.48$, Oy7-11 IW7: $r = -0.33$). The relatively weak correlations reflect the different d excess courses on both sides of the youngest ice wedge parts (Figures 4.5a-c), which exhibit the lowermost d excess values (about 5‰ - 6‰), comparable to that of the recent ice wedges (Table 1). These low d excess values probably point to a significant contribution of regional moisture to the winter precipitation at the Oyogos Yar Coast in modern times. A recharge of continental surface water can be excluded due to its frozen state in winter. As mentioned above, possible sources for moisture generation at colder temperature conditions than in the North Atlantic Ocean, leading to lower d excess values, could be the North Pacific Ocean as well as the Laptev or East-Siberian Seas (see also Meyer et al., 2002b). Mainly two factors are assumed to control the contribution of regional moisture to the winter precipitation: the sea ice extent and atmospheric circulation patterns. In winter, the Laptev and East-Siberian Seas are still completely covered with sea

ice, except for polynyas. Therefore, substantial changes in the sea ice cover could not have caused the higher proportion of regional moisture. However, larger polynyas or a later freeze up of the Laptev and East-Siberian Seas may have provided more regional moisture in modern times. Another possibility is a change in the atmospheric circulation patterns, in particular the dynamics between the Siberian High and the Aleutian Low. A strengthened Aleutian Low could have led to increased precipitation of regional moisture, possibly due to a higher frequency of cyclones.

Together with the warmest $\delta^{18}\text{O}$ data of the studied ice wedges, this higher proportion of regional moisture is interpreted as feature of the recent Arctic warming. However, also kinetic fractionation due to sublimation/evaporation effects before and during melting and percolation of melt water through the snowpack might have contributed to the d excess shift to relatively low values.

On both sides of the youngest parts, shifts from higher to lower d excess values and vice versa are clearly detectable in the ice wedge profiles (Figures 4.5a-c). They comprise short-term changes (based on 1 to 2 samples only) as well as more stable conditions represented by 5 to 10 samples. At least the latter should be regarded as climate-related changes, whereas short-term variations are more likely influenced by the secondary fractionation processes mentioned above. These changes in d excess records point to varying proportions of different moisture sources throughout the last millennia (see above). This contradicts Meyer (2003) who supposed the North Pacific as constant moisture source for the nearby Bol'shoy Lyakhovsky Island to explain the observed low d excess values. However, we assume that lower d excess values represent a higher contribution of regional moisture (i.e. from North Pacific or polynyas), whereas higher d excess data point to a greater influence of Atlantic moisture.

4.8 Conclusions

The study of ice wedges in an Alas at the Dmitrii Laptev Strait (Oyogos Yar Coast) reveal a Late Holocene (since about 3,500 years BP) ice wedge growth syngenetically to the enclosing sediments. The initial stage of ice wedge growth (epigenetically in the enclosing sediments) probably took place in the Early Holocene after the drainage of a thermokarst lake. Recent ice wedge growth exhibits an isotopic composition close to the GMWL. Consequently, climate

signals are obtained from the ice wedges. Even though isotope values are differently distributed, high resolution sampled Late Holocene ice wedge profiles show similar isotopic composition (maximum, mean and minimum values as well as slope and intercept) leading to a significant LMWL for winter precipitation, only slightly deviated from the GMWL.

This study is the first attempt to interpret high-resolution (1-3 cm) isotopic signals from Holocene ice wedges in terms of a climate record, using AMS ^{14}C dating of organic matter enclosed in the ice wedges. Different effects in ice wedge formation make a climate interpretation difficult. However, $\delta^{18}\text{O}$ data reveal considerable changes in winter temperatures in the Late Holocene with a warming trend towards recent times. This trend is superimposed by a marked variability that may reflect well-known climate epochs like the Medieval Warm Period or the Little Ice Age. The youngest ice wedge parts reflect an enormous warming in the last decades to centuries and exhibit the highest temperatures of the whole record, which may be related to recent Arctic climate change. The d excess record exhibits a pronounced variability, probably caused by changing proportions of Atlantic, Pacific and polynya moisture in the precipitation feeding the studied ice wedges at the Oyogos Yar Coast.

Acknowledgements

This study is part of the Russian-German cooperative scientific project “System Laptev Sea” and the International Polar Year project “Past Permafrost” (IPY project 15). It was partly funded by the state of Berlin (NaFöG PhD scholarship and travel costs for T. Opel). We thank all Russian and German colleagues of the expedition „Lena – New Siberian Islands 2007” for support during fieldwork. Sampling and analytical work in the AWI Potsdam laboratories was greatly supported by Bernhard Chapligin, Antje Eulenburg and Lutz Schönicke. We thank Rossana Raffi and an anonymous reviewer for helpful comments which helped to improve the quality of the manuscript.

5 Synthesis

The overarching goal of this thesis was to gain new insights into the Late Holocene Eurasian Arctic climate and environmental history. In order to contribute to the understanding and assessment of past and recent Arctic climate changes, glacier ice and ground ice from the Russian Arctic were studied. On the one hand, new paleoclimatic information was derived from the Akademii Nauk (AN) ice core drilled on Severnaya Zemlya (SZ, Central Siberian Arctic). On the other hand, a new approach was used to study syngenetic ice wedges from the Oyogos Yar coast of the Dmitrii Laptev Strait (East Siberian Arctic) as paleoenvironmental archive.

While both archives cover the same Late Holocene time interval, the deduced proxy data exhibit different temporal resolution; annual to decadal for the AN ice core and centennial to millennial for the Oyogos Yar ice wedges. Owing to a year-round precipitation, the AN ice core data represent mostly annual information. In contrast, the ice wedges provide winter signals, given that winter snow melt is the predominant source for frost-crack filling.

As both studied archives are composed of ice from precipitation, similar analytical methods (e.g. mass spectrometry) were applied to derive paleoclimatic proxy data (e.g. stable water isotope composition) (Table 1.1).

5.1 Main paleoclimatic results and implications for the Late Holocene climate history of the Eurasian Arctic

Using $\delta^{18}\text{O}$ as proxy for surface air temperatures and d excess as proxy for evaporation conditions (e.g. Dansgaard, 1964; Rozanski et al., 1993; Jouzel et al., 1997), paleoclimatic information was extracted from both studied archives, complemented mainly by major ion concentration data from the Akademii Nauk ice core. The following essential paleoclimatic information was extracted.

- The AN $\delta^{18}\text{O}$ record reflects the variations of the Eurasian sub-Arctic and Arctic surface air temperature (SAT) as shown by comparisons with meteorological data (Figures 2.5 and 3.5). This is particularly evident for the SAT time series of Vardø in Northern Norway, indicating a strong climatic connection, probably the influence of the North Atlantic. Viewing the AN

$\delta^{18}\text{O}$ record of the 20th century, two features are particularly important. First, in the early 20th-century maximum the temperature was higher than in the 1990s, which, in contrast, were warmer on a hemispheric scale. Second, the early 20th-century maximum exhibits a double-peak structure, which is evident only in a few meteorological records of the Western Eurasian Arctic and sub-Arctic in contrast to other Arctic regions (Figure 2.5).

- In the 20th century, variations in AN d excess are connected with sea ice extent changes in the Kara Sea, which serves as regional moisture source (Figure 2.6). Low sea-ice extent allows a higher contribution of regional moisture, leading to lower d excess due to colder evaporation conditions. In turn, a high sea-ice extent prevents a considerable regional moisture contribution to the precipitation on Akademii Nauk ice cap, which is therefore characterized by higher d excess values. This pattern indicates that d excess can provide information on the proportion of regional moisture in the precipitation and therefore on regional sea ice extent changes.
- Major ions concentrations in the AN ice core reflect the atmospheric aerosol content. Sulphate and nitrate reveal the anthropogenic pollution of the Eurasian Arctic (Figure 2.7). Outstanding peaks in sulphate represent major volcanic eruptions, which are used for dating the ice core.

Selected paleoclimatic characteristics and main isotopic features of both studied archives are presented in Table 5.1. Owing to its generation from winter precipitation, the mean stable isotope composition of the Oyogos Yar ice wedges is lighter than that of the AN ice core, which represents annual precipitation. In turn, the AN ice core exhibits higher d excess values. The ice wedges stable isotope composition is in line with that of the nearby Bol'shoy Lyakhovsky Island (Meyer et al., 2002b) and can therefore be regarded as representative for this region of the East Siberian Arctic.

Due to age reversals in dated ice wedge samples (Figure 4.5) only preliminary isotope curves, based on the AMS ^{14}C -dated samples from two Late Holocene ice wedges (Table 4.2) and on the recent ice wedge samples, were created in order to compare them with the AN ice core stable isotope data. Viewing the long-term $\delta^{18}\text{O}$ records of the AN ice core and of the Oyogos Yar ice wedges, a distinct unprecedented maximum is obvious during the last century (Figure 5.1), clearly

representing the warmest time period recorded in both archives. In the d excess records, the lowest values occurred in the most recent samples (Figure 5.2), indicating a higher proportion of regional moisture from the nearby Kara, Laptev and East Siberian Seas connected to a lower sea ice extent (see above).

Table 5.1: Overview of general paleoclimatic characteristics and stable water isotope composition of Akademii Nauk ice core (upper 535 m) and Oyogos Yar syngenetic ice wedges (for AN ice core, annual mean values from high-resolution stable isotope samples are used).

	Akademii Nauk ice core Severnaya Zemlya Central Siberian Arctic	Syngenetic ice wedges Oyogos Yar East Siberian Arctic
Dated time range	Ca. AD 300-2000	Ca. AD 500-2000
Spatial significance	Local to Western Eurasian Arctic	Local to Laptev / East Siberian Sea region
Temporal resolution	Annual to decadal	Centennial to millennial
Type of signals	Temperature Moisture source / Atmospheric circulation / Sea ice extent Atmospheric aerosol content	Temperature Moisture source / Atmospheric circulation / Sea ice extent
Resolution of signals	Annual and summer signals	Winter signals
Moisture source	North Atlantic / Regional Seas	North Atlantic / Regional Seas / North Pacific?
$\delta^{18}\text{O}$ min / mean / max (‰ vs. V-SMOW)	-26.5 / -21.6 / -16.5	-27.1 / -25.0 / -20.7
δD min / mean / max (‰ vs. V-SMOW)	-200.4 / -161.3 / -124.1	-207.8 / -192.1 / -159.9
d excess min / mean / max (‰ vs. V-SMOW)	6.8 / 11.2 / 15.1	4.8 / 8.0 / 11.3
Slope / intercept	7.7 / 4.6	7.6 / -1.6

The AN $\delta^{18}\text{O}$ record exhibits a decreasing trend until about AD 1750 (Figure 5.1). This coincides with several other paleo-temperature records from the Northern High Latitudes, which show a general cooling in the Middle and Late Holocene (Wanner et al., 2008). However, the AN $\delta^{18}\text{O}$ trend is at least partly caused by the growth of Akademii Nauk ice cap, as proven by decreasing sea-salt ion concentrations (Figure 3.6). In contrast, the ice wedge $\delta^{18}\text{O}$ data indicate a warming trend in the Late Holocene. This trend, however, is attributed to the winter season only (Figures 4.5 and 5.1). A review by Solomina and Alverson (2004) has

already pointed out the peculiar fact that different temperature trends have been recorded across the Russian Arctic and Subarctic, probably caused by the different nature of the used archives, e.g. tree rings, lake sediments, marine sediments and ice cores (see also Figure 3.7).

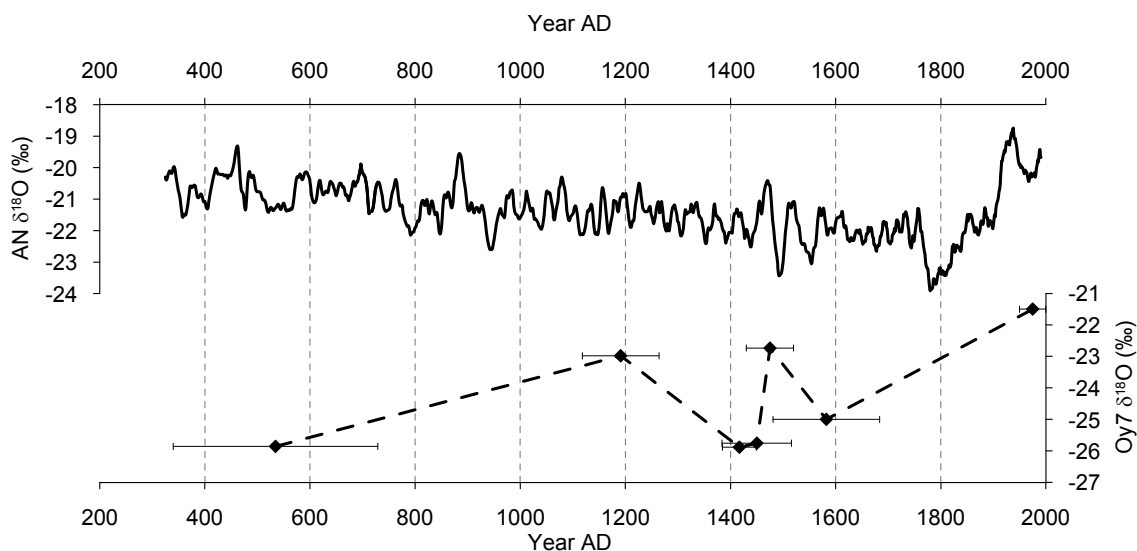


Figure 5.1: $\delta^{18}\text{O}$ data of the studied archives. Top: AN $\delta^{18}\text{O}$ data as running mean over 15 years based on the core chronology AN 2009/04. Bottom: Preliminary overview $\delta^{18}\text{O}$ record based on the AMS ^{14}C dated ice wedge samples from Oyogos Yar (Table 4.2). Black dots show the mean calibrated radiocarbon ages calculated from the minimum and maximum values (2σ range), indicated by the error bars. The modern value represents mean values of recent ice wedges and the most recent parts of the Holocene ice wedges and is assumed to represent the last decades.

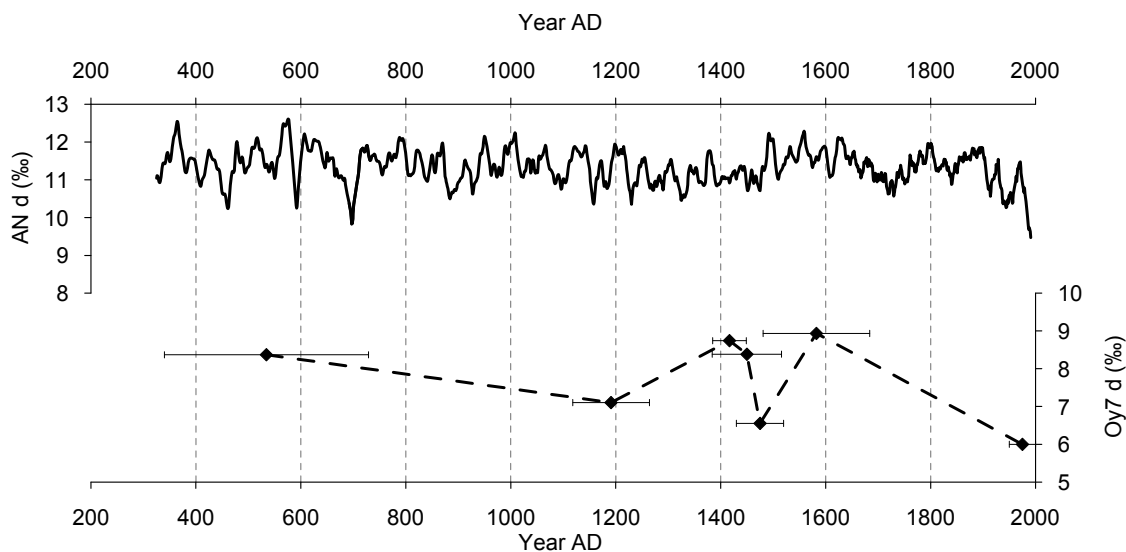


Figure 5.2: Deuterium excess (d excess) data of the studied archives. Top: AN d excess data as running mean over 15 years based on the core chronology AN 2009/04. Bottom: Preliminary overview d excess record based on the AMS ^{14}C dated ice wedge samples from Oyogos Yar (Table 4.2). See caption of Figure 5.1 for further details.

The general $\delta^{18}\text{O}$ trends are superimposed by a marked variability. This particularly applies to the AN $\delta^{18}\text{O}$ record due to its high resolution compared to the ice wedge record. However, no general coincidence of solar or volcanic forcing and AN $\delta^{18}\text{O}$ was found (Figure 3.7). Obviously, in the AN $\delta^{18}\text{O}$ record, neither a pronounced Medieval Warm Period (MWP; ca. AD 900-1200) nor a distinct Little Ice Age (LIA; ca. AD 1400-1900) are recorded. Only the absolute minimum around AD 1800 and the subsequent increase could be interpreted as termination of the LIA. In contrast, the preliminary ice wedge $\delta^{18}\text{O}$ record exhibits a maximum around AD 1200, which might be attributed to the MWP as well as a minimum in the 15th century, possibly corresponding to the onset of the LIA. However, a maximum is also recorded in the 15th century, discarding the hypothesis a long lasting cold phase.

An important feature of the AN $\delta^{18}\text{O}$ as well as d excess records are rapid changes, for instance in $\delta^{18}\text{O}$ at about AD 900, in the 15th and 16th centuries, at about AD 1750 and in the early 20th century (Figure 5.1), and in d excess around AD 600, at about AD 700 and in the 20th century (Figure 5.2). Comparable rapid changes in the 15th and 16th centuries can also be detected in the Oyogos Yar ice wedge records as well as in the Austfonna (Svalbard) $\delta^{18}\text{O}$ record (Figure 3.7). As these rapid changes are not directly connected to major changes of solar or volcanic forcing (Figure 3.7), they are probably caused by the internal dynamics of the climate system, including shifts in atmospheric and oceanic circulation patterns. In the case of the rapid climate changes in the 15th and 16th centuries this is supported by generally increased Icelandic Low and Siberian High intensities, resulting in strengthened westerlies with a very fast and strong onset (Mayewski et al., 2004). Substantial glacier advances at Franz Josef Land (Lubinski et al., 1999) and Novaya Zemlya (Polyak et al. 2004) between AD 1400 and 1600 are probably related to these changes. Accordingly, increased westerly to south-westerly winds leading to enhanced atmospheric and ocean heat transport to the Barents Sea as well as enhanced cyclonic circulation over the Barents Sea presumably caused the late 15th century and the early 20th century Arctic warming events (Bengtsson et al., 2004; Crespin et al., 2009), evident in the AN and Austfonna (Svalbard) $\delta^{18}\text{O}$ records (Figure 3.7).

The difference in mean d excess values between the AN ice core and the Oyogos Yar ice wedges indicates different moisture generation and transport patterns. The

relative low mean d excess values ($\sim 8\text{‰}$) in Holocene ice wedges from the Dmitrii Laptev Strait are typical for this Eastern Siberian Arctic region (“eastern province”) in contrast to study sites in the western and central parts of the Laptev Sea coast (Meyer, 2003). The higher mean d excess values ($\sim 11\text{‰}$) of the AN ice core fit well into this “western province”. Most probably, moisture from the North Pacific Ocean contributes to the precipitation at the Dmitrii Laptev Strait, whereas this can be excluded for the “western province” including Severnaya Zemlya. Nevertheless, the highly variable d excess in both records indicates no constant moisture source region but a mixture of North Atlantic moisture, moisture from the regional seas and, in the case of the Oyogos Yar ice wedges, potentially Pacific moisture.

5.2 Potentials and limitations of the studied paleoclimate archives

As shown above, both studied archives provide relevant data with a high potential for future paleoenvironmental applications. However, they are still fundamentally limited regarding their usability as paleoclimate archives and, therefore, regarding the significance of the derived data. These limitations are both archive- and site-specific peculiarities and are primarily related to dating issues.

5.2.1 Akademii Nauk ice core

Despite its position in the High Arctic, AN ice cap (SZ) is characterized by summertime surface melting due to its relatively low altitude (about 750 m NN). The subsequent melt water infiltration leads to an alteration of the originally deposited atmospheric signals (Koerner, 1997). Glaciers and ice caps with melting have been attracted less attention in ice core studies than e.g. the Greenland and Antarctic ice sheets. They have gained in importance in the last 20 years. Nevertheless, this study shows that valuable high-resolution paleoclimatic information can be obtained from ice cores drilled at ice caps with moderate melting, even though the seasonal signals are altered by melt water infiltration. Moreover, the annual to multi-annual stable water isotope and major ion signals derived from the AN ice core provide some highly significant paleoclimatic information for this poorly investigated region (Chapter 2).

The dating of the AN ice core is based on a combination of stable-isotope based annual layer counting and the detection of volcanic reference horizons. However, this approach proved to be problematic in the lower core part. Up to now, only a

few reference horizons could be identified at all and none before AD 1259 (Chapter 3). Due to the high sea salt ion concentrations and the altering affects of melting and infiltration, peaks in electrical conductivity are not necessarily linked to volcanic eruptions (Weiler et al., 2005). Moreover, sulphate, commonly used to identify volcanic horizons in ice cores, is more susceptible to melting and infiltration than other ions. Therefore, imprints of smaller volcanic eruptions, whose atmospheric sulphur load is often unknown, are more easily blurred. Furthermore, smaller volcanic eruptions, particularly from remote regions such as the Kamchatka Peninsula which is relatively close to Severnaya Zemlya, are not well-dated.

Standard ice-flow models underestimate the real annual layer thickness in the lower core sections. Therefore, they overestimate the age of the corresponding layers and are only of limited use for dating the AN ice core. This is most probably caused by the non-existence of dynamic steady-state ice-cap conditions due to the Late Holocene ice cap growth (Chapter 3). Hence, high-resolution sampling and the analysis of stable water isotope composition is necessary to date the ice core by counting annual layers as long as no additional reference horizons will be detected or independent age determinations will be available (Chapter 5.3).

In summary, it can be concluded that the relative small and low-altitude Akademii Nauk ice cap is highly sensitive to regional near-surface climate and environmental dynamics and has therefore a high potential for the reconstruction of the corresponding regional parameters, despite the above-mentioned limitations. As recently shown, the same is true for ice cores from comparable ice caps on Svalbard (Austfonna; Isaksson et al., 2005a, 2005b) and Franz Josef Land (Vetreniy; Henderson, 2002), whereas ice cores from higher elevated sites such as Greenland or Lomonosovfonna (Svalbard; Isaksson et al., 2005a, 2005b) contain signals of higher atmospheric layers.

In order to gain new ice-core based regional information on climate variability and forcing as proposed for instance within the framework of the IPICS 2000 year array (IPICS, 2009), ice core drilling should be conducted at such relative low-altitude ice caps in the Eurasian Arctic.

5.2.2 Syngenetic ice wedges (Oyogos Yar)

In a Holocene thermokarst depression (Alas) at the Dmitrii Laptev Strait three syngenetic ice wedges were studied. In contrast to previous studies in the Siberian Arctic (e.g. Meyer et al., 2002a; 2002b), a new approach, comprising horizontal high-resolution sampling and ^{14}C AMS radiocarbon dating, was used in order to derive continuous records from singular ice wedges. The stable-water isotope compositions of the studied ice wedges are close to the Global Meteoric Water Line (GMWL), proving the paleoclimatic significance of the isotope data. Despite some differences, all three stable-isotope profiles exhibit similar general characteristics. This indicates that the ice wedges recorded the same climate signals, such as the sub-recent strong warming accompanied by changes in moisture supply (Chapter 4).

Even though the ice wedges were dated to the Late Holocene, the derivation of continuous time series proved to be problematic because inconsistent AMS dating results (age reversals) appeared in the profiles (Figure 4.5). This contradicts the assumption of regular frost cracking and ice-wedge growth and poses the main issue regarding the extraction of time series from ice wedges. Most probably, temporal irregular frost cracking (Mackay, 1991) as well as changing positions of the frost cracks within the ice wedges are responsible and may also be related to local effects. Moreover, a careful selection of organic material is necessary to avoid dating of e.g. reworked material.

However, under favorable conditions and based on continuous ^{14}C AMS age sequences ice wedges can be studied with an about centennial resolution as recently demonstrated for ice wedges from Barrow/Alaska (Appendix II).

A second constraint is linked to the issue of which part of the winter snow cover provides the melt water that fills the frost crack during snow melt in spring. According to the annual temperature pattern, early winter snow is assumed to contain “warmer” isotopic signatures than late winter snow; a mixture of both would result in a mean signal. Additionally, the initial isotopic signal may be altered by fractionation during several processes such as snow metamorphism, snow melting and refreezing. Moreover, melt water from different stages of snow melt will exhibit different isotopic signatures with respect to the original snow cover (Lauriol et al., 1995). These processes and isotopic implications are hard to

determine and assess without a detailed monitoring and sampling at all stages of snow cover, ice vein formation and ice wedge growth.

Up to now, syngenetic ice wedges have been used predominantly to characterize climate and environmental conditions of different stratigraphic units during the Late Pleistocene and the Holocene, and to derive overview temperature trends (e.g. Meyer et al., 2002a; 2002b; Schirrmeister et al., 2003b; Wetterich et al., 2008b). Despite the mentioned limitations, they have the potential to serve as an important climate archive as impressively proven by the stable-isotope records of the Younger Dryas cold period in Barrow/Alaska (Appendix II). Therefore, further efforts should strive for using syngenetic ice wedges as climate archive and stable water isotopes as temperature and moisture proxies. Particularly as ice wedges are a widely distributed feature of permafrost regions, they allow for creating a network of stable-isotope based climate information in regions without other ice archives such as glaciers and ice caps.

5.3 Outlook and ideas for future research

This thesis contributes to a better understanding of Late Holocene climate and environmental change in the Eurasian Arctic by providing new substantial findings. Future research should continue the work on the studied archives and seek to transfer the findings and experiences to new study objects.

5.3.1 Akademii Nauk ice core

To overcome the dating issue and to develop a robust age model of the AN ice core, not only annual layer counting and the detection of additional volcanic reference layers using high resolution data should be continued, but independent physical dating approaches should be pursued as well. Such a project is envisaged within an cooperation with the working group of Dr. Wagenbach (Heidelberg University, Institute of Environmental Physics) and could include measurements of ^{10}Be for matching with the tree-ring based radiocarbon record of solar activity, as successfully applied to the Franz Josef Land ice core (Henderson, 2002; Kotlyakov et al., 2004). Also direct radiocarbon dating on the particulate organic carbon (POC), on dissolved organic carbon (DOC) in ice or on carbon in air bubbles could help to enhance the core chronology. A comprehensive effort to include all these age information could help to adjust a

standard ice-flow model to the AN ice core that would take into account the growth of AN ice cap. Putting reasonable age constraints on the lowermost core section would allow for detecting important paleoclimatic implications regarding the onset of a sustainable growth of the ice cap.

Based on robust information on age and growth of the AN ice cap, the correction of the ice core time series for the ice cap growth would facilitate the separation of surface elevation change from climate signals.

Another interesting issue would be the detailed influences of the North Atlantic Ocean, which is a main driver of the Eurasian Arctic climate due to its northward transport of heat and moisture. A west-to-east transect of ice-core based stable isotope and major ion data from Svalbard via Franz Josef Land to Severnaya Zemlya would help to assess the spatio-temporal variability of this North Atlantic Ocean influence. Of particular interest are rapid climate changes and the corresponding interactions of ocean, sea ice and atmosphere.

Additional attempts using AN ice core for paleoclimatic studies should include the measurements of new proxies, such as black carbon, a product of incomplete combustion, which absorbs heat in the atmosphere and reduces the surface albedo (McConnell et al., 2007).

Due to the formation of melt layers, air in the firn layers of the AN ice cap is trapped relatively fast as compared to the Greenland and Antarctic ice sheets, where firn-atmosphere interactions take place over several decades, leading to age offsets between the ice and the included air. Therefore, AN ice core could provide valuable information on past atmospheric composition, enabling also isotope studies on trapped air.

5.3.2 Syngenetic ice wedges

Follow-up research on the Late Holocene Oyogos Yar ice wedges should focus on an improved dating, leading to a better temporal resolution. Most promising for such a ^{14}C AMS dating effort would be the ice wedge Oy7-11 IW 7, which was sampled at high resolution (1 cm) under laboratory conditions. It exhibits the most symmetric stable isotope profiles (Figure 4.5), indicating an almost continuous growth, possibly without age reversals. Furthermore, several samples contained appropriate amounts of organic material for ^{14}C AMS dating.

Similar ice-wedge studies as the ones conducted within this thesis should be performed at several sites in the wide tundra regions of the Siberian Arctic and sub-Arctic to create comparable ground-ice based stable water isotope data sets. This should be done preferentially along climatic gradients, e.g. from West to East along the Eurasian North coast, considering also sites with existing ice core data, e.g. Svalbard, Franz Josef Land and Severnaya Zemlya for a more detailed archive inter-comparison. Older ice wedge generations should be studied in a similar manner, i.e. the huge syngenetic ice wedges of the Late Weichselian Ice Complex in Northeast Siberia, which also are in the age range for ^{14}C AMS dating. These studies should also include the analysis of the $^{36}\text{Cl}/\text{Cl}$ ratio to extend the available data set for this recently developed dating method (Appendix III). In particular, the yet not understood shift in the $^{36}\text{Cl}/\text{Cl}$ ratio between Late Pleistocene and Holocene ice wedges should be addressed.

To better understand and assess the temporal and spatial variations of frost cracking as well as the isotopic signals contained in the corresponding ice vein with respect to the original snow cover, a monitoring program is suggested. This monitoring of active syngenetic ice wedges should comprise repeated sampling of winter precipitation, detection of the timing of frost cracking and frost crack filling as well as sampling of the corresponding ice veins. Additionally, the monitoring should include measurements of chloride to gain more insights into the chlorine cycle, which would help to improve the dating approach for ground ice based on the $^{36}\text{Cl}/\text{Cl}$ ratio. In combination with automatic measurements of air temperature, existing isotope-temperature relationships (Vasil'chuk, 1992 and Nikolayev and Mikhalev, 1995) could be evaluated. This monitoring could be accompanied by laboratory-based experiments on stable isotope fractionation.

I A 275 year ice-core record from Akademii Nauk ice cap, Severnaya Zemlya, Russian Arctic

Diedrich Fritzsche¹, Rainer Schütt¹, Hanno Meyer¹, Heinz Miller², Frank Wilhelms², Thomas Opel^{1,4}, Lev M. Savatyugin³

¹Alfred Wegener Institute for Polar and Marine Research, PO Box 600149, D-14473 Potsdam, Germany

²Alfred Wegener Institute for Polar and Marine Research, PO Box 120161, D-27515 Bremerhaven, Germany

³Arctic and Antarctic Research Institute, 199397 St Petersburg, Russia

⁴Department of Geography, Humboldt University Berlin, Unter den Linden 6, D-10099 Berlin, Germany

Annals of Glaciology 42, 361-366.

Abstract

Between 1999 and 2001, a 724 m long ice core was drilled on Akademii Nauk, the largest glacier on Severnaya Zemlya, Russian Arctic. The drilling site is located near the summit. The core is characterized by high melt-layer content. The melt layers are caused by melting and even by rain during the summer. We present high-resolution data of density, electrical conductivity (dielectrical profiling), stable water isotopes and melt-layer content for the upper 136 m (120 m w.e.) of the ice core. The dating by isotopic cycles and electrical conductivity peak identification suggests that this core section covers approximately the past 275 years. Singularities of volcanogenic and anthropogenic origin provide well-defined additional time markers. Long-term temperatures inferred from 12 year running mean averages of $\delta^{18}\text{O}$ reach their lowest level in the entire record around 1790. Thereafter the $\delta^{18}\text{O}$ values indicate a continuously increasing mean temperature on the Akademii Nauk ice cap until 1935, interrupted only by minor cooling episodes. The 20th century is found to be the warmest period in this record.

I.1 Introduction

In the Eurasian Arctic, Severnaya Zemlya is the easternmost archipelago, which is covered by large ice caps. This allows regional climate signals to be accessed from ice-core records. The Akademii Nauk ice cap, covering an area of 5575 km², is the largest in the Russian Arctic, with a maximum elevation of about 800 m a.s.l. (Dowdeswell et al., 2002). The first 761 m long surface-to-bedrock core on this ice cap was drilled in 1986/87 by a Russian team (Savatyugin and Zagorodnov, 1988; Klement'yev et al., 1991). The core has been sampled in a relatively low resolution. A chronology was published for that core indicating a Late Pleistocene near-bottom age (Klement'yev et al., 1988, 1991; Kotlyakov et al., 1990).

Between 1999 and 2001 the new ice core discussed here was drilled to bedrock on Akademii Nauk (Figure I.1) to improve the data resolution and to revise the previous timescale. For this new core, the drilling site was selected close to the summit considering the form and flow of the ice cap (Dowdeswell et al., 2002). Fritzsche et al. (2002) report details of the drilling site at 80°31' N, 94°49' E, as well as recent accumulation rates. For technical details of the operation see Savatyugin et al. (2001). The mean annual air temperature at the drilling site was -15.7°C for the period May 1999–April 2000 (Kuhn, 2000). During summer, air temperature can even be above 0°C. In April 2000 a temperature of -10.2°C was measured at 10 m depth. Latent heat from percolating water affects the difference between mean annual air temperature and temperature in firn. In 2000/01 the borehole temperature was between -12.40°C at 100 m depth and -7.49°C at the bottom, with a minimum of -14.35°C at 209 m depth (Kotlyakov et al., 2004). Consequently Akademii Nauk is a cold glacier.

Reconstructing annual signals (e.g. $\delta^{18}\text{O}$) in ice cores from the percolation zone of glaciers can be problematic owing to the effect of meltwater infiltration (Koerner, 1997). The variation of stable isotopes in ice (δD and $\delta^{18}\text{O}$) can be eroded, but, at least in particular cases, seasonal cycles still persist (Pohjola et al., 2002a). Sometimes the deuterium excess d ($d = \delta\text{D} - 8 \delta^{18}\text{O}$) resolves the annual variation better than the corresponding δD or $\delta^{18}\text{O}$ data, as shown for the Vernagtferner, Oetztal Alps, Austria (Stichler et al., 1982).

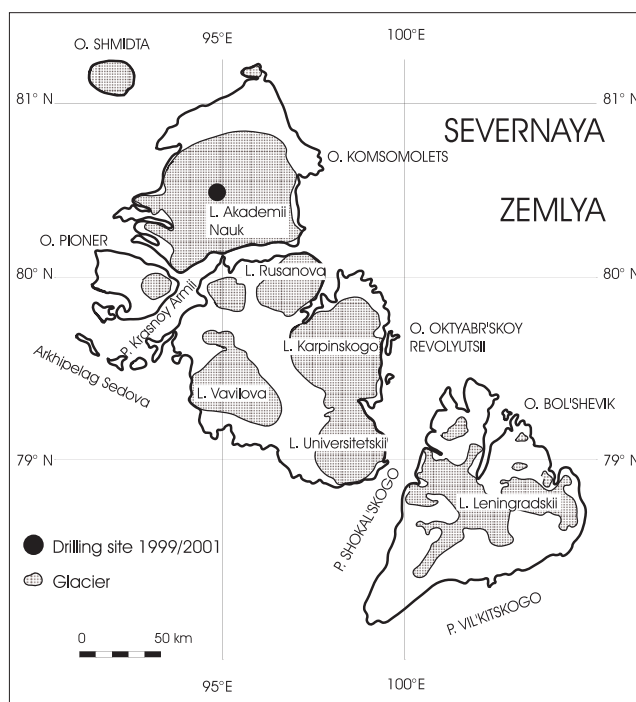


Figure I.1: Location of Severnaya Zemlya and its glaciers.

We present density, $\delta^{18}\text{O}$, δD and d profiles as well as the melt-layer content from the uppermost 136 m of the new Akademii Nauk ice core. These parameters are compared to electrical conductivity obtained by dielectrical profiling (DEP) of the same core sequence. A chronology is given based on the annual-layer thickness determined from $\delta^{18}\text{O}$ and d and using the time markers from volcanic events detected by DEP measurements. According to this depth-age model, the core section under investigation covers approximately 275 years.

I.2 Analytical methods

The core was processed in the cold laboratory of the Alfred Wegener Institute in Bremerhaven. Processing included the following steps:

1. Quasi-continuous density measurements (γ -densimeter) and DEP (Moore and Paren, 1987) were taken non-destructively at 5 mm resolution on a combined bench, which was also used for analysis of ice cores from Greenland (NorthGRIP) and Dronning Maud Land, Antarctica (EPICA). For a detailed description refer to Wilhelms (2000).
2. Following the DEP measurements, two slices were cut with a horizontal band-saw parallel to the core axis. The first 11 mm thick segment was sampled for isotopes ($\delta^{18}\text{O}$, δD); the second, a 30 mm thick plate, was

- polished for optical scanning of the internal structure, and subsequently sampled for chemical investigations (Weiler et al., 2005).
3. The stable isotopes were sampled from the segment in 25 mm long increments. To obtain a first overview, samples for each 1 m segment of core were collected by abrading 1-2 mm off the surface over the whole segment length with a microtome knife. The frozen samples were melted for the determination of δD and $\delta^{18}O$ with a Finnigan-MAT Delta S mass spectrometer. The analytical precision is better than $\pm 0.8\%$ for δD and $\pm 0.1\%$ for $\delta^{18}O$ (Meyer et al., 2000).
 4. The melt layers were visually identified on scanned pictures of coplanar slices. The scanning resolution is better than 0.1 mm, but because of irregular boundaries between melt layers and firn the fixing of layers was less precise. Accurate distinction between firn-ice and melt-impacted layers was difficult in the deeper parts of the core, but less problematic in the section discussed in this paper.

Following Madsen and Thorsteinsson (2001), we call glacial ice formed by firn only 'firn-ice'. In the manner of Paterson (1994) we use the term 'firn' for aggregates of several crystals with interconnecting air passages between the grains. Ice consisting of firn infiltrated by a visible content of water we call, independent of the amount of water, 'melt-layer ice' or 'melt layer'. Most melt layers in this core are formed by infiltration of water into the porous firn structure. Close to the surface, the firn has a porosity of 50%, which can be filled with percolating water. The melt-layer content is calculated by the proportion of melt-layer ice per metre by weight. In general, the amounts of melt-layer ice are a proxy parameter for warm summers, but superimposed sporadic melt features can make this interpretation complicated (Koerner, 1977).

1.3 Results and discussion

A shallow core (SZ 99-2) was drilled about 200 m eastsoutheast of the main coring site (SZ 99) in order to estimate the stratigraphic noise in the $\delta^{18}O$ and melt-layer records. The two datasets are in good agreement, with a 0.55 m depth offset (Figure I.2). This offset could be caused by a compression of the uppermost winter snow during drill-tower assembly and/or by roughness of the snow surface. The uppermost 0.43 m of the main core and 0.2 m of the shallow core were lost

because of their poor consolidation. Discrete, massive melt layers are found in the main core (e.g. at 2.9 or 7.8 m depth), and equivalent layers are found in the shallow core at corresponding depths. Many more small ice layers are observed in both cores. As expected, melt layers consisting of partially saturated firn are often found at various depths. The firn is not a homogeneous medium, and internal surfaces are undulated, so heterogeneous flow of vertical and horizontal percolating meltwater is the rule. Nevertheless, the two $\delta^{18}\text{O}$ profiles look similar, but the differences in infiltration are clearly visible in detail. For example, at 8.5 m depth of SZ 99 the deformed $\delta^{18}\text{O}$ minimum indicates infiltration of less depleted water. On the whole, the correlation of $\delta^{18}\text{O}$ between the two cores is good, with a correlation coefficient of $r = 0.67$ (2.5 cm resolution, 906 samples each, 14 years). An increase to more than $r = 0.75$ is possible with a visual piecewise adjustment (cores shifted against each other, six breaks, none overlapping).

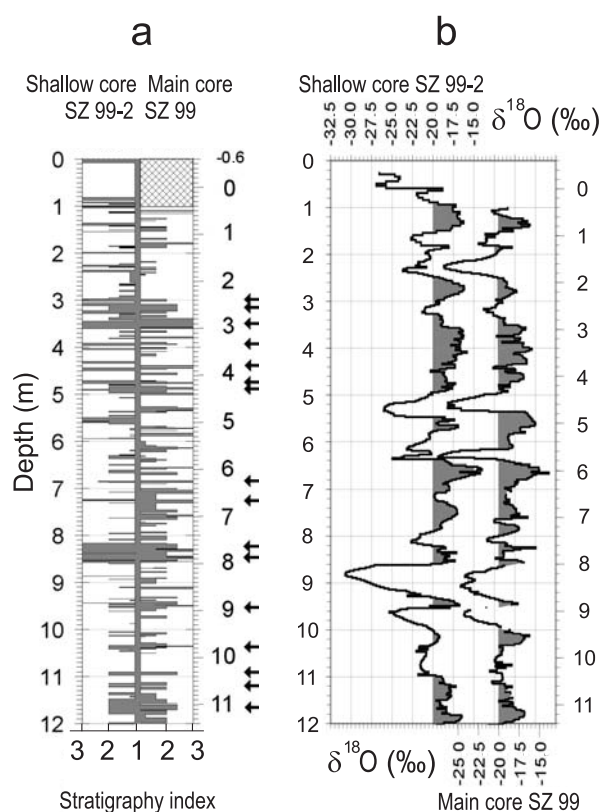


Figure I.2: Comparison of visible stratigraphy (a) and $\delta^{18}\text{O}$ (b) in the upper part of the main core SZ 99 and the shallow core SZ 99-2 drilled some 200 m apart. Stratigraphy index numbers in (a): 1. firn not impacted by water; 2. partially saturated melt layers; 3. saturated melt layers. The abscissa is mirrored for easier comparison. Arrows indicate melt layers occurring in both cores at the same depth. Shading in (b) is for easy comparison.

Figure I.3 shows the ice-core density profile at 5 mm resolution. Melt layers are obvious already in the uppermost metres of the core, with a density about 900 kg m^{-3} . Between these layers, firn horizons appear with a typical density of $300\text{-}400 \text{ kg m}^{-3}$ near the surface, and increasing density with depth. From the density profile it is apparent that the core originates from the percolation zone of the glacier. The transition from firn to ice occurs at about 60 m depth. The density profile is used to convert the depth scale into metres water equivalent (m w.e.).

Air bubbles are found throughout the core in varying size and concentration. Only very few parts of the core are almost free of bubbles. The homogeneously distributed bubbles suggest air entrapment between firn crystals. Hence, most of the melt-impacted layers were not made entirely from refrozen (bubble-free) meltwater. For the uppermost 30 m, where the density of ice and firn is sufficiently different, the calculation of infiltration from the density log (Figure I.3) agrees well with the visual recording of the melt-layer content.

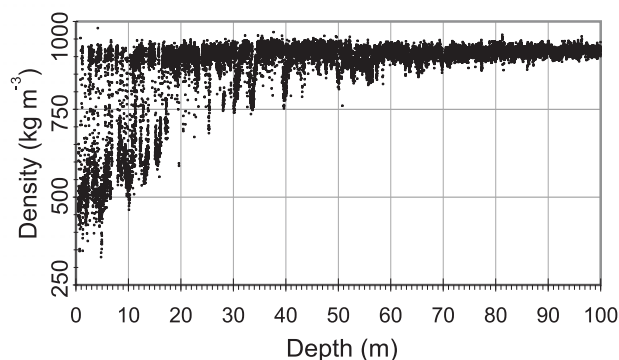


Figure I.3: Density-depth profile of the core (5 mm resolution).

The electrical conductivity record (Figure I.4d) exhibits some of the volcanogenic time markers which were used to establish the core chronology. The conductivity peak at about 20 m w.e. depth was related by chemical analysis (Weiler et al., 2005) to the 1956 eruption of Bezymianny, Kamchatka, with an attributed volcanic explosivity index (VEI) of 5 (Siebert and Simkin, <http://www.volcano.si.edu/gvp/world>). This is the largest conductivity peak observed in the whole core. The other peaks in conductivity are assumed to be of volcanogenic origin, and the assigned age is based on correlation with ice-core records from Greenland (e.g. from Hans Tausen Iskappe (Clausen et al., 2001)). The chronology of the core section discussed here is established by identifying

peaks in the conductivity record. In between the peaks the timescale is refined by counting seasonal signals in the stable-isotope records, mostly the d oscillations together with the $\delta^{18}\text{O}$ variations. As an example, Figure I.5 presents the stable-isotope variations between the Bezymianny event (1956) and the assumed Katmai (Alaska, USA) eruption (1912). On the graph's righthand side, our interpretation of annual cycles is marked with tags. An annual mark is defined by a minimum in δD and $\delta^{18}\text{O}$ and simultaneously a maximum in d . But four more years (arrows) could possibly be counted as well (error +10%). When counting the peaks, one finds probably more and not less years in this core, because of the appearance of additional infiltration peaks.

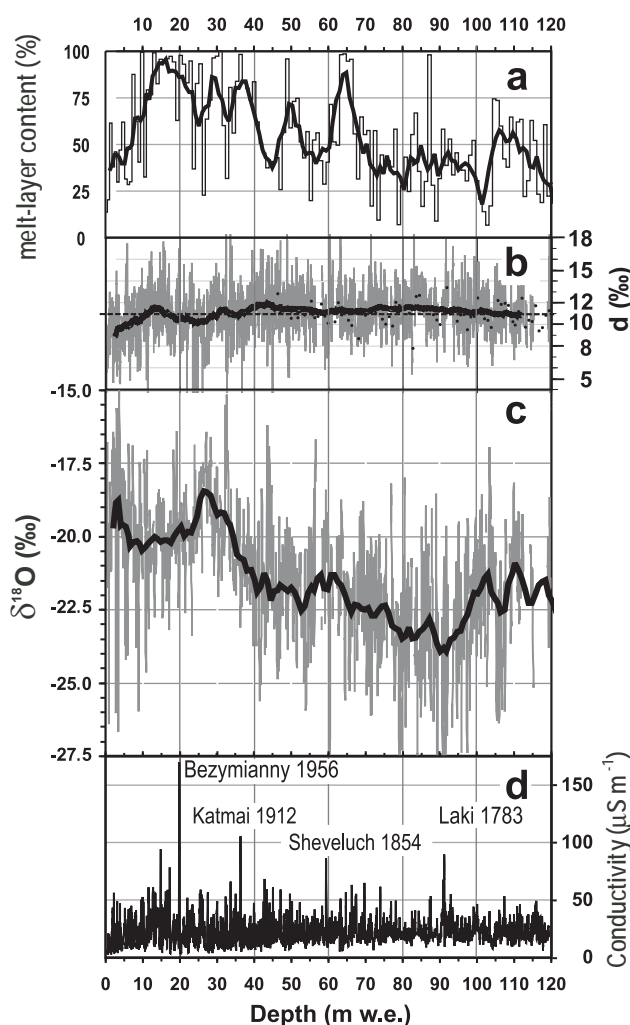


Figure I.4: Profiles from the upper 120 m w.e. (136 m depth) of the main core from Akademii Nauk ice cap. (a) Melt-layer content. Step function gives 1 m values, and black curve is 5 m running mean. (b, c) D excess d (b) and $\delta^{18}\text{O}$ (c). Grey indicates 25 mm data, and black curve is 5 m running mean. (d) Electrical conductivity (DEP) (5 mm resolution).

The melt-layer content (Figure I.4a) shows maxima at around 65, 50 and 40-10 m w.e., corresponding to the 1840s, 1880s and 1900-70 respectively. Following Koerner (1977), the amount of meltwater can be considered as a proxy for summer warmth. The $\delta^{18}\text{O}$ profile (Figure I.4c) shows a minimum at 90 m w.e. (AD 1790). An increasing trend of $\delta^{18}\text{O}$ is obvious between 90 and 27 m w.e. The d record exhibits annual cycles (Figure I.5), but the long-term trend is nearly constant (Figure I.4b): mean: $d = 11.0\text{‰}$ (dotted line).

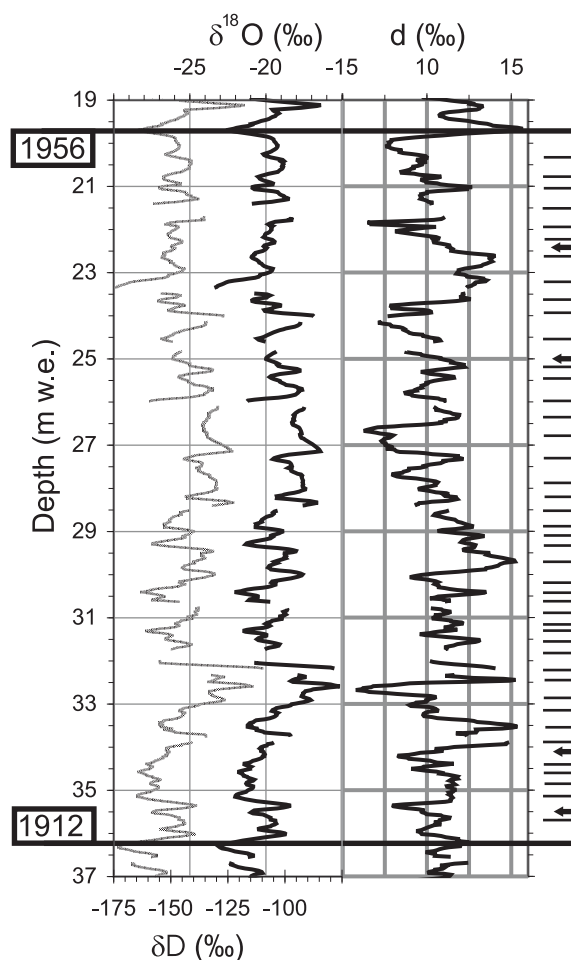


Figure I.5: Stable-isotope variations between the 1956 Bezymianny event and the layer with high electrical conductivity assumed to originate from the eruption of Katmai in 1912. Tags on righthand side indicate our interpretation of annual cycles. Arrows mark peaks which can be interpreted as additional years.

The derived annual-layer thickness for the top 120 m w.e. of the core, corresponding to the period 1725-1999, is plotted in Figure I.6. The annual-layer thickness is presented as found in the core (none decompressed). The modern

mean annual-layer thickness of about 0.46 m w.e. agrees with the recent mean annual accumulation rate at the drill site as calculated earlier from ^{137}Cs measurements (Fritzsche et al., 2002; Pinglot et al., 2003) as well as with the mean accumulation rate of 0.46 m w.e. a^{-1} in the period 1986/87 published by Zagorodnov et al. (1990). In deeper parts of the core (not shown here) the annual-layer thickness was determined over discrete 1 m intervals by high-resolution analysis of seasonal $\delta^{18}\text{O}$, δD and d and variations of electrical conductivity assumed to be seasonal. We found an annual-layer thickness of about 0.12 m w.e. for the near-bottom layers. From a linear decrease in annual-layer thickness with depth as observed in the DEP profile and assuming no discontinuity in the record, we calculated a bottom age of roughly 2500 years. This is less than the age computed by a Nye model (Paterson, 1994) with an accumulation rate of 0.46 m w.e. a^{-1} . Therefore our results imply that this ice cap was not in dynamic steady state throughout its existence, but has been growing until modern times. Similar conclusions have been drawn for Hans Tausen Iskappe, North Greenland (Hammer et al., 2001).

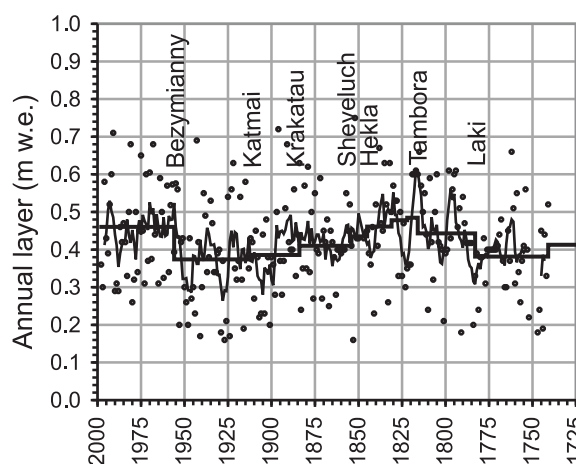


Figure I.6: Annual-layer thickness, AD 1725-1999, derived from $\delta^{18}\text{O}$ and d oscillations and from interpolation between volcanic time markers. Dots show thickness of a single year, black curve the 5 year running mean and the step line the mean annual-layer thickness between presumed volcanic eruptions.

The new $\delta^{18}\text{O}$ record from Akademii Nauk (Figure I.7) looks similar to the Vardø (Norway) temperature record (data: <http://www.giss.nasa.gov/data/update/gistemp/TMPDIR/tmp.634010980003.1.1/634010980003.1.1.txt>) and a composite of surface air temperatures in the Arctic (Polyakov et al., 2003b) (data: <http://denali.frontier.iarc.uaf.edu:8080/~igor/research/data/airtemppres.php>). The

good agreement suggests that $\delta^{18}\text{O}$ from Akademii Nauk is a good proxy for mean annual air temperature. Our $\delta^{18}\text{O}$ record shows an absolute minimum at about 1790, following the eruption of more than ten volcanoes with a VEI ≥ 4 since 1750, including Laki, Iceland, in 1783. Thereafter the $\delta^{18}\text{O}$ value increased until 1935, interrupted by a 10-20 year long reverse trend following huge volcanic eruptions during the 1850s. For the same period, Kotlyakov et al. (2004) present a long-term warming trend, which was reconstructed from borehole temperature logging in the Akademii Nauk 1986/87 borehole with a model considering the effects of vertical heat transfer by meltwater and its refreezing. The warming trend until the late 1930s was recorded by many meteorological stations in different regions of the Arctic (e.g. at Svalbard (Brázdil, 1988)). This trend is also a strong signal in composite air-temperature datasets from the Arctic as well as in data for the Northern Hemisphere at 64-90°N (<http://www.giss.nasa.gov>). The increasing temperature in the 19th and at the beginning of the 20th century can also be found in glaciers on Svalbard (Isaksson et al., 2003) and in Franz Josef Land (Henderson, 2002) as well as North Greenland (Hans Tausen Iskappe (Hammer et al., 2001)).

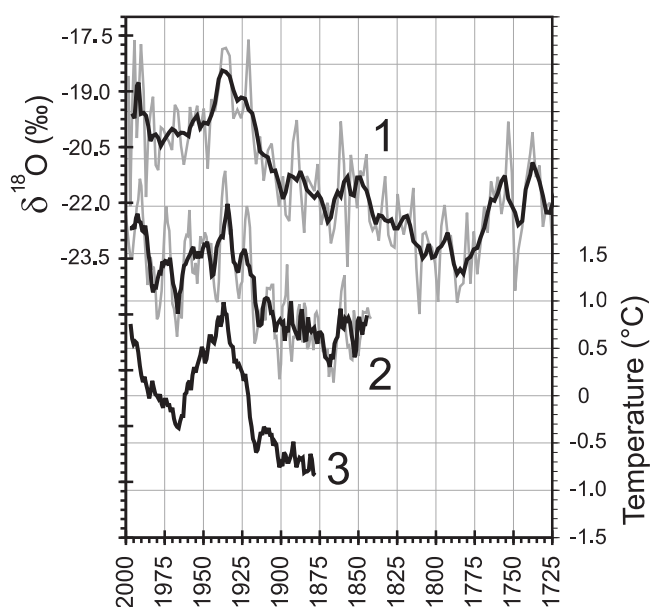


Figure I.7: Comparison of (1) dated $\delta^{18}\text{O}$ curve for the segment of ice core shown in Figure I.4 (1 m mean values and 5 m running means (approximately 2.3 and 12 years respectively); (2) air temperature measured at Vardø, North Norway (5 and 10 year running mean values); and (3) trend of composite surface air temperature in the Arctic (6 year running mean; deviation from mean temperature 1961-2000) (data from Polyakov et al., 2003b).

I.4 Conclusions

Our investigations on the newly drilled ice core from Akademii Nauk revealed:

Annual layers could be identified in the upper 136 m of core presented in this paper using a combination of high-resolution (2.5 cm) d and $\delta^{18}\text{O}$ data.

The core was dated by combining the annual-layer thickness measurements from stable-isotope studies with volcanogenic signals in the electrical conductivity record used as time markers.

The $\delta^{18}\text{O}$ time series is very similar to trends in air temperature measured in the Arctic. Thus the $\delta^{18}\text{O}$ data are a good proxy for mean annual air temperature.

The accumulation rate over the period 1956-99 is about 0.46 m w.e. a^{-1} based on stable-isotope investigations. This finding agrees with the rates we found earlier by ^{137}Cs radioactivity measurements and the annual accumulation rate published for 1986/87 (Zagorodnov et al., 1990). It is in disagreement with a modern annual-layer thickness of 0.26-0.28 m suggested by Klement'yev et al. (1988) and used by Kotlyakov et al. (1990) for dating the Akademii Nauk ice core drilled in 1986/87.

Our preliminary chronology of the ice core dates the lowermost part to roughly 2500 years BP.

Acknowledgements

The drilling project was funded by the German Ministry of Education and Research (03PL027A/3). The analysis of the core was financially supported by the Alfred Wegener Institute for Polar and Marine Research. We thank A. Lambrecht for assistance with the DEP measurements, H. Henschel for correcting the English and two anonymous reviewers for their helpful comments.

II Permafrost evidence for a Younger Dryas cold event in northern Alaska

Hanno Meyer¹, Lutz Schirrmeister¹, Kenji Yoshikawa², Thomas Opel¹,
Hans-W. Hubberten¹, Jerry Brown³

¹Alfred Wegener Institute for Polar and Marine Research, Research Unit
Potsdam, Telegrafenberg A43, 14473 Potsdam, Germany.

²Water and Environmental Research Center, Institute of Northern
Engineering, University of Alaska, Fairbanks, Alaska, 99775, USA

³P.O. Box 7, Woods Hole MA 02543, USA

In preparation for submission to Nature.

Abstract

The reaction of the North Pacific region to a „shutdown“ or reduction of the thermohaline circulation in the North Atlantic during Younger Dryas has been a matter of debate. We present a radiocarbon-dated stable water isotope record from northern Alaskan permafrost (ice wedges) near Barrow, Alaska, to demonstrate centennial-scale Late Glacial-Holocene winter climate variations. Our results provide the first stable isotope evidence for a Younger Dryas cold event recorded in permafrost and for a change in atmospheric moisture conditions similar to the Greenland ice core records, but with a lag of about 500 years and likely associated with the successive opening of the Bering Strait.

The debate on the susceptibility of permafrost to global warming has gained interest in the last decade (Lemke et al., 2007), particularly with regard to positive feedback mechanisms of a potential release of stored carbon (Zimov et al., 2006; Walter et al., 2006). As permafrost in North America and Siberia warmed in the late 20th century (Osterkamp, 2005; Romanovsky et al., 2007), enhanced thawing of frozen ground caused dramatic environmental consequences, particularly in warmer discontinuous permafrost regions and along ice-rich Arctic coastlines. Climatological records extending beyond the Late Glacial-Holocene transition are

rather sparse within permafrost regions, often restricted to lake sediments and rely mostly on summer indicators such as pollen, especially in the North Pacific sector (Kokorowski et al., 2008). Ground ice, defined as all types of ice contained in frozen ground (van Everdingen, 1998) including ice wedges provide paleoclimate archives that can be studied by stable water isotope methods analogously to glacier ice (Mackay, 1983; Meyer et al., 2002b). Ice wedges are widely distributed in non-glaciated high northern latitudes, are diagnostic of permafrost and, in general, indicative of periods of cold climate conditions. They are found in both continuous and discontinuous permafrost zones and may also have formed during and survived interglacials (Froese et al., 2008). Ice wedges are distinctive due to their vertically-oriented foliations and air bubbles. They form as winter thermal contraction cracks are periodically filled by surface water (mainly from snow melt), which quickly (re)freezes at negative ground temperatures (Lachenbruch, 1962). The seasonality of thermal contraction cracking and of the infill of frost cracks are generally related to winter and spring, respectively. Ice wedges are, thus, interpreted to be indicative of winter climate conditions.

We investigated a relict, buried ice-wedge system within the continuous permafrost zone near Barrow, northern Alaska (Figure II.1). The Barrow ice-wedge system (BIWS) is buried under about 3 meters of Late Glacial/early Holocene ice-rich sediments. Permafrost in this area is cold (about -9°C) and extends to over 300 meters in depth. The BIWS consists of two intersecting ice wedges, which were sampled horizontally, i.e. perpendicular to its growth structure, covering the complete time interval of ice wedge formation (Figure II.3). Organic material such as leaves, twigs or lemming pellets contained within the BIWS were selected for direct AMS ^{14}C (accelerator mass spectrometry radiocarbon) dating. AMS ^{14}C -dates of organic matter enclosed in the BIWS suggest continuous ice-wedge formation for about 3000 years duration between 14.4 and 11.3 kyr cal B.P. (before present = before 1950; Table II.1), comprising the Bølling-Allerød Interstadial (BA), the Younger Dryas Stadial (YD) as well as the onset of the Preboreal warming (PB).

We present the stable oxygen ($\delta^{18}\text{O}$, ‰ V-SMOW) and d excess records (d excess = $\delta\text{D} - 8 * \delta^{18}\text{O}$; Dansgaard, 1964) from the BIWS (Figure II.2). The $\delta^{18}\text{O}$ values are interpreted as a proxy for air temperatures in the region of precipitation,

whereas the d excess characterizes sea surface conditions (i.e. relative humidity, temperature) in the moisture source region. The chronology of the BIWS stable isotope record is based upon mean calibrated AMS ^{14}C -ages. We interpolate linearly between ^{14}C -dated samples to enhance the stable isotope record of the BIWS, assuming regular ice-wedge growth, which is supported by the sequence of AMS ^{14}C -dates in the BIWS, as well as constant horizontal growth rates between two ^{14}C -dated samples. The BIWS stable isotope data is compared to the N-GRIP (North Greenland Ice Core Project) $\delta^{18}\text{O}$ and d excess records (Steffensen et al., 2008; Figure II.2) for the time interval between 15 and 10 kyr cal B.P. N-GRIP is the most recently published Greenland ice-core record with highest resolution and dating accuracy for the Late Glacial-Holocene transition.

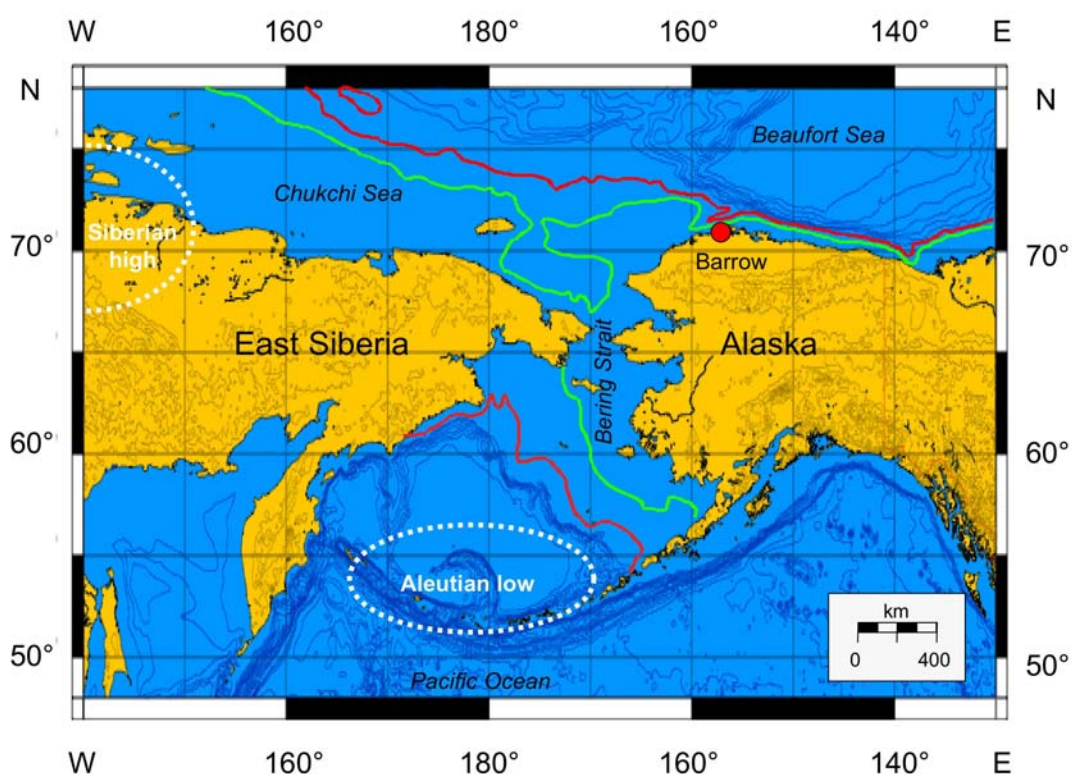


Figure II.1: Location of the Barrow ice-wedge system (BIWS) in northern Alaska (red dot). Red and green contours indicate the -100 m and -50 m isobaths, respectively. The -100 m isobath corresponds widely to the position of the shoreline at 18 kyr cal B.P. (PALE Beringian Working Group, 2002). White-dotted lines give the approximate positions of the modern dominant atmospheric pressure centers (Aleutian low and Siberian high; Mock et al., 1998).

Table II.1: Radiocarbon dates of organic remains in ice wedges of the Barrow ice-wedge system (BIWS)

N°	Sample ID	Radiocarbon age		Calibrated age	Mean calibrated	Lab ID
				2 σ range	age	
		[yr B.P.]		[yr cal B.P.]	[yr cal B.P.]	
1	BAR-IW- ¹⁴ C-1	12 370	+/-60	14 770 - 14 082	14 426	KIA 25339
2	BAR-IW- ¹⁴ C-3	11 700	+/-100	13 761 - 13 338	13 550	KIA 33159
3	BAR-IW- ¹⁴ C-5	11 310	+/-45	13 275 - 13 107	13 191	KIA 25656
4	BR06-IW-4.1	11 250	+/-90	13 284 - 12 956	13 120	KIA 33157
5	BAR-IW- ¹⁴ C-7	10 740	+/-60	12 861 - 12 681	12 771	KIA 25657
6	BR06-IW-4.9	10 730	+/-60	12 857 - 12 674	12 766	KIA 33158
7	BAR-IW- ¹⁴ C-11	10 480	+/-65	12 690 - 12 141	12 416	KIA 25658
8	BAR-IW- ¹⁴ C-22	10 290	+/-45	12 367 - 11 830	12 099	KIA 25659
9	BR06-IW-3.11	9990	+/-80	11 811 - 11 238	11 525	KIA 33156
10	BR06-IW-3.5	9850	+230/-220	12 098 - 10 585	11 342	KIA 33155

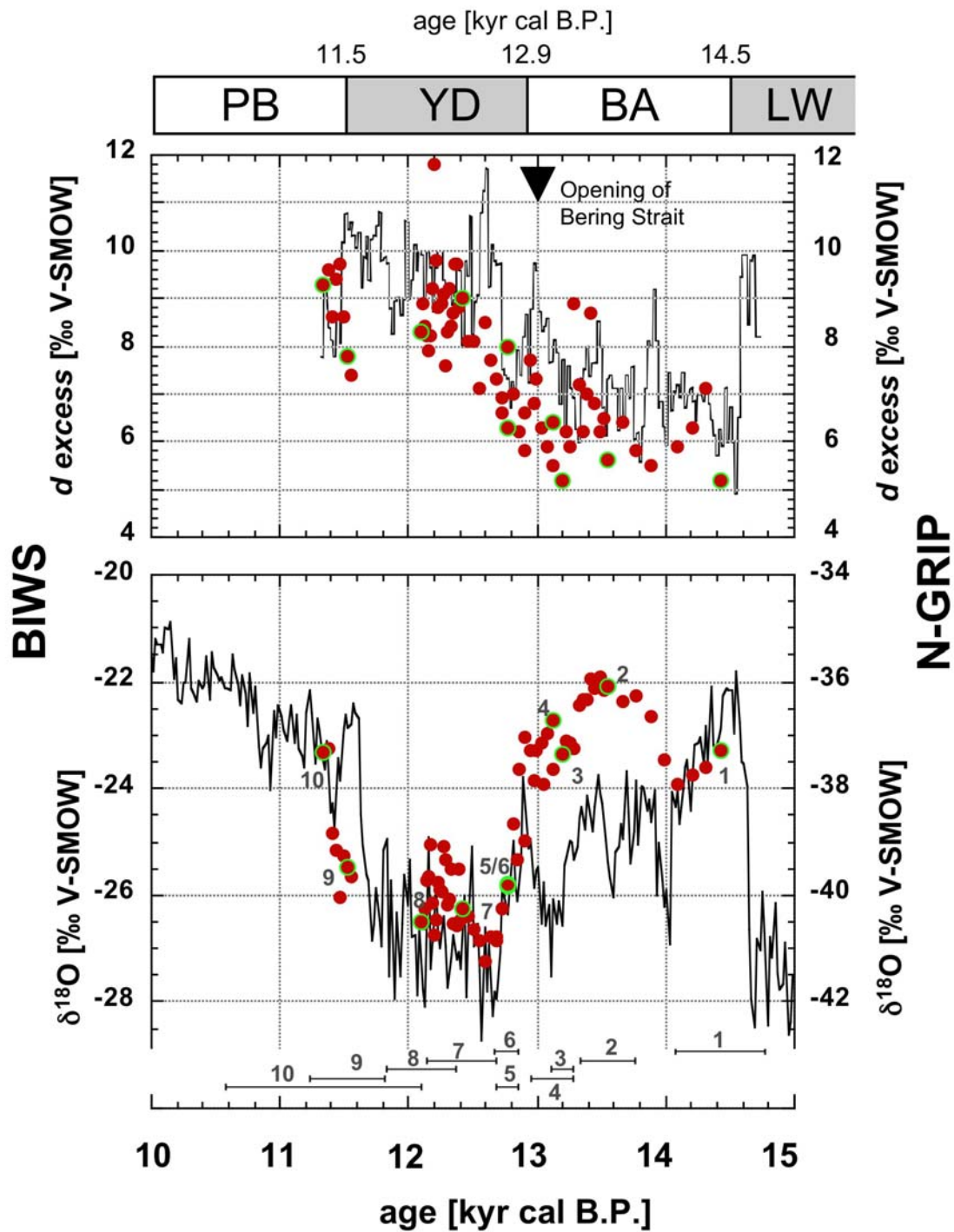


Figure II.2: Stable isotope record (top: d excess; bottom: $\delta^{18}\text{O}$) of the Barrow ice-wedge system (BIWS, red dots) in comparison with the N-GRIP ice core in 20-yr resolution (Steffensen et al., 2008; black line) for the time interval between 10 and 15 kyr cal B.P. Green circles indicate directly AMS ^{14}C -dated samples (mean calibrated ages), which are numbered as in Table II.1. Bottom: 2σ error bars of each date are displayed. Main chronological units are given: LW= Late Wisconsin, BA = Bølling-Allerød; YD = Younger Dryas; PB = Preboreal.

The similarity between N-GRIP and BIWS $\delta^{18}\text{O}$ records is striking with a prominent decrease in $\delta^{18}\text{O}$ at 12.9 kyr cal B.P. and subsequent increase at around 11.5 kyr cal B.P. bracketing the YD cold stadial. Although the absolute N-GRIP $\delta^{18}\text{O}$ values are lower reflecting colder mean annual air temperatures at the Greenland drill site, both N-GRIP and BIWS records display $\delta^{18}\text{O}$ variations of the same order of magnitude (6‰ in BIWS; 7‰ in N-GRIP ice core). The decrease in $\delta^{18}\text{O}$ reflecting colder temperatures at around 12.9 kyr cal B.P. occurs nearly contemporaneously both in N-GRIP and BIWS records, whereas the increase in $\delta^{18}\text{O}$ at 11.5 kyr cal B.P. is interpreted as early PB warming pulse, which is recorded first in the N-GRIP ice core, followed by a more gradual change in the BIWS $\delta^{18}\text{O}$ record with a lag of 100 to 200 years. The coldest phase in both records is around 12.5 kyr cal B.P. These observations contrast with re-evaluation of paleoclimate (mostly palynological) data from Alaska and Northeast Siberia, which suggest that the YD cold event has been absent or reduced in northern Alaska (Kokorowski et al., 2008). Modern synoptic climatology studies provide further insight to the interpretation of paleoclimate records. During the second half of the 20th century, atmospheric circulation patterns were seasonally and spatially heterogeneous. Changes in position and intensity of the Aleutian low as well as of the Siberian high are responsible for large parts of the climate variability in this region (Mock et al., 1998). Accordingly, the cold season during the YD was associated with a stronger and more pronounced Aleutian low (Kokorowski et al., 2008). The evidence of a YD cold event in the BIWS $\delta^{18}\text{O}$ record emphasizes that the YD in northern Alaska was related to the winter season. This is supported by prominent YD evidence in southern Alaskan coastal regions, which are characterized by winter precipitation maxima (Kokorowski et al., 2008, Mock et al., 1998).

Both, N-GRIP ice core and BIWS data have a tendency for relatively low $\delta^{18}\text{O}$ values in their records at about 14.0 to 14.2 kyr cal B.P., but at higher temperature level than in YD. A cold phase between Bølling and Allerød stages is known from the Greenland ice cores as Older Dryas event and could also be detected in the BIWS $\delta^{18}\text{O}$ record. The major discrepancy between both records is a well-defined maximum in the BIWS $\delta^{18}\text{O}$ dataset during the BA period (at about 13.5 kyr cal B.P.), later by about 800-1000 years than the N-GRIP ice core $\delta^{18}\text{O}$ maximum at 14.5 kyr cal B.P. The BIWS $\delta^{18}\text{O}$ maximum is contemporaneous to the initial establishment of *Betula* shrub tundra in western Alaska (Hu et al., 2002) and

suggests that in Alaska not only the ecological response but also the winter climatic conditions differ from the Greenland BA temperature optimum.

It is generally agreed that oceanographic changes in the North Atlantic region (e.g. of the meridional overturning circulation, MOC) are responsible for the sudden Northern Hemispheric climate deterioration (McManus et al., 2004; Broecker, 2006). The YD cooling has been attributed to the release of meltwater from the Laurentide Ice Sheet to the North Atlantic or Arctic oceans (Tarasov and Peltier, 2005), which stopped or weakened North Atlantic deep water (NADW) formation and, thus, the thermohaline conveyor belt. The “shutdown” of the MOC and the subsequent lack of heat transport to the Arctic lead to a rapid temperature drop in the entire Northern Hemisphere. This was connected with altered atmospheric circulation patterns and the southward extent of Arctic sea ice. Global circulation model simulations suggest lower sea surface temperatures (SST) during the YD (Mikolajewicz et al., 1997), both in the North Atlantic (about 4 K) and North Pacific (about 2.5 K). Combining the $\delta^{18}\text{O}$ records from N-GRIP ice core and BIWS, we assume that the YD cooling occurred nearly contemporaneously at both sites, whereas warming pulses are lagged by centuries in northern Alaska. The warming pulse, i.e. at about 11.5 kyr cal B.P., could have originated in the North Atlantic likely due to the re-initiation of NADW formation.

The d excess records from both BIWS and N-GRIP ice core coincide in general trends and absolute values (Figure II.2). The BIWS varies from low d excess (of about 6‰) during BA to higher d excess (of about 9‰) in YD. A similar, but more abrupt shift in the N-GRIP d excess record from 6-7‰ in BA to about 9-10‰ in YD has been observed between 13.5 and 12.8 kyr cal B.P. (Steffensen et al., 2008). This shift has been interpreted as reorganization of the Arctic atmospheric circulation and was accompanied by an increase of precipitation rates in Greenland (Dansgaard et al., 1989; Alley, 2000). The shift in the BIWS d excess record illustrates that Alaskan atmospheric circulation patterns were part of this reorganization process, but more smoothly and, with a lag of about 500-600 years, later than in Greenland. A rise in d excess is indicative of a different (e.g. southward shifted) moisture source (or changing conditions within a stationary moisture source) characterized by lower relative humidities and/or higher SSTs. However, for both North Pacific and North Atlantic, lower SSTs were modeled (Mikolajewicz et al., 1997). A similar counter-intuitive shift in d excess has been

described for Greenland high elevation sites with low d excess in mild phases and high d excess in cold phases (Johnsen et al., 1989). This has been explained by a southward shift of the polar front as well as of a more southern sea-ice limit leading to higher latitudinal temperature gradients and stronger zonal wind patterns. Therefore, a shift to a different (warmer or less humid) moisture source for winter precipitation in northern Alaska is likely. We suggest that the lag of this shift behind the Greenland record and the gradual increase of BIWS d excess is likely related to oceanographic changes such as the opening of the Bering Strait between about 12 and 11 kyr ^{14}C B.P. 23. Bradley and England (2008) refined this estimate to about 13 kyr cal BP, when inflow of Pacific water through the Bering Strait brought first Pacific bivalves to the Arctic Ocean. The breaching of the Bering Strait initialized a northward flow of large amounts of low-saline Pacific water to the Arctic Ocean. A local cold-SST moisture source for winter precipitation in northern Alaska, however, can be ruled out as our d excess data suggests. Additionally, the Bering Strait was frozen in winter and low temperatures imply a low moisture-carrying capacity of air masses. Therefore, we hypothesize that this general change of oceanographic circulation patterns in the North Pacific region, especially of the sea surface water, might have caused this gradual change of the BIWS moisture source region.

In summary, these findings highlight the potential of permafrost, especially ice wedges, as centennial-scale paleoclimate archives to enable us to expand the spatially-restricted glacier ice records to larger continental areas of the Northern Hemisphere. The BIWS record represents the first isotope-based permafrost climate record of the Late Glacial-Holocene transition including well-documented evidence for the YD cold stadial. Since ice wedges are investigated by stable isotope methods, this certainly accounts for temperatures of the winter season. Similar d excess records from the Greenland ice sheet and its permafrost “analogue” in Alaska underline the atmospheric-oceanographic teleconnection between both regions.

Methods

The Barrow permafrost tunnel intercepts a buried ice-wedge system horizontally about 10 m in E-W direction and 3 m in N-S direction. The section was excavated and first described in the early 1960s (Brown, 1965). The Barrow ice-wedge

system (BIWS) is covered by about 3 m of frozen ice-rich deposits. An access shaft reaches the ice wedge level at 3.6 m depth below surface (m b.s.). The BIWS was sampled for stable isotopes horizontally at a depth of 4.5 m b.s (compare Figure II.3). In total, 131 samples were taken from two intersecting ice wedges in five sampling transects, which were sampled with an electric chain saw (1.5 cm slices in 10 cm intervals). All ice samples were transported frozen to the cold laboratory at Alfred Wegener Institute for Polar and Marine Research (Bremerhaven, Germany), where they were cut for stable isotope and radiocarbon analyses.

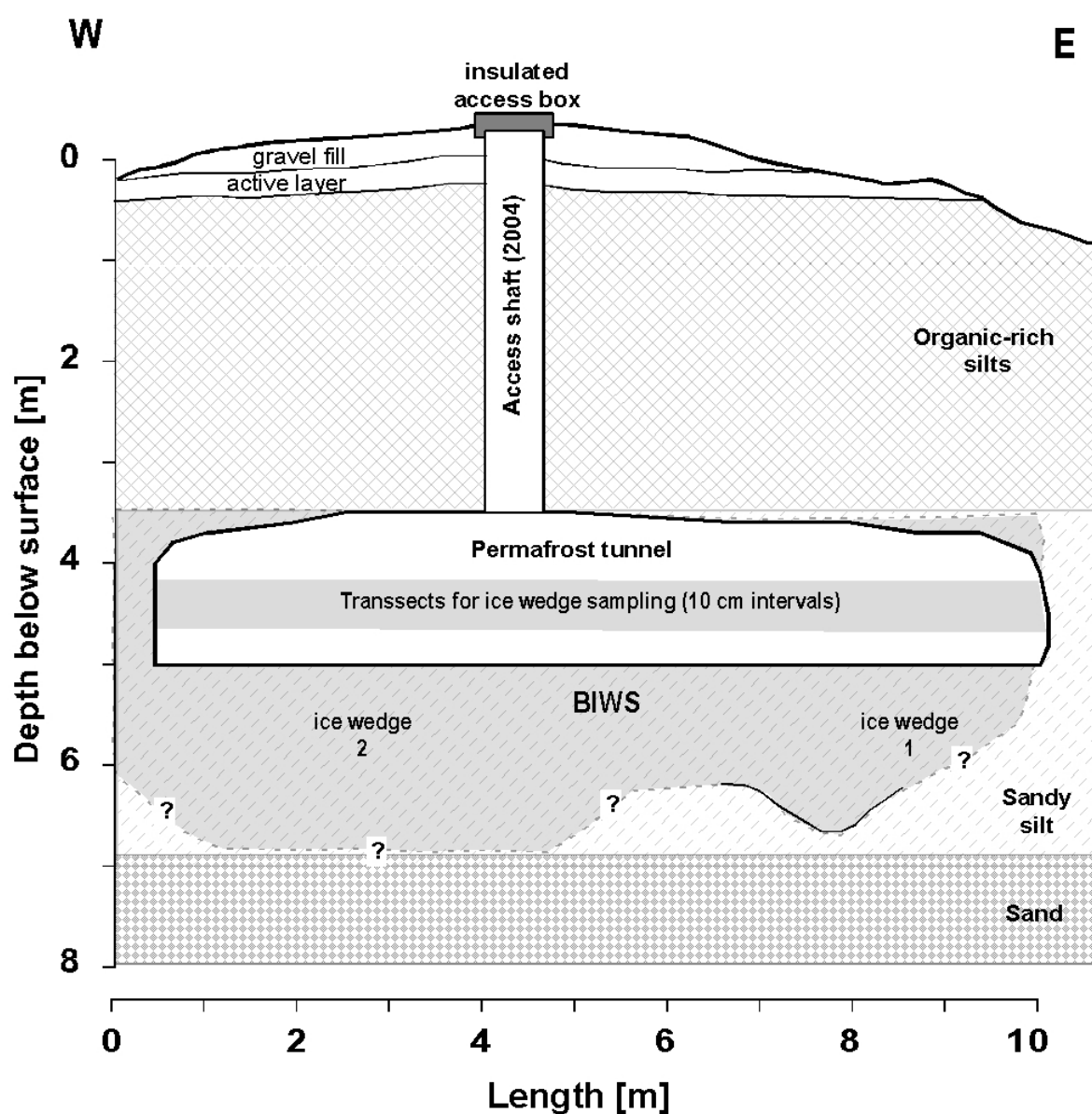


Figure II.3: Schematic drawing of the Barrow ice wedge system (BIWS, side view). Grey sections indicate the position of the ice-wedge sampling transects.

Ages of organic remains in the buried ice wedge system were determined by Accelerator Mass Spectrometry (AMS) ^{14}C -dating of plant remains (mainly lemming pellets, small roots, leaves or twigs) picked under light microscope. The measurements were carried out in the AMS facility of the Leibniz Laboratory in Kiel, Germany (Nadeau et al., 1997; 1998). In order to eliminate contamination by younger organic acids only the leached residues were used for dating. AMS ^{14}C -ages were calibrated using the CALIB rev. 5.02 Software, Calibration dataset: intcal04.14c (Reimer et al., 2004). Mean calibrated ages were calculated from the minimum and maximum values (2σ range).

Stable water isotopes were measured with a Finnigan MAT Delta-S mass spectrometer at the Alfred Wegener Institute, Research Unit Potsdam using equilibration techniques. Hydrogen and oxygen isotope ratios are given as per mil difference relative to V-SMOW (‰, Vienna Standard Mean Ocean Water), with internal 1σ errors better than 0.8‰ and 0.1‰ for δD and $\delta^{18}\text{O}$, respectively (Meyer et al., 2000).

Acknowledgements

Field logistics was provided by the Barrow Arctic Research Consortium (BASC) in support of the U.S. National Science Foundation Project OPP-0327664, Barrow Permafrost Observatory. The site is owned by the Ukpeagvik Iñupiat Corporation (UIC), the Barrow Village Corporation.

III ³⁶Cl/Cl ratio in ground ice of East Siberia and its application for chronometry

Alexander Blinov¹, Vasily Alfimov², Jürg Beer³, David Gilichinsky⁴, Lutz Schirrmeister⁵, Alexander Kholodov⁴, Pavel Nikolskiy⁶, Thomas Opel⁵, Dmitry Tikhomirov¹ and Sebastian Wetterich⁵

¹St. Petersburg State Polytechnic University, St. Petersburg, Russia

²Ion Beam Physics, ETH Zürich, Switzerland

³Swiss Federal Institute of Aquatic Science and Technology, Dübendorf, Switzerland

⁴Soil Cryology Laboratory, Institute of Physicochemical and Biological Problems in Soil Science, Pushchino, Russia

⁵Alfred Wegener Institute for Polar and Marine Research, Department of Periglacial Research, Potsdam, Germany

⁶Laboratory of Quaternary Deposits, Geological Institute, Russian Academy of Sciences, Moscow, Russia

Geochemistry, Geophysics, Geosystems (G3). Resubmitted after revision.

Abstract

Abundance of the cosmogenic nuclide chlorine-36 (³⁶Cl) was measured together with the chloride (Cl⁻) concentration in different horizons of Quaternary permafrost samples collected from various types of ground ice in the northeastern part of Siberia. The ³⁶Cl/Cl in 32 samples ranged in value from 2.4x10⁻¹⁴ to 1.4x10⁻¹². Nonetheless, after a few extreme values were excluded these ³⁶Cl/Cl ratios provide a local permafrost chronometry. The general concordance of the modelled ages with geological expectations and other chronological methods supports the potential power of the proposed dating method. However, the large observed change in ratios from higher to lower values during the transition from Last Glacial Maximum (LGM) to Holocene climatic conditions remains unexplained. An attempt to make use of the corresponding Beryllium-10 (¹⁰Be) absolute concentrations in the same samples failed because input of ¹⁰Be attached to particulate matter into permafrost is unknown. Further ³⁶Cl/Cl serial measurements of modern

precipitation and fossil ground ice are needed to refine this dating method into a practical tool with a clear protocol.

III.1 Introduction

Permafrost is a palaeo-environmental archive that contains several proxy records such as fossil faunal, floral, and microbial communities and greenhouse gases that existed before human environmental impact. In the Eurasian Arctic, ancient frozen ground exists because of the persistent harsh, cold climatic conditions. Permafrost underlies most of the Siberian territory; however, the question of whether it has existed permanently since its first occurrence remains unresolved. The oldest signs of permafrost conditions are related to frost-crack pseudomorphs in late Pliocene deposits at the Krestovka River in the Kolyma lowlands (Sher, 1971, 1974) and in the Val'karai lowlands on the northern coast of Chukotka (Arkhangelov et al., 1985). The palaeo-ecological data of Sher (1997) indicated that most ancient permafrost records are about 3 million years old.

The potential of permafrost as a palaeo-environmental archive of geochemical, cryolithological, and biological characteristics with ages that correspond to those of permafrost makes the development of an accurate permafrost chronology an essential objective of geological, climatological, and palaeoecological studies. Permafrost chronology is important for outlining the stratigraphy and Quaternary history of the permafrost region as well as for detecting the temporal vertical dynamics of the permafrost.

Previous palaeo-environmental studies in Arctic permafrost have used different chronological methods such as radiocarbon dating (e.g. Mackay et al., 1972; Moorman et al., 1996; Murton et al., 1997; Sulerzhitsky and Romanenko, 1997; Vasil'chuk and Vasil'chuk, 1998; Vasil'chuk et al., 2000; Schirrmeister et al., 2002b; Grosse et al., 2007), luminescence dating (e.g. Krbetschek et al., 2000; Andreev et al., 2004, 2009), and the ²³⁰Th/U disequilibria method (e.g. Schirrmeister et al., 2002a, 2003b; Wetterich et al., 2008b). Using these dating methods, only the age of sedimentation and of organic remains within permafrost were determined; the age of the permafrost aggradation, especially for early Pleistocene to late Pleistocene deposits, could not be determined. Continuous chronologies of permafrost do not extend beyond the limit of radiocarbon, and there are but few reports with indirect dates of mid-Pleistocene permafrost (e.g.

Froese et al., 2008). The recently proposed geochronology method using the long-lived cosmogenic radionuclide ³⁶Cl (Gilichinsky et al., 2007) could potentially extend the dating range beyond several hundred thousand years; in so doing, this method would find a wide variety of applications in Quaternary palaeo-environmental and palaeo-ecological reconstructions, e.g. estimating the time scale for the long-term preservation of fossils, tracing the history of greenhouse gases, and determining the age of inclusions of viable microorganisms adapted to a permanently frozen environment.

Common ground-ice features within the permafrost are ice wedges formed by annually repeated contraction cracking of upper frozen ground layers. The precipitation that falls in winter enters the ice wedge frost crack as melt water during melt season and refreezes there, forming a new vertical ice vein and subsequently growing ice wedges. Two main types of ice wedges are distinguished: syngenetic ice wedges form synchronously with accumulation and freezing of the surrounding sediments; epigenetic ice wedges form during freezing of already existing sediments (van Everdingen, 2005). Depending mainly on the temperature regime, the water supply, and the substrate, other ground-ice types such as segregation ice, pore ice, or buried ice bodies of various structure and extent are also substantial parts of permafrost.

The global chlorine cycle has been intensively studied, mostly in connection with atmospheric ozone depletion (Graedel and Keene, 1996). Most stable chlorine enters the troposphere in sea spray. Volcanoes add not more than 15-20% to the tropospheric chlorine injection in the form of HCl (Graedel and Keene, 1996); this source is highly sporadic and unevenly distributed on the surface. The addition of dust-borne chlorine from the surface is usually neglected in the contemporary atmospheric budget. Under standard atmospheric conditions, the chlorine atoms produced occur as Cl⁻ due to this element's strongly hydrophilic nature and high electron affinity. This is advantageous for many environmental and hydrological applications because chloride acts as a conservative tracer and undergoes minimal chemical interactions in the environment. In the course of its geochemical cycle, chlorine is removed from the atmosphere by wet and, to a smaller extent, by dry precipitation. The deposition flux depends on the distance from the oceans and on wind direction and speed (Johnston and McDermott, 2008).

Under contemporary conditions, the Siberian regions west of 140°E receive most of the moisture from the relatively warm northern Atlantic Ocean as indicated by the west-to-east direction of the main moisture fluxes in northern Eurasia (Kuznetsova, 1998). In contrast, moisture transport from the cold, predominantly ice-covered Arctic Ocean to Siberia is considered to be negligible. Therefore, the varying distance of northern Siberian regions from the Arctic Ocean is not expected to influence the deposition flux of stable chlorine. During ice wedge formation, the stable chlorine contained in the precipitation is incorporated into the ice.

The cosmogenic radionuclide ³⁶Cl has a half-life of 301,000 years, and is produced in the Earth's atmosphere by nuclear reactions of cosmic rays (CR) with atoms of air. The primary CR penetrating the atmosphere generate secondary cascades which develop in the downward direction, so the stratosphere yields about 55% of the mean atmospheric production of ³⁶Cl and the troposphere contributes the remaining 45% (Masarik and Beer, 1999). The dominant contribution comes from Argon-40 (⁴⁰Ar) spallation, with a minor addition from neutron activation of ³⁶Ar and ³⁵Cl. According to calculations, the mean global atmospheric production rate of cosmogenic ³⁶Cl is close to 20 atoms m⁻²s⁻¹. The production rate has a strong latitudinal dependence caused by the shielding effect of the Earth's dipole magnetic field. However, most of this effect is eliminated by strong mixing of the stratospheric air masses (Heikkila et al., 2008).

The production of ³⁶Cl, as well as other cosmogenic nuclides, is affected by temporal changes in solar magnetic activity, which modulates the CR flux via the solar wind. A stronger solar wind deflects more CR away from Earth decreasing ³⁶Cl production, and vice versa. The eleven-year cycle and hundred-year-long intervals of depressed solar activity are apparent in annually-resolved radionuclide records (Muscheler et al., 2007); however, these cycles are negligible when averaged on the geological time scale. Long-term variations of the ³⁶Cl production rate on multi-millennial time scales is caused by slow changes of the geomagnetic field intensity (Baumgartner et al., 1998).

³⁶Cl that has been produced and circulated in the stratosphere is preferentially transported to the troposphere at mid-latitudes, in the regions of the polar and sub-polar jet-streams, causing maximum ³⁶Cl fallout between 30° and 60° in both hemispheres (Lal and Peters, 1967; Heikkila et al., 2008). After a residence time of

about one week, ³⁶Cl is then removed from the troposphere by wet and dry deposition (Bentley et al., 1986). Its local surface flux is strongly influenced by the precipitation rate, and corrections should be applied to account for this effect (Blinov et al., 2000). Obviously, the atmospheric air transport is influenced by climatic, as well as meteorological conditions (Heikkila et al., 2008). Thus, temporal and spatial variations seen in the ³⁶Cl local surface flux reflect a combination of variations in production, transport, and depositional processes. Recently, new surface precipitation measurements have estimated the mean fallout rate of ³⁶Cl in European mid-latitudes (30–70° N) as 43.7 atoms m⁻²s⁻¹ (Johnston and McDermott, 2008).

The mean lifetime of ³⁶Cl is $\tau_{36} = T_{1/2}/\ln 2 = 434,000$ a. After the meteoric component following the surface water flow is incorporated into the permafrost, the ratio of ³⁶Cl to stable chlorine decreases with time by the process of exponential radioactive decay:

$$\frac{d\left(\frac{{}^{36}\text{Cl}}{\text{Cl}}\right)}{\frac{{}^{36}\text{Cl}}{\text{Cl}}} = -\frac{dt}{\tau_{36}}. \quad (1)$$

It was assumed (Gilichinsky et al., 2007) that after an ice wedge system closed, the time interval Δt since formation of its horizons could be calculated according to (1) from the corresponding ³⁶Cl/Cl ratios:

$$\Delta t = t_2 - t_1 = \tau_{36} \cdot \ln \left(\frac{{}^{36}\text{Cl}/\text{Cl}(t_1)}{{}^{36}\text{Cl}/\text{Cl}(t_2)} \right). \quad (2)$$

For a surface base sample of zero age, equation (2) gives the absolute age of the deeper sample. The precondition of the proposed method's validity is the constant surface ³⁶Cl/Cl over Δt .

Ground-water ages in the range of up to one million years established on the basis of ³⁶Cl concentration measurements have been reported (Bentley et al., 1986). It is expected that syngenetic permafrost ice samples with ages up to 1-2 million years can be dated with a similar procedure. The ³⁶Cl/Cl method was tested on the late and mid-Pleistocene syngenetic permafrost ice wedges from Cape Svyatoy Nos and Bol'shoy Lyakhovsky Island, resulting in an age range of 460 ± 130 thousand years for regional Pleistocene permafrost, a range that was supported by indirect palaeontological and geochronological data (Gilichinsky et al., 2007). This work,

which applied the ³⁶Cl/Cl method to additional permafrost samples from various stratigraphical units from the same region, mainly aimed to confirm the principles and improve the database.

III.2 Sampling of ground ice

Quaternary syngenetic permafrost deposits with two levels of large ice wedges exist in the western part of the East Siberian Sea along the Dmitry Laptev Strait; these deposits are located on both the west and north coasts of Cape Svyatoy Nos and Oyogos Yar, and on the southern coast of Bol'shoy Lyakhovsky Island. A special sampling campaign was organized in this region during the summer seasons from 2004 to 2007 (Figure III.1). The samples of ice wedges (Figure III.2) were extracted either from the boreholes, or from outcrops with well-defined horizon structure. A summary of the ice wedge data appears in Table III.1. The majority of the samples come from several generations of ice wedges. A few samples consist of segregation ice or buried ice lenses.

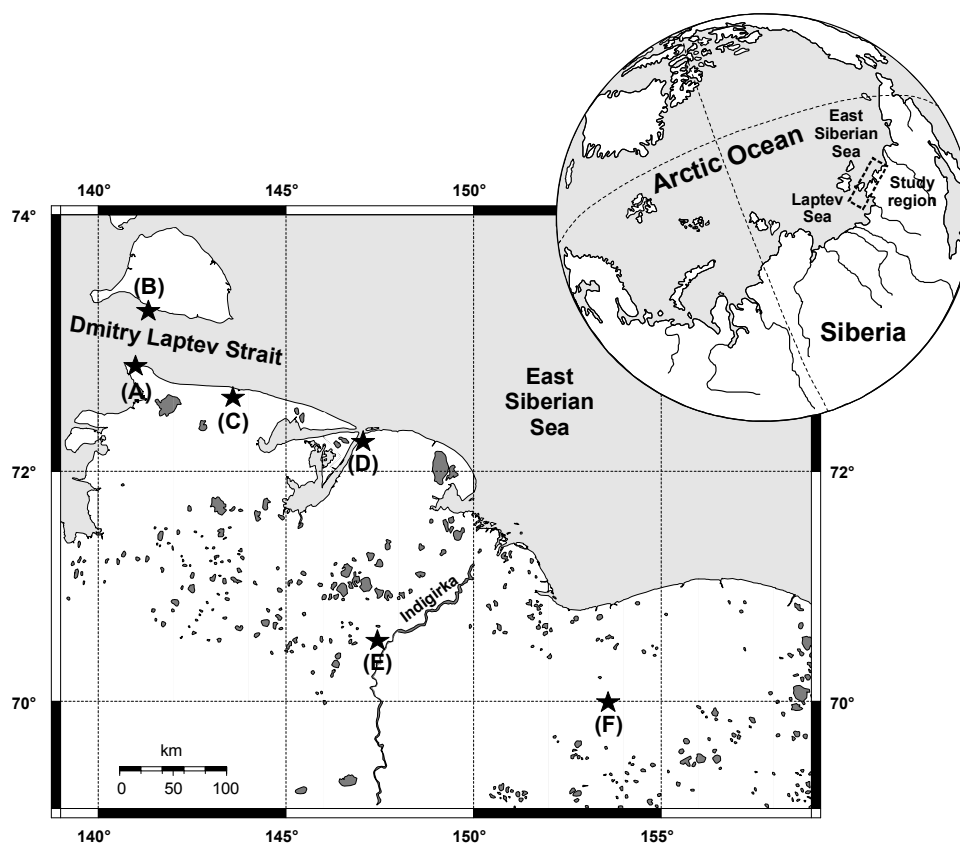


Figure III.1: Location of sampling sites in Northeast Siberia: (A) – Cape Svyatoy Nos, (B) – Bol'shoy Lyakhovsky Island, (C) – Oyogos Yar coast, (D) – Cape Khaptashinsky Yar, (E) – Allaikha River and (F) – Bol'shoy Khomus Yuryakh River.

Permafrost samples (Table III.1, № 1-4) from the cross section of Cape Svyatoy Nos (A in Figures III.1 and III.2) were delivered for dating in summer of 2004. This section included two different systems of syngenetic ice wedges formed during the mid-Pleistocene (Yukagir Suite) and late Pleistocene (Yedoma Suite). The sample (Table III.1, № 5) of a middle Pleistocene syngenetic ice wedge (Yukagir Suite) from Bol'shoy Lyakhovsky Island was collected in order to confirm the dating result from Cape Svyatoy Nos.

Sixteen ice wedge samples (Table III.1, № 6-21) were collected from cliff exposures on both coasts of Dmitry Laptev Strait in 2007. Ten samples (Table III.1, № 6-15) were collected at the south coast of Bol'shoy Lyakhovsky Island (B in Figures III.1 and III.2). Six samples were taken at the coast of Oyogos Yar (C in Figures III.1 and III.2). The studied sequences cover the Saalian Ice Complex deposits of the Yukagir Suite (Table III.1, № 5, 6, 8), pre-Eemian epigenetic ice wedges in fine-grained flood plain deposits of the Kuchchugui Suite (Table III.1, № 7, 12), probable Early Weichselian syngenetic ice wedges of the Bychchaguy Suite (Table III.1, № 14, 18, 19), huge syngenetic ice wedges of the late Pleistocene Yedoma Suite (Table III.1, № 10, 13, 15, 16, 21), and young syngenetic ice wedges formed in Holocene thermokarst depressions (Table III.1, № 9, 11, 17, 20). The exposed sequences were surveyed, described, photographed, and sketched according to sediment structures and cryostructures (Schirmer et al., 2008b; Opel et al., 2009a; Wetterich et al. 2009). Most ice wedge samples were taken with an axe; one of them (Table III.1, № 8) was obtained with a chain saw.

In 2006, five samples of ground ice (Table III.1, № 22-26) were collected at Khaptashinsky Yar on the right bank of the Khroma Bay of the East Siberian Sea (D in Figures III.1 and III.2). The first three samples (№ 22-24) were taken near the sea shore from different depths in the same borehole. They belong to a syngenetic ice wedge of the Yedoma Suite. Sample № 25 was collected from another borehole at the same location. It belongs to a syngenetic ice wedge of the middle Pleistocene Ice Complex. Sample № 26 was taken from an ice lens of a nearby river section. This exposure presumably corresponded to the same middle Pleistocene Ice Complex as sample № 25, and the quality of the sample was marked as poor.

Table III.1: Field data, analytical results and calculated ages. The sample type is indicated as ice wedge (IW) or segregation ice (SI).

No	Sample ID	Sample type	Sample depth below surface (m, b.s.)	Expected age, 10 ³ years	Local stratigraphy	N(Cl), ppm	N(³⁶ Cl/Cl), 10 ⁻¹²	N(³⁶ Cl), 10 ⁴ at·g ⁻¹	³⁶ Cl/Cl age, 10 ³ years
1	2	3	4	5	6	7	8	9	
Cape Svyatoy Nos (2004) 72°51'N, 141°05'E									
1	2/01	IW	3.35-4.35	17-25	Yedoma ¹	7.2 ± 0.6	0.25 ± 0.06	3.06 ± 0.78	34 (base)
2	3/01a	IW	4.35-5.1	25-50	Yedoma ¹	6.2 ± 0.5	0.37 ± 0.08	3.9 ± 0.9	484 ± 161
3	4/01	IW	7.85-8.4	200-400	Yukagir ¹	50.8 ± 1.2	0.11 ± 0.02	9.49 ± 2.08	581 ± 166
4	3/01b	IW	20.5-20.7	200-400	Yukagir ¹	27.1 ± 0.9	0.088 ± 0.018	4.05 ± 0.84	341 ± 43
Bol'shoy Lyakhovskiy Island (2005) 73°17'N, 141°20'E									
5	PFBL05	IW	25	200-400	Yukagir	8.1 ± 0.5	0.13 ± 0.008	1.79 ± 0.16	309 ± 40
Bol'shoy Lyakhovskiy Island (2007) 73°17'N, 141°20'E									
6	L7-01-108	IW	28	> 150	Yukagir ²	3.8 ± 0.3	0.14 ± 0.007	0.90 ± 0.08	552 ± 37
7	L7-01-117	IW	27	130-150	Kuchchugui ²	7.4 ± 0.3	0.08 ± 0.003	1.01 ± 0.06	341 ± 43
8	L7-02-101	IW	27	> 150	Yukagir ²	7.3 ± 0.3	0.13 ± 0.008	1.61 ± 0.12	< 11
9	L7-07-101	IW	3	1-10	Holocene ³	10.4 ± 0.4	0.23 ± 0.008	4.06 ± 0.21	40 (base)
10	L7-07-201	IW	4	30-50	Yedoma ³	6.2 ± 0.3	0.23 ± 0.008	2.42 ± 0.14	< 11
11	L7-08-201	IW	1.9	1-10	Holocene ^{3,4}	14.2 ± 0.5	0.19 ± 0.01	4.58 ± 0.29	609 ± 42
12	L7-12-101	IW	28	130-150	Kuchchugui ²	10.3 ± 0.4	0.07 ± 0.004	1.22 ± 0.08	500 ± 41
13	L7-14-201	IW	22	40-50	Yedoma ^{3,4}	4.1 ± 0.2	0.09 ± 0.005	0.63 ± 0.05	failed
14	L7-15-101	IW	11	100-120	Bychchagy ²	3.5 ± 0.2	0.89 ± 0.005	5.29 ± 0.30	40 (base)
15	L7-18-101	IW	13.2	30-50	Yedoma ³	3.1 ± 0.2	0.29 ± 0.018	1.53 ± 0.14	40 (base)
Oyogos Yar coast (2007) 72°36'N, 143°36'E									
16	Oy7-01-301	IW	1	30-50	Yedoma	6.1 ± 0.3	0.109 ± 0.007	1.13 ± 0.13	< 11
17	Oy7-02-101	IW	2	1-10	Holocene ⁵	20.1 ± 0.4	0.031 ± 0.003	1.06 ± 0.15	68 ± 31
18	Oy7-03-101	IW	15	100-120	Bychchagy	4.0 ± 0.2	0.30 ± 0.01	2.04 ± 0.21	98 ± 31
19	Oy7-03-201	IW	15	100-120	Bychchagy	4.0 ± 0.2	0.28 ± 0.01	1.90 ± 0.20	< 11
20	Oy7-04-201	IW	1.5	1-10	Holocene ⁵	9.4 ± 0.2	0.032 ± 0.003	0.51 ± 0.07	40 (base)
21	Oy7-08-101	IW	3.5	30-50	Yedoma	4.4 ± 0.2	0.52 ± 0.02	3.89 ± 0.38	25 (base)
Khaptashinsky Yar (2006) 72°14'N, 147°03'E									
22	INT 01	IW	0.5-2	20-30	Yedoma	5.9 ± 0.3	0.087 ± 0.012	0.87 ± 0.13	2.19 ± 0.17
23	INT 02	IW	8-9	20-30	Yedoma	3.4 ± 0.2	0.38 ± 0.02	2.19 ± 0.17	3.50 ± 0.28
24	INT 03	IW	11.5-12.2	20-30	Yedoma	7.1 ± 0.3	0.29 ± 0.02	3.50 ± 0.28	

Table III.1 continuation

25	INT 04	IW	12.3-15.3	200-300	Khroma ⁶	9.8 ± 0.4	0.22 ± 0.01	3.66 ± 0.22	80±56
26	INT 05	SI	>15.3	>300	Khroma ⁶	83.8 ± 0.8	0.11 ± 0.01	15.65 ± 1.71	381±65
Allaikha River (2006) 70°34'N, 147°27'E									
27	INT 07	IW	6-8	20-30	Yedoma ⁶	7.4 ± 0.3	0.29 ± 0.02	3.64 ± 0.29	25 (base)
28	INT 08	SI	10.3-11.2	300-500	Achagy ⁶	38.2 ± 0.6	0.19 ± 0.014	12.32 ± 0.93	209±44
Bol'shoy Khomus Yuryakh River (2005) 70°00'N, 153°37'E									
29	INT 1A	SI	1.4-5.4	200-400	--	6.2 ± 0.3	0.34 ± 0.04	3.58 ± 0.46	300 (base)
30	INT 2A	SI	0.7-2.7	200-400	--	6.8 ± 0.3	0.31 ± 0.02	3.58 ± 0.28	< 11
31	INT 3A	IW	12	200-400	--	7.7 ± 0.4	0.024 ± 0.005	0.31 ± 0.07	< 11
32	INT 4C	SI	8.4-12	500-600	--	12.7 ± 0.4	0.21 ± 0.02	4.53 ± 0.45	496±78
Lower Kolyma River (2004, 2005) 68° 45'N, 161° 20'E									
33	INT-2004-S	Snow	Surface	zero age	modern	0.7 ± 0.1	0.012 ± 0.002	0.014 ± 0.003	< 11
34	INT-2005-S	Snow	Surface	zero age	modern	1.3 ± 0.2	0.014 ± 0.001	0.030 ± 0.005	< 11
Yana River (2006) 67°41'N, 135°44'E									
35	INT-10W	River water	Surface	zero age	modern	0.5 ± 0.1	0.39 ± 0.02	0.33 ± 0.067	< 11

¹ Gilichinsky et al. (2007); ² Andreev et al. (2004); ³ Andreev et al. (2009); ⁴ Wetterich et al. (2009); ⁵ Opel et al. (2009a); ⁶ Kaplina (1981)

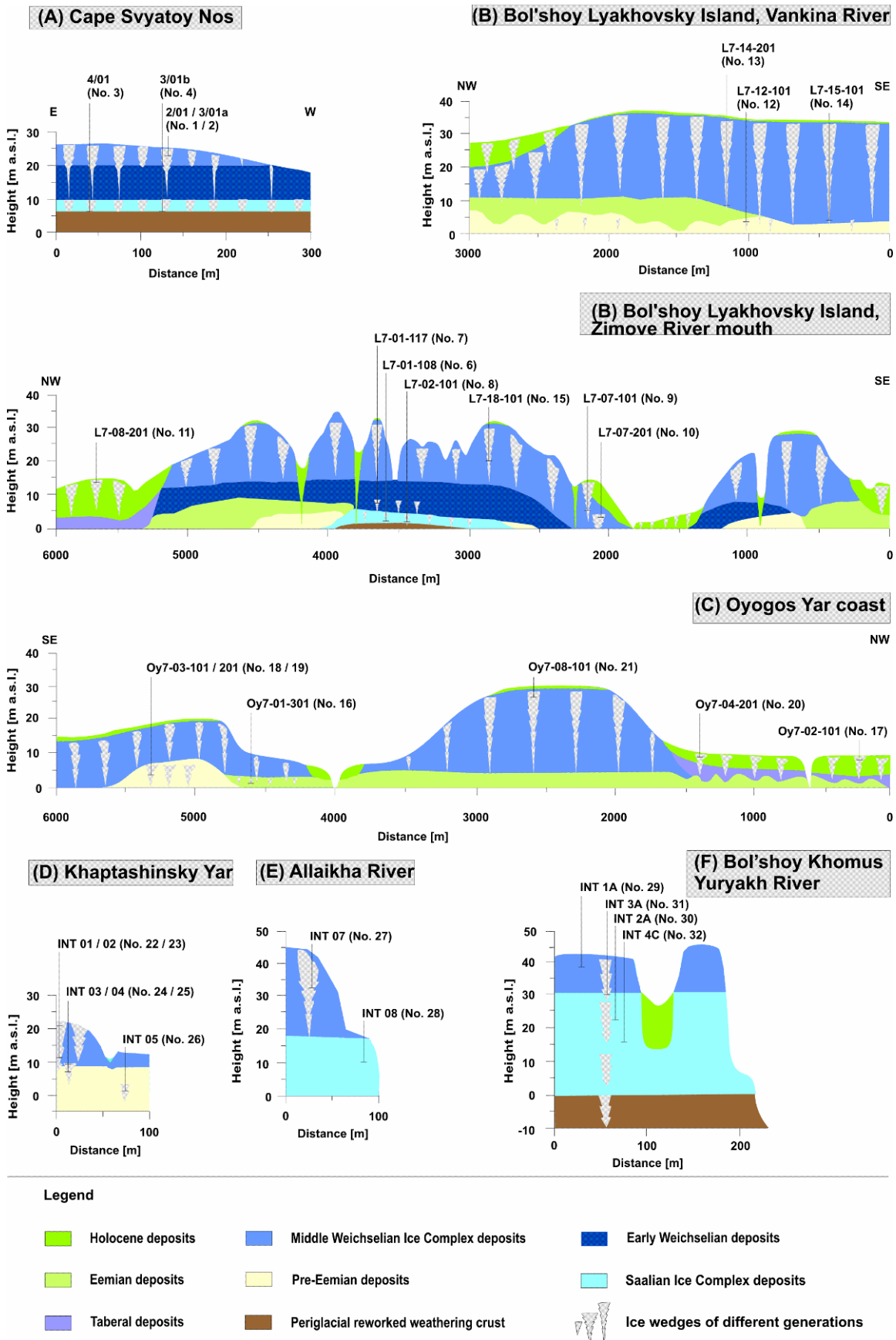


Figure III.2: Generalized overview schemes of the studied exposures: (A) – Cape Svyatoy Nos, (B) – Bol'shoy Lyakhovsky Island, (C) – Oyogos Yar coast, (D) – Cape Khaptashinsky Yar, (E) – Allaikha River, (F) – Bol'shoy Khomus Yuryakh River.

Two samples (Table III.1, № 27, 28) were collected on the banks of Alliakha River, the left tributary of the Indigirka River at a distance of about 100 km from the Arctic Ocean (E in Figures III.1 and III.2). Sample № 27 was taken from a borehole and belonged to a syngenetic ice wedge of the late Pleistocene Ice Complex (Yedoma Suite). Sample № 28 was cut from the middle Pleistocene Ice Complex (Achagy Suite) exposure on the river bank section with an estimated age of more than 300 thousand years. This was the only sample of segregated ice-cement finally obtained by melting out the frozen permafrost sample.

Four samples (Table III.1, № 29-32) were obtained in the Kolyma lowlands in 2005, in the upper reaches of the Bol'shoy Khomus Yuryakh River (F in Figures III.1 and III.2). They represent two middle Pleistocene horizons. The upper horizon is represented by three samples. Two samples of segregated ice (Table III.1, № 29, 30) melted from a frozen deposit that may be 300-400 thousand years old, according to palaeontological evidence. The third sample (Table III.1, № 31) was cut out of a syngenetic ice wedge from the same horizon. The fourth sample (Table III.1, № 32) was collected from a nearby borehole and also consists of melted, segregated ice from permafrost deposits of a lower horizon with an age of about 500-600 thousand years.

In addition, three samples from modern precipitation and surface water were collected from a nearby geographical region to serve as references (Table III.1, № 33-35). Two snow samples were collected in the vicinity of the Kolyma River's lower reach at the beginning of springtime in 2004 and 2005. They represent the contemporary concentration of chemical elements and cosmogenic nuclides in winter precipitation, although they could not be attributed to a specific time interval and could be subject to local conditions such as wind advection and mixing. One water sample was collected from the Yana River in summer 2006.

III.3 Methods

During the field stage a volume of ca. 2 litres of the initial sample was melted, poured into a clean plastic bottle, marked, and shipped to a laboratory for follow-up studies. The experimental procedure for samples № 1-4 was described in Gilichinsky et al. (2007). Chloride concentrations were measured on filtered aliquots using ion chromatography (IC, Dionex DX-320): samples № 6-21 were measured at the Alfred Wegener Institute for Polar and Marine Research Potsdam

(Germany), and samples № 5 and 22-35 were measured at the Swiss Federal Institute of Aquatic Science and Technology (Eawag, Switzerland). Afterwards, the samples for ³⁶Cl measurements were prepared at the Swiss Federal Institute of Aquatic Science and Technology (Eawag, Switzerland) following the standard method (Synal et al., 1994). One sample only (Table III.1, № 11) required the addition of 3.8 mg Cl carrier solution to increase the total chlorine content. Measurements of ³⁶Cl/Cl ratios were carried out by Accelerator Mass Spectrometry (AMS) at the Swiss Federal Institute of Technology facility (ETH Zurich, Switzerland).

III.4 Results

III.4.1 Concentrations and Ratio

Measured chloride concentrations and ³⁶Cl/Cl for the ice samples are summarized in Table III.1. The results for the first four samples were already presented in Gilichinsky et al. (2007). The chloride concentrations range from 3 parts per million (ppm), typical of continental rainwater, up to 84 ppm which exceeds even the mean groundwater concentration. Note that Holocene ice wedges from Bol'shoy Lyakhovsky Island and Oyogos Yar exhibit significantly higher Cl⁻ concentration than those of the Late Pleistocene (Yedoma Suite), possibly related to sea spray effects due to the Holocene transgression; uncertainties in the Cl⁻ concentration measurements were systematically less than 10%. The ³⁶Cl/Cl ratios range from 2.4×10^{-14} to 3.9×10^{-13} for ice; uncertainties in ³⁶Cl/Cl ratios were dominated by an average relative error of about 12% in counting the rare ³⁶Cl isotope. The chloride concentration and ³⁶Cl/Cl ratios in permafrost both exceed the values measured for modern snow and river water (Table III.1, № 33-35). For comparison, values of $0.02\text{--}0.5 \times 10^{-12}$ were measured for ³⁶Cl/Cl in modern rain water collected in Europe (Johnston and McDermott, 2008).

³⁶Cl concentrations do not show any clear dependence on chloride concentration, but rather appear to depend on changing atmospheric transport and climatic conditions. The scatter in the data presumably reflects complicated dynamics of ³⁶Cl fallout and local fixation conditions in ice. The main feature of the calculated concentrations is their general excess, by a factor of about 20, over the values known for the Holocene-related part of Greenland ice cores that directly reflect atmospheric production by CR. Apparently these ³⁶Cl concentrations do not reflect

direct freezing out of surface water containing a constant meteoritic value. At the same time, any contamination of the deeper sediment horizons by recent bomb-produced surface radioactivity could be excluded by the depth profile of the results.

The expected geologic age of the permafrost samples (Table III.1, column 4) corresponds to a wide time interval. The ³⁶Cl/Cl scattering demands an additional explanation. Arctic ice cores could have provided further data on a comparable time-scale, but due to the very low chlorine content, the ³⁶Cl/Cl was not systematically measured there. The ³⁶Cl concentration in the GRIP ice core (Wagner, 1999) decreased by a factor of 2 to 2.5 at the transition from the LGM to the Holocene. However, this decrease was reasonably explained by the corresponding increase in the precipitation rate which diluted the cosmogenic ³⁶Cl in the ice volume. In our analysis we have assumed that the ³⁶Cl/Cl ratio, naturally averaged over a thousand-year interval of constant climatic conditions and fixed in the permafrost ice, was insensitive to changes in the supply of surface water. However, additional sources of chlorine, like eroded dust or sea-salt aerosol input, may alter the local balance. Similar to the GRIP record, the transition from late Pleistocene (Yedoma Suite) to Holocene is reflected in Siberian ground ice as a change of ³⁶Cl/Cl from $(2.5-3.5) \times 10^{-13}$ to $(1.5-2.5) \times 10^{-14}$, except for samples from Bol'shoy Lyakhovsky Island (Table III.1, column 7, № 9, 11). This discrepancy was probably caused by local peculiarities of thermokarst-related processes at Bol'shoy Lyakhovsky Island.

The excess of ³⁶Cl in older samples could be a result of *in situ* production. Some *in situ* ³⁶Cl produced in ice wedges after deposition is also stored in permafrost together with meteoric ³⁶Cl. However, according to our calculations (Tikhomirov and Blinov, 2009) the build-up of *in situ* ³⁶Cl is negligible in late Pleistocene and Holocene Siberian permafrost, and is unlikely to be important for any permafrost horizons younger than one million years.

The ¹⁰Be concentrations were measured in sixteen of the studied samples. The long-lived cosmogenic radionuclide ¹⁰Be was initially considered a supplementary source of information about the transport of surface water to the ice wedges. In modern water samples (snow, river water) its concentration was measured at about 10^4 at. g⁻¹, close to the value for Greenland ice cores or for rain water collections. In contrast, the concentration of ¹⁰Be in permafrost samples showed

values extending from 10^5 up to 10^7 at. g⁻¹ with a ³⁶Cl/¹⁰Be ratio as low as 0.001, excluding an atmospheric origin. The excess may represent an influx of ¹⁰Be to permafrost ice with dust from eroded rock material. The fine particulate component was present in all studied ice samples and the division of ¹⁰Be between particles and water is unknown. After this fact had become clear, measurements of ¹⁰Be concentrations in the next samples were cancelled.

III.4.2 Age determination

The ³⁶Cl/Cl ratios of the ice wedges were used for permafrost age determination. Ground ice samples with a ³⁶Cl/Cl ratio below 5×10^{-14} belonging to the Holocene period defined as < 11 ka were excluded from the following procedure because their initial ³⁶Cl/Cl clearly differs from that of the older samples. For all study sites, we assumed the age of the samples representing the youngest late Pleistocene horizon (Yedoma Suite) according to stratigraphy classification and geological interpretation (Table III.1, column 4). The resulting ages were used as the base age for each local chronology. The ages of the middle Pleistocene samples were calculated as the sum of the median base age and the time interval was determined according to (1). The results are given in Table III.1, column 9 and are illustrated by lines of local permafrost chronologies in Figure III.3. The age determination errors were calculated as a statistical sum which included measurement errors of the ³⁶Cl/Cl ratio and the stable Cl concentration. Geological uncertainties for base samples were not included in the errors because of their non-statistical nature. As noted above, the ³⁶Cl/Cl ratios of Holocene samples do not lay on the decay curves because of the change from higher to lower ratio values during the transition from late Pleistocene to Holocene. Elucidating the reasons for the changes in the ³⁶Cl/Cl ratio during the Holocene will require additional research.

III.4.3 Discussion

Stratigraphic ages coincide with those calculated from ³⁶Cl/Cl for middle Pleistocene (Late Saalian) ground ice at the Khomus Yuryakh River, Khaptashinsky Yar, Bol'shoy Lyakhovsky Island, and Cape Svyatoy Nos study sites as well as for late Pleistocene (Early Weichselian) ground ice on the Oyogos Yar coast. These results confirm the general utility of ground ice dating with ³⁶Cl/Cl

contaminated by ion exchange between small ice wedges and the more concentrated pore ice in the surrounding permafrost deposits. Electrical conductivity transects through these ice wedges show clear and symmetric increases towards the margins (Meyer et al., 2002a).

Extrapolating local chronologies to their base ages, as shown in Figure III.3, provides an estimate of the range of the assumed ³⁶Cl/Cl surface input. For all the sites but one, this input falls within a factor of two of 0.3×10^{-12} . The single exclusion is of the much higher values from the Bol'shoy Khomus Yuryakh River site, though the two measurements made there are not enough for definite conclusions.

No sizeable fractionation of the chlorine isotope ratio in the water phase during transport from the surface to ice wedges could be caused either by physical processes like evaporation/condensation or by simple chemical binding. Non-constant input of sea-borne chloride could produce variations in ³⁶Cl/Cl, but they would be negatively correlated with the chloride concentration. From the geological point of view such anomalous ³⁶Cl/Cl ages could result from lateral ion exchange between ground ice and the surrounding frozen sediment as water migrated along concentration gradients. Assuming an approximate exchange rate of 10 cm per 10 ka, small ice wedges are more sensitive to such exchange than are larger ones. Chemical analysis of pore ice from similar deposits showed certain layers with very high chloride concentrations (100–3000 ppm) and high electrical conductivity (1–10 mS cm⁻¹) (H. Meyer, AWI Potsdam, pers. comm.). A possible explanation was the high aridity and evaporation in the previous period, which resulted in increased ion concentrations in near-surface soils due to repeated freezing-thawing cycles. Strong evaporation due to high continentality is a rather common climate phenomenon in East Siberia today, with potential evapotranspiration approximately twofold higher than real precipitation (Rivas-Martínez, 2007; Wetterich et al., 2008a). In addition, there are several palaeo-environmental records of stronger continentality in the study area during the middle and late Pleistocene (Andreev et al., 2004, 2009; Kienast et al., 2005, 2008; Wetterich et al., 2009).

The enhanced ionic composition of surrounding ground water could be transmitted to post-sedimentary epigenetic ice wedges, leading to the false dates. Another process that could be important is thawing of ground ice during warming periods

like the Eemian interglacial as described by Wetterich et al. (2009) for both coasts of the Dmitry Laptev Strait. Such a thermokarst-related process could result in remobilization of a highly-concentrated soil solution and its intrusion into older ground ice bodies.

III.5 Summary and Conclusions

³⁶Cl/Cl measured in ground ice provides valuable information about the timing of permafrost formation. For the first time, previously unknown permafrost ages were estimated for the vast territory of the eastern Arctic. Except for a few samples, the age of all ice wedges and segregation ice syngenetically formed in cryochrones, demonstrating a good correlation with expected ages as confirmed by other geochronological methods and stratigraphic evidence. Several local chronologies were constructed for syngenetic middle and late Pleistocene ground ice samples from Northeast Siberia. Because the lifetime of ³⁶Cl is 434,000 years, the method is more applicable to old (Saalian) ice wedges than to young (Weichselian) ice wedges. More detailed cryolithological (i.e. ice texture) and chemical analyses, such as major ion and trace element concentrations and stable isotope ratios, are necessary to refine this method for determining ice wedge chronology as well as contamination patterns. The results of this study suggest that the reliability of dating permafrost using ³⁶Cl/Cl ratios depends on the size and on the formation type of the sampled ground ice. In this context synsedimentary- (syngenetically-) formed large ice wedges are preferred over postsedimentary- (epigenetically-) formed wedges, in order to avoid the influence of brines within surrounding deposits on the initial (precipitation-controlled) ³⁶Cl/Cl ratio in the ice.

The main conclusion is that the chlorine level and ³⁶Cl/Cl ratios in the Yedoma Suite, which formed in Weichselian cryochrones (12-15 to 50 thousand years ago), may serve as a zero point (or base) for dating Ice Complex sequences formed in middle and early Pleistocene cryochrones under more or less similar climatic conditions, including precipitation.

The systematic changes of the Holocene samples require additional studies, and the observed change in ³⁶Cl/Cl ratios during the late-Pleistocene-to-Holocene transition requires additional explanation. Such studies should be connected with comparable analyses of Northern Hemisphere glacier ice as well as of precipitation in the catchment area.

Acknowledgments

We are grateful to all our colleagues from ETH Zurich, Eawag (Silvia Bollhalder Lueck), AWI Potsdam (Antje Eulenburg) and Moscow State University (Vladimir Tumskoy and Alexander Dereviagin) who helped during the field seasons and with permafrost shipping, chemical analysis, and AMS measurements. We also acknowledge Hanno Meyer (AWI Potsdam) for valuable information and highly constructive discussions. The research was supported by the INTAS grant 05-1000008-8133, the Russian Fund for Basic Research grant 04-05-64226, and was part of the IPY project 15 "PAST PERMAFROST". We thank Robert Ackert and an anonymous reviewer for helpful comments, which considerably improved the quality of the manuscript. The paper really benefited by valuable comments and English language correction from Candace O'Connor (University of Alaska, Fairbanks).

References

- ACIA. 2005. Arctic Climate Impact Assessment. Cambridge University Press: Cambridge, New York, Melbourne, Madrid, Cape Town, Singapore, São Paulo; 1042 p.
- Alexandrov EI, Radionov VF, Svyaschennikov PN. 2000. Climatic regime and its changes in the region of the Barents and Kara seas. In *Transport and fate of contaminants in the northern seas. Sea ice project package. AARI final report*. Arctic and Antarctic Research Institute: St. Petersburg; chapter 3. http://npolar.no/transeff/transport/ice/aari_all.pdf.
- Alley RB. 2000. The Younger Dryas cold interval as viewed from central Greenland. *Quaternary Science Reviews* **19**: 213-226.
- Andreev AA, Klimanov VA, Sulerzhitsky LD. 2001. Vegetation and climate history of the Yana River lowland, Russia, during the last 6400 yr. *Quaternary Science Reviews* **20**: 259-266.
- Andreev AA, Tarasov PE, Siebert C, Ebel T, Klimanov VA, Melles M, Bobrov AA, Dereviagin AYu, Lubinski DJ, Hubberten H-W. 2003. Late Pleistocene and Holocene vegetation and climate on the northern Taymyr Peninsula, Arctic Russia. *Boreas* **32**: 484-505.
- Andreev AA, Grosse G, Schirmermeister L, Kuzmina SA, Novenko EY, Bobrov AA, Tarasov PE, Kuznetsova TV, Krbetschek M, Meyer H, Kunitsky VV. 2004. Late Saalian and Eemian palaeoenvironmental history of the Bol'shoy Lyakhovsky Island (Laptev Sea region, Arctic Siberia). *Boreas* **33**: 319-348.
- Andreev AA, Lubinski DJ, Bobrov AA, Ingólfsson Ó, Forman SL, Tarasov PE, Möller P. 2008. Early Holocene environments on October Revolution Island, Severnaya Zemlya, Arctic Russia. *Palaeogeography, Palaeoclimatology, Palaeoecology* **267**: 21-30.
- Andreev AA, Grosse G, Schirmermeister L, Kuznetsova TV, Kuzmina SA, Bobrov AA, Tarasov PE, Novenko EY, Meyer H, Dereviagin AY, Kienast F, Bryantseva A, Kunitsky VV. 2009. Weichselian and Holocene palaeoenvironmental history of the Bol'shoy Lyakhovsky Island, New Siberian Archipelago, Arctic Siberia. *Boreas* **38**: 72-110.
- Arkhangelov AA, Plakht IR, Kolesnikov SF, Parmuzina OY. 1985. Vremya formirovaniya mnogoletnei merzloty na Severnoi Chukotke (The age of permafrost formation in Northern Chukotka). In: *Razvitie kriolitozony Evrazii v verkhnem kainozoe (Development of the Cryolithozone of Eurasia in the upper Cenozoic)*, Popov AI (ed.). Nauka: Moscow; 108-112 (in Russian).
- Bauch HA, Müller-Lupp T, Spielhagen RF, Taldenkova E, Kassens H, Grootes PM, Thiede J, Heinemeier J, Petryashov VV. 2001. Chronology of the Holocene transgression at the northern Siberian margin. *Global and Planetary Change* **31**(1-4): 125-139.
- Baumgartner S, Beer J, Masarik J, Wagner G, Meynadier L, Synal H-A. 1998. Geomagnetic Modulation of the ^{36}Cl Flux in the GRIP Ice Core, Greenland. *Science* **279**: 1330-1332.

- Bengtsson L, Semenov VA, Johanessen OM. 2004. The early twentieth-century warming in the Arctic – A possible mechanism. *Journal of Climate* **17**: 4045-4057.
- Bentley HW, Phillips FM, Davis SN, Habermehl MA, Airey PL, Calf GE, Elmore D, Gove HE, Torgersen T. 1986. Chlorine 36 dating of very old ground water 1. The Great Artesian Basin, Australia. *Water Resources Research* **22**(13): 1991-2001.
- Blinov A, Massonet S, Sachsenhauser H, Stan-Sion C, Lazarev V, Beer J, Synal H-A, Kaba M, Masarik J, Nolte E. 2000. An excess of ^{36}Cl in modern atmospheric precipitation. *Nuclear Instruments and Methods in Physics Research* **B172**: 537-544.
- Blinov A, Alfimov V, Beer J, Gilichinsky D, Schirrmeister L, Kholodov A, Nikolskiy P, Opel T, Tikhomirov D, Wetterich S. resubmitted after revision. $^{36}\text{Cl}/\text{Cl}$ ratio in ground ice of East Siberia and its application for chronometry. *Geochemistry, Geophysics, Geosystems (G3)*.
- Bolshiyarov DY, Makeyev VM. 1995. Arkhipelag Severnaya Zemlya: oledeniye, istoriya razvitiya prirodnoy sredy (Severnaya Zemlya Archipelago: glaciation and historical development of the natural environment). Gidrometeoizdat: St Petersburg; 216 p. (in Russian).
- Bradley RS. 1999. Paleoclimatology. Reconstructing Climates of the Quaternary. 2nd edition. Academic Press: San Diego et al.; 613 p.
- Bradley RS, England JH. 2008. The Younger Dryas and the Sea of Ancient Ice. *Quaternary Research* **70**: 1-10.
- Brázdil R. 1988. Variation of air temperature and atmospheric precipitation in the region of Svalbard. In *Results of investigations of the geographical research expedition Spitsbergen 1985*, Brázdil R (ed.). Univerzity J. E. Purkyně v Brně Geographia 24: Brno; 285-323.
- Broecker WS. 2006. Was the Younger Dryas triggered by a flood? *Science* **312**: 1146-1148.
- Brohan P, Kennedy JJ, Harris I, Tett SFB, Jones PD. 2006. Uncertainty estimates in regional and global observed temperature changes: a new data set from 1850. *Journal of Geophysical Research* **111**(12): D12106.
- Brown J. 1965. Radiocarbon dating, Barrow, Alaska. *Arctic* **18**: 36-47.
- Bunge AA. 1887. Bericht über den ferneren Gang der Expedition. Reise nach den Neusibirischen Inseln. Aufenthalt auf der Grossen Ljachof-Insel. In *Expedition nach den Neusibirischen Inseln und dem Jana-Lande (1885)*, Schrenk LV, Maximovicz CJ (eds.). *Beiträge zur Kenntnis des russischen Reiches und der angrenzenden Länder Asiens* **3**, Buchdruckerei der Kaiserlichen Akademie der Wissenschaften: St. Petersburg; 231–284.
- Castellano E, Becagli S, Hansson M, Hutterli M, Petit JR, Rampino MR, Severi M, Steffensen JP, Traversi R, Udisti R. 2005. Holocene volcanic history as recorded in the sulfate stratigraphy of the European Project for Ice Coring in Antarctica Dome C (EDC96) ice core. *Journal of Geophysical Research* **110**: D06114.
- Christensen JH, Hewitson B, Busuioc A, Chen A, Gao X, Held I, Jones R, Kolli RK, Kwon W-T, Laprise R, Magaña Rueda V, Mearns L, Menéndez CG,

- Räisänen J, Rinke A, Sarr A, Whetton P. 2007. Regional Climate Projections. In *Climate Change 2007: The Physical Science Basis. Contribution of Working Group I to the Fourth Assessment Report of the Intergovernmental Panel on Climate Change*, Solomon S, Qin D, Manning M, Chen Z, Marquis M, Averyt KB, Tignor M, Miller HL (eds.). Cambridge University Press: Cambridge and New York; 847-940.
- Clausen HB, Stampe M, Hammer CU, Hvidberg CS, Dahl-Jensen D, Steffensen JP. 2001. Glaciological and chemical studies on ice cores from Hans Tausen Iskappe, Greenland. *Meddelelser om Grønland, Geoscience* **39**: 123-149.
- Craig H. 1961. Isotopic variations in meteoric waters. *Science* **133**: 1702-1703.
- Crespin E, Goose H, Fichet T, Mann ME. 2009. Potential causes of 15th century Arctic warming using coupled model simulations with data assimilation. *Climate of the Past* **5**: 389-401.
- Dansgaard W. 1964. Stable isotopes in precipitation. *Tellus* **16**: 436-468.
- Dansgaard W, White JWC, Johnsen SJ. 1989. The abrupt termination of the Younger Dryas climate event. *Nature* **339**: 532-534.
- Dansgaard W, Johnsen SJ, Clausen HB, Dahl-Jensen D, Gundestrup NS, Hammer CU, Hvidberg CS, Steffensen JP, Sveinbjörnsdóttir AE, Jouzel J, Bond G. 1993. Evidence for general instability of past climate from a 250-kyr ice-core record. *Nature* **364**: 218-220.
- Dereviagin AYu, Meyer H, Chizhov AB, Hubberten H-W, Simonov EF. 2002. New data on the isotopic composition and evolution of modern ice edges in the Laptev Sea Region. *Polarforschung* **70**: 27-35.
- Derevyagin A, Opel T. 2009. Ground ice studies. In *The Expedition LENA - NEW SIBERIAN ISLANDS 2007 during the International Polar Year (IPY) 2007/2008*, Boike J, Bol'shiyanov DY, Schirrmeister L, Wetterich S. (eds.). *Reports on Polar and Marine Research* **584**, Alfred Wegener Institute for Polar and Marine Research: Bremerhaven; 115-138.
- Divine DV, Isaksson E, Pohjola V, Meijer H, van de Wal RSW, Martma T, Moore J, Sjögren B, Godtliebse F. 2008. Deuterium excess record from a small Arctic ice cap. *Journal of Geophysical Research* **113**: D19104.
- Dowdeswell JA, Bassford RP, Gorman MR, Williams M, Glazovsky AF, Macheret YY, Shepherd AP, Vasilenko YV, Savatyugin LM, Hubberten H-W, Miller H. 2002. Form and flow of the Academy of Sciences Ice Cap, Severnaya Zemlya, Russian High Arctic. *Journal of Geophysical Research* **107**(B4): 2076.
- Elias S A, Short SK, Nelson CH, Birks HH. 1996. Life and times of the Bering land bridge. *Nature* **382**: 60-63.
- Endlicher W. 2000. Nordasien. In *Regionale Klimatologie. Teil 2. Die Alte Welt. Europa, Afrika, Asien*, Weischet W, Endlicher W. B. G. Teubner: Stuttgart and Leipzig; 571-591.
- Fischer H, Werner M, Wagenbach D, Schwager M, Thorsteinsson T, Wilhelms F, Kipfstuhl J, Sommer S. 1998. Little ice age clearly recorded in northern Greenland ice cores. *Geophysical Research Letters* **25**: 1749-1752.

- French HM. 2007. The periglacial environment. 3rd edition. Wiley: Chichester; 458 p.
- Fritzsche D, Wilhelms F, Savatyugin LM, Pinglot JF, Meyer H, Hubberten H-W, Miller H. 2002. A new deep ice core from Akademii Nauk ice cap, Severnaya Zemlya, Eurasian Arctic: first results. *Annals of Glaciology* **35**: 25-28.
- Fritzsche D, Schütt R, Meyer H, Miller H, Wilhelms F, Opel T, Savatyugin LM. 2005. A 275 year ice-core record from Akademii Nauk ice cap, Severnaya Zemlya, Russian Arctic. *Annals of Glaciology* **42**: 361-366.
- Fröhlich K, Gibson JJ, Aggarwal PK. 2002. Deuterium excess in precipitation and its climatological significance. Study of environmental change using isotope techniques. *C&S Papers Series 13/P*, Vienna International Atomic Energy Agency: Vienna; 54–65.
- Froese DG, Westgate JA, Reyes AV, Enkin RJ, Preece SJ. 2008. Ancient permafrost and a future warmer Arctic. *Science* **321**: 1648.
- Gilichinsky DA, Nolte E, Basilyan AE, Beer J, Blinov AV, Lazarev VE, Kholodov AL, Meyer H, Nikolskiy PA, Schirrmeyer L, Tumskey VE. 2007. Dating of syngenetic ice wedges in permafrost with ^{36}Cl . *Quaternary Science Reviews* **26**: 1547–1556.
- Graedel TE, Keene WC. 1996. The budget and cycle of Earth's natural chlorine. *Pure and Applied Chemistry* **68**(9): 1689-1697.
- Gravis GF. 1978. Tsiklichnost' termokarsta na Primorskoi nizmenosti v verkhnem Pleistotsene i Golotsene (Cyclicity of thermokarst at the coastal lowlands during the late Pleistocene and Holocene). In *Third International Conference on Permafrost, Proceedings*. Vol. 1. Edmonton, Alberta, Canada; 283-287 (in Russian).
- Gray ST, Graumlich LJ, Betancourt JL, Pederson GD. 2004. A tree-ring based reconstruction of the Atlantic Multidecadal Oscillation since 1567 A.D. *Geophysical Research Letters* **31**(12): L12205.
- Grotes PM, Stuiver M, White JWC, Johnsen S, Jouzel J. 1993. Comparison of oxygen isotope records from the GISP2 and GRIP Greenland ice cores. *Nature* **366**: 552-554.
- Grosse G, Schirrmeyer L, Siegert Ch, Kunitsky VV, Slagoda EA, Andreev AA, Dereviagyn AYu. 2007. Geological and geomorphological evolution of a sedimentary periglacial landscape in Northeast Siberia during the Late Quaternary. *Geomorphology* **86**(1/2): 25-51.
- Hammer CU, Johnsen SJ, Clausen HB, Dahl-Jensen D, Gundestrup N, Steffensen JP. 2001. The paleoclimate record from a 345m long ice core from the Hans Tausen Iskappe. *Meddelelser om Grønland, Geoscience* **39**: 87-95.
- Heikkilä U, Beer J, Feichter J. 2008. Modeling cosmogenic radionuclides Be-10 and Be-7 during the Maunder Minimum using the ECHAM5-HAM General Circulation Model. *Atmospheric Chemistry and Physics* **8**: 2797-2809.
- Henderson KA. 2002. An ice core paleoclimate study of Windy Dome, Franz Josef Land (Russia): development of a recent climate history for the Barents Sea. PhD dissertation. Ohio State University, USA; 218 p.

- Hoffmann G, Jouzel J, Johnsen S. 2001. Deuterium excess record from central Greenland over the last millennium: Hints of a North Atlantic signal during the Little Ice Age. *Journal of Geophysical Research* **106**(D13): 14265-14274.
- Hu FS, Lee BY, Kaufman DS, Yoneji S, Nelson DM, Henne PD. 2002. Response of tundra ecosystem in southwestern Alaska to Younger-Dryas climatic oscillation. *Global Change Biology* **8**: 1156-1163.
- Hubberten H-W, Andreev A, Astakhov VI, Demidov I, Dowdeswell JA, Henriksen M, Hjort C, Houmark-Nielsen M, Jakobsson M, Kuzmina S and co-authors. 2004. The periglacial climate and environment in northern Eurasia during the last glaciation. *Quaternary Science Reviews* **23**: 1333-1357.
- Iizuka Y, Igarashi M, Kamiyama K, Motoyama H, Watanabe O. 2002. Ratios of Mg²⁺/Na⁺ in snowpack and an ice core at Austfonna ice cap, Svalbard, as an indicator of seasonal melting. *Journal of Glaciology* **48**(162): 452-460.
- Ilyashuk BP, Andreev AA, Bobrov AA, Tumskoy VE, Ilyashuk EA. 2006. Interglacial history of a palaeo-lake and regional environment: A multi-proxy study of a permafrost deposit from Bol'shoi Lyakhovsky Island, Arctic Siberia. *Journal of Paleolimnology* **35**: 855-872.
- IPA (International Permafrost Association). 1998. Circumpolar Active-Layer Permafrost System (CAPS). Version 1.0.
- IPICS (International Partnerships in Ice Core Sciences). 2009. The IPICS 2000 Year Array: Ice core contributions to quantitative assessment of recent climate forcing and climate variability. Science and coordination plan. http://www.pages.unibe.ch/ipics/data/IPICS_2K_final.pdf.
- Isaksson E, Pohjola V, Jauhiainen T, Moore J, Pinglot JF, Vaikmäe R, van de Wal RSW, Hagen JO, Ivask J, Karlöf L, Martma T, Meijer HAJ, Mulvaney R, Thomassen M, van den Broeke M. 2001. A new ice-core record from Lomonosovfonna, Svalbard: viewing the 1920-97 data in relation to present climate and environmental conditions. *Journal of Glaciology* **47**(157): 335-345.
- Isaksson E, Hermanson M, Hicks S, Igarashi M, Kamiyama K, Moore J, Motoyama H, Muir D, Pohjola V, Vaikmäe R, van de Wal RSW, Watanabe O. 2003. Ice cores from Svalbard - useful archives of past climate and pollution history. *Physics and Chemistry of the Earth* **28**: 1217-1228.
- Isaksson E, Divine D, Kohler J, Martma T, Pohjola V, Motoyama H, Watanabe O. 2005a. Climate oscillations as recorded in Svalbard ice core $\delta^{18}\text{O}$ records between AD 1200 and 1997. *Geografiska Annaler* **87A**: 203-214.
- Isaksson E, Kohler J, Pohjola V, Moore J, Igarashi M, Karlöf L, Martma T, Meijer H, Motoyama H, Vaikmäe R, van de Wal RSW. 2005b. Two ice-core $\delta^{18}\text{O}$ records from Svalbard illustrating climate and sea-ice variability over the last 400 years. *The Holocene* **15**(4): 501-509.
- Jansen E, Overpeck J, Briffa KR, Duplessy J-C, Joos F, Masson-Delmotte V, Olago D, Otto-Bliesner B, Peltier WR, Rahmstorf S, Ramesh R, Raynaud D, Rind D, Solomina O, Villalba R, Zhang D. 2007. Palaeoclimate. In *Climate Change 2007: The Physical Science Basis. Contribution of Working Group I to the Fourth Assessment Report of the Intergovernmental Panel on*

- Climate Change*, Solomon S, Qin D, Manning M, Chen Z, Marquis M, Averyt KB, Tignor M, Miller HL (eds.). Cambridge University Press: Cambridge, New York; 433-497.
- Johnsen SJ, Dansgaard W, White JWC. 1989. The origin of Arctic precipitation under present and glacial conditions. *Tellus* **41B**(4): 452-468.
- Johnston VE, McDermott F. 2008. The distribution of meteoric Cl-36 in precipitation across Europe in spring 2007. *Earth and Planetary Science Letters* **275**: 154-164.
- Jones PD, Mann ME. 2004. Climate over past millennia. *Reviews of Geophysics* **42**: RG2002.
- Jouzel J, Alley RB, Cuffey KM, Dansgaard W, Grootes P, Hoffmann G, Johnsen SJ, Koster RD, Peel D, Shuman CA, Stievenard M, Stuiver M, White J. 1997. Validity of the temperature reconstruction from water isotopes in ice cores. *Journal of Geophysical Research* **102**(C12): 26,471-26,487.
- Kaplina TN. 1981. History of Permafrost strata of the Northern Yakutia in the late Cenozoic period. In *History of development of Permafrost of the Eurasia*. Nauka: Moscow; 153-180 (in Russian).
- Kaufman DS, Ager TA, Anderson NJ, Anderson PM, Andrews JT, Bartlein PJ, Brubaker LB, Coats LL, Cwynar LC, Duvall ML, Dyke AS, Edwards ME, Eisner WR, Gajewski K, Geirsdóttir A, Hu FS, Jennings AE, Kaplan MR, Kerwin MW, Lozhkin AV, MacDonald GM, Miller GH, Mock CJ, Oswald WW, Otto-Bliesner BL, Porinchu DF, Rühland K, Smol JP, Steig EJ, Wolfe BB. 2004. Holocene thermal maximum in the western Arctic (0-180°W). *Quaternary Science Reviews* **23**: 529-560.
- Kekonen T, Moore J, Perämäki P, Mulvaney R, Isaksson E, Pohjola V, van de Wal RSW. 2005. The 800 year long ion record from the Lomonosofonna (Svalbard) ice core. *Journal of Geophysical Research* **110**: D07304.
- Kienast F, Siebert C, Dereviagin A, Mai D-H. 2001. Climatic implications of late quaternary plant macrofossil assemblages from the Taymyr Peninsula, Siberia. *Global and Planetary Change* **31**: 265-281.
- Kienast F, Schirmer L, Siebert C, Tarasov P. 2005. Palaeobotanical evidence for warm summers in the East Siberian Arctic during the last cold stage, *Quaternary Research* **63**(3): 283-300.
- Kienast F, Tarasov P, Schirmer L, Grosse G, Andreev AA. 2008. Continental climate in the East Siberian Arctic during the last interglacial: implications from palaeobotanical records. *Global and Planetary Change* **60**: 535-562.
- Klementyev OL, Korotkov IM, Nikolaev VI. 1988. Glyatsiologicheskiye issledovaniya v 1987-1988 gg. na lednikovakh kupolakh Severnoy Zemli (Glaciological studies on the ice domes of Severnaya Zemlya in 1987-1988). *Materialy Glyatsiologicheskikh Issledovaniy* **63**: 25-26 (in Russian).
- Klementyev OL, Potapenko VYu, Savatyugin LM, Nikolaev VI. 1991. Studies of the internal structure and thermal-hydrodynamic state of the Vavilov Glacier, Archipelago Severnaya Zemlya. In *Glaciers-Ocean-Atmosphere Interactions. Proceedings of the International Symposium held at St. Petersburg, Sept. 1990*, Kotlyakov VM, Ushakov A, Glazovsky A (eds.).

- IAHS Publication 208*. International Association of Hydrological Sciences: Wallingford; 49-59.
- Kloss AL. 2008. Water isotope geochemistry of recent precipitation in Central and North Siberia as a proxy for the local and regional climate system. Unpublished diploma thesis. Institute for Physical Geography and Landscape Ecology, Leibniz University of Hannover, Germany; 107 p.
- Koerner RM. 1977. Devon Island ice cap: core stratigraphy and paleoclimate. *Science* **196**(4285): 15-18.
- Koerner RM. 1997. Some comments on climatic reconstructions from ice cores drilled in areas of high melt. *Journal of Glaciology* **43**(143): 90-97.
- Koerner RM, Fisher DA. 2002. Ice-core evidence for widespread Arctic glacier retreat in the Last Interglacial and the early Holocene. *Annals of Glaciology* **35**: 19-24.
- Kokorowski HD, Anderson PM, Mock CJ, Lozhkin AV. 2008. A re-evaluation and spatial analysis of evidence for a Younger Dryas climatic reversal in Beringia. *Quaternary Science Reviews* **27**: 1710–1722.
- Konishchev VN, Kolesnikov SF. 1981. Osobennosti stroeniya i sostava pozdnokainozoiskikh otlozheniyakh b obnazhenii Oyagosskii Yar (Specifics of structure and composition of late Cenozoic deposits in the section of Oyogossky Yar). In *Problemy Kriolitologii (Problems of Cryolithology) Vol. IX*, Popov AI (ed.). Moscow University Press: Moscow; 107-117 (in Russian).
- Koronovsky N. 2002. Tectonics and Geology. In *The physical geography of northern Eurasia*, Shagedanova M (ed.). Oxford University Press: Oxford; 1-35.
- Kotlyakov VM, Zagorodnov VS, Nikolaev VI. 1990. Drilling on ice caps in the Soviet Arctic and on Svalbard and prospects of ice core treatment. In *Arctic research: advances and prospects*, Kotlyakov VM, Sokolov VYe (eds.). Nauka: Moscow; 5-18.
- Kotlyakov VM, Arkhipov SM, Henderson KA, Nagornov OV. 2004. Deep drilling of glaciers in Eurasian Arctic as a source of paleoclimatic records. *Quaternary Science Reviews* **23**: 1371-1390.
- Krbetschek MR, Gonser G, Schwamborn G. 2000. Luminescence dating results of Sediment sequences of the Lena Delta. *Polarforschung* **70**: 83-88.
- Kuhn M. 2000. Severnaja automatic weather station data (Severnaja Zemlja). In *The response of Arctic ice mass to climate change (ICEMASS). Third Year Report (January-December 2000)*, European Commission. Framework IV. Environment and Climate Research Programme (DG XII), contract ENV4-CT97–0490. University of Oslo, Norway; 7-8–7-14.
- Kurita N, Yoshida N, Inoue G, Chayanova EA. 2004. Modern isotope climatology of Russia: a first assessment. *Journal of Geophysical Research* **109**: D03102.
- Kurita N, Sugimoto A, Fujii Y, Fukazawa T, Makarov VN, Watanabe O, Ichiyanagi K, Numaguti A, Yoshida N. 2005. Isotopic composition and origin of snow over Siberia. *Journal of Geophysical Research* **110**: D13102.

- Kuznetsova LP. 1998. Atmospheric moisture content and transfer over the territory of the former USSR. In *Second International Workshop on Energy and Water Cycle in GAME Siberia, 1997*, Kotlyakov VM, Sokolov VYe (eds.). *Research Report of IHAS 4*, Institute for Hydrospheric-Atmospheric Sciences, Nagoya University: Nagoya, Japan; 145–151.
- Lachenbruch AH. 1962. Mechanics of thermal construction cracks and ice wedge polygons in permafrost. *Geological Society of America. Special Paper 70*; 65 p.
- Lal D, Peters B. 1967. Cosmic ray produced radioactivity on the earth. In *Handbuch der Physik*, Sitte K (ed.). 46/2, Springer-Verlag: Berlin; 551-612.
- Lauriol B, Duchesne C, Clark ID. 1995. Systématique du remplissage en eau des fentes de gel: les résultats d'une étude oxygène-18 et deutérium. *Permafrost and Periglacial Processes 6*: 47–55.
- Legrand M, Mayewski P. 1997. Glaciochemistry of polar ice cores: a review. *Reviews of Geophysics 35*(3): 219–243.
- Lemke P, Ren J, Alley RB, Allison I, Carrasco J, Flato G, Fujii Y, Kaser G, Mote P, Thomas RH, Zhang T. 2007. Observations: Changes in Snow, ice and Frozen Ground. In *Climate Change 2007: The Physical Science Basis. Contribution of Working Group I to the Fourth Assessment Report of the Intergovernmental Panel on Climate Change*, Solomon S, Qin D, Manning M, Chen Z, Marquis M, Averyt KB, Tignor M, Miller HL (eds.). Cambridge University Press: Cambridge and New York; 337-383.
- Lorenz H, Männik P, Gee D, Proskurnin V. 2008. Geology of the Severnaya Zemlya Archipelago and the North Kara Terrane in the Russian high Arctic. *International Journal of Earth Sciences 97*:519–547.
- Lubinski DJ, Forman SL, Miller GH. 1999. Holocene glacier and climate fluctuations on Franz Josef Land, Arctic Russia, 80°N. *Quaternary Science Reviews 18*: 85-108.
- Maasch KA, Mayewski PA, Rohling EJ, Stager JC, Karlén W, Meeker LD, Meyerson EA. 2005. A 2000-year context for modern climate change. *Geografiska Annaler 87A*: 7-15.
- Mackay JR, Rampton VN, Fyles JG. 1972. Relic Pleistocene permafrost, western Arctic, Canada. *Science 176*: 1321-1323.
- Mackay JR. 1974. Ice-wedge cracks, Garry Island, Northwest Territories. *Canadian Journal of Earth Sciences 11*: 1366–1383.
- Mackay JR. 1983. Oxygen isotope variations in permafrost, Tuktoyaktuk Peninsula area, Northwest Territories. *Current Research, Part B, Geological Survey of Canada Paper 83-1B*: 67–74.
- Mackay JR. 1992. The frequency of ice-wedge cracking (1967-1987) at Garry Island, western Arctic coast, Canada. *Canadian Journal of Earth Sciences 29*: 236-248.
- Madsen KN, Thorsteinsson T. 2001. Textures, fabrics and meltlayer stratigraphy in the Hans Tausen ice core, North Greenland – indications of late Holocene ice cap generation? *Meddelelser om Grønland, Geoscience 39*: 97-114.

- Mann ME, Bradley RS, Hughes MK. 1999. Northern Hemisphere Temperatures During the Past Millennium: Inferences, Uncertainties, and Limitations. *Geophysical Research Letters* **26**(6): 759–762.
- Mann ME, Jones PD. 2003. Global Surface Temperatures over the Past Two Millennia. *Geophysical Research Letters* **30**(15): 1820.
- Masarik J, Beer J. 1999. Simulation of particle fluxes and cosmogenic nuclide production in the Earth's atmosphere. *Journal of Geophysical Research* **104**(D10): 12099-12111.
- Mayewski PA, Rohling EE, Stager JC, Karlén W, Maasch KA, Meeker LD, Meyerson EA, Gasse F, van Kreveld S, Holmgren K, Lee-Thorp J, Rosqvist G, Rack F, Staubwasser M, Schneider RR, Steig EJ. 2004. Holocene climate variability. *Quaternary Research* **62**: 243-255.
- McConnell JR, Edwards E, Kok GL, Flanner MG, Zender CS, Saltzman ES, Banta JR, Pasteris DR, Carter MM, Kahl JDW. 2007. 20th-Century Industrial Black Carbon Emissions Altered Arctic Climate Forcing. *Science* **317**(5843): 1381-1384.
- McManus JF, Francois R, Gherardi JM, Keigwin LD, Brown-Leger S. 2004. Collapse and rapid resumption of Atlantic meridional circulation linked to deglacial climate changes. *Nature* **428**: 834-837.
- Meyer H, Schönicke L, Wand U, Hubberten H-W. 2000. Isotope studies of hydrogen and oxygen in ground ice – experiences with the equilibration technique. *Isotopes in Environmental and Health Studies* **36**: 133-149.
- Meyer H, Dereviagin AY, Siegert C, Hubberten HW. 2002a. Paleoclimate Studies on Bykovsky Peninsula, North Siberia – Hydrogen and Oxygen Isotopes in Ground Ice. *Polarforschung* **70**: 37-51.
- Meyer H, Dereviagin AY, Siegert C, Schirrmeister L, Hubberten H-W. 2002b. Paleoclimate reconstruction on Big Lyakhovsky Island, North Siberia – Hydrogen and oxygen isotopes in ice wedges. *Permafrost and Periglacial Processes* **13**: 91-105.
- Meyer H. 2003. Late Quaternary climate history of Northern Siberia – evidence from ground ice. *Reports on Polar and Marine Research* **461**, Alfred Wegener Institute for Polar and Marine Research: Bremerhaven; 1-111.
- Meyer H, Mogens D, Dereviagin, AY, Schirrmeister L. in preparation a. Water isotopes of ground ice at Cape Mamontov Klyk, Western Laptev Sea region, North Siberia. *Permafrost and Periglacial Processes*.
- Meyer H, Schirrmeister L, Andreev A, Wagner D, Hubberten H-W, Yoshikawa K, Bobrov A, Wetterich S, Kandiano E, Brown J. in preparation b. Late Glacial and Holocene isotopic and environmental history of Northern Alaska – results from a buried ice wedge system at Barrow. *Quaternary Science Reviews*.
- Meyer H, Schirrmeister L, Yoshikawa K, Opel T, Hubberten H-W, Brown J. in preparation c. Permafrost evidence for a Younger Dryas cold event in northern Alaska. *Nature*.
- Michel FA. 1982. Isotope investigations of permafrost waters in northern Canada. Ph.D. thesis. Department of Earth Sciences, University of Waterloo, Canada.

- Mikolajewicz U, Crowley TJ, Schiller A, Voss R. 1997. Modelling teleconnections between the North Atlantic and North Pacific during the Younger Dryas. *Nature* **387**: 384-387.
- Mock C, Bartlein P, Anderson P. 1998. Atmospheric circulation patterns and spatial climatic variations in Beringia. *International Journal of Climatology* **10**: 1085-1104.
- Möller P, Lubinski DJ, Ingólfsson Ó, Forman SL, Seidenkrantz M-S, Bolshiyarov DYu, Lokrantz H, Antonov O, Pavlov M, Ljung K, Zeeberg J-J, Andreev A. 2007. Severnaya Zemlya, Arctic Russia: a nucleation area for Kara Sea ice sheets during the Middle to Late Quaternary. *Quaternary Science Reviews* **26**: 1149-1191.
- Moore JC, Paren JG. 1987. A new technique for dielectric logging of Antarctic ice cores. *Journal de Physique. Colloque C1, supplément au no. 3.* **48**: 155-160.
- Moore J, Kekonen T, Grinsted A, Isaksson E. 2006. Sulfate source inventories from a Svalbard ice core record spanning the Industrial Revolution. *Journal of Geophysical Research* **111**: D15307.
- Moorman BJ, Michel FA, Wilson A. 1996. ¹⁴C dating of trapped gases in massive ground ice, Western Canadian Arctic. *Permafrost and Periglacial Processes* **7**: 257-266.
- Moritz RE, Bitz CM, Steig EJ. 2002. Dynamics of Recent Climate Change in the Arctic. *Science* **297**(5586): 1497-1502.
- Murton JB, French HM, Lamothe M. 1997. Late Wisconsinan erosion and eolian deposition, Summer Island area, Pleistocene Mackenzie Delta, Northwest Territories: Optical dating and implications for glacial chronology. *Canadian Journal of Earth Sciences* **34**: 190-199.
- Muscheler R, Joos F, Beer J, Muller SA, Vonmoos M, Snowball I. 2007. Solar activity during the last 1000 yr inferred from radionuclide records. *Quaternary Science Reviews* **26**(1-2): 82-97.
- Murdmaa I, Polyak L, Ivanova E, Khromova N. 2004. Paleoenvironments in Russkaya Gavan' Fjord (NW Novaya Zemlya, Barents Sea) during the last millennium. *Palaeogeography, Palaeoclimatology, Palaeoecology* **209**: 141-154.
- Nadeau MJ, Schleicher M, Grootes PM, Erlenkeuser H, Gott dang A, Mous DJW, Sarnthein JM, Willkomm H. 1997. The Leibniz Labor facility at the Christian-Albrechts-University, Kiel, Germany. *Nuclear Instruments and Methods Physics Research* **B123**: 22-30.
- Nadeau MJ, Grootes PM, Schleicher M, Hasselberg P, Rieck A, Bitterling M. 1998. Sample throughput and data quality at the Leibniz Labor AMS facility. *Radiocarbon* **40**: 239-245.
- Naurzbaev MM, Vaganov EA, Sidorova OV, Schweingruber FH. 2002. Summer temperatures in eastern Taimyr inferred from a 2427-year late-Holocene tree-ring chronology and earlier floating series. *The Holocene* **12**(6): 727-736.
- Nikolayev VI, Mikhalev DV. 1995. An oxygen-isotope paleothermometer from ice in Siberian permafrost. *Quaternary Research* **43**(1): 14-21.

- North Greenland Ice Core Project (NorthGRIP) Members. 2004. High-resolution record of Northern Hemisphere climate extending into the last interglacial period. *Nature* **431**(7005): 147-151.
- Opel T, Dereviagin AYu, Meyer H, Schirrmeister L, Wetterich S. 2009a. Resubmitted after minor revisions. Paleoclimatic information from stable water isotopes of Holocene ice wedges at the Dmitrii Laptev Strait (Northeast Siberia). *Permafrost and Periglacial Processes*.
- Opel T, Fritzsche D, Meyer H, Schütt R, Weiler K, Ruth U, Wilhelms F, Fischer H. 2009b. 115 year ice-core data from Akademii Nauk ice cap, Severnaya Zemlya: high-resolution record of Eurasian Arctic climate change. *Journal of Glaciology* **55**(189): 21-31.
- Osterkamp TE. 2005. The recent warming of permafrost in Alaska. *Global and Planetary Change* **49**: 187-202.
- Overpeck J, Hughen K, Hardy D, Bradley R, Case R, Douglas M, Finney B, Gajewski K, Jacoby G, Jennings A, Lamoureux S, Lasca A, MacDonald G, Moore J, Retelle M, Smith S, Wolfe A, Zielinski G. 1997. Arctic environmental changes of the last four centuries. *Science* **278**: 1251-1256.
- The PALE Beringian Working Group. 1999. Paleoenvironmental Atlas of Beringia Presented in Electronic Form. *Quaternary Research* **52**: 270–271.
- Paterson WSB. 1994. The Physics of glaciers. 3rd edition. Elsevier: Oxford.
- Pinglot JF, Vaikmäe RA, Kamiyama K, Igarashi M, Fritzsche D, Wilhelms F, Koerner R, Henderson L, Isaksson E, Winther J-G, van de Wal RSW, Fournier M, Bouisset P, Meijer HAJ. 2003. Ice cores from Arctic sub-polar glaciers: chronology and post-depositional processes deduced from radioactivity measurements. *Journal of Glaciology* **49**(164): 149-158.
- Pohjola VA, Martma TA, Meijer HAJ, Moore JC, Isaksson E, Vaikmäe R, van de Wal RSW. 2002a. Reconstruction of three centuries of annual accumulation rates based on the record of stable isotopes of water from Lomonosovfonna, Svalbard. *Annals of Glaciology* **35**: 57-62.
- Pohjola VA, Moore JC, Isaksson E, Jauhiainen T, van de Wal RSW, Martma T, Meijer HAJ, Vaikmäe R. 2002b. Effect of periodic melting on geochemical and isotopic signals in an ice core from Lomonosovfonna, Svalbard. *Journal of Geophysical Research* **107**(D4): 4036.
- Polyak L, Murdmaa I, Ivanova E. 2004. A high-resolution, 800-year glaciomarine record from Russkaya Gavan', a Novaya Zemlya Fjord, Eastern Barents Sea. *The Holocene* **14**(4): 628-634.
- Polyakov IV, Alekseev GV, Bekryaev RV, Bhatt US, Colony R, Johnson MA, Karklin VP, Walsh D, Yulin AV. 2003a. Long-term ice variability in Arctic marginal seas. *Journal of Climate* **16**(12): 2078-2085.
- Polyakov IV, Bekryaev RV, Alekseev GV, Bhatt US, Colony RL, Johnson MA, Maskhtas AP, Walsh D. 2003b. Variability and trends of air temperature and pressure in the maritime Arctic, 1875-2000. *Journal of Climate* **16**(12): 2067-2077.
- Przybylak R. 2007. Recent air-temperature changes in the Arctic. *Annals of Glaciology* **46**: 316-324.

- Raab A, Melles M, Berger GW, Hagedorn B, Hubberten H-W. 2003. Non-glacial paleoenvironments and the extent of Weichselian ice sheets on Severnaya Zemlya, Russian High Arctic. *Quaternary Science Reviews* **22**: 2267-2283.
- Reimer PJ, Baillie MGL, Bard E, Bayliss A, Beck JW, Bertrand CJH, Blackwell PG, Buck CE, Burr GS, Cutler KB, Damon PE, Edwards RL, Fairbanks RG, Friedrich M, Guilderson TP, Hogg AG, Hughen KA, Kromer B, McCormac G, Manning S, Ramsey CB, Reimer RW, Remmele S, Southon JR, Stuiver M, Talamo S, Taylor FW, van der Plicht J, Weyhenmeyer CE. 2004. INTCAL04 terrestrial radiocarbon age calibration, 0-26 cal kyr BP. *Radiocarbon* **46**: 1029-1058.
- Rivas-Martínez S. 2007. Global bioclimatics. Data set. Available online at <http://www.globalbioclimatics.org>, Phytosociological Research Center, Madrid, Spain.
- Rivas-Martinez S, Rivas-Saenz S. 1996-2009. Phytosociological Research Center, Spain. Worldwide Bioclimatic Classification System. <http://www.globalbioclimatics.org>.
- Romanovsky VE, Sazonova TS, Balobaev VT, Shender NI, Sergueev DO. 2007. Past and recent changes in air and permafrost temperatures in eastern Siberia. *Global and Planetary Change* **56**: 399-413.
- Rozanski K, Araguás-Araguás L, Gonfiantini R. 1993. Isotopic patterns in modern global precipitation. In *Climate Change in Continental Isotopic Records*, Swart PK, Lohmann KC, McKenzie J, Savin S (eds.). *Geophysical Monograph No 78*, American Geophysical Union: Washington; 1-36.
- Ruth U, Wagenbach D, Mulvaney R, Oerter H, Graf W, Pulz H, Littot G. 2004. Comprehensive 1000 year climatic history from an intermediate-depth ice core from the south dome of Berkner Island, Antarctica: methods, dating and first results. *Annals of Glaciology* **39**: 146-154.
- Samyn D, Tison J-L, Meyer H, Schütt R, Fritzsche D. 2008. Insights into basal ice processes at Akademii Nauk ice cap, Severnaya Zemlya archipelago, High Russian Arctic. Poster (CGG01619P) at 33rd International Geological Congress, August 2008, Oslo, Norway.
- Savatyugin LM, Zagorodnov VS. 1988. Glyatsiologicheskiye issledovaniya na lednikovom kupole Akademii Nauk (Glaciological studies on the Academy of Sciences ice cap). *Materialy Glyatsiologicheskikh Issledovaniy* **61**: 228 (in Russian).
- Savatyugin LM, Arkhipov SM, Vasiliev NI, Vostretsov RN, Fritzsche D, Miller H. 2001. Rossiysko-germanskkiye glyatsiologicheskiye issledovaniya na Severnoy Zemle i prilegayushchikh ostrovakh v 2000 g (Russian-German glaciological studies on Severnaya Zemlya and adjacent islands in 2000). *Materialy Glyatsiologicheskikh Issledovaniy* **91**: 150-162 (in Russian).
- Schirrmester L, Oezen D, Geyh MA. 2002a. ²³⁰Th/U dating of frozen peat, Bol'shoy Lyakhovsky Island (North Siberia). *Quaternary Research* **57**: 253-258.
- Schirrmester L, Siegert Ch, Kunitzky VV, Grootes PM, Erlenkeuser H. 2002b. Late Quaternary ice-rich permafrost sequences as an paleoenvironmental

- archive for the Laptev Sea Region in northern Siberia. *International Journal of Earth Sciences* **91**: 154-167.
- Schirrmeister L, Siegert C, Kuznetsova T, Kuzmina S, Andreev AA, Kienast F, Meyer H, Bobrov AA. 2002c. Paleoenvironmental and paleoclimatic records from permafrost deposits in the Arctic region of Northern Siberia. *Quaternary International* **89**: 97-118.
- Schirrmeister L, Grosse G, Kunitsky V, Meyer H, Derivyagin A, Kuznetsova T. 2003a. Permafrost, periglacial and paleo-environmental studies on New Siberian Islands. In *Russian-German Cooperation System Laptev Sea The Expeditions Lena 2002*, Grigoriev MN, Rachold V, Bolshiyarov DY, Pfeiffer EM, Schirrmeister L, Wagner D, Hubberten HW (eds.). *Reports on Polar and Marine Research* **466**, Alfred Wegener Institute for Polar and Marine Research: Bremerhaven; 195-314.
- Schirrmeister L, Kunitsky VV, Grosse G, Schwamborn G, Andreev AA, Meyer H, Kuznetsova T, Bobrov A, Oezen D. 2003b. Late Quaternary history of the accumulation plain north of the Chekanovsky Ridge (Lena Delta, Russia) - a multidisciplinary approach. *Polar Geography* **27**(4): 277-319.
- Schirrmeister L, Wetterich S, Kunitsky V, Tumskoy V, Dobrynin D, Derevyagin A, Opel T, Kienast F, Kuznetsova T, Gorodinski A. 2008a. Palaeoenvironmental studies on the Oyogos Yar coast. In *The Expedition LENA - NEW SIBERIAN ISLANDS 2007 during the International Polar Year (IPY) 2007/2008*, Boike J, Bol'shiyanov DY, Schirrmeister L, Wetterich S. (eds.). *Reports on Polar and Marine Research* **584**, Alfred Wegener Institute for Polar and Marine Research: Bremerhaven; 85-154.
- Schirrmeister L, Wetterich S, Tumskoy V, Kunitsky V, Derevyagin A, Opel T, Kuznetsova T. 2008b. Permafrost and environmental dynamics during Quaternary climate variations – studies along the Dmitrii Laptev Strait. In *The Expedition LENA - NEW SIBERIAN ISLANDS 2007 during the International Polar Year (IPY) 2007/2008*, Boike J, Bol'shiyanov DY, Schirrmeister L, Wetterich S. (eds.). *Reports on Polar and Marine Research* **584**, Alfred Wegener Institute for Polar and Marine Research: Bremerhaven; 35-154.
- Serreze MC, Walsh JE, Chapin III FS, Osterkamp T, Dyurgerov M, Romanovsky V, Oechel WC, Morison J, Zhang T, Barry RG. 2000. Observational evidence of recent change in the northern high-latitude environment. *Climatic Change* **46**: 159-207.
- Shagedanova M. 2002. The climate at present and in the historical past. In *The physical geography of northern Eurasia*, Shagedanova M (ed.). Oxford University Press: Oxford; 70-102.
- Sher AV. 1971. Mlekopitayushchie i stratigrafia pleistotsena krainego Severo-Vostoka SSSR i Severnoi Ameriki (Pleistocene mammals and stratigraphy of the far Northeast USSR and North America). Nauka: Moscow; 310 p. (in Russian).
- Sher AV. 1974. Pleistocene mammals and stratigraphy of the Far Northeast USSR and North America. *International Geology Review, Book Section, American Geological Institute* **16**: 7-10.

- Sher AV. 1997. A brief overview of the late Cenozoic History of the Western Beringian lowlands. In *Terrestrial Paleoenvironmental Studies in Beringia. Joint Russian-American Paleocology Workshop*, Edwards M, Sher A, Guithrie D (eds.). Fairbanks, Alaska; 134-145.
- Siebert L, Simkin T. 2002. Volcanoes of the world: an illustrated catalogue of Holocene volcanoes and their eruptions. Smithsonian Institution Digital Information Series GVP-3. <http://www.volcano.si.edu/gvp/world>.
- Siegert C, Derevagin AYu, Shilova GN, Hermichen W-D, Hiller A. 1999. Paleoclimatic evidences from permafrost sequences in the Eastern Taymyr lowland. In *Land–Ocean Systems in the Siberian Arctic: Dynamics and History*, Kassens H, Bauch HA, Dmitrenko IA, Eicken H, Hubberten H-W, Melles M, Thiede J, Timokhov LA (eds.). Springer: Berlin; 477–499.
- Solanki SK, Usoskin IG, Kromer B, Schüssler M, Beer J. 2004. An unusually active Sun during recent decades compared to the previous 11,000 years. *Nature* **431**(7012): 1084-1087.
- Solomina O, Alverson K. 2004. High latitude Eurasian paleoenvironments: introduction and synthesis. *Palaeogeography, Palaeoclimatology, Palaeoecology* **209**(1-4): 1-18.
- Steffensen JP, Andersen KK, Bigler M, Clausen HB, Dahl-Jensen D, Fischer H, Goto-Azuma K, Hansson M, Johnsen SJ, Jouzel J, Masson-Delmotte V, Popp T, Rasmussen SO, Röthlisberger R, Ruth U, Stauffer B, Siggaard-Andersen M-L, Sveinbjörnsdóttir ÁE, Svensson A, White JWC. 2008. High-resolution Greenland ice core data show abrupt climate change happens in few years. *Science* **321**: 680-684.
- Stein R, Dittmers K, Fahl K, Kraus M, Matthiessen J, Niessen F, Pirrung M, Polyakova Ye, Schoster F, Steinke T, Fütterer DK. 2004. Arctic (palaeo) river discharge and environmental change: evidence from the Holocene Kara Sea sedimentary record. *Quaternary Science Reviews* **23**(11-13): 1485-1511.
- Stichler W, Baker D, Oerter H, Trimborn P. 1982. Core drilling on Vernagtferner (Oetztal Alps, Austria) in 1979: Deuterium and oxygen-18 contents. *Zeitschrift für Gletscherkunde und Glazialgeologie* **18**(1): 23-35.
- Stiévenard M, Nikolaëv V, Bolshiyarov DYu, Fléhoc C, Jouzel J, Klementyev OL, Souchez R. 1996. Pleistocene ice at the bottom of Vavilov ice cap, Severnaya Zemlya, Russian Arctic. *Journal of Glaciology* **42**(142): 403-406.
- Stuiver M, Polach HA. 1977. Discussion: Reporting of ^{14}C data. *Radiocarbon* **19**: 355-363.
- Sulerzhitsky LD, Romanenko FA. 1997. Vozrast i rasselenenie "Mamontovoi" fauny aziatskogo zapolyar'ya (Age and distribution of the "Mammoth" fauna of the Polar Region of Asia). *Earth's Cryosphere* **1**(4): 12-19 (in Russian).
- Svendsen JI, Alexanderson H, Astakhov VI, Demidov I, Dowdeswell JA, Funder S, Gataullin V, Henriksen M, Hjort C, Houmark-Nielsen M, Hubberten H-W, Ingolfsson O, Jacobsson M, Kjær K, Larsen E, Lokrantz H, Lunkka JP, Lysa A, Mangerud J, Matushkov A, Murray A, Moeller P, Niessen F, Nikolskaya O, Polyak L, Saarnisto M, Siegert C, Siegert MJ, Spielhagen RF, Stein R.

2004. Late Quaternary ice sheet history of northern Eurasia. *Quaternary Science Reviews* **23**: 1229–1272.
- Svensson A, Nielsen SW, Kipfstuhl S, Johnsen SJ, Steffensen JP, Bigler M, Ruth U, Röthlisberger R. 2005. Visual stratigraphy of the North Greenland Ice Core Project (NorthGRIP) ice core during the last glacial period. *Journal of Geophysical Research* **110**: D02108.
- Synal H-A, Beer J, Bonani G, Lukaszczuk C, Suter M. 1994. ^{36}Cl measurements at the Zurich AMS facility. *Nuclear Instruments and Methods in Physics Research* **B92**: 79-84.
- Tarasov L, Peltier WR. 2005. Arctic freshwater forcing of the Younger Dryas cold reversal. *Nature* **435**: 662-665.
- Tarussov A. 1992. The Arctic from Svalbard to Severnaya Zemlya: climatic reconstructions from ice cores. In *Climate since A.D. 1500*, Bradley RS, Jones PD (eds.). Routledge: London and New York; 505-516.
- Tikhomirov DA, Blinov AV. 2009. Cosmogenic ^{36}Cl as a tool for dating permafrost ice. *Bulletin of the Russian Academy of Sciences: Physics* **73**(3): 384-386.
- Traufetter F, Oerter H, Fischer H, Weller R, Miller H. 2004. Spatio-temporal variability in volcanic sulphate deposition over the past 2 kyr in snow pits and firn cores from Amundsenisen, Antarctica. *Journal of Glaciology* **50**(168): 137-146.
- Trenberth KE, Jones PD, Ambenje P, Bojariu R, Easterling D, Klein Tank A, Parker D, Rahimzadeh F, Renwick JA, Rusticucci M, Soden B, Zhai P. 2007. Observations: Surface and Atmospheric Climate Change. In *Climate Change 2007: The Physical Science Basis. Contribution of Working Group I to the Fourth Assessment Report of the Intergovernmental Panel on Climate Change*, Solomon S, Qin D, Manning M, Chen Z, Marquis M, Averyt KB, Tignor M, Miller HL. (eds.). Cambridge University Press: Cambridge and New York; 237-336.
- Vaikmäe R. 1989. Oxygen isotopes in permafrost and ground ice – A new tool for paleoclimatic investigations. In *5th Working Meeting "Isotopes in Nature", Proceedings*. Leipzig, Germany; 543-553.
- van Everdingen R (ed.). 1998. revised May 2005. Multi-language glossary of permafrost and related ground-ice terms. National Snow and Ice Data Center/World Data Center for Glaciology: Boulder, CO. <http://nsidc.org/fgdc/glossary/>.
- Vasil'chuk YuK. 1991. Reconstruction of the palaeoclimate of the late Pleistocene and Holocene on the basis of isotope studies of subsurface ice and waters of the permafrost zone. *Water Resources* **17**(6): 640–674.
- Vasil'chuk YuK. 1992. Oxygen isotope composition of ground ice. Application to paleogeocryological reconstructions. Vol. 1 and 2. Geological Faculty of Moscow State University, Russian Academy of Sciences: Moscow; 418 and 263 p. (in Russian).
- Vasil'chuk YuK, Vasil'chuk AC. 1998. Oxygen isotope and C14 data associated with Late Pleistocene syngenetic ice-wedges in mountains of Magadan region, Siberia. *Permafrost and Periglacial Processes* **9**: 177-183.

- Vasil'chuk YuK, van der Plicht J, Jungner H, Sonninen E, Vasil'chuk AC. 2000. First direct dating of Late Pleistocene ice-wedges by AMS. *Earth and Planetary Science Letters* **179**: 237-242.
- Vinogradova AA, Egorov VA. 1996. Long-range pollutant transport into the Russian Arctic. *Izvestiya Atmospheric and Oceanic Physics* **32**(6): 731-737.
- Vinogradova AA, Ponomareva TYa. 1999. Air exchange between the Russian Arctic and the surrounding atmosphere in spring–summer periods from 1986 to 1995. *Izvestiya Atmospheric and Oceanic Physics* **35**(5): 532-539.
- von Toll EV. 1895. Wissenschaftliche Resultate der von der Kaiserlichen Akademie der Wissenschaften zur Erforschung des Janalandes und der Neusibirischen Inseln in den Jahren 1885 und 1886 ausgesandten Expedition. Abtheilung 3. Die fossilen Eislager und ihre Beziehungen zu den Mammuthleichen. *Mémoires de L'Académie impériales des Sciences de St. Pétersbourg VII Série, Tome XLII, No. 13*, Commissionnaires de l'Académie Impériale des Sciences: St. Pétersbourg; 1-86.
- Wagner G. 1999. Die kosmogenen Radionuklide ^{10}Be und ^{36}Cl im Summit-GRIP-Eisbohrkern. Dissertation. ETH Zurich, Switzerland; 156 p.
- Walter KM, Zimovs SA, Chanton JP, Verbyla D, Chapin III FS. 2006. Methane bubbling from Siberian thaw lakes as a positive feedback to climate warming. *Nature* **443**: 71-75.
- Wanner H, Beer J, Bütikofer J, Crowley TJ, Cubasch U, Flückiger J, Goosse H, Grosjean M, Joos F, Kaplan JO, Küttel M, Müller SA, Prentice IC, Solomina O, Stocker TF, Tarasov P, Wagner M, Widmann M. 2008. Mid- to Late Holocene climate change: an overview. *Quaternary Science Reviews* **27**: 1791–1828.
- Watanabe O, Motoyama H, Igarashi M, Kamiyama K, Matoba S, Goto-Azuma K, Narita H, Kameda H. 2001. Studies on climatic and environmental changes during the last few hundred years using ice cores from various sites in Nordaustlandet, Svalbard. *Memoirs of National Institute of Polar Research Special Issue* **54**: 227-242.
- Weiler K, Fischer H, Fritzsche D, Ruth U, Wilhelms F, Miller H. 2005. Glaciochemical reconnaissance of a new ice core from Severnaya Zemlya. *Journal of Glaciology* **51**(172): 64-74.
- Wetterich S, Herzsuh U, Meyer H, Pestryakova L, Plessen B, Lopez CML, Schirrmeister L. 2008a. Evaporation effects as reflected in freshwaters and ostracod calcite from modern environments in Central and Northeast Yakutia (East Siberia, Russia). *Hydrobiologia* **614**: 171-195.
- Wetterich S, Kuzmina S, Andreev AA, Kienast F, Meyer H, Schirrmeister L, Kuznetsova T, Sierralta M. 2008b. Palaeoenvironmental dynamics inferred from late Quaternary permafrost deposits on Kurungnakh Island, Lena Delta, Northeast Siberia, Russia. *Quaternary Science Reviews* **27**(15-16): 1523-1540.
- Wetterich S, Schirrmeister L, Andreev AA, Pudenz M, Plessen B, Meyer H, Kunitsky VV. 2009. Eemian and Late Glacial/Holocene palaeoenvironmental records from permafrost sequences at the Dmitry

-
- Laptev Strait (NE Siberia, Russia). *Palaeogeography Palaeoclimatology Palaeoecology* **279**: 73-95.
- Wilhelms F. 2000. Messung dielektrischer Eigenschaften polarer Eiskerne. *Reports on Polar Research* **367**, Alfred Wegener Institute for Polar and Marine Research: Bremerhaven; 171 p.
- Yershov ED. (ed). 1989. Geokryologiya SSSR, Vostochnaya Sibir' i Dal'nii vostok (Geocryology of the USSR, Vol. Eastern Siberia and Far East). Nedra: Moscow; 515 p. (in Russian).
- Zagorodnov VS, Klement'yev OL, Nikiforov NN, Nikolaëv VI, Savatyugin LM, Sasunkevich VA. 1990. Hidrotermicheskiy rezhim i l'dobrazovaniye v tsentral'noy chasti lednika Akademii Nauk na Severnoy Zemle (Hydrothermal regime and ice formation in the central part of the Akademiya Nauk glacier, Severnaya Zemlya). *Materialy Glyatsiologicheskikh Issledovaniy* **70**: 36-43 (in Russian).
- Zielinski GA, Mayewski PA, Meeker LD, Whitlow S, Twickler MS, Morrison M, Meese DA, Gow AJ, Alley RB. 1994. Record of volcanism since 7000 B.C. from the GISP2 Greenland ice core and implications for the volcano-climate system. *Science* **264**: 948-952.
- Zimov SA, Schuur EAG, Chapin III, FS. 2006. Permafrost and the global carbon budget. *Science* **312**: 1612-1613.

Note: The reference list has been updated and arranged according to the structure of the thesis. Therefore, slight differences to citations in the already published original papers may occur.

Acknowledgements

This thesis would not exist in this form without the help and support of many people. Thank you all!

First, I am particularly grateful to Prof. Wilfried Endlicher, Prof. Hans-Wolfgang Hubberten and Prof. Heinrich Miller for reviewing this thesis.

I would like to thank Prof. Wilfried Endlicher for his support of my scientific career from my university studies to the accomplishment of this thesis.

I am grateful to Prof. Hans-Wolfgang Hubberten for providing the opportunity to work at the Alfred Wegener Institute for Polar and Marine Research in Potsdam (AWI). Thank you also for enabling my participation in the expedition to the Dmitrii Laptev Strait in 2007.

I want to thank Dr. Diedrich Fritzsche for introducing me to ice core studies, for attending my research, for his interest in my work, for the supervision of the ice-core related part of my thesis, for constructive discussions at any time and for shared days in the cold laboratory in Bremerhaven.

I thank my colleagues from the AWI for being interested in my work. Particular gratitude merit Dr. Lutz Schirrmeister, Dr. Hanno Meyer and Dr. Sebastian Wetterich for their support, for their ongoing interest in my research, for their valuable comments and ideas, for fruitful and inspiring discussions (supported by coffee, chocolate and Hobbits) and for introducing me to permafrost and ground ice research. I also thank Dr. Rainer Schütt and Sebastian Breitenbach for fruitful discussions.

Furthermore, I thank all co-authors and reviewers of the relevant papers. Their substantial contributions and valuable comments have always been greatly appreciated. Not only in the final phase of my PhD I benefited a lot from quick and constructive proof-reading by Dr. Diedrich Fritzsche, Dr. Lutz Schirrmeister, Dr. Sebastian Wetterich and Dr. Hanno Meyer.

I want to thank the team of the expedition to the Dmitrii Laptev Strait in 2007, particularly Alexander Dereviagin, Dr. Lutz Schirrmeister, Dr. Sebastian Wetterich and Dr. Frank Kienast, for the great teamwork and a great expedition in an exciting area of the Arctic. I benefited much from your broad knowledge and experience and very much enjoyed the expedition – despite the all-encompassing mud...

For supporting me in the laboratories in Potsdam and Bremerhaven, I additionally thank Antje Eulenburg, Ute Bastian, Lutz Schönicke, Bernhard Chaplignin as well as Dr. Urs Ruth, Dr. Anna Wegner, Birthe Twarloh and Anika Schmidt.

This thesis was supported by a NaFöG PhD scholarship and travel grants from the state of Berlin, which were highly appreciated.

I want to thank my office mates and all other PhD candidates (It was an honour to be your president!) and diploma students during my time at the AWI for a great atmosphere, for scientific and non-scientific discussions and for lots of fun; not to forget the AWI Polar Runners Potsdam for great company at numerous running events.

Great thanks, of course, also deserves my family, particularly my parents, who supported my under- and graduate studies not only financially but also with continuous interest in my work. Thank you for your patience and trust!

Finally and most importantly I thank Anne for her support, encouragement, patience and love during the last years, but especially the last weeks of my work on this thesis. This thesis is dedicated to you.

Eidesstattliche Erklärung

Hiermit erkläre ich, die vorliegende Dissertation selbständig und ohne unerlaubte Hilfe angefertigt zu haben.

Die Dissertation wird erstmalig und nur an der Humboldt-Universität zu Berlin eingereicht.

Die dem Verfahren zugrunde liegende Promotionsordnung ist mir bekannt.

Thomas Opel

Berlin, d. 13. August 2009